Andreia Filipa Morgado Furtado
Mestre em Controlo da Qualidade e Toxicologia dos Alimentos

Rastreabilidade Metrológica das Medições de Massa Volúmica e das Determinações Reológicas de Líquidos

Dissertação para obtenção do Grau de Doutor em
Ciência e Engenharia de Materiais,
Especialidade em Ciência de Materiais

Orientador: Doutora Maria Teresa Varanda Cidade,
Professora Auxiliar com Agregação,
Faculdade de Ciências e Tecnologia da
Universidade Nova de Lisboa

Júri:

Presidente:	Prof. Doutor João Jorge Ribeiro Soares Gonçalves de Araújo
Arguentes:	Prof. Doutora Catarina Almeida da Rosa Leal
	Doutor Markus Schiebl
Vogais:	Prof. Doutora Maria Teresa Varanda Cidade
	Doutor João Luís Vieira Alves e Sousa

FACULDADE DE CIÊNCIAS E TECNOLOGIA
UNIVERSIDADE NOVA DE LISBOA

Setembro, 2019

A vós,
às minhas doces Marias
e aos meus desafiantes Estarolas.

AGRADECIMENTOS

"*Panta Rhei*", Heraclitus. Tudo flui. Por terem tornado possível e incentivarem a elaboração desta tese, de todas as experiências e projetos nos quais me envolvi ao longo destes anos, o meu mais sincero agradecimento ao Instituto Português da Qualidade, e à Direção de Departamento de Metrologia, a Doutora Isabel Godinho e à Direção do Laboratório Nacional de Metrologia, ao Doutor João Alves e Sousa, muito obrigada. À Faculdade de Ciências e Tecnologia da Universidade Nova de Lisboa, também a minha casa há quase 20 anos, e em especial à minha Orientadora, à Professora Maria Teresa Varanda Cidade, pelo seu envolvimento, pela sua ajuda e preciosa orientação, por me fazer chegar até aqui. Também agradeço a especial importância dos membros da CAT no suporte e finalização desta tese, obrigada.

My acknowledgment to the EMRP and EMPIR projects in which I was involved and that allowed the development of parts of this thesis work. These projects were carried out with funding of European Union and are jointly funded by the participating countries within EURAMET and the European Union.

"*Se um dia não souberes algo, escreve um livro sobre esse assunto*", e foi o que fiz. Disse-me, há alguns anos atrás, o meu colega de trabalho, e de buscas incessantes a respostas às mais variadas questões, Olivier Pellegrino. E a ele agradeço o constante incentivo por essa busca. Mas não poderia ficar por aqui. Aliás, os protagonistas são vários, e a todos eles agradeço, dedico, e em certo modo "devo", os resultados deste trabalho: à Adelaide Rodrigues, pelo contante apoio "maternal", por me manter "viva" e por sempre acreditar em mim, todos os dias, nestes últimos 13 anos; à Ana Rita Madeira, pelo companheirismo neste crescimento; ao Jorge Pereira, ao meu companheiro de batalha nestes assuntos dos líquidos, obrigada por acreditares (em mim) e por toda a confiança, acho que fazemos uma ótima equipa; ao Luís Ribeiro, pela sua pluripotência e paciência na resolução de problemas e pela partilha de conhecimento; ao Vítor Cabral, o meu vizinho da frente, pela sua curiosa e simpática inquietude, a todos vós do "clube do café com docinhos e curiosidades", e a tantos outros colegas do IPQ, a quem devo, minutos, horas, dias, anos de sorrisos, gargalhadas e de consolo, a quem não nunca poderei agradecer de igual modo.

"Apfelschörle, Quark und Physik". Ihnen, mein lieber Freund Henning Wolf, dafür, dass Sie an meine Arbeit, an mich und an meine Zukunft glauben, dass Sie so geduldig sind, dass ich in dieser Metrologie-Welt „wachsen"kann.

"*Porque eu sou do tamanho do que vejo, e não do tamanho da minha altura*", Fernando Pessoa. À minha família de estarolas, por me quererem fazer "ser mais, ser melhor": ao Pedro Matos, o nosso comandante e pacificador, por todos os conselhos, e por partilhares as dores comigo; ao João Fadista, por seres o meu doce estarola; ao André Santos, por todas as guerrilhas; ao meu querido André Rosa, ao meu austero assentimental, por seres um dos mosqueteiros, por me fazeres acender a luz no fundo do túnel, por fazeres as flores brotar e os flocos de neve tomarem formas inimagináveis, a ti devo conseguir olhar além; à Vitória Cunha, por toda a energia, por todo o apoio em momentos angustiantes, por me ouvires, por não me teres deixado baixar os braços; a todos vós estarolas que trago e sempre levarei no meu coração: André Galvão, Irene Izquierdo, Verónica Azevedo; Elizabete Almiro, Mónica Estevão, Hélder Cruz, a todas as nossas mini-estarolinhas, a todos a vós devo.

Às flores do meu caminho. Às "Marias" do meu coração: à minha avó, à minha querida e doce mãe-avó que me carrega e carregou; à minha mãe amiga, por crescermos juntas e juntas estaremos sempre; à minha irmã Joana por seres a minha pequenina e tão grande; à minha tia Zézinha, por nos completares; ao meu pai ("grande maluco"); aos meus irmãos "gémeos" (Rúben e Daniela); a todos os meus tios-pai (Zézinho e Chico), tia Lena, Tia Teresa, Tété (por ter feito crescer em mim este "bichinho das ciências"), primos e primas irmãos (Sara, Marcos, Carina, Daniela, Isa, Pedro e Nádia); aos meus avós paternos, à minha Família, por me sempre fazerem acreditar que posso ser aquilo que anseio, por me deixarem descansar nos vossos colos, por me secarem as lágrimas e por me fazerem sorrir e querer sorrir, dia após dia, mesmo que as "pedras do nosso caminho" se transformem em montanhas. A vós dedico todo este trabalho, porque ele a vós devo. Obrigada.

Abstract

Density is one of the main drivers of economic transactions in a wide range of products, from fuels to food products. Actual consumption of liquids of high commercial value, such as wine, olive oil and fuels, can and should be regarded as of high importance within the European economy. The physical properties of these liquids, such as density, surface tension, viscosity and elasticity, among others, cover a wide range of variation. Furthermore, such liquids are often handled over a wide range of temperatures and pressures during the processing, control and transport steps. Since currently available density measurement methods are influenced by one or more of these properties inherent in liquids, as well as temperature and pressure, their robustness should be carefully evaluated. Still being urgent the establishment of an adequate density metrological traceability chain, not only in Portugal, but also in the European space, and throughout the world. Thus, the main objective of this thesis work was to study the influence of such properties of liquids on the result of measurements made by oscillation-type density meters, from ambient pressure to pressures up to 600 bar. The influence of viscosity in Newtonian liquids, and viscoelasticity in non-Newtonian liquids, on the accuracy and precision of the density measurement results was investigated using hydrostatic weighing and pycnometry as comparative methods. The mechanical characterization of viscoelastic samples was performed using rotational rheometry. The knowledge acquired during this work will be disseminated in international guides and standards of scientific and applied metrology (EURAMET guides and ISO standards) and legal metrology (OIML and WELMEC documents), in order to fill the lack of documentation in this area of knowledge.

Another aspect of high importance and impact in the scientific field is the development of methods for determining the salinity of seawater. This parameter allows describing the ocean currents that will be used as a basis for climate modelling. In this sense, the investigations carried out were able to prove the compatibility of salinity determinations by measuring density and refractive index.

Keywords: Liquids' Metrology; Metrological Traceability; Density; Viscosity; Viscoelasticity; Rheology

Resumo

A massa volúmica é um dos principais elementos impulsionadores de transações económicas dos mais variados produtos, desde combustíveis até produtos alimentícios. O consumo real de líquidos de elevado valor comercial, tal como o vinho, o azeite e os combustíveis, pode e deve ser encarado de elevada importância no seio da economia europeia. As propriedades físicas destes líquidos, tais como: a massa volúmica, tensão superficial, viscosidade e elasticidade, entre outras, cobrem um amplo espectro de variação. Além disso, esses líquidos são frequentemente manipulados num amplo intervalo de temperaturas e pressões, durante as etapas de processamento, controlo e transporte. Dado que os métodos de medição de massa volúmica atualmente disponíveis são influenciados por uma ou mais destas propriedades inerentes aos líquidos, bem como pela temperatura e pela pressão, a sua robustez deve ser cuidadosamente avaliada. Sendo ainda premente, o estabelecimento de uma cadeia de rastreabilidade metrológica de massa volúmica adequada, não só em Portugal, como no espaço europeu, e em todo o mundo. Assim, o objetivo principal deste trabalho prendeu-se com o estudo da influência de tais propriedades dos líquidos no resultado das medições efetuadas por densímetros de tubo vibrante, a pressão ambiente e altas pressões (até 600 bar). A influência da viscosidade, em líquidos Newtonianos, e da viscoelasticidade, em fluidos não-Newtonianos, na exatidão e na precisão dos resultados de medição da massa volúmica foi investigada usando como métodos comparativos a pesagem hidrostática e a picnometria, respetivamente. A caracterização mecânica das amostras viscoelásticas foi realizada por recurso a reometria rotacional. Os conhecimentos adquiridos durante este trabalho serão disseminados em guias e normas internacionais de metrologia científica e aplicada (guias EURAMET e normas ISO) e de metrologia legal (documentos OIML e WELMEC), com intuito de colmatar a falta de documentação existente nesta área de conhecimento.

Outro aspeto de elevada importância e impacto, no meio científico, prende-se no desenvolvimento dos métodos de determinação da salinidade da água do mar. Parâmetro que permite descrever as correntes oceânicas que serão utilizadas como base para a modelação climática. Neste sentido, as investigações realizadas conseguiram comprovar a compatibilidade das determinações de salinidade por meio da medição da massa volúmica e do índice de refração.

Termos chave: Metrologia de Líquidos; Rastreabilidade Metrológica; Massa volúmica; Viscosidade; Viscoelasticidade; Reologia

Content Index

Index of Figures

Index of Tables

List of Abbreviations and Acronyms

API	American Petroleum Institute
ASTM	American Society for Testing and Materials (standards, USA)
BEV-PTP	Federal Office of Metrology and Surveying - Physico-technical testing service (the Austria's NMI, in German: *Bundesamt für Eich- und Vermessungswesen -Physikalisch-technische Prüfdienst*)
BIPM	International Bureau of Weights and Measures (in French, *Bureau international des poids et mesures*)
BRML	*Biroul Roman de Metrologie Legala* (the Romania's NMI)
BS	British standards
CCM	Consultative Committee for Mass and Related Quantities (in French, *Comité Consultatif pour la Masse et les Grandeurs Apparentées*)
CGPM	General Conference on Weights and Measures
CIPM	International Committee for Weights and Measures (in French, *Comité International des Poids et Mesures*)
CIPM MRA	*Comité international des poids et mesures* - Mutual Recognition Arrangement
CMC	Calibration and Measurement Capability
CMI	*Ceský metrologický institut* (the Czech Republic's NMI)
CP	cone-and-plate (measuring systems)
(C)RM	(Certified) Reference Material
CSD (or CD)	controlled shear deformation
CSR (or CR)	controlled shear rate
CSR (or CR)	controlled shear rate
CSS (or CS)	controlled shear stress
DI	Designated Institute

DIN	*Deutsches Institut für Normung* (the German's standards organization)
DMA	Dynamic-Mechanical Analysis
DMDM	*Ministarstvo privrede Direkcija za mere i dragocene metale* (the Serbia's NMI)
EC	European Commission
EMPIR	European Metrology Programme for Innovation and Research
EMRP	European Metrology Research Programme
EURAMET	European Association of National Metrology Institutes
EURAMET TC-M	EURAMET Technical committee for metrology in Mass and Related Quantities
FCT/UNL	Faculdade de Ciências e Tecnologia da Universidade Nova de Lisboa
GUM	Guide to the Expression of Uncertainty in Measurement
GUM	GUM Central Office of Measures (the Poland's NMI, In Polish: *Glowny Urzad Miar*)
HP	High-Pressure
HW	Hydrostatic Weighing
IMBiH	*Institut za mjeritejstvo Bosne i Hercegovine* (the Bosnia and Herzegovina's NMI)
INM	*I.P. Institutul National de Metrologie* (the Republic of Moldova's NMI)
IPK	International Prototype of the Kilogram
IPQ	Portuguese Institute for Quality (in Portuguese, *Instituto Português da Qualidade*)
IPR	Intellectual Property Rights
ISO	Internal Organization for Standardization
JRP	Joint Research Project
JV	*Justervesenet* (the Norway's NMI)
KC	Key Comparison
KCDB	Key Comparison Database
LNM	National Metrology Laboratory (in Portuguese, *Laboratório Nacional de Metrologia*)
LPL	Laboratory of Properties of Liquids (in Portuguese, *Laboratório de Propriedades de Líquidos*)
LVE	Linear viscoelastic
MKEH	Hungarian Trade Licensing Office (the Hungary's NMI), now renamed as to Government Office of the Capital City Budapest, BFKH
NIST	National Institute of Standards and Technology (North American NMI)
NL	Newtonian liquid
NMI	National Metrology Institute
NNL	Non-Newtonian Liquid
NPL	National Physical Laboratory (the UK's NMI)
OD	Oscillation-type density meter

OIML	International Organization of Legal Metrology (in French, *Organisation Internationale de Métrologie Légale*)
PAO	Poly-alpha-olefin
PP	Parallel plate (measuring systems)
PRT	Platinum resistance thermometer
PT	Proficiency Testing
PTB	*Physikalisch-Technische Bundesanstalt* (the Germany's NMI)
RMO	Regional Metrology Organisation
SC	Stakeholder Committee
SC	Subcommittee
SDS	Safety Data Sheet
SI	International System of Units (in French, *système international d'unitées*)
SMOW	Standard Mean Ocean Water
SVM	Stabinger's viscometer
TC	Technical Committee
TUBITAK	*Türkiye Bilimsel ve Teknolojik Araştırma Kurumu* (the Turkey's NMI)
VIM	International Vocabulary of Metrology (in French, *Vocabulaire International de Métrologie*)
VSL	*Van Swinden Laboratory* (the Netherlands' NMI)
VSMOW	Vienna Standard Mean Ocean Water
WELMEC	Western European Legal Metrology Cooperation

List of symbols and signs

Latin characters (small letters)

f	frequency [Hz]
g	gravitation constant [m/s^2]
h	gap dimension, layer thickness, fluid level [m]
k	coverage factor (JCGM 100:2008)
lg	logarithm (to the basis 10)
ln	natural logarithm (to the basis e, Euler's number)
m	mass [kg]
p	pressure [0,1 MPa =1 bar]
r	radius [m]
t	temperature [ºC]
u	standard uncertainty (JCGM 100:2008)
U	expanded uncertainty (JCGM 100:2008)
v	velocity [m/s]
V	volume [m^3]

Latin characters (capital letters)

A	area [m^2]
F	force [N]
G	shear modulus [Pa]
G^*, G', G''	complex shear modulus, storage modulus, loss modulus [Pa]
J	(shear) compliance (creep tests) [Pa^{-1}]
M	torque [mNm]
Q	quality factor (of a harmonic oscillation) [1]
Re	Reynolds number [1]

T	(absolute) temperature [K]

GREEK CHARACTERS

γ	deformation or strain [%], [1]
$\dot{\gamma}$	shear rate (strain rate; $d\gamma/dt$) [s^{-1}]
δ	phase shift angle, loss angle [º]
$tan\delta$	loss factor, damping factor [1]
η	(shear) viscosity [Pa s]
η^*, η', η''	complex viscosity, and its real and imaginary part [Pa s]
ν	kinematic viscosity [m^2/s]
ρ	density [$kg \cdot m^{-3}$]
τ	shear stress [Pa]
ω	angular velocity (rotation), angular frequency (oscillation) [rad/s], [s^{-1}]

FACULDADE DE CIÊNCIAS E TECNOLOGIA
UNIVERSIDADE NOVA DE LISBOA

I

Thesis Research Framework

The dimension of the impact of metrological traceability of density measurements and rheological determinations of liquids in our daily life may not be very clear at first sight for all citizens. A Metrology Scientist will take only few minutes to get a rough idea on the influence of these two parameters in our Society. In terms of economic impact, one can think of the commercial transactions that are made with basis on the density of the liquids, such as in the oil and food industries. It is easy to realize that the liquids produced, controlled and manipulated by these industries have very different physical properties, such as density, viscosity and viscoelasticity that may influence the density measurements results when some types of measurement methods are used. Of equal importance is to be able to obtain accurate density and viscosity measurements, of all these liquids, with application in the design of the production and filling lines in these industries. For instance, the economic impact of a correct line design can be, among others, related with the efficiency of the use of the pumps, namely when non-Newtonian liquids are concerned. In other hand, and not less important, the knowledge of these parameters has a great impact in operational safety. As example, one can think about the disaster occurred in 2010 in the Deepwater Horizon drilling rig at Gulf of Mexico, with great impact in terms of Human and animal lives loss as well as environmental. When drilling deep for gas and oil or for the purpose of building bridge piles or taking core samples for a future tunnel, non-Newtonian drilling fluids are used. Other example is when the pressurised fluids transports hydraulic power to the down hole drilling assembly and the drill bit, the balance of fluid pressure in the pores of the surrounding formation, stabilises the borehole walls, washes the cuttings out of the well, and lubricates the drill bit.

Practical metrological needs and requirements can illustrate the relevance of this topic. Other situation, with a large importance in the actual consumption patterns, are the prepacked products, i.e. a product contained inside a package that is sale with the quantity (volume or mass) displaying a predetermined value. When the quantity of a liquid product in a package is expressed in terms of volume but verified by weighing, it is also necessary to determine the density of this product. The quantities of prepacked products are regulated by European Directives (Council Directive 76/211/EEC; Council Directive 80/232/EEC and Directive 2007/45/EC of the European Parliament and of the Council). It has been seen that, in practice, the methods for measuring density of these liquid products are frequently not well understood by the end-users, leading to significant systematic errors (OIML G 14:2011). The Guide 14

(2011) and the Bulletin number 96 (1984), produced by the International Organization of Legal Metrology (OIML, in French, *Organisation Internationale de Métrologie Légale*), pointed out oscillation-type density meters as suitable measuring instruments to determine the density of several of these types of liquids, such as: liquids without dissolved carbon dioxide or other gases; viscous liquids, e.g., lubricating oils, paints, varnishes; solvents; cleaning, cosmetic and washing products. This wide variety of liquids, ranging in a broad density, viscosity and viscoelastic ranges requires sophisticated calibration procedures of these instruments. In addition, some of these products are produced, manipulates, packed and transport at high temperatures and pressures. The European Directives regarding the mandatory control of the volume of the liquid contained in prepacked products for consumer protection as well as the introduction of these products in the market, had intensified the request of these industries, and others stakeholders, to National Metrology Institutes (NMI) to provide the proper calibration services. For this, and other for reasons, the improvement of the metrological quality of density, viscosity and viscoelasticity measurements will have direct an impact on the industrial site, leading, for instance, to a reduction of the production of non-conforming products in pre-packaged industries and, therefore, leading to a better competitiveness. In terms of society, having the proper methods to control the volume inside a prepacked liquid will boost the confidence on the markets.

In short, the establishment of a proper and recognised traceability chain for density, viscosity and viscoelasticity measurements of liquids is mandatory for the enhance of the confidence and competitiveness of national industries, as well to potentiate the research developed in several laboratories. Additionally, from the environmental site, a highest-level aspect is the need for accurate density measurement of seawater (for salinity determination) in the European marginal seas to be used for the description of oceanic currents as base for climate modelling.

II

INTRODUCTION

This chapter aims to frame, in the big picture, the question discussed in this work. For that, the metrological traceability of density, viscosity and viscoelasticity measurements, of liquids, are described in some extent, including the realization and dissemination of the respective units, all way through the metrological hierarchy pyramid, from the SI, to primary standards down to the working instruments used for field measurements. Thus, given state-of-the-art information about the uncertainties associated with the existing measurement methods used to determine these quantities, allowing to frame the magnitude of uncertainties obtained throughout the present work. Another explored point, to some extent, was the calculation of measurement uncertainties by presenting their assumptions and describing practical examples, specifically in the case of rheometry. The roadmap of liquids' density metrology at IPQ is also described in detail.

II.A

METROLOGICAL TRACEABILITY OF DENSITY MEASUREMENTS OF LIQUIDS

The density ρ, of a body is defined as the quotient of its mass m, and its volume V ($\rho = m/V$). The unit of density is therefore kg·m^{-3}. Given this relation, and mainly in liquids, it is often the case that their mass is determined based on volume and density measurements. Density is of great economic importance, for instance, everywhere the price of a product is related with its volume, but where the mass is measured (or vice-versa). Whereas for this purpose, a relative standard uncertainty of density measurements from $1{\cdot}10^{-4}$ up to $1{\cdot}10^{-3}$ is found sufficient, while in oceanography, in which the ocean currents caused by density differences are studied, relative uncertainties lower than $1{\cdot}10^{-5}$ are found as required. Within the scope of the discussions on climate change, such measurements are of great interest, especially for model calculations where an accurate knowledge of water density as a function of temperature and pressure is necessary. The existence of reference tables and formulas for water density allow the use of ultra-pure water as a liquid density standard, with a low relative uncertainty of $1{\cdot}10^{-5}$ (Bettin, Borys & Nicolaus, 2008). Similarly, vacuum oils (a recent substitution of pure mercury) are used as a density standard to trace back the pressure measurement to the height measurement of a vacuum oil column (the pressure p of a liquid column is $p = g\,\rho\,h$, where g is the gravitational acceleration of the Earth, ρ the density of the liquid and h the height of the liquid column) (Ehlers *et al.*, 2019).

II.A.1. REALISATION OF DENSITY UNIT

The concept of metrological traceability is defined as the property of a measurement result whereby the result can be related to a reference through a documented unbroken chain of calibrations, each contributing to the measurement uncertainty (JCGM 200:2012). This property of a measurement result is assured by ensuring a documented, unbroken chain of instrument calibrations, from the working instruments used for field measurements, all the way up the metrological hierarchy pyramid to the primary standard (JCGM 200:2012). At the top of this pyramid is an internationally defined and accepted

reference, in most cases the International System of Units (SI), whose technical and organizational infrastructure has been implemented and developed by the International Bureau of Weights and Measures (BIPM, in French *Bureau International des Poids et Mesures*).

The SI was previously defined in terms of seven base units, and derived units that where defined as products of powers of the base units. The seven base units were chosen, for historical reasons, and were, by convention, regarded as dimensionally independent: the meter, the kilogram, the second, the ampere, the kelvin, the mole, and the candela. In a landmark decision, the BIPM's Member States voted on the 16th of November 2018 to revise the SI, changing the world's definition of the kilogram, the ampere, the kelvin and the mole. This decision, made at the 26th meeting of the General Conference on Weights and Measures (CGPM), would mean that from 20th of May 2019, all SI units will be defined in terms of constants that describe the natural world. This would assure the future stability of the SI and would open the opportunity for the use of new technologies, including quantum technologies, to implement the definitions. So, the present SI is now defined in terms of seven defining constants: caesium hyperfine frequency $\Delta\nu_{Cs}$; speed of light in vacuum c; Planck constant h; elementary charge e; Boltzmann constant k; Avogadro constant N_A; and luminous efficacy of a defined visible radiation K_{cd}.

As the authors Cabiati & Bich (2009) described, to define the units by reference to fundamental constants implies to abandon the identification of the unit with its primary standard, as in the old metrological tradition. Meaning that to realise a unit will consist in assigning a value to a primary standard, consistent with the fixed values of the reference constants, by means of an experimental procedure, independent of a specific definition. The primary standard should be suitable to dissemination by direct comparison, thus essentially stable and accessible with the highest precision, while the role of the realisation experiment would be mainly related to indirect measurements, typical of scientific activity, which involves the coherence of the unit system. The two distinct roles, of unit realisation and primary standard, correspond to different uncertainty components, of which only one is implied in dissemination activity, just aiming at compatibility of measurements of a specific quantity. Each of the two uncertainty components has a different evolution from the time of the unit redefinition.

At the national level, practical realisation, maintenance and dissemination of the SI quantities, is one of the main tasks of the National Metrology Institutes (NMI), that it is the case of the Portuguese Institute for Quality (IPQ). So, each NMI must maintain the national primary standards and intercompare them periodically, issuing quantitative equivalence statements published in the key comparisons database of the BIPM (KCDB-BIPM). The third link in the traceability assurance chain is from the responsibility of calibration laboratories, accredited in accordance to the international standard ISO/IEC 17025 (2017). Accreditation ensures that the calibration methods they employ are appropriate, well executed and recognised worldwide. Importantly, it also ensures that the unbroken chain of calibrations is well documented, i.e. metrological traceability is assured.

In the past hundred years, the accuracy of the realization of the density unit has improved by a factor of nearly 100. At the beginning of the 20th century, an uncertainty of approximately $2 \cdot 10^{-6}$ was achieved when it was checked whether the mass of the kilogram prototype was in agreement with the former definition as the mass of 1 dm^3 of water at 4 °C. Currently, the most accurate primary density standards have an uncertainty of approx. $4 \cdot 10^{-8}$, whereby an improvement to $1 \cdot 10^{-8}$ was aspired within the scope of the Avogadro Project (Bettin, Borys & Nicolaus, 2008).

After the implementation of the revised SI, the kilogram changed from being equal to the mass of the International Prototype of the Kilogram (IPK) to a quantity related to a fixed numerical value of the Planck constant. At this point the IPK changed from having a fixed mass without uncertainty to having a mass with a finite uncertainty which can change with time. Directly after the implementation date of the revised SI, the IPK will inherit the uncertainty that had previously been associated with the Planck constant,

equal to 10 µg (k =1). Prior to the decision to redefine the kilogram, all NMI took traceability, directly or indirectly, from the IPK. This will continue to be the case immediately after the 20th of May 2019. The only change is that the mass of the IPK will then have an associated uncertainty of 10 µg.

II.A.2. DISSEMINATION OF DENSITY UNIT

The hierarchy scheme that defines the order of disseminating the density unit from a primary measurement standard to secondary measurement standards, working standards and working measuring instruments, in the interval from 0,5 to 24 000 kg·m^{-3}, was prepared by the OIML Subcommittee SC4 ("Densities") of the Technical Committee TC9 ("Instruments for measuring mass and density"), as an international recommendation, and can be found illustrated in Figure II.1. This hierarchy scheme sets up a uniform method to realize the density unit by the absolute method for density unit realization through two base units of physical quantities, mass and length. The primary standard of the density unit is traceable to primary standards of length and mass units. The countries that do not possess equipment to be used as the primary standard can use secondary standards of density, and so on.

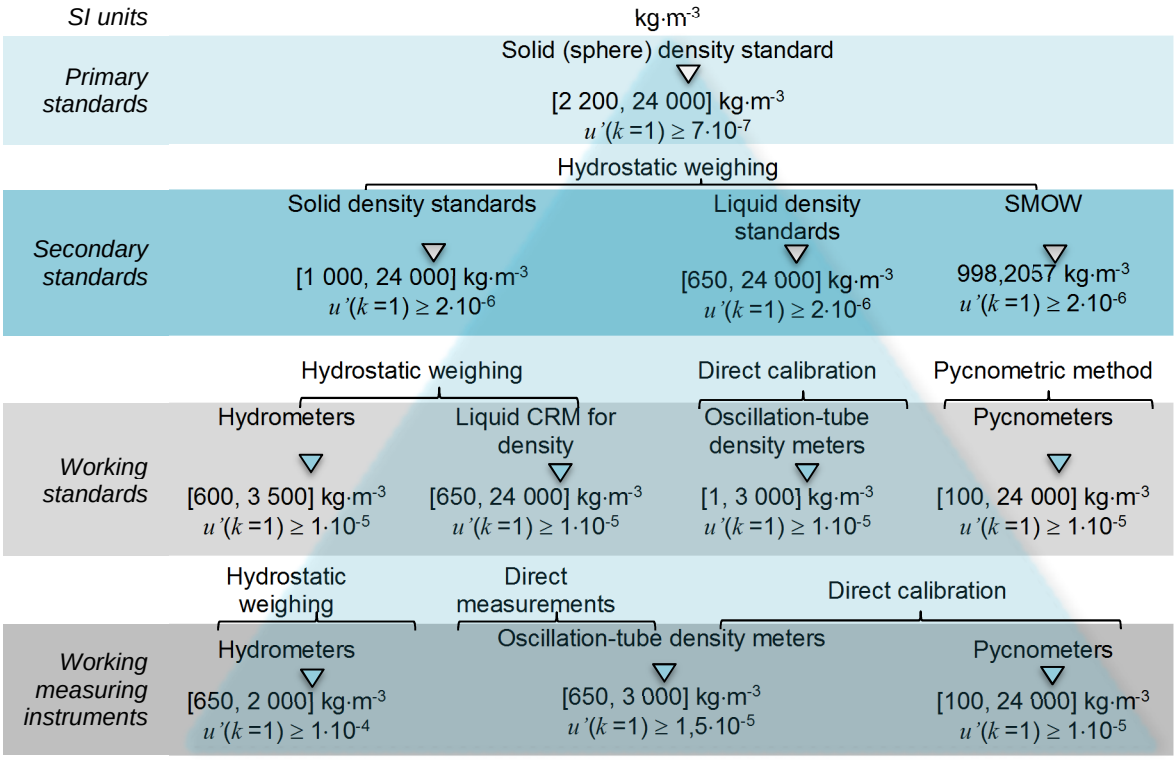

Figure II.1 Hierarchy scheme of dissemination of the density unit for liquids.

II.A.2.1 Primary measurement standard of the density unit

The primary measurement standard is intended for reproduction and dissemination of the density unit by means of secondary and working measurement standards to working density measuring instruments. As primary density standard, a solid body of regular geometric shape is used, typically of spherical form, with mass and diameter to ensure the lowest uncertainty of density measurements. The mass of the density standard is traceable to the IPK, and its volume is determined directly by measuring its diameter using an optical interferometer, so that the unit of the density is directly traceable to the SI units of mass and length. The range of transmission of the density unit to secondary measurement standards varies from 650 to 24 000 $kg \cdot m^{-3}$ (Fig. II.1). The primary measurement standard is used for dissemination of the density unit to secondary measurement standards by the method of hydrostatic weighing with a relative measurement standard uncertainty above $7 \cdot 10^{-7}$ (k =1).

Since the primary link-up is extremely laborious and only possible for almost perfectly shaped solids, comparison methods are used to determine the density of other solids, but also of liquids and gases (Spieweck & Bettin, 1992). Most methods use Archimedes' principle, according to which a solid in a liquid apparently loses as much weight as the displaced liquid weighs. The apparent weight of a solid (as compared to calibrated mass standards) is thus measured by means of a hydrostatic balance. Based on this result, it is possible to calculate, if the mass is known, the apparent weight loss or the buoyancy $\rho_L \cdot V_s \cdot g$ and, if the volume V_s of the solid is known, the density ρ_L of the liquid (Fig. II.2). Vice-versa, if the density of the liquid is known, it is possible to determine the volume of a solid sample. In this way it is possible to determine, for example, the volume of other, secondary density standards, of weights of artefacts for the measurement of the air density. If the sample and the standard have a very similar mass and volume, the highest accuracy is achieved if the apparent weights of the sample and the standard are compared both in the liquid and in air and only the (small) differences are measured. In this way, volumes (and densities) can be compared with a relative uncertainty below $5 \cdot 10^{-8}$ (Fujii, 2006).

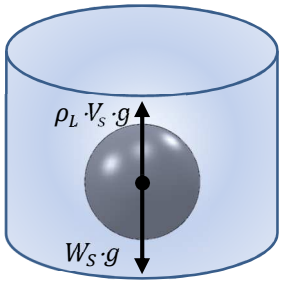

Figure II.2 Schematic representation of the actuating forces on sphere in liquid.

In floatation procedures, the special case of Archimedes' principle is used the weight is fully compensated by the buoyancy in the liquid. The exact adjustment of the densities can be realized, for example, by means of a pressure change in the liquid ("pressure-of-floatation"). From the difference of the pressures at which two samples are floating it is then possible to calculate, by means of the compressibility of the liquid, the density difference of the samples. Whereas in hydrostatic weighing, a wire is used to lead to the balance, no wire is used in this method, which permits to achieve a much higher accuracy. In this way, silicon spheres with relative uncertainties of $2 \cdot 10^{-8}$ can be compared. This fact was exploited within the scope of the Avogadro Project to detect density differences in the silicon crystal and to seek crystal defects (Becker *et al.*, 2005). In the magnetic floatation method, a permanent magnet which hangs on the sample and on a float is used to keep the sample in a state of floatation. The density of water was redetermined by means of this method (Wolf, Bettin & Gluschko, 2006). But it can also be used for comparing the density of solids. The main advantage here, again, is that there is no wire leading to the balance and traversing the surface of the liquid (Bettin, Borys & Nicolaus, 2008).

II.A.2.2 Secondary measurement standard of the density unit

Secondary measurement standards of the density unit are intended for dissemination of the unit to working measurement standards, i.e. to Certified Reference Materials (CRM) of density of solids, to CRM of density of liquids and to hydrometers, by the method of hydrostatic weighing, by direct and pycnometric methods. The range of nominal values of density, reproduced by the secondary measurement standard is from 650 to 24 000 $kg \cdot m^{-3}$ with a relative measurement standard uncertainty above $2 \cdot 10^{-6}$ (k =1) (Fig. II.1). Others, not so common, secondary measurement standards consist of a solid sinker covering the density range from 1 000·to 24 000 $kg \cdot m^{-3}$; and samples of Standard Mean Ocean Water (SMOW) with known isotopic composition and density at 20 °C and atmospheric pressure of 101,325 kPa.

Hydrostatic weighing is also used for the calibration of hydrometers, according to the, so-called, Cuckow's method (Cuckow, 1949). Thereby, the hydrometer is weighed while it is immersed up to the scale line to be checked, into a liquid of known density (and surface tension) (Spieweck & Bettin, 1992). Hydrometers are a cheap and reliable means to determine density or, indirectly (if the density dependence is known) the concentration of dissolved substances in liquids. In legal metrology, they are used to measure alcohol content. Nowadays, density meters of oscillation-type are used more often to determine the density of liquids because they only need a very small amount of liquid, can be automated and can be integrated into industrial processes.

II.A.2.3 Working measurement standards and instruments

The following materials and instrumentation are used as working standards: hydrometers, liquid CRM for density, oscillation-type density meters and pycnometers, in the density interval from 1 to 24 000 $kg \cdot m^{-3}$; with a relative measurement uncertainty above $1 \cdot 10^{-5}$ (k =1) (Fig. II.1).

In the base of the pyramid can be found the working measurement standards, which in the case of liquids' density can be hydrometers, oscillation-type density meters and pycnometers. For these instruments the dissemination of the density unit is done via hydrostatic weighing in the case of hydrometers (more specifically by Cuckow's method), and by direct measurements or calibration in the case of the oscillation-type density meters and pycnometers. The relative measurement uncertainties of the working standards should be comprised between $1 \cdot 10^{-5}$ and $1 \cdot 10^{-4}$ (k =1) (Fig. II.1).

II.B

METROLOGICAL TRACEABILITY OF VISCOSITY AND RHEOMETRIC MEASUREMENTS

The viscosity of a liquid is a measure of its resistance to deformation at a given rate, being therefore conceptualized as quantifying the frictional force that arises between adjacent layers of fluid that are in relative motion. Thus, dynamic viscosity, η, also known as dynamic viscosity coefficient or simply viscosity (ISO 3104:1994), is a measure of liquids' internal resistance to flow. The unit derived from the SI of dynamic viscosity is Pa·s, i.e. $N \cdot m^{-2} \cdot s$, and is expressed in terms of SI base units in $m^{-1} \cdot kg \cdot s^{-1}$. On other hand, kinematic viscosity, ν, is defined as the resistance of a liquid to gravity flow. Algebraically it results from the quotient between dynamic viscosity and density, both measured at the same temperature and pressure conditions (ISO 3104:1994). The SI derived unit of kinematic viscosity is $m^2 \cdot s^{-1}$. Viscosity can be measured with various types of instruments, as e.g. viscometers, viscosity cups, rheometers. A rheometer is used for those liquids that cannot be defined by a single value of viscosity and therefore require more parameters to be set and measured. These liquids are called non-Newtonian.

II.B.1 REALISATION AND DISSEMINATION OF VISCOSITY UNIT

The base of all viscosity measurements is the internationally accepted viscosity of double-distilled water at 20 °C (ISO TR 3666:1998; Swindells, Coe & Godfrey, 1952). The dissemination of the viscosity unit is initiated in each country, through the practical realization of the kinematic viscosity scale by each NMI through the step-up method, using a set of standard glass viscometers and reference liquids, using as a starting point the conventionally established and accepted water viscosity value (ISO TR 3666:1998; Swindells, Coe & Godfrey, 1952; Lorefice & Saba, 2017) (Fig. II.B.3). With this method is possible to cover the kinematic viscosity interval from 0,4 $mm^2 \cdot s^{-1}$ to above 700 000 $mm^2 \cdot s^{-1}$, in the temperature interval from 10 to 150 °C (Lorefice & Saba, 2017). The degree of equivalence of each National Viscosity Scale (NVS) is in turn assessed by participating in international comparisons (Fig. II.B.3). Countries that do not establish their own scale ensure the traceability of national viscosity measurements by calibrating

their standard viscometers by their own scale or by calibrating them with viscosity certified reference liquids, this being the current situation of Portugal.

At secondary levels the dissemination of the viscosity is accomplished by calibrating capillary viscometers or by using reference liquids for viscosity at a given temperature (Fig. II.3). Glass viscometers are the most stable and accurate representation of viscosity, but their use is limited to Newtonian liquids with viscosities up to 106 mPa·s, at temperatures below 300 °C and close to atmospheric pressure. For all other instruments, including those used for non-Newtonian liquid measurements, suitable reference liquids are required for calibration. To be considered reference liquids they must have well-known and established flow behavior, be homogeneous, have long-term stability, and be thermally stable (ISO 17034:2016).

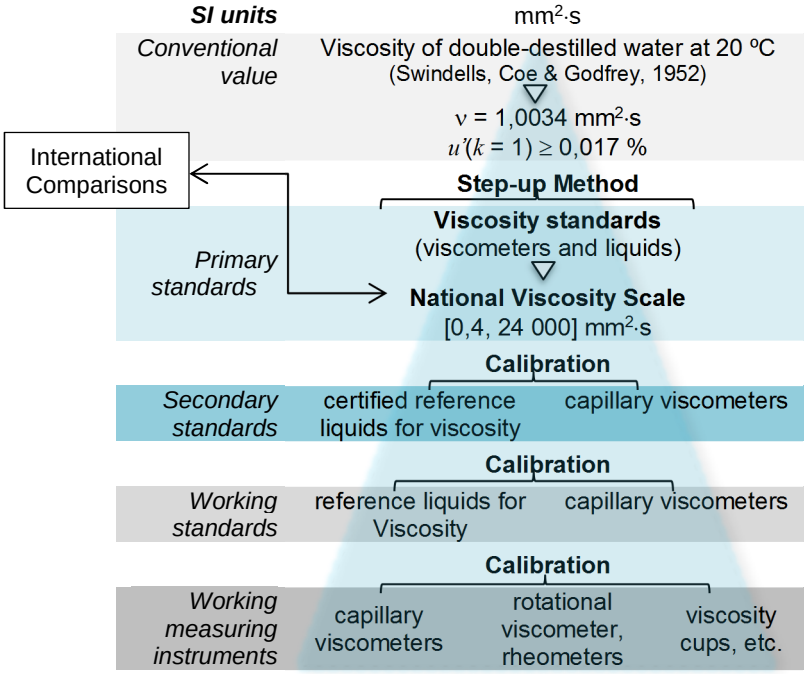

Figure II.3 Hierarchy scheme of dissemination of viscosity measurements (adapted from (Lorefice & Saba, 2017)).

II.B.2 TRACEABILITY OF RHEOLOGICAL DETERMINATIONS

As previously mentioned, the establishment of standards is a practical, and useful, way of providing comparable results for a specified type of measurement. Metrology, as the science of measurement, goes way beyond by ascertaining that quantities are generally transferable between physical relations. The two key issues are the traceability to a common set of base units (the SI) and the estimation of the uncertainty of each quantity. The steps for evaluating the uncertainty of a measurement result are summarized in the Guide to the expression of uncertainty in measurement (GUM) (JCGM 100:2008). The first step consists in expressing a mathematical function *f* which relates the measurand to the input quantities on which the measurand depends, i.e. "function *f* should contain every quantity, including all corrections and correction factors, which can contribute a significant component of uncertainty to the result of the measurement" (JCGM 100:2008).

This part of the thesis aims to specify general methods for the calibration of rheometers and intent to cover the uncertainty budget of viscosity measurements performed by rotational methods. It should be noted that, the approach and the methodology here presented were applied to the determination of the uncertainty of the measurand studied in this work.

According to the International Vocabulary of Metrology (VIM) (JCGM 200:2012) a metrological traceability chain is described as a "sequence of measurement standards and calibrations that is used to relate a measurement result to a reference". In order to relate the measurement results obtained by viscosity sensors, specifically rotational rheometers, to the SI base units the following sequence of steps need to be accomplished: (1) calibration of the standard rotational rheometer traceable to the SI units; (2) use of CRM for viscosity (by tracing flow and viscosity curves); (3) calibration of a laboratory rheometer (each of the following parameters need to be calibrated independently: viscosity by using CRMs; shear rate (indirectly through rotational velocity) and shear stress (indirectly through torque); temperature; dimensions of the measuring geometries; measuring gap; etc.; (4) production of a reference material (RM) with specified viscosities by a standardized method and subsequent determination of its viscosities at specified shear rates by using the laboratory rheometer calibrated in step 3; (5) calibration of the viscosity sensors by using the RM from step 4. Uncertainty necessarily increases with every step in this sequence. Steps 1 and 2 would be carried out by NMI and the following steps 3-5 by the laboratory itself.

Input quantities are specific for a given measurement principle. Following are listed a few quantities which are considered significant when determining the viscosity of non-Newtonian liquids by using a rotational rheometer: torque; rotational speed; temperature (due to the drastic increase in uncertainty at high shear rates generate by the friction heating); dimensions (radiuses, lengths, angles, measuring gap); end effect correction (Highgate & Whorlow, 1969; Bauer & Boese, 1990; Kelessidis *et al.*, 2010; Wein *et al.*, 2015); mathematical model (choice of representative location, "narrow gap" approximation); measurement time (affects temperature via friction heating and laminar flow field establishment within the gap) (Giesekus & Langer, 1977); repeatability; reproducibility; sample shear history. Particles and wall slip are secondary considerations for CRM in comparison to the above. The above listed quantities are not only significant for the determination of the uncertainty of the viscosity of a CRM, but they also represent the parameters which must be controlled carefully when applying the CRM to the calibration of subsequent rheometers.

II.B.2.1 Calibration of Rheometers

As the purpose of use of a rotational rheometer is not always the same, the calibration method applied should fit the purpose. For this motive two calibrations method can be consider. A direct method, were all the measured input quantities, i.e. torque, angular velocity, temperature and dimensions of the measuring geometries are compared with reference values. And an indirect method where viscosity CRM are used to indirectly determinate the shear rate and shear stress measurement errors of a set composed by the measuring instrument (rotational viscometer or rheometer) and a measuring geometry (together with the temperature sensors). In order to obtain reliable viscosity results the steady state flow should be achieved in each measurement.

II.B.2.1.1 Direct method

The direct method for calibration of a rotational viscometer or a rheometer requires a separate calibration of the torque and of the angular velocity of the measuring geometry. Additionally, the dimensions (diameters and angles) of the measuring geometry and the temperature should also be calibrated by proper means. The direct method is described in standard documents such as DIN 53019-2 (2001); ASTM E2510-07 (2013) (for torque calibration) and ASTM E2509-14 (2014) (for temperature calibration).

II.B.2.1.2 Indirect method

The calibration of a rheometer by indirect method is described in the American standard ASTM E2975 (2016). The calibration procedure consists in determining the correction factor F for the selected measuring geometry in its whole viscosity range, by changing its rotational speed or its torque, thus in controlled rate (CR) and controlled stress (CS) modes by using a Newtonian CRM with a traceable viscosity value. The F factor is defined as the ratio between the viscosity value of the standard liquid (η_{std}) and the average of the viscometer readings (η_{rdg}) at the test temperature of 20 °C.

II.C

MEASUREMENT UNCERTAINTY

Measurement uncertainty includes components arising from systematic effects, such as components associated with corrections and the assigned quantity values of measurement standards, as well as the definitional uncertainty. Sometimes estimated systematic effects are not corrected for but, instead, associated measurement uncertainty components are incorporated (JCGM 200: 2012).

Measurement uncertainty comprises, in general, many components. Some of these may be evaluated by Type A evaluation of measurement uncertainty from the statistical distribution of the quantity values from series of measurements and can be characterized by standard deviations. The other components, which may be evaluated by Type B evaluation of measurement uncertainty, can also be characterized by standard deviations, evaluated from probability density functions based on experience or other information (JCGM 200: 2012).

In this work, the evaluation of measurement uncertainty followed the methods described in GUM (JCGM 100:2008). The method consists of the following steps: (1) expressing, in mathematical terms, the relationship between the measurand and its input quantities; (2) determining the expectation value of each input quantity; (3) determining the standard uncertainty, u of each input quantity; (4) determining the degree of freedom, ν for each input quantity; (5) determining all covariances, $\mathrm{cov}(x_{ij})$ between the input quantities; (6) calculating the expectation value for the measurand, Y; (7) calculating the sensitivity coefficient, $c_i\big(y(x_i)\big)$ of each input quantity; (8) calculating the combined standard uncertainty, $u_c(y)$ of the measurand; (9) calculating the effective degrees of freedom, ν_{ef} of the combined standard uncertainty; (10) choosing an appropriate coverage factor, k to achieve the required confidence level and (11) calculating the expanded uncertainty, U. It should be noted that for steps 6 to 11 suitable computer programs exist which can replace manual calculation. Step 1 is the most important part in the whole GUM procedure (JCGM 100: 2012).

The result of a test results from the function of a series of quantities. If we denote by Y the measurand and X_i the input quantities with i = 1, 2,...n, to which are associated a function, we obtain the following functional relation: $Y = f\,(X_1, X_2, X_3, \ldots, X_N)$.

In the evaluation of type A of uncertainties, these are estimated by means of statistical treatment (presupposes repeatability), that is, they are calculated from experimental work. The statistical treatment of the experimental work involves estimating the value of measurements standard deviation, *s*. The Eq. II.1 allows to calculate the standard deviation of n independent observations, where $\bar{x}$ corresponds to the arithmetic mean of the individually observed values x_j.

$$s = \sqrt{\frac{1}{n-1}\sum_{j=1}^{n}(x_j - \bar{x})^2} \qquad \text{(II.1)}$$

The standard uncertainty $u(x_i)$ is given by the experimental standard deviation of the mean through Eq. II.2.

$$u(x_i) = \frac{s}{\sqrt{n}} \qquad \text{(II.2)}$$

In the type B evaluation of measurement uncertainty, these are evaluated by scientific assessment, based on all available information on the possible variability of X_i. In this category belong values from previous measurement data, experience or general knowledge of the behavior, specifications of manufacturers, data from calibration and other certificates, uncertainties attributed to reference data from manuals, etc.

In the case of uncorrelated input quantities, the square of the standard uncertainty of the output quantity estimate, *y,* is given by Eq. II.3.

$$u^2(y) = \sum_{i=1}^{N} u_i^2(y) \qquad \text{(II.3)}$$

The quantity $u_i(y)$ (i = 1, 2, ... , n) is the contribution to the standard uncertainty associated with the estimate of output quantity y, which results from the standard uncertainty associated with the estimate of input quantity x_i.. The algorithm that defines it is as follows:

$$u_i(y) = c_i \cdot u(x_i) \qquad \text{(II.4)}$$

In this equation (Eq. II.4), c_i is the coefficient of sensitivity associated with the estimate of the input quantity x_i, ie, $c_i\big(y(x_i)\big) = \left(\frac{\partial y}{\partial x_i}\right)$.

The combined uncertainty $u_c(y)$ (Eq. II.5) is obtained through the error propagation equation, where all sources of uncertainty are combined in the standard uncertainty form, if the errors of the variables x_1, x_2, … x_n are completely independent of each other.

$$u_i(y(x_1, \ldots, x_n)) = \sqrt{\sum_{i=1,n}\left(\frac{\partial y}{\partial x_i}\right)_i^2 u(x_i)^2 + 2\sum_{i=1,n-1}\sum_{j=i+1,n}\left(\left(\frac{\partial y}{\partial x_i}\right)\left(\frac{\partial y}{\partial x_j}\right) \times cov(x_{ij})\right)} \qquad \text{(II.5)}$$

In this equation x_i (i = 1, ..., n) refers to the contributions that affect the measurement result, whereas $u(x_i)$ is the uncertainty of parameter i and $\mathrm{cov}(x_{ij})$ is the covariance between x_i and x_j. Considering that all parameters that contribute to the measurement result are independent, the covariance term is zero.

The combined uncertainty, $u_c(y)$, is estimated from the various standard uncertainties $u_i(y)$ that contributed to it by the square root of the sum of the squares of each of them (root of the quadratic sum).

For the determination of the combined standard uncertainty of the mensurand, $u_c(\ldots)$, the value of the square root of the variance, $u_c^2(x)$, of the influence quantities is estimated. For this purpose, it is considered that there is no correlation between the variables, and the equation of propagation of the errors can be used:

In a simplified form, the combined uncertainty $u_c^2(y)$ is estimated according to the Eq. II.6.

$$u_c^2(y) = \sum_{1}^{n} \frac{\delta z}{\delta y_i}(y_1) \tag{II.6}$$

In which $u_c^2(y)$ represents the standard uncertainty of the measurand y_1 and $\frac{\delta z}{\delta y_i}$ are the sensitivity coefficients that are derived from the calculation algorithm. The number of effective degrees of freedom was calculated using the Welch-Satherwaite formula (Eq. II.7).

$$\nu_{ef} = \frac{u^4(y)}{\sum_{i=1}^{N} \frac{u_i{}^4(y)}{\nu_i}} \qquad \text{where} \qquad u_i(y)\ (i = 1, 2, \ldots, N) \tag{II.7}$$

The calculation of the expanded uncertainty, U, gives us a confidence interval where the true value of the measurement is expected. The expanded uncertainty is obtained by multiplying the value of the combined uncertainty, $u_c(y)$, by an expansion factor, k, considering a normal distribution (Eq. II.8).

$$U = k \cdot u_c(y) \tag{II.8}$$

At the end of the uncertainty estimation, the measurement result is expressed as:

$$Y = y \pm U \tag{II.9}$$

II.C.1 UNCERTAINTY BUDGET OF RHEOMETERS' CALIBRATION

II.C.1.1 Direct method calibration

Taking the determination of viscosity by a rotational rheometer with a concentric cylinder system as an example and knowing that the definition equation of dynamic viscosity is given by Eq. II.10.

$$\eta = \frac{\tau}{\dot{\gamma}} \tag{II.10}$$

Where η is viscosity, τ is the shear stress and $\dot{\gamma}$ is the shear rate the viscosity is given by Eq. II.11.

$$\eta = \frac{M\left[\left(\frac{R_a}{R_i}\right)^2 - 1\right]}{8\pi^2 nLR_i^2 c_L \left(\frac{R_a}{R_i}\right)^2}\left[1 - \beta_T(T - T_{ref})\right] \tag{II.11}$$

Where M is torque, R_a is the outer radius of the gap, R_i is the inner radius of the gap, n is the number of rotations per time unit, L is the length of the cylinder mantle, c_L is the end effect correction factor, β_T is the linear coefficient of change of viscosity with temperature, T is measurement temperature and T_{ref} is reference temperature.

The analysis of a measurement of a Newtonian oil, at 20 ºC, using a rheometer with a concentric cylinder system, according to DIN 53019, at a shear rate of 1 s^{-1}, considering the input quantities described in Table II.1, resulted in a viscosity of 1,091 Pa·s with an expanded uncertainty of 0,018 Pa s. This uncertainty budget showed that roughly 40 % of the uncertainty originates from the end effect correction factor, 36 % from torque, 17 % from temperature stability and 7 % from R_a (Table II.1). These numbers can change drastically by varying measurement conditions. At lower shear rates, for example, the measured torque will be smaller, but its absolute uncertainty is constant which increases its share in the uncertainty of the viscosity. On the other hand, at higher shear rates the temperature stability becomes questionable due to friction heating. Consequently, the uncertainty of the viscosity will increase drastically and be dominated by temperature uncertainty.

Table II.1 Example of an uncertainty budget of the measurement of a Newtonian oil using a rheometer with a concentric cylinder system according to DIN 53019 with the following input quantities (and t = 20 °C).

Quantity	Symbol	Value	u (k = 1)	Distribution	Relative contribution for u
Torque	M	$5{,}7938\cdot10^{-5}$ Nm	$2{,}89\cdot10^{-7}$ Nm	rectangular	35,9 %
number of rotations per time unit	n	0,0128985 s^{-1}	$5{,}00\cdot10^{-7}$ s^{-1}	normal	-
Outer radius of the gap	R_a	0,014458 m	$2{,}89\cdot10^{-6}$ m	rectangular	7,4 %
Inner radius of the gap	R_i	0,0133295 m	$2{,}89\cdot10^{-7}$ m	rectangular	0,1 %
Length of the cylinder mantle	L	0,040009 m	$2{,}89\cdot10^{-7}$ m	rectangular	-
End effect correction factor	c_L	1,1	$5{,}77\cdot10^{-3}$	rectangular	39,8 %
Measurement temperature	T	20 °C	$5\cdot10^{-2}$ K	normal	16,8 %
Linear coefficient of change of viscosity with temperature	β_T	0,0683 K^{-1}	$5{,}77\cdot10^{-5}$ K^{-1}	rectangular	-

This example does by far not cover all input quantities but is a first approach to give an impression of the complexity at which one soon arrives. Additionally, it demonstrates that uncertainty estimation needs to be backed by real measurements.

II.C.1.2 Indirect method calibration

As described in the ASTM E2975 standard, the uncertainty of the correction factor, $u(F)$, was calculated by the sum of squares of the standard deviation of the experimental viscosities and the standard viscosity uncertainty $u(\eta_{rdg})$. The F values were used to correct the shear rate in CS mode and the shear stress in CR mode. For more details this standard should be consulted.

II.D

LIQUIDS' DENSITY METROLOGY AT IPQ

The Portuguese Institute for Quality (IPQ), in Portuguese *Instituto Português da Qualidade*) is the national organization that manages and promotes the development of the Portuguese Quality System, the legal framework for matters of quality in Portugal, which includes the Metrology Subsystem. The mission of IPQ's National Metrology Laboratory (LNM, in Portuguese *Laboratório Nacional de Metrologia*) is to ensure the accuracy and the traceability of the measurements performed in Portugal and the metrological control of measuring instruments satisfying Portuguese industrial and societal needs. IPQ is responsible for national measurement standards, for the traceability of Portuguese reference standards, for technical support to legal metrology activities, for the realization of national calibration laboratories comparisons and for participation in relevant international comparisons.

One of the LNM's metrological domains is the Laboratory of Properties of Liquids (LPL) that is responsible for the development, and maintenance of the national standards of liquids density, viscosity, viscoelasticity and surface tension, handling to: participate and coordinate interlaboratory comparisons, perform measurement audits, develop new measurement methods (for these quantities), conduct training activities in metrology field of liquids' properties and participate in national and international projects of development and research. LPL is also in endorsed to calibrate the measuring instruments of these quantities, such as hydrometers and oscillation-type density meters, for density; capillary viscometers and Stabinger's viscometers for viscosity; rotational viscometers and rheometers, for viscoelasticity; and tensiometers, for surface tension.

The next sub-chapters aimed to describe the work performed, by the author, to implement and develop density measurement methodologies at LPL/IPQ, finalizing by presenting the ongoing joint efforts to develop liquid's density metrology in Europe.

II.D.1 PRIMARY METHOD: HYDROSTATIC WEIGHING

In 2005, a hydrostatic weighing apparatus was implemented at IPQ by the *Istituto Nazionale di Ricerca Metrologica* (INRIM, the Italian NMI). At that time, the apparatus was constituted with a set of equipment, as described in Table II.4, and assembled as can be seen in Fig. II.4: a balance (Mettler Toledo, AT400 with a resolution of 0,1 mg), equipped to weigh a suspended load underneath; a sinker of known mass and volume (a silicon sphere); suspension copper wire (with a diameter of 0,15 mm) and holders; mechanism to load and unload the sinker inside the test liquid; a set of mass standard (of stainless non-magnetic steel and of OIML class E1); instruments to measure ambient conditions (pressure, temperature and relative humidity) for correction of the air buoyance effect (Barometer Druck, DP1 141 and a thermo-hygrometer Rotronic, HW4); a 100 ohm platinum resistance thermometer to measure the temperature of the tested liquid (connected to a measuring unit F250 RH from Automatic Systems Laboratory); and a 70 litre water bath (TAMSON, TV 7000) cooled/heated by water delivered from another water bath (LAUDA, RE 104).

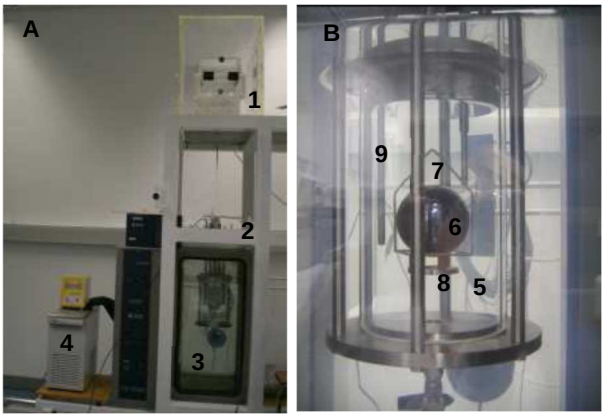

Figure II.4 First implemented IPQ's hydrostatic weighing apparatus (A) for density of liquids used from 2005-2011. Legend: 1- balance (Mettler Toledo, AT400); 2- lifting device; 3.-70 L regulated water bath (Tamson, TV70); 4- 10 L regulated water bath (Lauda, RE104); (B) measuring vessel: 5- liquid sample; 6- sinker (~233 g silicon sphere); 7- suspension; 8- loading device; 9- 100 ohm Platinum resistance thermometer (F250 RH, ASL).

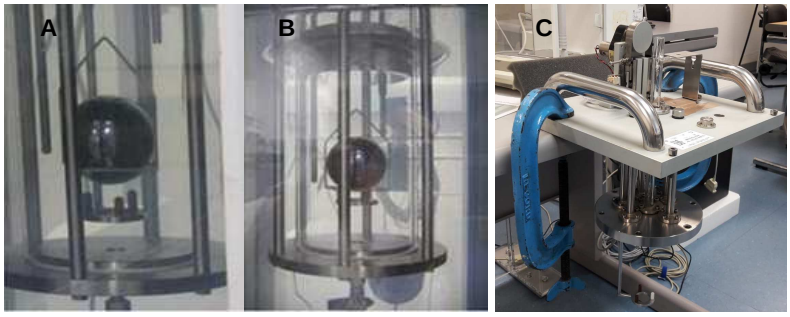

Figure II.5 First IPQ's measuring vessel filled with the liquid sample during the weighing of the sinker (A) and then during the weighing of the suspension (B); and lifting device (C).

In this apparatus, the liquid sample and the silicon sphere was contained in a sealed borosilicate cell (Fig. II.4-B). During weighing, the sphere rests on a suspension connected to a balance (Fig. II.4-A.1). The silicon sphere is raised from its suspension (Fig. II.4-B.7) by means of a support (Fig. II.4-B.8) connected to a driving motor (Fig. II.5-C) controlled by a LabView developed program. In order to maintain the liquid sample temperature, the measuring cell was completely immersed in a thermostatic unit (Fig. II.4-A.3). During measurements, the balance reading of the silicon sphere on the suspension

(Fig. II.5-A) and the balance reading of the suspension were alternately determined (Fig. II.5-B). The apparatus was automated though electronic controls and a software designed for running the weighing and acquiring the data from the balance.

Table II.2 Metrological features of the measuring instruments used by LPL in the hydrostatic weighing apparatus from 2005-2011.

Measuring instruments (Brand, Model)	Resolution	U calibration (k =2)
Balance (Mettler Toledo, AT400)	0,1 mg	1,2 mg
Barometer (Druck, DPI 141)	0,01 hPa	0,04 hPa
Thermo-hygrometer (Rotronic, HW4)	0,01 ºC	0,10 ºC
	0,01 %	0,88 %
Temperature sensor PRT 100 (ASL, F250 RH)	0,001 ºC	0,014 ºC

The weighing procedure was, and still is, performed in a set of ten of the following weighing sequence: (1) empty suspension (5x); (2) set of mass standards related to the empty suspension (5x); (3) empty suspension (5x); (4) silicon sphere (5x); (5) empty suspension (5x); (6) set of mass standards related to the empty suspension (5x); (7) empty suspension (5x).

The liquid temperature and the environmental conditions (pressure, temperature and relative humidity) are measured and the entire procedure is recorded. One weighing set takes approximately one hour and half to be completed.

II.D.1.1 Participation in International Comparisons

As previously mentioned, to maintain the national primary standards it is necessary to intercompare them periodically. For this reason, LPL/IPQ participated in several international comparisons, with peers NMI, to establish the degree of equivalence of density measurements performed with the primary method.

II.D.1.1.1 EURAMET Project 858

In 2008, a bilateral comparison has been carried out between the INRIM (the Italian NMI) and IPQ, in the framework of the EURAMET Project 858 “Hydrostatic weighing-exchange of experiences”. As, INRIM and IPQ were using similar hydrostatic weighing apparatus, the main purpose of this project was to promote the exchange of information regarding measurement procedures and uncertainty budgets, though the comparison of the density measurements results of two liquids (n-Nonane (99,7 %) and Trichloroethylene (95 %)) for the temperatures of 15 °C, 20 °C and 30 °C.

As example, the obtained values for the n-Nonane sample are given in Table II.3 and were assessed by means of the normalized error, En, statistical analysis (ISO 13528:2015).

Table II.3 Resume of the IPQ and INRIM results obtained for the n-Nonane sample on EURAMET Project 858.

t	IPQ		INRiM		$\lvert\rho_{IPQ} - \rho_{INRIM}\rvert$	En
	ρ_{IPQ}	U_{IPQ}	ρ_{INRIM}	U_{INRIM}		
(ºC)	(kg·m^{-3})	(kg·m^{-3})	(kg·m^{-3})	(kg·m^{-3})	(kg·m^{-3})	(1)
15	721,763	0,053	721,708	0,004	0,055	1,0
20	717,883	0,051	717,837	0,004	0,046	0,9
30	710,088	0,052	710,041	0,004	0,047	0,9

Legend: U – expanded uncertainty for a coverage factor k =2; En - normalized error (ISO 13528:2015).

IPQ obtained satisfactory results in this comparison, i.e. $En \leq 1$ meaning that the condition of Eq. II.12 was verified (Table II.3).

$$\left|\rho_{IPQ} - \rho_{INRIM}\right| \leq \sqrt{{U_{IPQ}}^2 + {U_{INRIM}}^2} \quad \text{(II.12)}$$

These results were used to pinpoint the major contributions of IPQ's uncertainty, that needed to be minimized, that included: the high uncertainty of the volume of the sinker (U_{V0} = 0,0066 cm³) obtained by the IPQ Laboratory of Mass, with a contribution of ~37 % for density uncertainty; the low repeatability of sphere's weighing results, likely related with the variation of meniscus formation in the suspension wire (also the contribution of this parameter was only estimated) and the low repeatability of the standards mass weighing, mainly coming from eccentricity effects, with a contribution of ~15 % for density uncertainty; and finally the uncertainty arising from temperature instability of the sample due to inefficient control of the thermoregulation systems. In addition, it was also suspected a possible contamination of the tested liquids with the water from the bath due to some gaps between the O-ring, glass cylinder and metallic structure of the measuring vessel.

II.D.1.1.2 EURAMET.M.D-K2 (Project 1019)

The aim of the EURAMET Project 1019 "Comparison of liquid density standards" was analogous to the Key Comparison CCM.D-K2 "Comparison of liquid density standards". The *Bundesamt für Eich- und Vermessungswesen - Physikalisch-technische Prüfdienst* (BEV-PTP, the Austria's NMI) organized this comparison, which was supported by the *Physikalisch-Technische Bundesanstalt* (PTB, the Germany's NMI). For the comparison, samples of n-pentadecane, water, tetrachloroethylene and an oil of high viscosity (EF 170) were measured in the temperature interval from 5 °C to 60 °C. The measurements have been carried out at atmospheric pressure by hydrostatic weighing of a solid density standard.

The resume of IPQ results on this project are given on Table II.4. Again, the results were assessed by means of the En statistical analysis, where if the condition of Eq. II.13 is verify, the results are considered satisfactory (ISO 13528:2015).

$$\left|\rho_{IPQ} - \rho_{ref}\right| \leq \sqrt{{U_{IPQ}}^2 + {U_{ref}}^2} \quad \text{(II.13)}$$

IPQ obtained satisfactory results, i.e. $En \leq 1$, for all samples tested except for the viscous oil (EF170) (Table II.4).

Table II.4 Resume of IPQ's results obtained on EURAMET Project 1019.

Sample	t (ºC)	ρ_{IPQ} (kg·m^{-3})	$U\rho_{IPQ}$ (kg·m^{-3})	ρ_{IPQ}-ρ_{ref} (kg·m^{-3})	$U(\rho_{IPQ}$-$\rho_{ref})$ (kg·m^{-3})	$U\rho_{ref}$ (kg·m^{-3})	En (1)
Water	20	998,489	0,034	-0,030	0,035	0,0040	0,9
n-Pentadecane	20	768,856	0,084	0,066	0,084	0,0033	0,8
n-Pentadecane	15	772,373	0,248	0,081	0,248	0,0047	0,3
Tetrachloroethylene	20	1622,723	0,065	0,047	0,0664	0,0142	0,7
Oil (EF 170)	20	831,729	0,037	-0,216	0,0376	0,0071	5,8

Legend: U – expanded uncertainty for a coverage factor k =2; En - normalized error (ISO 13528:2015).

Like in EURAMET Project 858, the same was observed in terms of major contributions for the uncertainty of density measurement values obtained by IPQ (Table II.5). The major contributors for the uncertainty value were the volume of the sinker (with ~47 %) and the experimental standard deviations mainly due to the low reproducibility of liquid meniscus formation between the suspension wire and the surface of the test liquid and the eccentricity effect during weighing.

Table II.5 Uncertainty budget of IPQ's results for water at 20 ºC obtained on EURAMET project 1019 (Comparison of liquid density standards).

Influence quantity	U'_ρ (%)
Mass of sinker	0,92%
Volume of sinker at its reference temperature	47,02%
Thermal expansion of sinker volume	0,00%
(Isothermal) compressibility of sinker	0,02%
Mass of weights	0,10%
Volume of weights	0,00%
Meniscus mass difference	0,46%
Temperature of liquid at sinker	1,22%
Cubic thermal expansion coefficient of liquid	5,04%
Isothermal compressibility of liquid	0,01%
Balance indication difference with/without sinker	0,00%
Density of air	0,17%
Pressure in liquid at sinker	0,01%
Height difference of weights and sinker	0,00%
Gradient of gravitational acceleration	0,00%
Method	8,88%
Density of weights	0,00%
Mean density and experimental standard deviation	13,35%

II.D.1.2 Apparatus' improvements after comparisons

IPQ's results from EURAMET Projects 858 and 1019 clearly demonstrated that IPQ's apparatus was requiring improvements. So, the laboratory had invested in the following equipment: a new regulated bath for replacement able to achieve a temperature stability, Δt, of $\pm$ 0,02 ºC (Tamson, TV7000LT) against the Δt ±0,5 ºC at 20 ºC and Δt ±1 ºC at 15 ºC of the former set of baths; calibration of silicon sphere's volume with lower uncertainty by calibration at PTB with an uncertainty value of U_{V0} =2,5 10^{-4} cm^3 (k =2) against the former value of U_{V0} = 6,6 10^{-3} cm^3 (k =2); acquisition of a new shaped measuring cell (Fig. II.D.6); replacement of the 0,15 mm diameter copper wire used by a 0,1 mm diameter hard stainless steel (ASI 302, Fe 78%/Cr 18 %/Ni 8 %, from Goodfellow), first to reduce the diameter and consequently the effect of the meniscus mass during the weighing, and secondly to use a non-reactive material with a reduce change of interact with the air and with the sample.

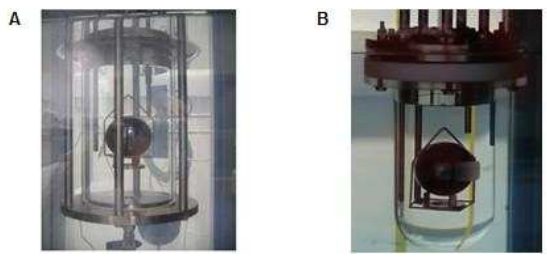

Figure II.6 IPQ's hydrostatic weighing vessels. (A) used in EURAMET Projects 858 and 1019; (B) actual measuring cell.

The actual IPQ's hydrostatic weighing apparatus can be seen in Fig. II.7 and the metrological features of the measuring instruments used in this apparatus are described in Table II.6.

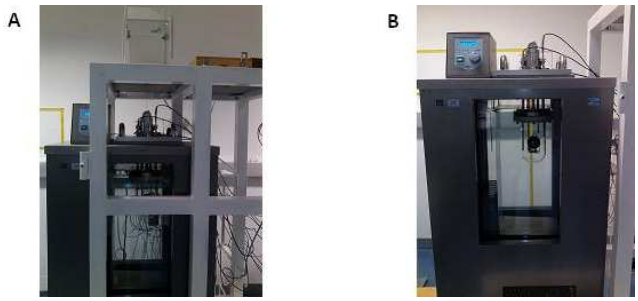

Figure II.7 Actual hydrostatic weighing apparatus at IPQ for density measurements of liquids; A: suspension connected to the balance; B: no balance connection.

Table II.6 Metrological features of the measuring instruments presently used in IPQ in hydrostatic weighing apparatus.

Quantity / Measuring instrument (Brand, Model)	Resolution / Measuring interval	Expanded uncertainty U
Mass m Balance (Mettler Toledo, AT400)	0,1 mg [0, 400] g	2,5 mg*
Mass m Set of mass standards OIML E1 or E2 (Stainless steel cylindrical shape) (Mettler Toledo)	[1, 200] g	E1 → 0,0033 mg to 0,033 mg E2 → 0,006 mg to 0,06 mg
Ambient pressure p, temperature t and relative humidity hr Thermo-hygrometer barometer (VAISALA, PTU303)	0,1 mbar [500, 1100] ºmbar	0,1 mbar* (including errors)
	0,1ºC [0, 60] ºC	≤ 0,17 ºC* (including errors)
	0,1% [0, 100] %	≤ 6,7%* (including errors)
Liquid temperature t 100 ohm PRT and measuring unit (Anton Paar, MKT50)	0,1 mK [0, 100] ºC (limited by the calibration range)	≤ 0,010ºC*
Silicon sphere	$V_{20\,ºC,\,101325\,Pa}$:100,47314 cm^3 m_{real}: 234,01350 g	$U_{V20\,ºC,\,101325\,Pa}$:2,5 10^{-4} cm^3 U_{mreal}: 1,5 10^{-4} g

Legend: U - Expanded uncertainty (k =2) that includes U from calibration, resolution, short and long-term drifts.

II.D.2 SECONDARY METHOD: OSCILLATION-TYPE DENSITY METERS

The first steps with oscillation-type density meters at IPQ were done in 2003 with a DMA 60 and a DMA 602 from Anton Paar. But only on late 2006, already with a DMA 5000 model (Anton Paar) (whose main metrological features are described in Table II.7), the quest to understand in detail this instrument had begun.

Table II.7 Main metrological features of the IPQ's oscillation-type density meter.

Oscillation-type density meter	Density measurements	Temperature measurements
Anton Paar, DMA 5000	ρ interval: [0; 2 000] kg·m^{-3} ρ resolution: 0,001 kg·m^{-3} atmospheric p up to 10 bar	t interval: [0; 90] °C t resolution: 0,001 ºC

This density meter (used as 2nd level density measurement method) is (annually) calibrated in density, viscosity and temperature. This calibration is performed with a set of CRM for density produced by H&D Fitzgerald (an UK accredited laboratory), in the density interval from 690 to 1615 kg m^{-3}, in the temperature interval from 10 to 50 °C, and in the dynamic viscosity interval of from 1 to 800 mPa s. In addition, CRM from other producers (from the National Institute of Standards and Technology (NIST, the North American NMI) and from the *Glowny Urzad Miar* (GUM, the Polish NMI)) are also used for quality control of density measurement results.

The temperature indication of DMA 5000 is calibrated by comparison with a 100 ohm PRT (MKT50, Anton Paar) and this related with the obtained density errors for the set of CRM dependence with temperature. Despite the last be an indirect method to infer about temperature indication errors, it has been proofed to be a more accurate approach to evaluate the real temperature error. This might be related with the fact that when inserting a PRT inside the measuring cell, first it is difficult to isolate the cell from the exterior and second the position of the PRT inside the measuring cell is not perfectly coincident with the position of the internal PRT.

With the data from the calibration, a calibration curve is performed and, after, used to correct density indication values. This curve is from main concern for viscous liquids.

A daily conformity check is performed before a set of density measurements, by measuring the density of an air sample, and comparing the indication value with the one given by the CIPM-2007 formula (Picard *et al.*, 2008, and a sample of ultra-pure water, and comparing the indication value with the one given in (Tanaka *et al.*, 2001). These two fluids (air and ultra-pure water) are also used to adjust and define the oscillator parameters. An adjustment of the oscillator with a high viscosity liquid is also necessary for accurate damping corrections due to viscosity.

The first IPQ steps in the metrology field of liquid density measure at high-pressure was done in the scope of the participation in the European Metrology Programme for Innovation and Research (EMPIR) Joint Research Project (JRP) 14IND06 pres2vac “Industrial standards in the intermediate pressure-to-vacuum range”, from 2015 to 2018[1]. A special measuring setup was prepared for this purpose as can be seen in Fig. II.8. This comprises an oscillation-type density meter for high pressure density measurements (DMA HP, Anton Paar) (A in Fig. II.8) connected to a regular density meter (DMA 5000, Anton Paar) for data processing (B in Fig. II.8). The pressure inside the system is generated by using

[1] Related publication: Ehlers, S., Könemann, J., Ott, O., Wolf, H., Šetina, J., Furtado, A., & Sabuga, W. (2019). Selection and characterization of liquids for a low pressure interferometric liquid column manometer. *Measurement*, 132, 191-198. https://doi.org/10.1016/j.measurement.2018.09.017

nitrogen gas with a purity of 99,99 % (C in Fig. II.8). The internal pressure of the system is measured with a pressure gauge IPI300 from Ametek JOFRA (D in Fig. II.8). A membrane degasser (Degasi GPC from Biotech) (E in Fig. II.8) was used to degas the candidate liquids under test.

Figure II.8 IPQ's setup assembled to measure fluids' density for pressures up to 10 bar. Legend: oscillation-type density meters from Anton Paar: A – DMA 5000 (for density measurements at atmospheric pressure); B – DMA HP (for density measurements up to 600 bar); C – pressure generator – nitrogen gas cylinder; D – pressure gauge (IPI300 from Ametek JOFRA); E – membrane degasser (Degasi GPC from, Biotech).

The expanded uncertainty of density measurements using this apparatus is commonly around U_ρ = 0,14 kg·m^{-3} (k =2) and the expanded uncertainty of pressure measurements of around U_p = 0,012 bar (k =2) (Table II.8).

The high-pressure density measurement cell is calibrated in density, with ultra-pure degassed water, at 20 ºC, in the pressure interval from atmospheric pressure up to 10 bar. The relative error of DMA HP density indication dependency with pressure, measured in the outlet with a pressure sensor IPI300, Ametek JOFRA, was obtained by using, as reference values, the CIPM formulation (Tanaka *et al.*, 2001) for water density. In order to validate the results obtained with the high-pressure density apparatus under test, the correlation equation for n-Nonane, at 20 °C, described by Schilling *et al*. (2008) was used.

Table II.8 Main features of the actual IPQ's setup to measure liquids' density at high-pressure.

Oscillation-type density meter	Density measurements	Temperature measurements	Pressure measurements	High pressure generator apparatus
Anton Paar, DMA HP	ρ: [0; 3 000] kg·m^{-3} ρ resolution: 0,01 kg·m^{-3} p: [1, 700] bar	t interval: [-10; 200] °C t resolution: 0,01 °C	IPI300, Ametek JOFRA p: [0, 21] bar U_p (k =2): 0,12 %	Nitrogen (purity of 99,99 %) 1/8" O.D. inox tubes (Swagelok) and ball valves (Swagelok)

II.D.2.1 Participation in International Comparisons

The establishment of the degree of equivalence of the density measurements performed with the national secondary standards for density, i.e. by density meters of oscillation type, may be performed by means of comparison with primary standards for density (by using liquid CRM whose density was determined in the hydrostatic weighing apparatus), or alternatively, by means of international comparisons with peers NMI., depending on the goal of the laboratory.

II.D.2.1.1 Tri-Lateral DMA Comparison

In this "informal" comparison, *Van Swinden Laboratory* (VSL, the Dutch NMI) provided the 3 reference liquids (double distilled de-mineralised water, n-heptane (biotech grade solvent, 99 %) and vitrea oil 10 (Shell)) and PTB acted as the pilot laboratory. The reference liquids were tested at the temperatures of 15 ºC, 20 ºC, 40 ºC and 60 ºC.

In general terms, the obtained results were compatible for the low viscosity samples (i.e., water and n-heptane). However, the results obtained for the vitrea oil 10, especially at lower temperatures, were not concordant. It was clear at the time that the internal adjustment of the density meters for high viscosity liquids was not properly done and that the calibration curve used by these NMI to correct the density indication was not accurate for viscous liquids.

Even if was not possible to conclude about the degree of equivalence of these density measurements, this exercise was an opportunity to confirm that further work needed to be done to harmonize this methodology.

II.D.2.1.2 EURAMET Project 1214

A follow-up comparison was agreed to investigate the discrepancy and to provide preparatory information for the EURAMET supplementary density comparison (using the same devices). The EURAMET Project 1214 "Density measurement of viscous oils (using vibrating tube density meters)" aimed to establish the level of equivalence regarding the density correction of viscous oils and to gain insight into the various methods used for the calibration of oscillation tube density meters. In this, NPL (National Physical Laboratory, the UK's NMI) was the pilot, counting with the participation of: VSL (density), IPQ, VSL (flow), Mettler-Toledo and H&D Fitzgerald.

The density of three increasingly viscous oils (vitrea 10, vitrea 100 and vitrea 220) was measured at temperatures of 10 °C, 20 °C, 40 °C and 70 °C. Reference values were calculated for each oil, at each measurement temperature by least squares analysis of the (consistent) measurement results considering the uncertainties of the measured values.

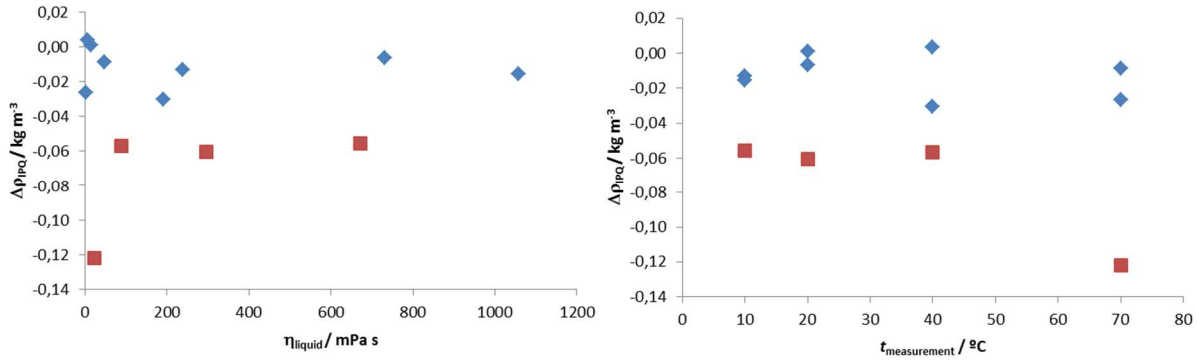

Figure II.9 Resume of IPQ's results in the EURAMET Project 1214. Legend: IPQ density deviation from the reference value ($\Delta\rho_{IPQ}$ in kg m^{-3}) against the dynamic viscosity of the liquid (η_{liquid} in mPa s) (A) and against measurement temperature ($t_{measurement}$ in ºC) (B). IPQ measurement uncertainty, $U\rho_{IPQ}$, was 0,03 kg·m^{-3}. Blue diamonds represent the values within the $U\rho_{IPQ}$ and the red squares represent $\Delta\rho_{IPQ} > U\rho_{IPQ}$.

Fig. II.9 shows the resume of IPQ's results. For IPQ the obtained measurement uncertainty, $U\rho_{IPQ}$, was 0,03 kg·m^{-3}. Satisfactory results were obtained for vitrea 10 and vitrea 200 samples, i.e. $\Delta\rho_{IPQ} \leq U\rho_{IPQ}$ (represented by the blue diamonds in both graphs of Fig. II.9). Also, for IPQ no relation was found

between the viscosity of the liquids (η_{liquid}, represented on the left-hand side graph of Fig. II.9) or against temperature ($t_{measurement}$, represented on the right-hand side graph of Fig. II.9). The red squares represent IPQ's results for vitrea 100, that were non-satisfactory, i.e. $\Delta\rho_{IPQ\ Vitrea\ 100} > U\rho_{IPQ}$. At that time IPQ associated this deviation with the CRM (used to correct the viscosity damping effect. As result, IPQ needed to perform further investigations on these deviations.

In general terms, the results of this comparison showed a reasonable level of equivalence between the participants and the results allowed the participants to investigate individual discrepancies in the results. The results of the participants have been assumed to be uncorrelated. However, some correlation would be expected because; the same model of density meter has been used by five of the six participants; the same method has been used to characterize the meter and apply viscosity dependent correction by four of the participants and there was some common traceability for CRMs (from H&D Fitzgerald) between four of the six participants.

This comparison led to an important conclusion: in future comparisons the assignment of the reference values to the transfer standard densities needed to be carefully considered. Ideally the transfer standard liquids should be characterized using a fundamental density determination technique (e.g. hydrostatic weighing) to avoid correlation effects between participants' measurements influencing the calculated reference value.

II.D.2.1.3 EURAMET Project 1240

The aim of this comparison, entitled EURAMET Project 1240 "Density determinations of liquid samples by density meters" was to investigate, eliminate and to pinpoint discrepancies between the frequently used density meters by NMIs and the density determination by hydrostatic weighing of standards, used as a national standard. Furthermore, to establish an "official" link between the density determination by the hydrostatic weighing and the density meters.

This project supposed to support the discussion about the criteria of the acceptability of density meters in metrological affairs. The participants determined the density of 3 different liquid samples (in the density interval from 760 to 1 000 kg·m^{-3}) at 3 different temperatures (15 °C, 20 ºC and 40 °C). BEV-PTP was the pilot of this project; supported by MKEH (the Hungary's NMI, now renamed as Government Office of the Capital City Budapest, BFKH). BEV and MKEH established the link to the hydrostatic weighing registered as EURAMET project 1019 "Comparison of liquid density standards" registered in the KCDB: EURAMET.M.D-K2.

The IPQ's results were satisfactory for all the samples, as one can see in Table II.9. With these results IPQ was able to conclude about the validity of the calibration curve used to correct the indication of the density meter, mainly for the viscous sample. It was also seen that IPQ was overestimating the measurement uncertainty.

Table II.9 Resume of the IPQ's results obtained in EURAMET Project 1240.

Sample / t	Viscosity	Density					
		$\rho_{ref.}$	$U\rho_{ref}$	ρ_{IPQ}	$U\rho_{IPQ}$	ρ_{IPQ}-$\rho_{ref.}$	En
(ºC)	(mPa s)	(kg·m^{-3})	(kg·m^{-3})	(kg·m^{-3})	(kg·m^{-3})	(kg·m^{-3})	(1)
Water / 20 °C	1	998,4713	0,0037	998,473	0,022	0,002	0,08
Pentadecane / 20 °C	2,85	768,8099	0,0033	768,822	0,035	0,012	0,34
Pentadecane / 15 °C	3,21	772,3103	0,0040	772,315	0,035	0,005	0,13
Pentadecane / 40 °C	1,89	754,8354	0,0031	754,839	0,035	0,004	0,10
Oil / 20 °C	144	831,9427	0,0056	831,925	0,032	-0,018	0,54

Legend: U – expanded uncertainty for a coverage factor k=2; En - normalized error (ISO 13528:2015).

II.D.2.1.4 Next scheduled comparisons: Key comparison CCM.D-K5

The next scheduled comparison is a key comparison CCM.D-K5 "Comparison on density determination of liquid samples using oscillation-type density meters" with the aim of compare the results of the density determinations of liquid samples by oscillation-type density meters of the participating laboratories. The BEV-PTP is going to be the Pilot Laboratory and will be supported by the MKEH. The comparison will be a CIPM key comparison according to the Mutual Recognition Arrangement (MRA).

In this comparison, samples of dodecane, perfluoro-compound C10HF22N (Fluorinert FC-40), and of oil with a high viscosity will be measured. The temperature range is going to be from 15 °C to 40 °C. The measurements will be carried out at atmospheric pressure by using oscillation-type density meter. The reference values for the comparison liquids will be determined by the hydrostatic method (BEV, MKEH). There will be 14 participants including IPQ.

The goal of IPQ participation in CCM.D-K5 will be to extend the density range and to decrease the uncertainty: from [770; 1000] kg·m^{-3} with $U\rho$ (k=2): [0,010; 0,020] kg·m^{-3} (EURAMET Project 1240) to [600; 1900] kg·m^{-3} with $U\rho$ (k=2): [0,005; 0,010] kg·m^{-3}, in the same temperature interval ([15, 40] ºC) at atmospheric pressure.

II.D.3 ROADMAPS FOR NEXT DEVELOPMENTS IN LIQUIDS' DENSITY METROLOGY

In Europe, only four NMI (BEV-PTP, GUM, MKEH, and PTB) currently possess the appropriate expertise to perform liquid density measurements at primary-level, i.e. with hydrostatic weighing apparatuses with a level of accuracy and uncertainty that meets national (e.g. to fulfil national laws) and international (e.g. to fulfil European Directives and standards) needs. As consequence the national's traceability chains of liquid density measurements, down to the second and third levels, which are used in industry and in research laboratories, are often compromised in less experienced European countries. For these reasons, emerging countries are keen to prepare their markets, for integration into the EU single market, by harmonizing their national legislation in order to the meet the standards set out in EU directives.

In addition, there is also a lack of EURAMET guides on liquid density measurements and existing international standards (ISO 15212-1:1998, ISO 15212-2: 2002) and the reference documents used in Legal Metrology (OIML G14: 2011, WELMEC Guide 6.4) are outdated and incomplete.

II.D.3.1 Establishing traceability for liquid density measurements in Europe: 17RPT02-rhoLiq a new EMPIR joint research project

In order to bridge this gap in the scientific knowledge in liquid's density metrology, a 3 years duration project, the 17RPT02-*rho*Liq[2] "Establishing traceability for liquids density measurements", with a total budget of 0,5 M€, counting with a Consortium composed by 11 NMI: IPQ (Portugal, as project coordinator), BEV-PTP (Austria), BRML (Romania), CMI (Czech Republic), DMDM (Serbia), GUM (Poland), IMBiH (Bosnia and Herzegovina), JV (Norway), PTB (Germany), TUBITAK (Turkey), INM (Moldova) and one density meters manufacturer Anton Paar (Austria) has started May 2018. This JRP belongs to EMPIR developed as an integrated part of Horizon 2020, the EU Framework Programme for Research and Innovation.

One of the focus of this project is to promote the development of high-level measurements and calibration services, and the production of density reference materials to fulfill the needs of the national stakeholders, e.g. from food, chemical, pharmaceutical and petroleum industries. The international recognition of these NMI in this metrological field will indirectly lead to the reinforcement of mutual confidence and cooperation at regional and international levels.

This project will facilitate compliance with economically relevant EU Directives, and it will further reinforce the competitiveness of production industries. These NMI will be able to develop strategies for accurately measuring the density of liquids with non-classical physical and mechanical properties, i.e. with physical properties that differ from water or hydrocarbons which are normally used as standard liquids. This will include a joint effort to perform robustness studies using liquids with high viscosities, with viscoelastic behavior, including liquids with dissolved gases or suspended particles. These kinds of liquids are the most commonly measured by the end-users, therefore, the knowledge gained about possible interferences and corrections, will be crucial to obtain accurate and traceable density

[2] The EMPIR project "17RPT02-rhoLiq" is carried out with funding of European Union under the EMPIR. The EMPIR is jointly funded by the EMPIR participating countries within EURAMET and the European Union. More information about this project can be found in the official website: www.rholiq.org

Furtado, A., Pereira, J., Schiebl, M., Mares, G., Popa, G., Bartos, P., ... & Neuvonen, P. (2018). Establishing traceability for liquid density measurements in Europe: 17RPT02-rhoLiq a new EMPIR joint research project. *Journal of Physics: Conference Series* (Vol. 1065, No. 8, p. 082013). IOP Publishing. doi:10.1088/1742-6596/1065/8/082013

measurement results. These kinds of measurements can be performed under limited conditions and will often result in larger uncertainties.

The knowledge gained in this project will be disseminated in international guides and standards for scientific, applied, and legal documents, via creation of new EURAMET guides, by revision of existing ISO standards, and of OIML and WELMEC guides, addressing in this way, the issue concerning the lack of adequate reference documentation on this field of metrology.

III

METROLOGICAL ASSESSMENT OF OSCILLATION-TYPE DENSITY METERS

Many thousands of liquids' density measurements are made worldwide every day. Among others physical properties of a substance is density, which can be used to inquire about others physical and chemical properties by means, for example, of its derived mechanical coefficients, isothermal compressibility coefficient or the thermal expansion coefficient. For liquids it is usually interpreted using equations of state (EOS) of state representative of liquid state. Furthermore, the importance of density goes beyond the strictly scientific domain to assume a useful economic function: it is, for example, one of the factors considered in calculations performed to optimize the conditions of exploitation and commercial distribution of petroleum products (Lagourette *et al.*,1992).

As described in previous chapters, density of a fluid can be determined by means of several types of measurement methods. From one point of view, these can be divided as *static* and *dynamic* methods. Normally, the *static* methods, as the hydrostatic weighing or the hydrometry, can produce density measurement results with a lower uncertainty and higher accuracy, when compare it the one obtained by *dynamic* methods (Webster, & Eren, 2016). One of the reasons for this difference, may be related with the fact that whenever a strain (e.g. the flow in on-line sensors, or the oscillation in a density meter) is applied to a fluid, physical (e.g. viscosity), chemical (e.g. pH and solubility of gases in a fluid) and mechanical (e.g. elasticity) changes may happen, causing possible measurement errors. In general, *static*-type density measurements are employed in laboratory conditions, and *dynamic* methods are employed in real-time measurements where the properties of a fluid can vary from time to time (Webster, & Eren, 2016).

The research undergone in this third chapter was focused on a specific *dynamic* method, the oscillation-type density meter. First invented by Stabinger *et al.* (1967), are nowadays and ever since, used in, and for several applications. The principal advantages of these instruments are associated with their simple operationally, small volume of needed sample and especially to their wide range of density and temperature measurements, and more recently also pressure.

As described, although most oscillation-type density meters possess mechanism and algorithms to correct viscosity-caused damping these are still found insufficient to obtain accurate density values able to fit the purpose of their use. Additionally, only a few studies have been undertaken to assess the metrological robustness of this instruments when measuring viscoelastic samples and/or when measuring in high-pressure ranges (up to 650 bar). Thus, this research focused on assessing the metrological robustness of oscillation-tube density meters regarding viscosity, viscoelasticity and pressure (from atmospheric pressure up to 650 bar) aiming to establish appropriate and valid correction mechanisms and algorithms. Therefore, this work intended to provide the basis for the future development of procedures for the calibration and use of oscillation-type density meters, all aiming to ensure the traceability of the oscillation-type density meters measurements to SI.

III.1 OSCILLATION-TYPE DENSITY METERS

III.1.1 Measuring Principle

The measuring principle of an oscillation-type density meter is based on the law of harmonic oscillation (Stabinger, 1994). In short, in these instruments, the measuring cell, that will act like a flexural oscillator, is filled with the fluid sample and is subjected to an oscillating force. The measuring cell oscillates at its own fundamental frequency, which is a function of the mass of the system (under vacuum), M_0. Assuming that, the oscillator inner volume, V is unchangeable, the volume of sample, inside the cell will be therefore also constant, so the frequency, f (Eq. III.1) and period, τ (Eq. III.2) of the oscillation result in a function of sample's density, ρ, and of the oscillator spring constant (stiffness), k, as described by a mass-spring model.

$$f = \frac{1}{2\pi}\sqrt{\frac{k}{M_0 + \rho V}} \tag{III.1}$$

$$\tau = 2\pi\sqrt{\frac{M_0 + \rho V}{k}} \tag{III.2}$$

The fluid's viscous behaviour during the oscillation leads to a damping and by this to a lower resonance frequency of the measuring system. The sample's viscosity will also have the effect of apparently slightly move the oscillation nodes, thus increasing the apparent volume of the cell. To overcome this, some density meters were built perform induce the measurement cell to oscillate at additional higher harmonics, allowing the damping due to the sample to be measured and in some extent to be corrected. From these data, the density meter determines the not viscosity-corrected density value dnc and a viscosity-corrected density value d.

Most of these instruments, the density of the fluid, ρ is obtained by a second order empirical relation with the square of the (measured) oscillation period, τ, (Eq. III.3). This relation describes the oscillation of straight rod mounted to an infinite mass.

$$\rho(t,p) = A(t,p)\tau^2 - B(t,p) \tag{III.3}$$

Where A and B are instruments characteristics of the oscillator which are determined by calibration with fluids of known density (Eq. III.4-5).

$$A = \frac{k(t,p)}{4\pi^2 V(t,p)} \quad \text{(III.4)}$$

$$B = \frac{M_0}{V(t,p)} \quad \text{(III.5)}$$

Where k is the oscillator's stiffness, V is the inner volume of the oscillator and $M_0$is the mass of the evacuated oscillator, i.e. in low vacuum or more commonly filled with air. Both characteristics of the oscillator, k and V are strongly dependent of temperature, t and pressure, p.

Although A and B coefficients are physically meaningful parameters of the oscillator, they are usually evaluated by calibration with, at least two, fluid of known density (typically, air or vacuum and ultra-pure water), and if necessary, for the whole temperature t, and pressure p, ranges. However, different calibration methods have been described to calibrate this type of density meters in order to fit the purpose of its use (Lagourette *et al.*, 1992; Sousa, 1994; Fehlauer & Wolf, 2006; Outcalt & McLinden, 2007; Lampreia & de Castro, 2011; Lorefice & Sardi, 2012, Outcalt, 2018).

Despite Eq. III.3 represented a second order approximation to the actual behavior of a oscillation tube density meter containing a fluid; different types of mathematical models for both the calibration of the oscillators and the density calculations can be used, as can be found seen in (Lagourette *et al.*, 1992; Holcomb & Outcalt, 1998; Bouchot, & Richon, 2001).

Webster, & Eren (2016) described as major design problem of the oscillation tube method as the conflict of limiting the oscillation element to a finite length and fixing the nodes accurately. Additionally, special attention must to be paid to avoid any exchange of vibration energy outside the measuring cell. It was also identified as one limitation the fact that has not been feasible so far to transform it in an absolute instrument, due to the lack of a correct modelling of its working equations (Lampreia & Castro, 2011). It is therefore necessary to analyse the theoretical basis of this type of flexural oscillators, trying to understand the physical meaning of the calibration constants and find the means to improve their density measurement accuracy.

III.1.2 Functional Units

According to the standard ISO 15212-1 (1998), an oscillation-type density meter must be composed of the following functional units: (A) a density sensor capable of, either being filled with the sample, or of being immersed in it; (B) a device to excite and control sensor oscillation; (D) a device to determine and display the density and the oscillation frequency f or period τ; (E) a device to determine and display the sample temperature for which the measured density is valid; (F) a system to detect and display malfunctions and operator errors (Fig. III.10).The functional units (A) to (C) are designated as the oscillation system. In addition, oscillation-type density meters can incorporate the following functional units: (G) a unit for controlling the temperature of the sample and density sensor; (H) sampling devices; (I) sensor cleaning devices. All functional units (A) to (I) can be integrated into a single instrument or can be separate units.

Density sensors can be made of glass (e.g. borosilicate glass 3.3 in accordance with ISO 3585), metal, metal alloys (e.g. Hastelloy), or plastics, and can be designed as straight, U-formed (as can be seen in Fig. III.10) or omega-formed tubes. Other designs are tuning-forks, cylinders, bells or membranes. All these designs should in conformity with the functional principle in accordance to the previously described measuring principle (ISO 15212-1:1998). Resonant frequencies in the range of 300 Hz are found in glass oscillator and in the range of 5000 Hz in metal oscillators.

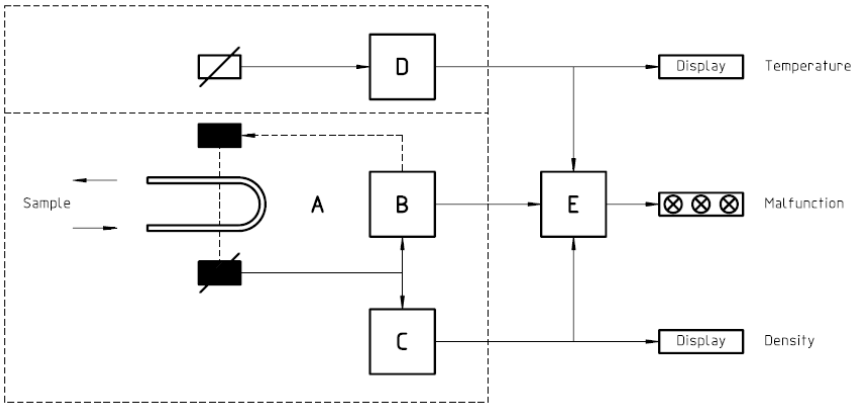

Figure III.10 Schematic representation of the functional units of an oscillation-type density meter (image from ISO 15212-1:1998). Legend: A - density sensor; B – excitation transmitter; C – signal evaluation; D – temperature measurement; E – functional monitoring.

In some constructions, a counter mass is linked to the measuring sensor to reduce parasitic resonances (i.e. external oscillations) from other components, e.g. electronic parts. It is commonly linked to the housing of the density meter by elastic supports and acts like a mechanical filter for external oscillations. The counter mass has a resonance frequency that lies far below the frequencies used for density measurement. The counter mass also ensures that the nodal points of the tube are constantly in position. The sample volume is set by the nodal points and therefore only the mass changes depending on the filled fluid while the volume remains stable (ISO 15212-1:1998). A counter mass is need if a Y-oscillator is used.

Some density meters, that possess a glass-made oscillator, also incorporate a built-in reference oscillator to eliminate, not only long-term drifts due to the aging effects of the material, but also temperature changes that influence the elasticity. A reference oscillator therefore makes it possible that only one single adjustment is needed to cover the whole temperature range and temperature scans of a sample can be performed (Fritz *et al.*, 2000).

In these instruments, the temperature regulation of the measuring cell is typically performed by means of Peltier elements.

III.1.3 Excitation and Evaluation of the Oscillation

The excitation of the oscillator can be either provided, mechanically, by a system of magnets and coils, or electrically, by Piezo-electric actuators (Fig. III.11). While magnets are comparatively inexpensive, the major drawback is that they put additional weight on the oscillating sensor, which has a negative influence on the achievable accuracy. The most precise method to excite a sensor is to use a Piezo element, a crystal or ceramic material that changes its dimension upon applied electrical voltage. However, this technology requires some safety measures in the electronic circuits as this requires high voltages.

After the oscillator excitation, optical pick-ups determine the period, τ of the oscillation (Fig. III.11). Optical pick-ups can detect a light beam that is interrupted by a minute coating on an oscillating glass sensor. Piezo elements can also be used to represent the period of oscillation if the usable effect of the element is inverted: A second Piezo element is then pressurized by the oscillator periodically and generates electric voltage that represents the period of oscillation very accurately. Magnets can be used to measure the period of oscillation as well. Whenever a magnet passes the coil, a little current is induced which can be evaluated.

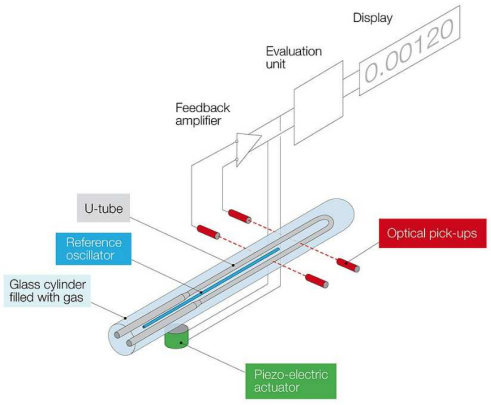

Figure III.11 Schematic representation of a commercial version of an oscillation-type density meter. (Note: in some density meters magnetic actuator are used instead of Piezo-electric) (image from Anton Paar®).

The processing of the oscillation pattern can be made analogically or by means of digital signal processors (DSP). Although analog processing of the oscillation pattern is affordable and less prone to errors, the precision is limited. Nowadays, digital signal processors (DSP) are state of the art and provide great advantages over the analog technology, even allowing the recognition of energy loss connected to sample viscosity. This is possible due to simultaneous determination of not only the characteristic frequency but also its first harmonic oscillation and the quality factor. Evaluation of the oscillation pattern is performed by keeping the measuring cell continuously oscillating at the characteristic frequency. By recording this constant oscillation not only the frequency of oscillation but also damping can be measured. In more recent density meters, is now used the pulsed excitation method, where the evaluation of the oscillation pattern of the oscillator includes an interruption of the characteristic frequency that leads to a natural fade-out of the oscillation. This procedure is repeated continuously and allows evaluation of the fade-out behaviour of the oscillation as well.

III.1.4 Mathematical Model

As described, the measurement principle of oscillation-type density meters is based on the change of the natural frequency of a hallow oscillator when filled with different fluids. So, Eq. III.3 can be derived considering a system represented by a hollow body mass M_0, under vacuum, and volume $V(t,p)$, filled with a sample of density $\rho(t,p)$, at temperature t and pressure p. This body would be suspended on a spring with a stiffness $k(t,p)$. The natural frequency f, of this system is then given by Eq. III.1.

The measurand density, $\rho(t_0,p_0)$ at target temperature, t_0 and pressure, p_0, results from the function of a series of input quantities, of which the functional equation can be found in Eq. III.6 and the mathematical relation can be found in Eq. III.7. To be noticed that this model does not include all the possible quantities of influence in density results, but only the more important ones.

$$\rho(t,p) = f(\tau, V, M_0, A, B, t, p, \alpha_{fluid}, \gamma_{fluid}, \alpha_{oscillator}, \gamma_{oscillator}, \varepsilon\tau, \varepsilon t, \varepsilon p, \varepsilon\eta, \varepsilon V, \varepsilon k, \varepsilon_{fluid}) \quad \text{(III.6)}$$

Where α_{fluid} is the cubic thermal expansion coefficient of the fluid; γ_{fluid} the isothermal compressibility coefficient of the fluid; $\alpha_{oscillator}$ the cubic thermal expansion coefficient of the oscillator; $\gamma_{oscillator}$ the isothermal compressibility coefficient of the oscillator; $\varepsilon\tau$ the deviation associate to an incorrect pickup and evaluation of the oscillation signal; εt the temperature-induced deviation, arising especially from position of the PRT that, due to constructions constraints, is not in direct contact with the sample); εp the pressure-induced deviation (sometimes caused by the use of high-volume syringes in closed measuring loops); $\varepsilon\eta$ the viscosity-induced deviation (from the sample); εV is the oscillator volume-induced deviation (from contamination and aging); εk the oscillator constants-induced deviation; and

finally ε_{fluid} the deviation coming of the unknown air saturation of the liquid. In this way, the potential sources of deviation can be easily grouped in the ones related with oscillator properties (for instance incorrect determination of A and B parameters due to incorrect calibration, or even due to the aging or contamination of the material, that will influence its elasticity); and with ones arising from the sample.

$$\rho(t_0, p_0) = \left[\left(\frac{k(t,p)}{4\pi^2 V(t,p)}\tau^2 - \frac{M_0}{V(t,p)}\right) - \alpha_{fluid}(t - t_0)\right]\left[1 + \gamma_{fluid}((p_0 - p)\right] + \varepsilon\tau + \varepsilon t + \varepsilon p + \varepsilon\eta + \varepsilon V + \varepsilon k + \varepsilon_{fluid} \quad \text{(III.7)}$$

III.1.5 Calibration and Adjustment[3]

Oscillation-type density meters are proven to be able to measure density of Newtonian fluids in a wide density, viscosity, and temperature ranges, with an uncertainty better than 0,010 kg·m^{-3} (Schmidt *et al.*, 2016) when using adequate calibration methods, as the substitution method. In earlier studies made using several instruments of the same type (DMA 5000, Anton Paar) and using a wide range of density CRM and water (Fitzgerald, 2000), it found that that once correctly calibrated, this instruments, would be capable of measuring density of any liquid, between 650 to 1 650 kg·m^{-3}, in the viscosity interval from 0 to 600 mPa·s, with a maximum absolute error of 0,030 kg·m^{-3}, and over a narrower viscosity range, i.e. below 30 mPa·s, with a maximum absolute error of 0,015 kg·m^{-3}.

Like all measuring instruments, the measurement results obtained by an oscillation-type density meter may also drift with time. Measurement errors may be caused, among other reasons, by: instrumental changes due to physical changes in the oscillator, i.e. in its mass, volume or elasticity coefficient; changes in the electronic operation of the measuring instrument; damage due to mishandling; instrument movement during measurement, especially if at a different angle to the horizontal; effects of liquid on the inner surface of the tube, such as deposition of material or erosion by the sample or by the cleaning method. Therefore, the calibration is an essential key to understand and consider the measuring behaviour of the measuring instruments (Furtado *et al.*, 2015a).

As previously described, calibration is a set of operations to establish a relationship between the reference density of a density standard and the corresponding density reading of the instrument. No intervention is made which permanently modifies the instrument (Fritz *et al.*, 2000). A calibration is performed with the purpose of validate the quality of the density measurements and adjustments of the oscillator. Each calibration is related to the actual set of instrument constants (ISO 15212-2:2002). For testing and calibrating density meters in accordance to ISO 15212-1 (1998), reference liquids shall be used whose density values and, if required, viscosities are known within the intended working range of temperature, pressure and flow.

Calibration shall be performed within the density measuring range and within the working ranges of temperature and viscosity and, where appropriate, pressure, which are suitable for the density meter. The density values of the reference liquids shall be determined in a manner traceable to national standards.

To obtain instrument constants A, B from the corresponding frequency values, at least two reference liquids with known densities must be filled into the cell. The instrument constants comprise the cell volume and its mass as well as the spring constant (Fehlauer & Wolf, 2006). Setting the instrument constants of a density meter is called adjustment. An adjustment is an operation to bring the instrument

[3] Furtado, A., Batista, E., Spohr, I., & Filipe, E. (2009). Measurement of Density Using Oscillation-Type Density Meters Calibration, Traceability and Uncertainties. *Proceedings of the 14ème Congrès International de Métrologie*.

(density meter) into a state in which it is suitable for use, by setting or adjusting the instrument constants. Systematic measuring deviations are removed to an extent which is necessary for subsequent sample measurements (Fritz *et al.*, 2000). The calibration and adjustments procedures performed at IPQ were previously described in point II.D.2. *Secondary Method: Oscillation-type density meters*.

III.1.6 Uncertainty Budget[4]

A generic uncertainty budget of density, ρ measurements performed with an oscillation-type density meter (with A and B spring constants), at temperature, t and pressure, p, of a fluid sample with viscosity, η, performed according to GUM (JCGM 100:2008) methodology is presented in Table III.10, where all the input quantities described previously in point *III.1.4 Mathematical Model* were included.

Table III.10 Generic uncertainty budget of density, ρ measurements performed with an oscillation-type density meter (with A and B constants), performed at temperature, t and pressure, p, of fluid sample with viscosity, η.

Source of uncertainty	Relative standard uncertainty	Type of evaluation	Distribution	Degrees of freedom
Density ρ				
Resolution of the density meter	$\frac{\rho\ resolution}{\sqrt{12}}$	B	Rectangular	50
Calibration and drift	$u_{\rho_{cal\,\&\,drift}}$	A	Normal	n-1
Repeatability	$\frac{\sigma_\rho}{\sqrt{n}}$	A	Normal	n-1
Temperature t				
Resolution of the density meter	$\frac{t\ resolution}{\sqrt{12}}$	B	Rectangular	50
Calibration and drift	$u_{t_{cal\,\&\,drift}}$	A	Normal	n-1
Temperature hysteresis of the oscillator	$u_{hyst.oscillator}$	B	Rectangular	50
εt	εt	B	Rectangular	50
Pressure p				
Resolution of the pressor transducer	$\frac{p\ resolution}{\sqrt{12}}$	B	Rectangular	50
Calibration and drift of the pressor transducer	$u_{p\ sensor_{cal\,\&\,drift}}$	A	Normal	n-1
Calibration and drift of the oscillator in pressure	$u_{p\ oscillator_{cal\,\&\,drift}}$	B	Rectangular	50
εp	$\frac{\varepsilon p}{\sqrt{12}}$	B	Rectangular	50
Sample properties				
α_{fluid}	$u_{\alpha_{fluid}}$	B	Rectangular	50
γ_{fluid}	$u_{\gamma_{fluid}}$	B	Rectangular	50
$\varepsilon\eta$	$\frac{\varepsilon\eta}{\sqrt{12}}$	B	Rectangular	50
ε_{fluid}	$\frac{\varepsilon_{fluid}}{\sqrt{12}}$	B	Rectangular	50
Other sources				
$\tau, V, M_0, A, B, \alpha_{oscillator}, \gamma_{oscillator}, \varepsilon\tau, \varepsilon V, \varepsilon k$	-	B	Rectangular	50
Density relative combined standard uncertainty	u_ρ			
Density relative expanded uncertainty	$u_\rho k = U$			
Coverage factor (95 %)	k			
Effective degrees of freedom	ν_{eff}			

Legend: The relative combine standard uncertainty of the result, u_c, was obtained from the square root of the sum of the relative standard uncertainties, considering a unitary sensitive coefficient for all the contributions. The effective degrees of freedom, ν_{eff},

[4] Furtado, A., Batista, E., Spohr, I., & Filipe, E. (2009). Measurement of Density Using Oscillation-Type Density Meters Calibration, Traceability and Uncertainties. *Proceedings of the 14ème Congrès International de Métrologie*.

for the relative combine standard uncertainty were calculated by the Welch-Satterthwaite formula. The coverage factor, k, is chosen to be the $t_{1-\alpha/2,\nu}$ critical value from the t-table with ν_{eff} degrees of freedom. The relative expanded uncertainty of the result, U, was obtained by multiplying the relative combined standard uncertainty of the result, u_c, by the coverage factor, k. The presented terms are in accordance with GUM (JCGM 100:2008).

III.A

VISCOSITY-INDUCED ERRORS

During the oscillation, the viscous component of a liquid, causes, on one hand, a formation of a boundary layer which increases the inertial mass of the resonator and on the other hand a damping of the oscillation due to the wall shear stress acting on the resonator. Consequently, these two parasitic effects lead to a lower resonance frequency of the measuring system and, thus, to an inaccurate density measurements. The detection of these influences is performed, by the instruments, by analyzing the frequency of harmonics of the oscillation. So, these effects can be corrected by means of algorithms obtained during the calibration of the oscillator with viscous CRM.

Thus, this part of the work consisted in a set of investigations on the effect of sample viscosity in density measurements performed with oscillation-type density meters with two different types of oscillators construction materials: borosilicate-made (DMA 5000 and DMA 5000M, Anton Paar) and Hastelloy C-276 made (DMA HP, Anton Paar). With this, two different excitation modes, regular (in DMA 5000 and DMA HP, Anton Paar) and pulsed (DMA 5000M, Anton Paar) could be also be evaluated. The main goal of this investigation was to produce a reference damping curve due to samples' viscosity, using Newtonian reference liquids, to be used in further studies to correlate the expected damping with the ones produce by the viscoelastic samples.

III.A.1 VISCOSITY TESTS WITH DMA 5000 – PART I

III.A.1.1 Materials and Methods

III.A.1.1.1 Density meter calibration for viscosity damping

An oscillation-type density meter DMA 5000 (Anton Paar), with a 10^{-3} kg·m^{-3} density resolution and a temperature resolution of 0,001 ºC, was calibrated, at 20 ºC, with 8 reference liquids with viscosity from 1 to 583 mPa·s: three liquids from EURAMET Comparison Project 1240 "Comparison of density determinations of liquid samples by density meters" (deutered water, pentadecane and viscosity oil) and four CRM from H&D Fitzgerald (lube oil largo 3 and 32, lube oil 110 and A90 and dimethyl phthalate). The density reference values of these liquids were measured by hydrostatic weighing. The deviation from density reference value of measuring results were analyzed for both DMA 5000 indication of density with internal algorithm of correction of viscosity damping, δd, and for indication without internal corrections algorithm of correction, δd_{nc}. The difference between these two indications was also analyzed, (d_{nc}-d). The temperature measurements are traceable to the IPQ primary Laboratory of Temperature. The uncertainty budget was performed according to GUM methodology (JCGM 100:2008) and as previously established (Furtado *et al.*, 2009).

III.A.1.2 Results and Discussion

III.A.1.2.1 Density meter calibration for viscosity damping

The calibration results for viscosity-induced damping of DMA 5000 (Anton Paar) density meter are presented in Table III.11. The expanded measurement uncertainty of the density values presented in this table, U, for a coverage factor, k, of 2,00, at a 95 % level of confidence, is 0,030 kg·m^{-3}, corresponding to a maximum relative expanded uncertainty of 0,0039 %. The relative expanded uncertainty of the difference (d_{nc}-d), was calculated according to $U'_{(d_{nc}-d)} = \sqrt{(U'_{d_{nc}})^2 + (U'_{d})^2}$, where a maximum value of 0,0050 % was obtained (for a coverage factor, k, *of* 2,00, at a 95% level of confidence).

Table III.11 Calibration results of DMA 5000 (Anton Paar) calibration for viscosity-induced errors with Newtonian reference liquids.

Reference liquid	η (mPa·s)	$\rho_{ref.}$ (kg·m^{-3})	δd (kg·m^{-3})	δd (%)	δd_{nc} (kg·m^{-3})	δd_{nc} (%)	(d_{nc}-d) (kg·m^{-3})	(d_{nc}-d) (%)
Deuterated water[1]	1,00	998,470	0,016	0,0016	0,016	0,0016	0,000	0,000
Pentadecane[1]	2,85	768,809	0,016	0,0021	0,031	0,0040	0,015	0,0020
Lube oil Largo 8[2]	16,60	823,934	0,058	0,0070	0,118	0,0143	0,060	0,0073
Dimethyl phthalate[2]	24,16	1191,261	0,059	0,0050	0,171	0,0144	0,112	0,0094
Lube oil Largo 32[2]	76,27	866,689	0,071	0,0082	0,365	0,0421	0,294	0,0339
Viscosity oil[1]	144,24	831,943	0,027	0,0032	0,492	0,0591	0,465	0,0559
Lube oil 110[2]	317,0	881,783	0,025	0,0028	0,643	0,0729	0,618	0,0701
Lube oil A90[2]	583,00	886,653	0,058	0,0065	0,679	0,0766	0,621	0,0700

Legend: 1 - Liquids from EURAMET Comparison Project 240 "Comparison of density determinations of liquid samples by density meters"; 2 – CRM oils from H&D Fitzgerald; $\rho_{ref.}$ - the density reference values were determinate by hydrostatic weighing; δd, δd_{nc} - deviation from density reference value of density meter indication of density with correction of viscosity, and the indication without corrections; The expanded measurement uncertainty for the density values presented, U, for a coverage factor, k, *of* 2,00, at a 95% level of confidence, is 0,030 kg·m^{-3} (corresponding to a maximum relative expanded uncertainty U' of 0,0039 %); The relative expanded uncertainty of the difference (d_{nc}-d), was calculated according to $U'_{(d_{nc}-d)} = \sqrt{(U'_{d_{nc}})^2 + (U'_{d})^2}$, where a maximum value of 0,0050 % was obtained (for a coverage factor, k, *of* 2,00, at a 95% level of confidence).

The obtained results display that DMA 5000 density indication with viscosity correction, ρ, evidences a maximum relative deviation from the reference density value of 0,0082 % (0,071 kg·m^{-3}) and no dependence was observed with viscosity. On other hand, DMA 5000 density indication without viscosity correction, d_{nc}, increases with viscosity and evidences a similar behaviour to (d_{nc}-d) , as can be seen on Fig. III.12.

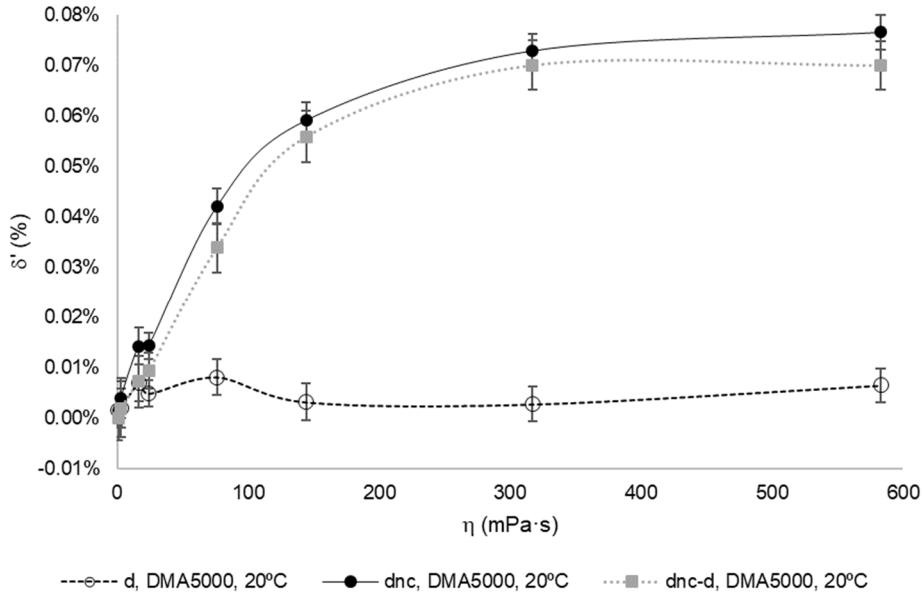

Figure III.12 Relative density deviations, in %, of the density indication with viscosity correction, δd of the density indication without viscosity correction, δd_{nc} and difference between the indication without and with viscosity correction(d_{nc}-d), against dynamic viscosity, in mPa·s, obtained in the tests with CRM oils performed at 20 ºC with a DMA 5000 (Anton Paar) density meter. Legend: the vertical bars represent the relative expanded uncertainty for a 95 % confidence level.

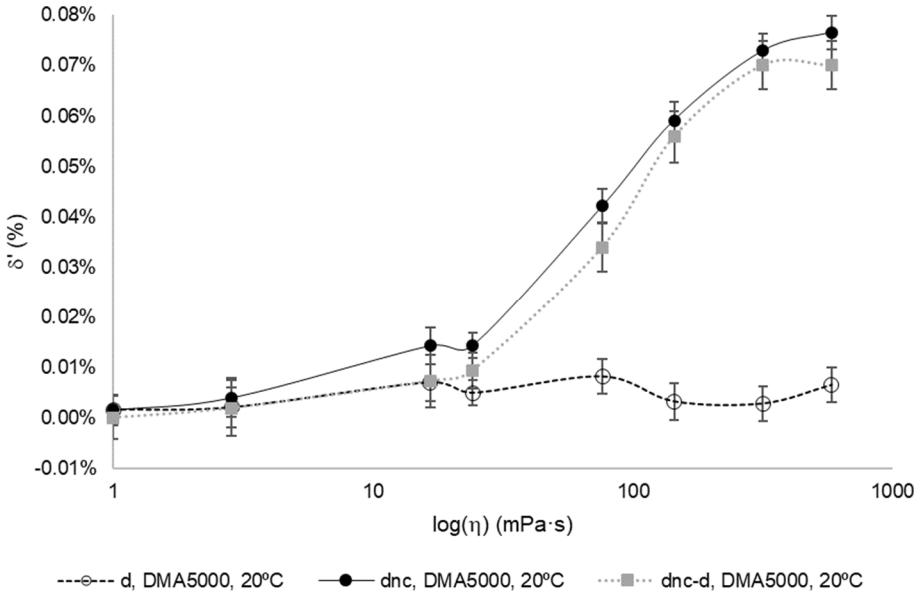

Figure III.13 Relative density deviations, in %, of the density indication with viscosity correction, δd, of the density indication without viscosity correction, δd_{nc} and difference between the indication without and with viscosity correction (d_{nc}-d), against the log(η), in mPa·s, obtained in the tests with CRM oils performed at 20 ºC with a DMA 5000 (Anton Paar) density meter. Legend: the vertical bars represent the relative expanded uncertainty for a 95 % confidence level.

A linearization of the curves presented in Fig. III.13 was obtained by representing the relative density deviation errors, in % (δd and δd_{nc}) and their difference (d_{nc}-d) against the logarithm (base 10) of dynamic viscosity, η in mPa·s. This representation allows a better understanding about the evolution of the density errors. It is now clear that a different correction algorithm is applied to viscosities above ~25 mPa·s, as can be proved by the change of slope in the curve of (d_{nc}-d)(log(η)).

A linear relation was obtained between the relative density deviation without viscosity correction, $\delta' d_{nc}$, of DMA 5000 and the difference between the indication without and with viscosity correction, (d_{nc}-d), in the viscosity interval from 1-590 mPa·s, as can be found in Fig. III.14. The maximum deviation of this linear regression was within the order of magnitude of the expanded uncertainty of the density measurements, i.e. 0,031 kg·m^{-3}, corresponding to a maximum relative expanded uncertainty of 0,0036 %.

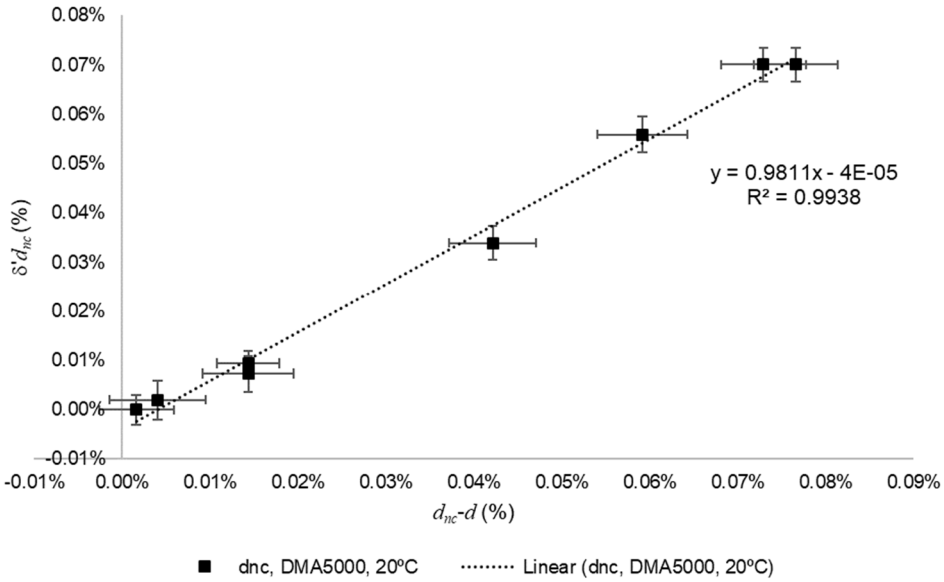

Figure III.14 Linear relation was obtained between the relative density deviation without viscosity correction, $\delta' d_{nc}$, against the difference between the indication without and with viscosity correction d_{nc}-d, obtained in the tests with CRM oils performed at 20 ºC, in the viscosity interval from 1-590 mPa·s, with a DMA 5000 (Anton Paar) density meter. Legend: the vertical and the horizontal bars represent the relative expanded uncertainty for a 95 % confidence level.

III.A.1.3 Conclusions

An interesting relation between the difference of density indication without viscosity correction, d_{nc} and density indication with viscosity correction, d, i.e. from (d_{nc}-d), was observed in the calibration results, performed with CRM oils at 20 ºC, with a density meter DMA 5000 (Anton Paar), allowing, without knowing the viscosity of the sample, to predict the correction to apply.

The maximum deviations obtained in this work are much larger than the one described by (Fitzgerald, 2000). For liquids with viscosity below 30 mPa·s the maximum density measurement error, δd was 0,059 kg·m^{-3} (corresponding to a $\delta' d$ of 0,0050 %) for ρ, and δd_{nc} of 0,171 kg·m^{-3} (corresponding to a $\delta' d_{nc}$ of 0,0144 %) for d_{nc}. For liquids with viscosity within the interval from 30 to 600 mPa·s the maximum obtained density measurement error, δd was 0,071 kg·m^{-3} (corresponding to a $\delta' d$ of 0,0082 %) for d, and δd_{nc} of 0,679 kg·m^{-3} (corresponding to a $\delta' d_{nc}$ of 0,0766 %) for d_{nc}.

Even if the deviations and relations obtained in this investigation had been deduced with a density meter DMA 5000 (Anton Paar) with factory default, they must to be validated for each density meter. Indeed, the relationships could depend on other parameters (very likely from the oscillator constants, and adjustments algorithms, etc.) than the sample viscosity.

III.A.2 VISCOSITY TESTS WITH DMA 5000M – PART II[5]

III.A.2.1 Materials and Methods

Two oscillation-type density meters DMA 5000M (Anton Paar) (referred as (1) and (2)) were tested at a temperature of 20 °C, and the second one additionally at 23 °C, with 13 Newtonian liquids (NL): ultra-pure water (ISO 3696:1987), n-Nonane, and 11 oils (mineral and PAO oils). The dynamic viscosity η of the tested liquids, at 20 ºC, ranged from 0,70 to 220 mPa·s.

III.A.2.1.1 Viscosity estimation from oscillation quality factor

The effect of sample viscosity on the DMA 5000M oscillation quality factor, Q, was studied, at 20 °C and 23 °C, for samples with dynamic viscosity η in the interval from 0,70 to 220 mPa·s, using the liquids described above.

III.A.2.1.2 Viscosity estimation from density indication

Both density indications of the density meter, the density not viscosity-corrected d_{nc} and the density viscosity-corrected d, were analysed. The difference between these two density indications d_{nc}-d, for simplification denoted from now on as D, was studied using the same premises of the previous point.

III.A.2.1.3 Samples characterization

The dynamic viscosity value of ultra-pure water was taken from ISO TR 3666 (1998). For the other test liquids, the kinematic viscosity values were measured with capillary viscometers (ISO 3104:1994; DIN 51562-1:1999). The dynamic viscosity was calculated using these values and the density values, measured by means of a hydrostatic weighing method (Fehlauer, & Wolf, 2006). The expanded uncertainty of these measurements is 0,20 % (with a coverage factor k =*2*,95 %).

The uncertainty of the dynamic viscosity values was obtained according to GUM methodology (JCGM 100:2008). This uncertainty is negligible compared to the uncertainty of the viscosity estimated by density measurements as shown in the following.

III.A.2.1.4 Viscosity-induced errors

In these studies, it was evidenced the possibility to use data obtained by oscillation-type density meters, Anton Paar DMA 5000M, to estimate the viscosity value of Newtonian liquids. In this type of density meters, the viscous behaviour of the liquid during the oscillation leads to a damping and by this to a lower resonance frequency of the measuring system and, thus, to an incorrect density indication. However, these instruments have been developed to overcome this error by applying a viscosity-related correction. Among other outputs, the density indication values without viscosity correction d_{nc} and with viscosity correction d and a damping indication parameter Q are given by these density meters in each measurement performed.

In these investigations has been proved to be possible to estimate the viscosity of the Newtonian liquids tested, at 20 °C and 23 ºC, in the viscosity interval from 7 mPa·s to 220 mPa·s, with a relative standard uncertainty of 3 %, by using a third-order polynomial regression of the kinematic viscosity against the difference of the density indication values with and without viscosity correction given by a DMA 5000M.

[5] This work was presented as a poster communication on AERC 2017 co-organized with the 26th Nordic Rheology Conference, (3-6 April 2017, Copenhagen, Denmark) and was published as: Furtado, A., Pagel, R., Lorenz, F., Godinho, I., & Wolf, H. (2017) Estimation of nominal viscosity of Newtonian liquids from data obtained by an oscillation-type density meter, *Annual Transactions of the Nordic Rheology Society*, Vol. 25.

A second more simple possibility is to calculate the viscosity from oscillation quality factor values Q. These findings might be considered being useful for laboratories that need a rough estimation of sample viscosity without having the opportunity to measure the viscosity directly by other methods.

The method to calculate the density correction was not published in detail thus, a physical model cannot be used for the calculation of viscosity. Instead of these mathematical approximations have been used.

III.A.2.2 Results and Discussion

III.A.2.2.1 Results for single devices

The data measured at 20 °C and 23 °C with two different density meters (1) and (2) is given in the Table III.12. The Q values are taken directly from the DMA indication values and the D values are calculated as described above.

Table III.12 Resume of the results of Q and D, in kg·m^{-3}, obtained at 20 °C and 23 C by density meters (1) and (2).

η (mPa s)	$Q_{(1)}$ (1)	$D_{(1)}$ (kg·m^{-3})	$Q_{(2)}$ (1)	$D_{(2)}$ (kg·m^{-3})
20 °C				
0,71	2844,9	-0,003	2760,2	-0,006
1,00	2761,2	0,000	2697,1	-0,004
1,45	2667,8	0,016	-	-
2,87	2468,7	0,042	-	-
7,68	2137,9	0,097	2075,5	0,095
10,03	2032,5	0,119	-	-
19,75	1774,3	0,184	-	-
31,70	1601,8	0,233	-	-
60,06	1386,1	0,317	1356	0,323
101,48	1224,9	0,399	-	-
125,00	1171,3	0,429	1133,9	0,440
224,06	1023,1	0,546	-	-
23 °C				
0,68	-	-	2745,18	-0,006
0,93	-	-	2685,97	-0,005
6,94	-	-	2094,03	0,089
27,72	-	-	1597,13	0,217
51,75	-	-	1400,33	0,300
106,87	-	-	1169,18	0,414

III.A.2.2.1.1 Viscosity estimation from quality factor

During the study of the relation between viscosity η and the oscillation quality factor values Q, it was observed that the lower the viscosity of the sample the higher was the oscillation quality factor Q indicated by the density meter. To the highest oscillation quality factor value (~2845) corresponded the lowest viscosity value tested (~0,7 mPa·s) and to the lowest oscillation quality factor value (~1023) corresponded the highest viscosity value tested (~220 mPa·s) (Table III.12). Proofing that there is an inverse relation between the expected physical damping of the oscillation and the oscillation quality factor value Q given by the density meter.

It was found that the dynamic viscosity η of the Newtonian samples versus oscillation quality factor Q, in the interval described above, at 20 °C and 23 °C, can be described by a simple exponential regression for both density meters tested ((1) and (2)) with an accuracy which is satisfying for many approaches. This is shown in Fig. III.15. The coefficients of the approximation and the relative standard deviations s of the regressions are given in Table III.13.

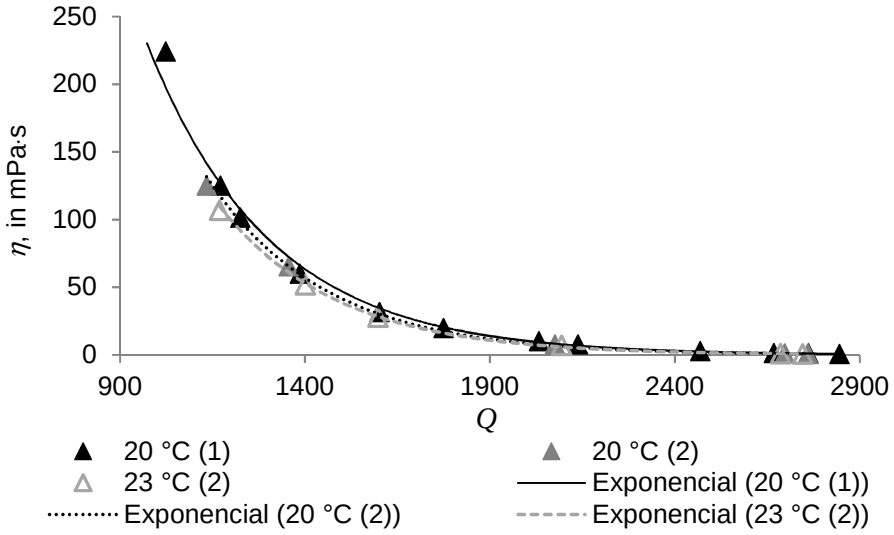

Figure III.15 Regression curve of the dynamic viscosity η, in mPa·s, at 20 ºC and 23 °C, against Q measured by density meters (1) and (2) (DMA 5000M, Anton Paar).

III.A.2.2.1.2 Viscosity estimation from density indications

The results of the difference between the density indication values not viscosity-corrected and viscosity-corrected, D, can be well described by polynomial regressions of third order for both density meters tested ((1) and (2)). The data are visualized in Fig. III.16. The coefficients of the approximation and the relative standard deviations s of the regressions are given in Table III.14.

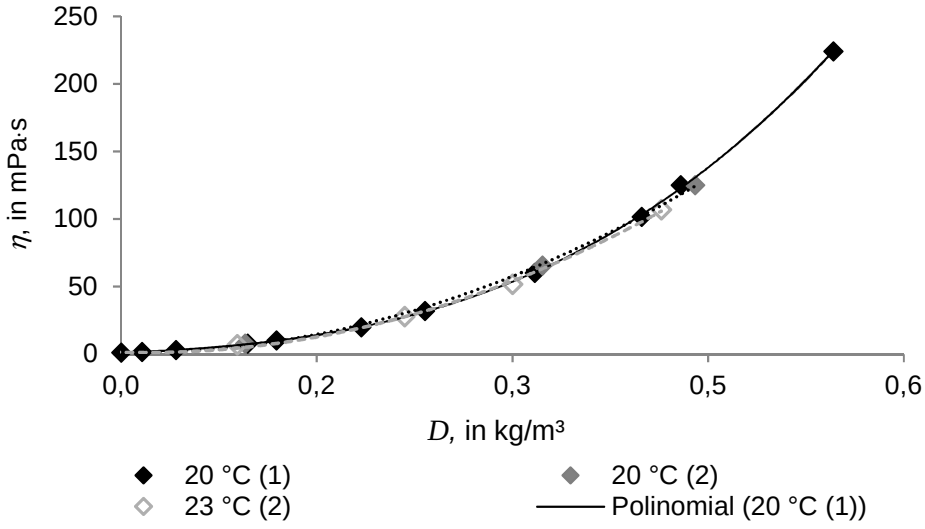

Figure III.16 Regression curve of the dynamic viscosity η, in mPa·s, at 20 ºC and 23 °C, against D, in kg·m^{-3}, measured by density meters (1) and (2) (DMA 5000M, Anton Paar).

Table III.13 Resume of the coefficients (a and b) and relative standard deviations s of the regressions of η, in mPa·s, against Q, at 20 °C and 23 °C, obtained by density meters (1) and (2) (DMA 5000M, Anton Paar), in the viscosity interval from 0,7 mPa·s to 220 mPa·s.

t (ºC)	Density meter	$\eta(Q) = a\, e^{-b\,Q}$ Regression coefficients		s
		a (mPa s)	b (1)	(%)
20	(1)	4339	-0,00302	9
	(2)	4670	-0,00314	8
23	(2)	4425	-0,00316	8

Table III.14 Resume of the coefficients (a, b, c, and d) and relative standard deviations s of the regressions of η, in mPa·s, against D, in kg·m^{-3}, at 20 °C and 23 °C, obtained by density meters (1) and (2) (DMA 5000M, Anton Paar), in two viscosity intervals (V1: 0,7 mPa s to 7 mPa s, V2: 7 mPa s to 220 mPa s).

t (ºC)	Density meter	$\eta(D) = aD^3 + bD^2 + cD + d$ Regression coefficients				s	
		a (mPa·s·kg^3·m^9)	b (mPa·s·kg^2·m^6)	c (mPa·s·kg^1·m^3)	d (mPa·s)	V_1 (%)	V_2 (%)
20	(1)	917	174	41	1	9	1,7
	(2)	390	404	29	1	15	0,3
23	(2)	822	163	47	1	11	1,3

III.A.2.2.1.3 Regressions residual analysis

In Fig. III.15 and III.16 the residuals of these approximations are shown. For the Q regression the maximum relative deviation in viscosity observed was 15 % (Table III.13). Residuals data follow a curvature clearly to be seen (Fig. III.17). This implies that another approximation curve could yield better results. Here we abstained from a more complex approximation to have the opportunity of getting a simple approximation.

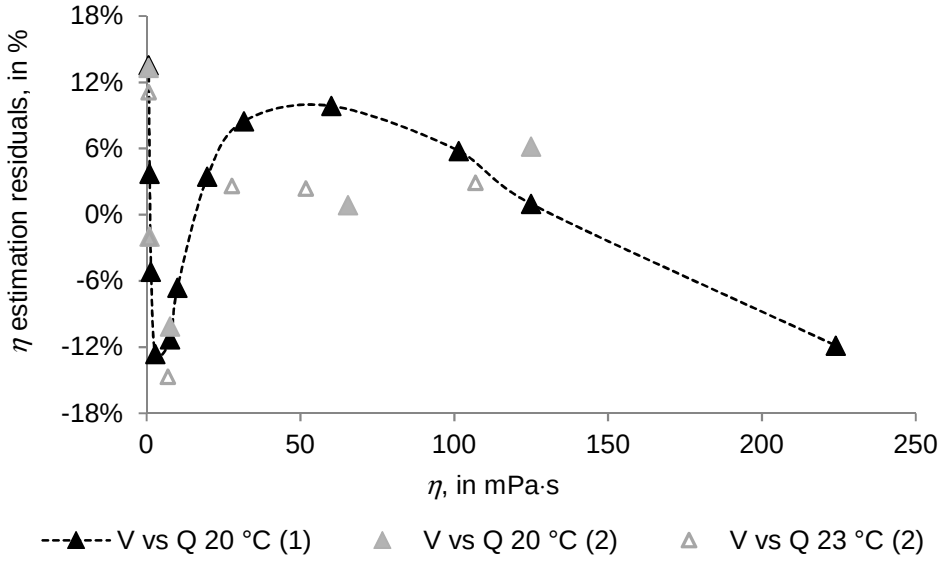

Figure III.17 Residuals analysis of the regressions curves of dynamic viscosity η (represented by V) against Q (represented by Q), measured by density meters (1) and (2) (DMA 5000M, Anton Paar), at 20 °C and 23 °C.

Table III.15 Resume of the relative residuals, in %, of the regression equations of dynamic viscosity η against Q, and against D, obtained at 20 °C and 23 °C, by density meters (1) and (2) (DMA 5000M, Anton Paar).

η (mPa s)	Curve relative residuals of the regression curves			
	$\eta(Q)_{(1)}$ (%)	$\eta(D)_{(1)}$ (%)	$\eta(Q)_{(2)}$ (%)	$\eta(D)_{(2)}$ (%)
20 °C				
0,71	14	24	13	18
1,00	4	0	-2	-11
1,45	-5	18	-	-
2,87	-13	8	-	-
7,68	-11	-3	-10	1
10,03	-7	-1	-	-
19,75	3	2	-	-
31,70	8	0	-	-
60,06	10	1	1	0
101,48	6	2	-	-
125,00	1	-2	6	0
224,06	-12	0	-	-
23 °C				
0,68	-	-	-2	-17
0,93	-	-	11	5
6,94	-	-	-15	2
27,72	-	-	3	-1
51,75	-	-	2	0
106,87	-	-	3	0

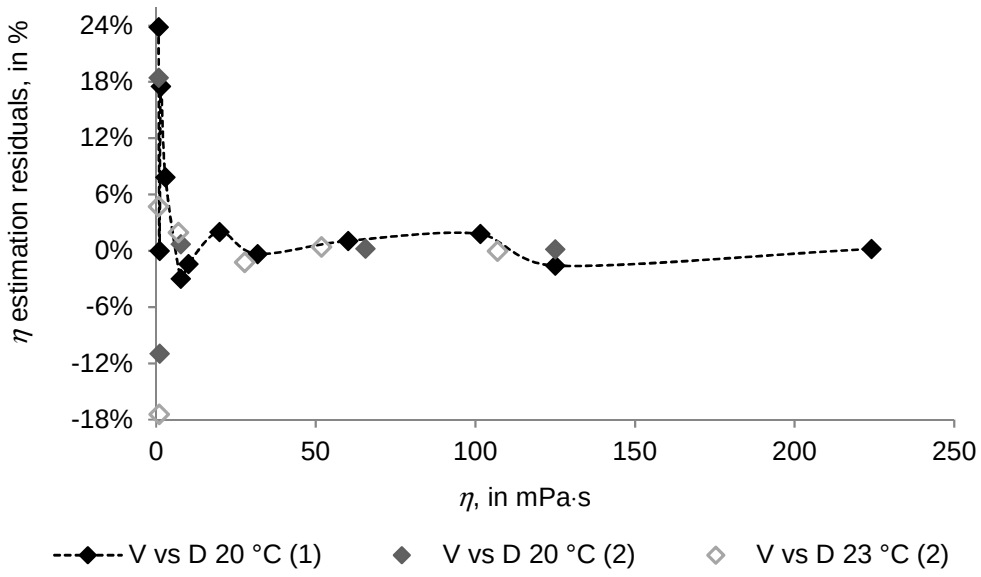

Figure III.18 Residuals analysis of the regressions curves of dynamic viscosity η (represented by V) against D (represented by D), measured by density meters (1) and (2) (DMA 5000M, Anton Paar), at 20 °C and 23 °C.

Looking for the D approximation using a third-order polynomial one can found comparably larger deviations only for viscosities below 7 mPa·s, the maximum relative deviation was here 24 % (Table III.15). This can be explained by the fact, according to the mechanical relations of a damped oscillator

D be proportional to the $\sqrt{\eta}$, meaning that the viscosity η will increase proportionally to D^2 and not with D^3. In the viscosity interval of 7 to 220 mPa·s, the viscosity can be determined from D values with a maximum deviation lower than 3 % (Table III.15).

The residuals obtained from the simple exponential regression of (η, Q) pairs of values, in the same viscosity interval, implies, in average, errors 9 times higher than the ones obtained with the third-degree polynomial regression of (η, D) pairs of values (Table III.15).

III.A.2.2.2 Combined results for two devices

To use a calculation procedure for the determination of the viscosity as described above, the results variation due to instrumental differences must be known. Thus, the study was performed at two different Anton Paar DMA 5000 M, mentioned as (1) and (2).

The data gained using both devices were put together and one approximation was calculated using all data. The results of this approximation are given in Tables III.16 and III.17, being equivalent to the Tables III.13 and III.14, which are for single devices. In Table III.21 the residuals to this combined approximation are given.

Table III.16 Resume of the coefficients (a and b) and relative standard deviations s of the regressions of η, in mPa·s, against Q, at 20 °C and 23 °C, for the combined data set obtained by density meters (1) and (2) (DMA 5000M, Anton Paar), in the viscosity interval from 0,7 mPa s to 220 mPa·s,

t	$\eta(Q) = a\, e^{-b\,Q}$ Regression coefficients		s
	a	b	
(°C)	(mPa s)	(1)	(%)
20	4413	-0,00308	13
20, 23	4413	-0,00308	15

Table III.17 Resume of the coefficients (a, b, c and d) and relative standard deviations s of the regressions of η, in mPa·s, against D, in kg·m^{-3}, at 20 °C and 23 °C, in two viscosity intervals (V1: 0,7 mPa s to 7 mPa·s, V2: 7 mPa s to 220 mPa·s), for the combined data set obtained by density meters (1) and (2).

t	$\eta(D) = aD^3 + bD^2 + cD + d$ Regression coefficients				s	
	a	b	c	d	V1	V2
(°C)	(mPa·s·kg^3·m^9)	(mPa·s·kg^2·m^6)	(mPa·s·kg^1·m^3)	(mPa·s)	(%)	(%)
20	1037	86	53	1	20	3,1
20, 23	1089	45	59	1	21	3,1

Using the data obtained for both density meters, the regression curves to obtain the dynamic viscosity η from Q and D values where plotted in Fig. III.19 and III.20, respectively, together with the deviations from the directly measured viscosity (right axis).

In the exponential regression for the data from both density meters tested a relative standard deviation in viscosity of 13 % was observed for the entire viscosity interval tested, i.e. from 0,7 mPa·s to 220 mPa·s (Table III.18). This value increased to 15 % when including the 23 °C data.

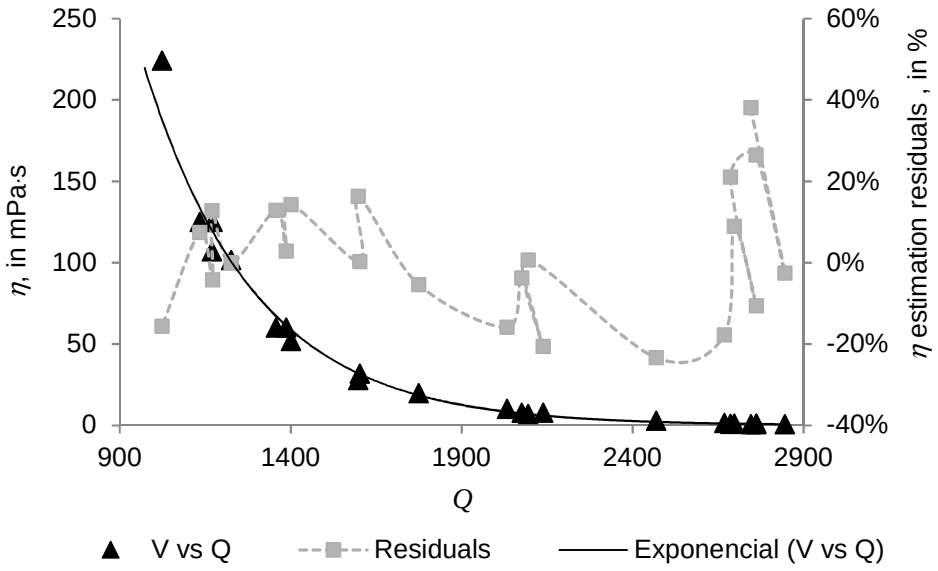

Figure III.19 Curve of the regression of dynamic viscosity η (left axis) against the Q obtained for the combined data set of density meters (1) and (2) (DMA 5000M, Anton Paar), at 20 °C and 23 °C, and residuals curve of dynamic viscosity η estimation, in %, from the exponential regression curve (right axis).

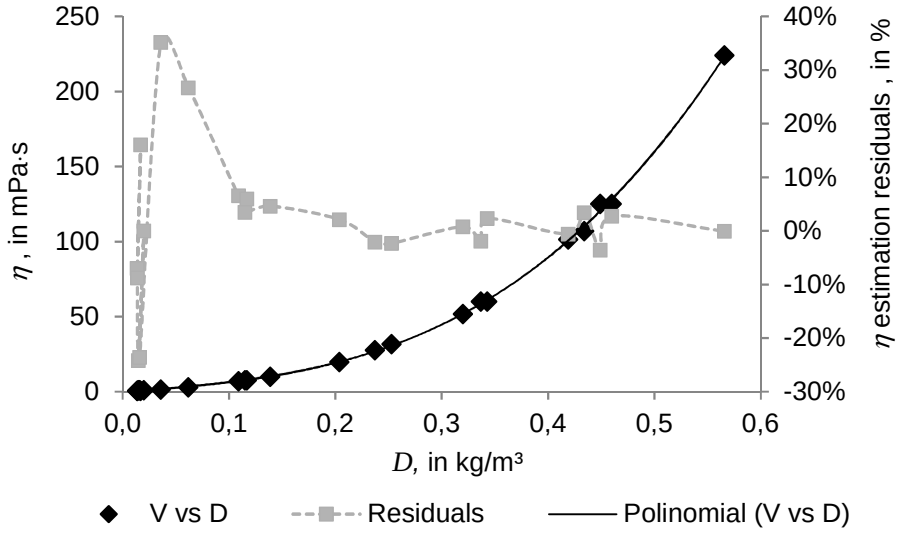

Figure III.20 Curve of the regression of dynamic viscosity η, in mPa·s (left yy-axis) against the D, in kg·m^{-3}, obtained for the combined data set of density meters (1) and (2) (DMA 5000M, Anton Paar), at 20 °C and 23 °C, and residuals curve of dynamic viscosity η estimation, in %, from third-degree polynomial curve (right yy-axis).

It was seen that a third-degree polynomial regression of viscosity against D can estimate the viscosity values in D interval from 0,097 to 0,546 kg m^{-3}, corresponding to a viscosity interval from 7,68 mPa·s to 224 mPa·s, with a relative standard deviation of 3,1 %. For viscosity values from 0,7 mPa·s to 7 mPa·s, corresponding to a D interval from -0,004 to 0,042 kg m^{-3}, a relative standard deviation in viscosity of 20 % was observed (Table III.18). Both standard deviations are nearly unchanged if including the 23 °C data (21 %).

Table III.18 Resume of the relative residuals, in %, of the combined regression of dynamic viscosity η against Q and against D obtained, at 20 °C and 23 °C, by density meters (1) and (2) (DMA 5000M, Anton Paar).

η (mPa·s)	Density meter (1) $Q_{(1)}$ (%)	Density meter (1) $D_{(1)}$ (%)	Density meter (2) $Q_{(2)}$ (%)	Density meter (2) $D_{(2)}$ (%)
20 °C				
0,71	-3	16	26	-9
1,00	-11	0	9	-24
1,45	-18	35	-	-
2,87	-23	27	-	-
7,68	-21	6	-4	3
10,03	-16	5	-	-
19,75	-5	2	-	-
31,70	0	-2	-	-
60,06	3	-2	13	2
101,48	0	-1	-	-
125,00	-4	-4	7	3
224,06	-16	0	-	-
23 °C				
0,68	-	-	38	-7
0,93	-	-	21	-24
6,94	-	-	1	7
27,72	-	-	16	-2
51,75	-	-	14	1
106,87	-	-	13	3

III.A.2.3 Conclusions

In this part of the work two different approaches were described and tested in order to determine the sample dynamic viscosity value η for Newtonian liquids from data measured by oscillation-type density meters DMA 5000M from Anton Paar. The study was performed using water, hydrocarbons, mineral and PAO oils, at measuring temperatures of 20 °C and 23 °C, in the viscosity interval from 0,7 to 220 mPa·s.

Two different approaches have been tested for the calculation of liquids viscosity. The first approach was to calculate the viscosity from the oscillation quality factor value Q and to describe these data by a simple exponential equation. The second approach was based in the calculation of the viscosity from the difference D in the density indications of the density meter, the not viscosity-corrected density d_{nc} and the viscosity-corrected density d and to use a polynomial approximation for the description of the viscosity-density difference relation.

The investigation was performed using two DMA 5000M to look for the effects of instrumental differences in the measurements results. The results were calculated for each individual device and for both together.

Using the viscosity estimation from Q it was possible to calculate the viscosity with a relative standard uncertainty of less than 15 % in the viscosity interval from 0,7 to 220 mPa·s. This method is usable as a fast estimation, where a precise knowledge of viscosity is not necessary.

The D approach was able to yield viscosity values with a relative standard uncertainty of 3 % in the viscosity interval from 7 to 220 mPa·s, corresponding to D values in the interval from 0,097 to 0,546 kg·m^{-3}. For lower viscosities in the range from 0,7 to 7 mPa·s the same approximation can be used only with a larger uncertainty of 20 %.

The relations are valid for both investigated devices, so it can be assumed that they are valid for any oscillation-type density meter DMA 5000 M. In all cases the inclusion of the 23 °C data does not increase the standard deviation significantly. Thus, these approximations can at least also be used in measurements performed at 23 °C.

The relations demonstrated in this study were derived for unbranched hydrocarbons with single and double bonds but containing no other functional groups. Different classes of Newtonian liquids, within the same density and viscosity range, but with different molecular structures, for instance siloxanes or ethers, may give different results.

III.A.3 VISCOSITY TESTS WITH DMA 5000M AND DMA HP

To determine the density indication error two oscillation-type density meters, DMA 5000M and DMA HP, both from Anton Paar, were tested with 10 Newtonian CRM (single bound hydrocarbons (n-Nonane and Dodecane), mineral oils (50B, 100B, 500A, 1000A and 2000A) and poly-alpha-olefin (PAO) oils (EF 162, EF 164 and EF 166) with dynamic viscosity, at 23 °C, in the interval from 0,7 to 1400 mPa·s.

III.A.3.1 Materials and Methods

III.A.3.1.1 Samples characterization

The kinematic viscosity of the Newtonian liquids was measured with capillary viscometers and with a Stabinger viscometer SVM 3000 from Anton Paar. The dynamic viscosity was then calculated by the product of the kinematic viscosity and density of the liquid. As the viscosity values will be used only as nominal values no uncertainty values will be presented.

The density of the tested liquids, to be taken as reference, was determined by means of two different methods: by hydrostatic weighing (Fehlauer & Wolf, 2006) and by gravimetric method using a Gay-Lussac glass pycnometer according to ISO 2811-1 (2011).

III.A.3.1.2 Viscosity induced errors

The density indication errors of the density meters were calculated by the difference between the density measured value and the reference density value (JCGM 200:2008).

III.A.3.2 Results and Discussion

III.A.3.2.1 Samples characterization

The values of dynamic viscosity, η and density, ρ, at 23 ºC, of the Newtonian liquids to be taken as reference are presented in Table III.19, together with the density measurement methods used for each sample and the obtained uncertainty of density values. The uncertainty of viscosity results is not given since these values will be used as nominal.

Table III.19 Dynamic viscosity η and density values ρ, at 23 ºC, of the Newtonian liquids tested.

Newtonian liquids	$\eta_{23\,°C}$ (mPa·s)	$\rho_{23\,°C}$ (kg·m^{-3})	U_ρ (kg·m^{-3})	U'_ρ (%)	Density determination method
n-Nonane	0,68	715,751	0,010	0,0014	HW
Dodecane	1,05	746,675	0,010	0,0013	PM
EF162	6,94	793,171	0,002	0,0003	HW
EF164	27,72	814,010	0,001	0,0001	HW
EF166	51,75	822,092	0,002	0,0002	HW
50B	48,10	863,829	0,055	0,0064	PM
100B	106,72	823,604	0,053	0,0064	PM
500A	315,28	836,481	0,054	0,0065	PM
1000A	888,54	843,105	0,054	0,0064	PM
2000A	1392,91	846,103	0,010	0,0012	PM

Legend: PM - Gravimetric method with a Gay-Lussac pycnometer, HW - Hydrostatic weighing; U – expanded uncertainty for a coverage factor $k = 2$; U' – relative expanded uncertainty for a coverage factor $k = 2$

III.A.3.2.2 Viscosity-induced errors

The density indication values, d_{nc} and d, and density relative indication errors, $\delta' d_{nc}$ and $\delta' d$, of both tested density meters (DMA 5000M and DMA HP, Anton Paar), obtained, at 23 ºC, with Newtonian CRM, are resumed in Tables III.20 and III.21, respectively. The relative expanded measurement uncertainty of the density values presented in these tables, U, is given for a coverage factor, k, of 2,00, at a 95 % level of confidence. In Table III.20 the relative expanded uncertainty of the difference, $U'_{(d_{nc}-d)}$ was calculated according as the $\sqrt{(U'_{d_{nc}})^2 + (U'_d)^2}$, and is presented also for a coverage factor, k, *of* 2,00, at a 95 % level of confidence.

Table III.20 Resume of density indication values, dnc and d, of the Newtonian liquids obtained at 23 ºC, with 2 different oscillation-type density meters (DMA 5000M and DMA HP, Anton Paar).

Newtonian liquids	DMA 5000M*						DMA HP*	
	d_{nc} (kg·m^{-3})	$U_{d_{nc}}$ (kg·m^{-3})	d (kg·m^{-3})	U'_d (kg·m^{-3})	$(d_{nc}-d)$ (%)	$U'_{(d_{nc}-d)}$ (%)	d_{nc} (kg·m^{-3})	$U_{d_{nc}}$ (kg·m^{-3})
n-Nonane	715,788	0,031	715,795	0,015	-0,0001	0,0050	715,856	0,036
Dodecane	746,961	0,015	746,949	0,015	0,0003	0,0037	746,884	0,028
EF162	793,625	0,020	793,536	0,019	0,0014	0,0037	793,370	0,029
EF164	814,236	0,015	814,018	0,015	0,0033	0,0037	814,023	0,030
EF166	822,479	0,014	822,178	0,014	0,0045	0,0036	822,203	0,030
50B	864,766	0,023	864,467	0,021	0,0041	0,0037	864,701	0,032
100B	825,115	0,017	824,701	0,016	0,0061	0,0041	825,120	0,034
500A	837,551	0,017	836,959	0,016	0,0085	0,0037	837,563	0,031
1000A	844,493	0,029	843,902	0,026	0,0083	0,0037	844,635	0,031
2000A	846,709	0,015	846,117	0,015	0,0083	0,0059	846,863	0,050

Legend: d_{nc} – density indication not corrected for viscosity damping; d – density indication; U' – relative expanded uncertainty for a coverage factor k = 2; *from Anton Paar; $U'_{(d_{nc}-d)} = \sqrt{(U'_{d_{nc}})^2 + (U'_d)^2}$

Table III.21 Resume of the density relative indication errors, $\delta' d_{nc}$ and $\delta' d$, obtained, at 23 ºC, for the Newtonian liquids tested with 2 different oscillation-type density meters (DMA 5000M and DMA HP, Anton Paar).

Newtonian liquids	DMA 5000M*				DMA HP*	
	$\delta' d_{nc}$ (%)	$U'_{\delta\, d_{nc}}$ (%)	$\delta' d$ (%)	$U'_{\delta\, d}$ (%)	$\delta' d_{nc}$ (%)	$U'_{\delta\, d_{nc}}$ (%)
n-Nonane	0,0052	0,0043	0,0061	0,0021	0,0147	0,0050
Dodecane	0,0383	0,0020	0,0367	0,0020	0,0280	0,0037
EF162	0,0572	0,0025	0,0460	0,0024	0,0251	0,0037
EF164	0,0278	0,0018	0,0010	0,0018	0,0016	0,0037
EF166	0,0471	0,0017	0,0105	0,0017	0,0135	0,0036
50B	0,1085	0,0027	0,0739	0,0024	0,1009	0,0037
100B	0,1835	0,0021	0,1332	0,0019	0,1841	0,0041
500A	0,1279	0,0020	0,0571	0,0019	0,1294	0,0037
1000A	0,1646	0,0034	0,0945	0,0031	0,1815	0,0037
2000A	0,0716	0,0018	0,0017	0,0018	0,0898	0,0059

Legend: d_{nc} – density indication not corrected for viscosity damping; d – density; U' – relative expanded uncertainty for a coverage factor k = 2; * from Anton Paar.

The obtained results display that for both tested density meters models, DMA 5000M and DMA HP, the density indication without viscosity correction, d_{nc}, evidences a maximum relative deviation, $\delta' d_{nc}$, of 0,18 % (for a viscosity of 107 mPa·s) (Fig. III.21). There was found two different areas, one below ~107 mPa·s, with a $\delta' d_{nc}/\eta$ ratio of 0,00168%·mPa^{-1}·s^{-1} for both DMA 5000M and DMA HP, and a $\delta' d/\eta$ ratio of 0,00121%·mPa^{-1}·s^{-1} for DMA 5000M. For viscosity values above ~107 mPa·s, a drastic decrease of damping sensitivity to viscosity was found, with a $\delta' d_{nc}/\eta$ ratio of 0,00009%·mPa^{-1}·s^{-1} for both DMA 5000M and 0,00007%·mPa^{-1}·s^{-1} DMA HP, and a $\delta' d/\eta$ ratio of 0,00011%·mPa^{-1}·s^{-1} for DMA 5000M (Fig. III.21). Meaning that in DMA 5000M for viscosities below ~107 mPa·s the damping sensitivity to viscosity is 11-fold, for d and 19-fold for d_{nc}, the one obtained for higher viscosities, and for DMA HP is 23-fold.

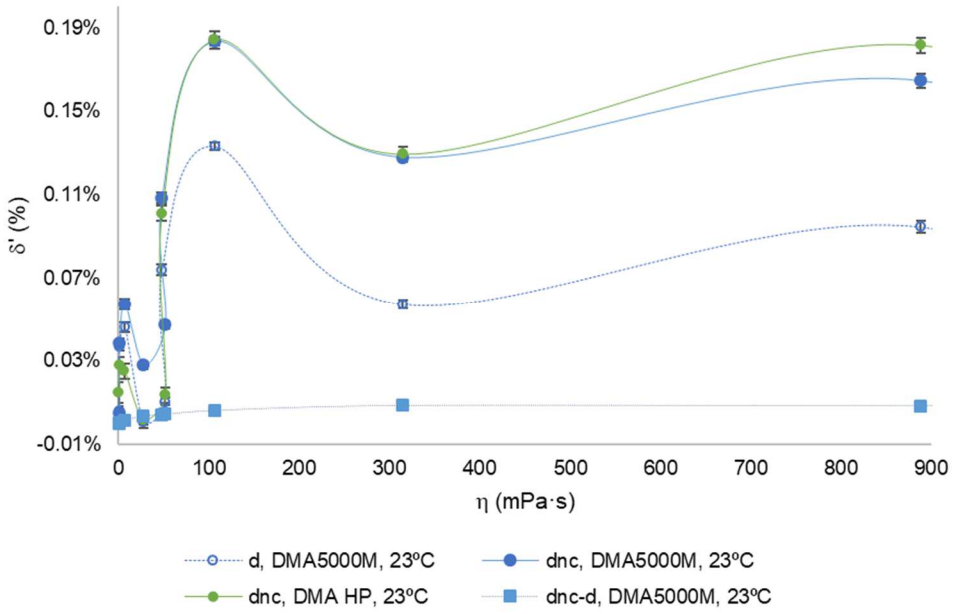

Figure III.21 Relative density deviations, in %, of the density indication with viscosity correction, δd (represented as d) of the density indication without viscosity correction, δd_{nc} (represented as dnc) and difference between the indication without and with viscosity correction (d_{nc}-d) (represented as dnc-d), against dynamic viscosity, in mPa·s, obtained in the tests with CRM oils performed at 23 ºC with a DMA 5000M and DMA HP (Anton Paar) density meters. Legend: the vertical bars represent the relative expanded uncertainty for a 95 % confidence level.

An attempt of linearization of the curves presented in Fig. III.22 was obtained by representing the relative density deviation errors, in % ($\delta' \rho$ and $\delta' \rho_{nc}$) and their difference (ρ_{nc}-ρ) against the logarithm (base 10) of dynamic viscosity, η in mPa·s. This representation allow a better understanding about the evolution of the density errors for. Again, similarly as happened for DMA 5000 model, it is clear that a different correction algorithm is applied, for both DMA 5000M and DMA HP models, to viscosities above ~28-48 mPa·s (for DMA 5000 was above ~25 mPa·s), as can be proved by the change of slope in the curve of (ρ_{nc}-ρ)(log(η).

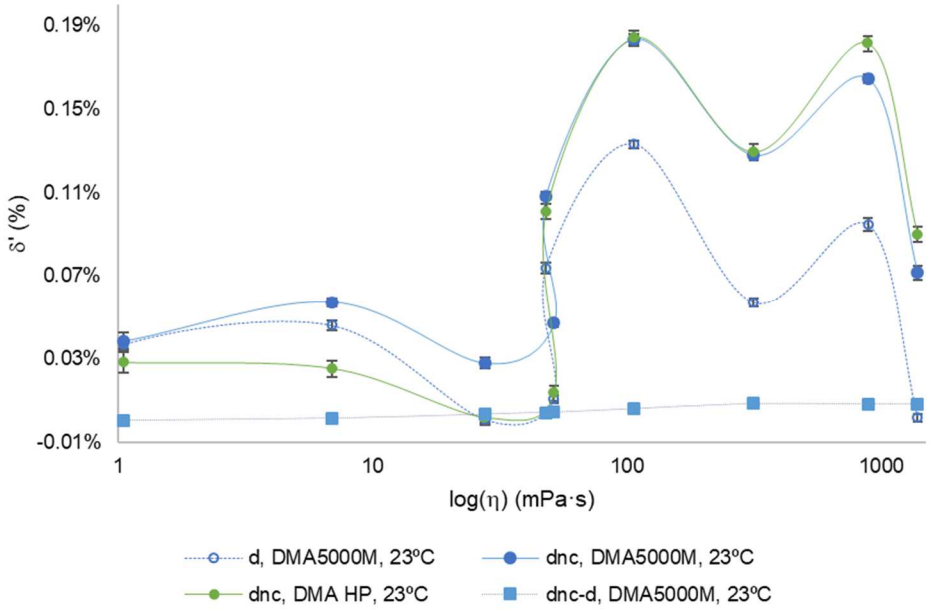

Figure III.22 Relative density deviations, in %, of the density indication with viscosity correction, $\delta\rho$ (represented as d), of the density indication without viscosity correction, $\delta\rho_{nc}$ (represented as dnc)and difference between the indication without and with viscosity correction (ρ_{nc}-ρ) (represented as dnc-d), against the log(η), in mPa·s, obtained in the tests with CRM oils performed at 23 ºC with a DMA 5000M and DMA HP (Anton Paar) density meters. Legend: the vertical bars represent the relative expanded uncertainty for a 95 % confidence level.

In contrary with was found in DMA 5000 results, no linear relation was obtained, in the interval of viscosity of 0,7-1400 mPa·s, between the density deviation of DMA 5000M density indication without viscosity correction, d_{nc}, and the difference between the indication without and with viscosity correction, (d_{nc}-d) as can be seen in Fig. III.23.

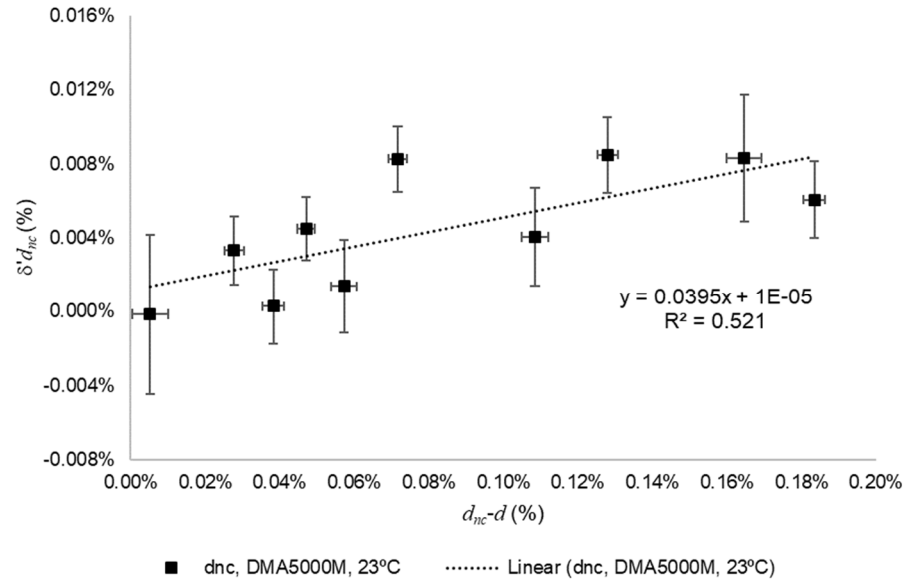

Figure III.23 Linear relation was obtained between the relative density deviation without viscosity correction, $\delta' d_{nc}$, against the difference between the indication without and with viscosity correction d_{nc}-d, obtained in the tests with CRM oils performed at 23 ºC, in the viscosity interval from 0,7 to 1400 mPa·s, with a DMA 5000M (Anton Paar) density meter. Legend: the vertical and the horizontal bars represent the relative expanded uncertainty for a 95 % confidence level.

III.A.3.3 Conclusions

The obtained results were able to be demonstrated that both models of density meters tested (DMA 5000M and DMA HP, Anton Paar) that density indication without viscosity correction, d_{nc}, evidences a maximum relative deviation, $\delta' d_{nc}$, of 0,18 % (for a viscosity of 107 mPa·s).There was also found two different the viscosity induced damping is more significant in the low viscosity interval below ~107 mPa·s, where is also met the higher density deviation value. Meaning that in this viscosity interval the calibration of viscosity-induced damping should be taken in great consideration if accurate density values are needed.

The difference between the two density indications ($dnc–d$) given by the DMA 5000M density meter have been proofed in former studies (Furtado *et al.*, 2016) to have a relation with the viscosity of Newtonian liquids, like unbranched hydrocarbons and mineral oils. For Newtonian liquids with viscosity above 315 mPa·s a plateau value of about 0,07 % was met for ($dnc - d$). For viscosities values below 300 mPa·s, particularly for viscosities from 0,7 to 107 mPa·s, shows that the data obtained can be fitted with the generic equation given by Furtado *et al.* (2016) as describing the dynamic viscosity of a Newtonian liquid from the density indications ($dnc–d$) of DMA 5000M density meter from Anton Paar. The maximum residuals expected for this equation are 21 % in the viscosity interval from 0,7 to 7 mPa·s and 3,1 % in the viscosity interval from 7 to 220 mPa·s. Despite the obtained residuals agreed with these values, dodecane (1,05 mPa·s) and the oil 50B (48,10 mPa·s) presented residuals above these values, 64,2 % and 8,3 %, respectively. These facts can be attributed to undetected experimental errors, for instance the possible presence of air bubbles in the sample that will lead to an incorrect higher viscosity and therefore to a higher difference between the density indications ($dnc–d$) given by the DMA 5000M density meter.

III.B

VISCOELASTICITY-INDUCED ERRORS

In order to provide a deeper insight into the damping effects produced by the viscoelasticity of non-Newtonian fluids during density measurements with oscillation-type density meters, the rheological behaviour, in oscillation mode, of several viscoelastic liquids was studied and the results correlated with the obtained density deviations. The results of these studies were one of the first insights to the knowledge of the measuring behavior of these density meters when measuring viscoelastic liquids, one of the scopes of the EMPIR Project 17RPT02-*rho*Liq.

This part of the work consisted in a set of investigations performed with two different oscillators (two made of borosilicate (DMA 5000 and DMA 5000M, Anton Paar) and a one made of Hastelloy C-276 (DMA HP, Anton Paar).

III.B.1 INTRODUCTION

III.B.1.1 Viscoelasticity

Viscoelastic materials are always showing viscous and elastic behavior simultaneously. The viscous portion behaves according to Newton's law and the elastic portion to Hooke's law. So, depending on their rheological behavior, viscoelastic materials may behave as viscoelastic liquids or viscoelastic solids.

III.B.1.1 Oscillatory tests

Oscillatory tests, performed with rheometers, are ideal to quantify the "amount" of viscosity and elasticity "hidden" in a material's structure. When performed in the non-destructive regime (meaning that the applied forces are too low to alter a material's microstructure), i.e. in the linear-viscoelastic (LVE) range, oscillatory tests can be used, for instance, to study the shelf-life stability of a material or to investigate different kinds of phase transitions, etc.

Couette flow is frequently used to illustrate shear-driven fluid motion. Couette flow is the flow of a fluid in the space between two surfaces, one of which is moving tangentially relative to the other. The configuration often takes the form of two parallel plates or the gap between two concentric cylinders. The simplest conceptual configuration of a Couette flow finds two infinite, parallel plates separated by a distance h (in m), where one plate is stationary and the motion of the other plate causes a shear stress τ (i.e. a force applied tangentially to the movable plate divided by the area, in $N \cdot m^{-2}$ or in SI units Pa) in the sample, which is placed between the plates, leading to deformation. The deflection path s (in m) movable plate, is measured and rheological evaluated as strain or deformation γ (in %). This flow assumes that there is an adhesive force between sample and plates and the produced flow is under laminar regime.

During rheological tests in oscillation mode, the material is exposed to a continuous sinusoidal excitation of either a shear deformation or a shear stress (produced by the rheometer). Depending on the type of excitation, the material will respond with a stress or a deformation (measured by the rheometer). When the amplitude values of the applied stress or deformation signal is low, within LVE range, the response of the sample will also show a sinusoidal shape. Depending on the type of sample, the applied sinusoidal signal and the response signal from the sample will show a phase shift, delta δ, between 0° and 90°. A phase shift of 0° indicates that the sample shows no viscous response and is considered purely elastic. Consequently, a phase shift of 90° implies that a material is behaving as purely viscous with no elastic response.

Storage modulus G', in Pa, is a measure of the deformation energy stored by the sample during the shear process, that will stay completely available after the deformation or a stress is removed and can act as driving force for the reformation process. On the other hand, loss modulus G'', in Pa, is a measure of the deformation energy used by the sample during the shear process and is, therefore, lost (i.e. dissipated) for the sample through the viscous friction. Thus, G' represents the elastic behavior of the material and G'' the viscous behavior. The loss (or damping) factor $tan\ \delta$, a dimensionless quantity, is calculated as the quotient of the lost (G'') and the stored deformation energy (G'), i.e. $tan\ \delta = G''/G'$. It therefore reveals the ratio of the viscous and the elastic portion of the viscoelastic deformation behavior. So, for the fluid or liquid state ("sol state") holds $tan\ \delta > 1$ (since G'' > G'), for the gel-like state or solid state holds $tan\ \delta < 1$ (since G' > G'') and for the sol/gel transition point holds $tan\ \delta = 1$ (since G' = G'').

Different measurements become available when an oscillatory deformation or stress is applied to a sample. These measurements include: Oscillatory Amplitude Sweep and Oscillatory Frequency Sweep.

III.B.1.1.1 Balance of materials' viscoelastic behaviour

If the viscous portion of a viscoelastic material is large enough (i.e. $tan\ \delta \rightarrow \infty$, viscoelastic liquid behavior), the absorption properties of the material are enhanced, e.g. to damp the effects of mechanical vibrations. The deformation arising from mechanical oscillations is used in the energy-absorbing material components (e.g. rubber buffers for damping of mechanical vibrations). On the other hand, if a material has a too large viscous portion, this can lead to excessive viscous heating, and at the end, to a high destructive degree of deformation. In this case, too much deformation energy would be transformed into heat, more than can be simultaneously stored or transport trough the material outside (Mezger, 2014).

III.B.1.1.2 Time-dependent structural decomposition and regeneration

A material that shows a thixotropic behavior presents a reduction of its internal structural strength under a sufficiently high shear deformation that is followed by a complete structural regeneration in the subsequent period of rest (e.g. dispersions and gels). On other hand, a rheopectic behavior means an increasing of the initial structural strength when performing a sufficiently high shear deformation, which is followed by a complete structural regeneration.

III.B.1.2 Viscoelasticity tests in oscillation-type density meters

The results from previous studies (Furtado *et al.*, 2017) indicated that oscillation of density meter measuring cell may cause modifications in the internal structure and arrangement of the molecules of viscoelastic samples, leading to a non-well described/characterized density deviation trend. In order to provide a deeper insight into the damping effects produced by these types of fluids when measuring density with an oscillation-type density meter, a total of 12 viscoelastic fluids were prepared, their mechanical properties were study resorting to a rheometer and their density measured by gravimetric method by using a pycnometer. These studies are divided, and will be presented, in different parts where different methodologies were used.

III.B.2 VISCOELASTICITY TESTS WITH DMA 5000 – PART I[6]

III.B.2.1 Materials and Methods

III.B.2.1.1 Test fluids

To carry out this study, 3 aqueous solutions of different polymers (Carbopol 940 (Fagron) at 0,15 cg·g^{-1}; polyvinyl alcohol (PVA, Sigma-Aldrich) and sodium borate (Borax, Dimor), both at 0,04 g·ml^{-1}; hydroxymethylcellulose (Sigma-Aldrich) at 0,01 g·ml^{-1}; all in ultrapure water) and 2 food liquids (mayonnaise and ketchup, both commercial formulations) were chosen.

III.B.2.1.2 Viscoelastic samples characterization

III.B.2.1.2.1 Density measurements

The oscillation-type density meter used in this study was a DMA 5000 from Anton Paar. The density indication errors were obtained by calibration of this density meter with Newtonian certified reference liquids (CRM) (from H&D Fitzgerald) within the dynamic viscosity, η, interval from 1 to 795 mPa·s. The reference density values of these liquids were determined by hydrostatic weighing. The density indication errors of the density meter were calculated by the difference between the density measured value and the reference density value (JCGM 200:2008).

The density of the 5 viscoelastic samples was measured by gravimetric method with a 50 mL Gay-Lussac pycnometer (Fig. III.24), according to ISO 2811-1 (ISO 2811-1:2016). The filling of the pycnometer with these samples was performed with a peristaltic pump (ICC, ISMATEC) in order to avoid the formation of air bubbles. The density of these 5 samples was also measured using the oscillation-type density meter at the same temperature of the pycnometer test, for comparison of results.

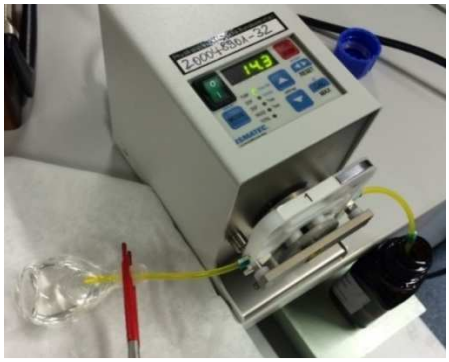

Figure III.24 Assembling used for filling the Gay-Lussac pycnometer with the non-Newtonian liquids tested by means of a peristaltic pump (ISM831C, ISMATEC) with a Tygon HC F-4040-A tube from ISMATEC.

Additionally, the density values of the 5 viscoelastic samples obtained by the oscillation-type density meter (i.e., d_{nc} - non-viscosity-corrected density value, d - viscosity-corrected density value and d'_c – density value corrected with the calibration curve obtained with the Newtonian liquids) were compared against the density results obtained by gravimetric method using a Gay-Lussac pycnometer (ρ_{pic}).

[6] This work was presented in an oral communication at the IMEKO TC1-TC7-TC13-TC18 Symposium 2019 (2-5 July 2019, St. Petersburg, Russia) and will be published on the *Journal of Physics: Conference Series*, as: Furtado, A., Gavina, J., Napoleão, A., Pereira, J., Cidade, M.T., Density measurements of viscoelastic samples with oscillation type density meters.

The uncertainty of density values obtained in both measuring methods, i.e. with the oscillation-type density meter (1) and with the pycnometer (2), was obtained according to GUM methodology (JCGM 100:2008), having into account the following major contributions for the uncertainty budget: (1) density meter (resolution, drift and calibration including CRM used), measurements repeatability; (2) calibration of pycnometer volume, balance (resolution, drift and calibration), air buoyancy (and instruments used to measure air temperature, relative humidity and pressure), mass standards used, measurements repeatability, temperature, temperature coefficient of the liquid. In this paper the reported expanded uncertainty, U, is stated as the standard measurement uncertainty multiplied by the coverage factor k = 2, which for a t-distribution corresponds to a coverage probability of approximately 95 %.

III.B.2.1.2.2 Rheological determinations

Dynamic viscosity, η', storage modulus, G', and loss modulus, G'', dependence on shear strain and on frequency, of the non-Newtonian samples tested were determined by oscillation tests in a rotational rheometer (Mars III, HAAKE ThermoScientific) using a plate-plate (PP35 TiL) measuring geometry. Two different oscillation mode tests were performed for each sample: (1) amplitude sweep at a constant angular frequency, ω, of 10 rad/s in the interval of shear strain, γ, from 0,01 to 100 % (log. ramp) for the determination of the linear viscoelastic regime (LVR) and (2) a frequency sweep at a constant shear strain, γ, of 0,1 to 1 % inside the LVR, for an angular frequency interval, ω, of 100 to 1 rad/s (from 0,016 to 16 Hz) (log. ramp). From the amplitude sweep tests it was possible to identify the prevalent behaviour of the sample (viscous or elastic) regarding the shear strain applied and to check for yield stress value, τ_y, and for the flow stress value, τ_f. The data from frequency sweeps ran for a non-destructive deformation range, will give information regarding the dependence of the dynamic viscosity, η', with the oscillation frequency, f, up to 16 Hz, the upper limit of the PP35 measuring geometry.

III.B.2.3 Results and Discussions

III.B.2.3.1 Comparison of density results

Because it is a static method of measuring the density of liquids, pycnometry has been chosen to be used in comparison with vibrating tube densimetry. As a static method it is expected that the viscoelastic properties of the samples would not influence the measurement result, as in oscillation-type density meters. However, phenomena related to these properties were observed during the filling of the pycnometer which may have influenced the measurement results, and which cannot be easily accounted for.

Table III.22 summarizes the deviations of the bulk density results of the test liquids obtained by oscillation-type density meter compared to the results obtained by gravimetric method using the Gay-Lussac pycnometer. A maximum relative expanded uncertainty, U' of 0,0054 % was obtained for the d_{nc}, d_c and d'_c values, with exception of the liquid foods (mayonnaise and ketchup) with maximum relative expanded uncertainty, U' of 0,030 %) possible related to the heterogeneity of this kind of samples, leading to a consequent low repeatability of the density measurements. On the other hand, the maximum relative expanded uncertainty, U' obtained for the pycnometric method was 0,0039 %. Given this, and considering the results from Table III.22, with exception of the PVA and Borax sample, all the others viscoelastic samples presented significant density deviations when compared (i.e. higher than the uncertainty, U' obtained for the pycnometric method).

Table III.22 Summary of the density deviations, δd, of the results obtained by the oscillation-type density meter (d_{nc}, d_c and d'_c) and the results obtained by gravimetric method using a Gay-Lussac pycnometer (ρ_{pic}) of the 5 viscoelastic samples, at 20 ºC.

Samples	ρ_{pic}	δd					
		δd_{nc}		δd		$\delta d'_c$	
	(kg·m^{-3})	(kg·m^{-3})	(%)	(kg·m^{-3})	(%)	(kg·m^{-3})	(%)
Carbopol	994,46	3,7	0,3721	3,7	0,3721	3,7	0,3721
PVA and Borax	1008,14	0,021	0,0021	-0,018	-0,0018	-0,054	-0,0054
Hydroxymethylcellulose	1003,09	-0,69	-0,0688	-0,86	-0,0857	-1,3	-0,1296
Mayonnaise	933,63	15*	1,61	14*	1,50	14*	1,50
Ketchup	1122,28	-0,81*	-0,07	-1,6*	-0,14	-1,4*	-0,12

Notes: d_{nc} - non-viscosity-corrected density value, d_c - viscosity-corrected density value and d'_c – density value corrected with the calibration curve obtained with Newtonian liquids; U – expanded uncertainty stated as the standard measurement uncertainty multiplied by the coverage factor k = 2, which for a t-distribution corresponds to a coverage probability of approximately 95 %, obtained according to GUM methodology (JCGM 100:2008); U'for d_{nc}, d_c and d'_c values: 0,0054 % and * 0,030 %; U' for ρ_{pic} values: 0,0039 %.

III.B.2.3.2 Rheological determinations

The extrapolated value of the dynamic viscosity, $\eta'_{ext.}$, of each viscoelastic sample at the same oscillation frequency, f_ρ, produced in the oscillation-type density meter during the density measurement, was obtained by extrapolating the experimental lines obtained from the linear regression of $\log(\eta') = a \log(f) + b$ for the interval of frequencies, f, analysed in the rheometer (Table III.23). The viscosity values estimated by the results of the oscillation-type density meter (DMA 5000, Anton Paar), $\eta_{est.\,\rho}$, are also given in Table III.23, together with the description of the viscoelastic character predicted for each sample for f_ρ and the damping factor, $tan\ \delta$, for the maximum frequency tested.

The hydroxymethylcellulose sample presented a predominant viscous behavior, G'' > G', in the entire range of frequencies tested. PVA/Borax and mayonnaise samples showed a predominant elastic behavior, with G' > G'', for frequencies higher than their crossover frequency, i.e. for f > 1,5 Hz, and for f > 2,3 Hz, correspondently. Ketchup sample showed a predominant elastic behavior, with G' > G'', in the entire range of frequencies tested. At last Carbopol sample showed a G' ≅ G''.

Earlier studies (Furtado *et al.*, 2017) showed a way of estimate the dynamic viscosity, $\eta_{est.\,\rho}$, of Newtonian fluids by using the density results given by an oscillation-type density meter, with an uncertainty of 18 %. The same approach was now applied to estimate $\eta_{est.\,\rho}$ for each non-Newtonian fluid tested. The $\eta_{est.\,\rho}$ were compared with the dynamic viscosity values extrapolated η'_{ext} from the curve $\log(\eta') = a \log(f) + b$, with an uncertainty of 10 %, and the relative deviation of the $\eta_{est.\,\rho}$ in relation to $\eta'_{ext.}$, $\delta\eta_\rho$ calculated (Table III.23). Despite Carbopol and PVA/Borax samples presented $\delta\eta_\rho$ values below the $U\eta_{est.}$, the $\delta\eta_\rho$ results for the other samples showed that this approach seems not to be suitable to be use for non-Newtonian fluids (Table III.23).

Table III.23 Summary of viscosity values estimated by the results of the oscillation-type density meter (DMA 5000, Anton Paar), $\eta_{est.\,\rho}$, and the dynamic viscosity values, $\eta'_{ext.}$, estimated by extrapolation of the $\log(\eta')$ curves as a function of $\log(f)$ determined by the rheometer (Mars III, ThermoScientific) with a plate-plate (PP35TiL) measurement geometry, for the frequency values, f_ρ, measured by the oscillation-type density meter for each sample.

Samples	Density meter		Frequency sweep tests				
	f_ρ (Hz)	$\eta_{est.\,\rho}$ (mPa·s)	Viscoelastic character predicted for f_ρ	$tan\,\delta$ (1)	$\eta'_{ext.}$ (mPa·s)	$\lvert\eta^*\rvert_{ext.}$ (mPa·s)	$\delta\eta_\rho$ (%)
Carbopol	278,62	< 6	G' ≈ G''	0,89	5,3	8119	13
PVA/ Borax	277,94	10,3	G' > G''	0,23	10,7	375	-4
Hydroxymethylcellulose	278,34	48,5	G'' > G'	2,16	29,1	34,2	67
Mayonnaise	282,13	> 795	G' > G''	0,44	88,5	329	798
Ketchup	270,52	> 795	G' > G''	0,60	245,5	313	224

Legend: f_ρ – oscillation frequency produced in the oscillation-type density meter (DMA 5000, Anton Paar) during the density measurement (Hz); $\eta_{est.}$ – viscosity value estimated by the results of the oscillation-type density meter; $\log(\eta') = a\ \log(f) + b$ – linear fitting of the dynamic viscosity η' results against frequency, f, obtained in the frequency tests in the rheometer (Mars III, ThermoScientific); $\lvert\eta^*\rvert_{ext.}$ - dynamic viscosity value extrapolated from the curve; $\lvert\eta^*\rvert_{ext.}$ – complex viscosity value extrapolated for f_ρ; relative deviation of the $\eta_{est.\,\rho}$ in relation to $\eta'_{ext.}$.

III.B.2.4 Conclusions

Oscillation-type density meters are a very robust, reliable and convenient instruments to measure the density of Newtonian liquids in wide range of density, viscosity and temperature with an expanded uncertainty from 0,01 to 0,03 kg·m^{-3}, by using a proper calibration curve, since the deviations due to viscosity may lead to a maximum density deviation of 0,62 kg·m^{-3} in the viscosity interval up to 795 mPa·s (Furtado *et al.*, 2017). This study showed that the knowledge of the effect of samples' viscoelasticity on the density measurements results using this kind of density meter is limited by the uncertainty of the pycnometer method (0,010 %), since these density meters are able to produce density results with lower uncertainty (0,0053 % for Newtonian liquids).

Additionally, one should have in consideration that these results may be instrument dependent. Despite the obtained data one cannot conclude about how the rheological properties of a fluid affect the density measurements and viscosity predictions with an oscillation-type density meter. Additionally, the results showed that the approach used to estimate the dynamic viscosity of Newtonian fluids by using the density results given by an oscillation-type density meter (Furtado *et al.*, 2017) cannot be used for non-Newtonian fluids.

As already suspected in earlier studies (Furtado *et al.*, 2017), these results are other indication that oscillation of the density meter cell during density measurements can cause modifications in the internal structure and arrangement of the molecules of the non-Newtonian samples, leading to a non-well described density deviation trend, which may be essentially due to the elastic portion of the viscoelastic behaviour of these samples. As planned in the 17RPT02-*rhoLiq* EMPIR Project the viscoelasticity effect on density results need to be study by a measurement method with a low uncertainty such as the hydrostatic weighing. This may lead to means of comparison that will be able to use the oscillation-type density meters in their maximum metrological capability also with non-Newtonian samples. Or even to know the real limitation of this measuring instrument, to give the most accurate insights for reference documents, such as standards and guides.

III.B.3 VISCOELASTICITY TESTS WITH DMA 5000 – PART II[7]

III.B.3.1 Materials and Methods

III.B.3.1.1 Test fluids

To carry out the Part II of this study of the influence of the viscoelasticity of the samples on the density measurement result of oscillation-type density meters, 5 aqueous solutions of different compositions were chosen: poly(vinyl alcohol) (PVA), at 0,036 g·mL^{-1} and sodium borate (Borax) at 0,0036 g·mL^{-1}; carboxylpolymethylene (Carbomer) solution at 0,15 cg·g^{-1}; hydroxyethyl-cellulose at 0,5 cg·g^{-1}; starch dispersion at 3 cg·g^{-1} and poly(acrylamide-co-diallyldimethylammonium chloride) (P(AAm-co-DADMAC) solution at 5,5 cg·g^{-1}. In addition, two commercial beverages (apple juice and grape juice) were also tested. For simplification further references to the test fluids will be given by using the codes attributed in Table III.24.

Table III.24 Codification of the test fluids (F#).

Codification	Fluid
F1	PVA and Borax
F2	Carbomer
F3	Hydroxyethyl-cellulose
F4	Starch dispersion
F5	P(AAm-co-DADMAC)
F6	Apple juice
F7	Grape juice

III.B.3.1.1.1 PVA and Borax solution

A solution of PVA, at 0,036 g·mL^{-1}, and Borax at 0,0036 g·mL^{-1}, was prepared as described below, based on (Savins, 1968).

The PVA solution, at 0,04 g·mL^{-1}, was prepared by slowly adding 40 g of PVA (87-90 % hydrolyzed, average molecular mass [30.000-70.000] g mol^{-1}, CAS: 9002-89-5, Sigma-Aldrich,) to 800 mL of deionized water preheated to 70 °C - 80 °C and stirred until all the polymer was dissolved. It was ensured that the solution did not boil. The mixture cooled to room temperature and transferred into a 1000 mL volumetric flask. Deionized water was then added until the mark and the solution was finally mixed by slowly inverting a few times.

The Borax solution, at 0,04 g·mL^{-1}, was prepared by transferring 4 g of sodium tetraborate decahydrate (anhydrous, Puriss P.A., ACS reagent, Reag. ISO, buffer substance, ≥ 99,5 %, CAS: 1303-96-4, Honeywell, Fluka) into a 100 mL volumetric flask to which ultrapure water was added, dissolving the borax, by heating, and then cooled to room temperature. The PVA and Borax solutions were finally jointed and mixed in a 2 L flask.

III.B.3.1.1.2 Carbopol solution

A Carbomer solution at 0,15 cg·g^{-1} was prepared as described below based on (Al-Malah, 2006). Carbomer requires a long time to swell properly for use. So, it is necessary to make a pre-gel before beginning the ultimate batch. Consequently, carbomer, type 940 (CAS: 9003-01-4, Carbomera, fagron),

[7] This work was accepted for oral communication at the on 19th International Metrology Congress - CIM 2019 (24-26 September 2019, Paris, France) and will be published in conference proceedings in Web of Conferences (by EDP Sciences), as: Furtado, A., Gavina, J., Napoleão, A., Pereira, J. and Cidade, M.T., Density measurements of viscoelastic samples with oscillation type density meters.

was weighted and added to a known volume of ultrapure water at room temperature. The sample was left for 24 h at room temperature. The sample was then stirred for 2 h at 350 rpm by using a magnetic stirrer, to assure homogeneity and dispersity of carbomer in the aqueous solution.

III.B.3.1.1.3 Hydroxyethyl-cellulose solution

A hydroxyethyl-cellulose (Sigma-Aldrich, CAS: 9004-62-0) solution at 0,5 cg·g^{-1} on ultrapure water was prepared by gravimetric method, based on (Benyounes *et al.*, 2018). The sample was stirred for 24 h at 350 rpm, at room temperature, by using a magnetic stirrer.

III.B.3.1.1.4 Starch solution

A starch dispersion (from potato soluble, reag. USP, Ph. Eur, for analysis, CAS: 9005-84-9, Panreac Applichem, ITW Reagents), at 3 cg·g^{-1}, was prepared by mixing starch with ultrapure water in a flask. The starch dispersion was appropriately stirred for 30 min at room temperature and then heated in a 90 °C water bath for 30 min with constant mild agitation using a magnetic stirrer in order to avoid sedimentation and agglomeration (adapted from (Chuin Won *et al.*, 2017)). Sorbic acid (synthesis grade, CAS: 110-44-1, Scharlau) was added to the solution to work as stabilizer (0,3 g per 1000 g of solution).

III.B.3.1.1.5 P(Aam-co-DADMAC) Carbopol solution

A poly(acrylamide-co-diallyldimethylammonium chloride) (P(AAm-co-DADMAC) solution 10 cg g^{-1} in water, CAS: 26590-05-06, Sigma-Aldrich) solution 5,5 cg g^{-1} in ultrapure water was prepared by weighing. The solution was stirred at 200 rpm with a magnetic stirrer for 24 h.

III.B.3.1.2 Viscoelastic samples characterization

III.B.3.1.2.1 Density measurements

To perform this study a commercial oscillation-type density meter was used (DMA 5000, Anton Paar). The density indication errors were obtained by calibration of this density meter with Newtonian certified reference liquids (CRM) within the dynamic viscosity, η, interval from 1 to 795 mPa·s. The reference density values of these CRM were determined by hydrostatic weighing. The density indication errors of the density meter were calculated by the difference between the measured density value and the reference density value (JCGM 200:2008).

Additionally, the density of the 7 test samples was determined by gravimetric method with the use of a 100 mL aluminium pycnometer (Erichsen), a mass comparator (Mettler Toledo, PR 2007) and a set of stainless-steel standard mass OIML class E2 (Mettler). The tests were performed by substitution weighing method and using the approach described in ISO 2811-1 (2016).

The density values of the test fluids obtained by the oscillation-type density meters (i.e., $\rho_{OD\,nc}$ non-viscosity-corrected density value, $\rho_{OD\,c}$ viscosity-corrected density indication value and $\rho'_{OD\,c}$ density value corrected with the calibration curve obtained with the Newtonian liquids) were compared against the density results obtained by gravimetric method using a pycnometer (ρ_{PN}). The method that the density meters uses to calculate the density correction is not published in detail, thus, a physical model cannot be used for the calculation of viscosity.

Additionally, to test the sensibility of density measurements to samples' time-dependent relaxation/recovery behavior, samples' density was measured at time 0 and at time 5 min, i.e. the same sample was measured twice with a relaxation time interval of 5 min in between. From these measurements, all the relevant data given by the density meter, i.e. the first and second oscillations periods, T_1 and T_2, respectively and the damping indication parameter Q, were related. The density meter cell filled with a fluid behaves like a damped harmonic oscillator due to the viscous portion of the

sample the *Q* factor is therefore a ratio between the energy stored (in the oscillating resonator) and the energy dissipated. These results were crossed with the results of the thixotropic tests.

III.B.3.1.2.2 Uncertainty budget

The uncertainty of density values obtained in both measuring methods, i.e. with the oscillation-type density meter (1) and with the pycnometer (2), was obtained according to GUM methodology (JCGM 100:2008), having into account the following major contributions for the uncertainty budget: (1) density meter (resolution, drift and calibration including CRM used), measurements repeatability; (2) calibration of pycnometer volume, balance (resolution, drift and calibration), air buoyancy (and instruments used to measure air temperature, relative humidity and pressure), mass standards used, measurements repeatability, temperature, temperature coefficient of the liquid. In this paper the reported expanded uncertainty, U, is stated as the standard measurement uncertainty multiplied by the coverage factor k = 2, which for a t-distribution corresponds to a coverage probability of approximately 95 %.

III.B.3.1.2.3 Rheological determinations

Complex viscosity $|\eta^*|$, storage modulus, G', and loss modulus, G'', dependence on shear strain γ and on frequency, *f*, of the 7 viscoelastic samples tested were determined by using a rheometer (HAAKE Mars III, ThermoScientific) using two different measuring geometries: a cone-plate (C35/2° Ti L) for P(AAm-co-DADMAC) and PVA and Borax samples and a concentric-cylinder (CC25 Din Ti) for the remaining samples.

III.B.3.1.2.3.a Oscillatory tests

Two different oscillation tests were performed in controlled deformation (CD) mode for each sample: (1) amplitude sweep, at constant frequency, *f*, of 1 Hz (1,592 Hz in case of P(AAm-co-DADMAC) sample) in the interval of shear strain, γ, from 0,1 to 100 % (for a total of 16 data points in logarithmic distribution) for the determination of the linear viscoelastic (LVE) range and (2) frequency sweep at a constant strain (deformation) γ, of 1 % (0,1 % in case of grape juice sample) inside the LVE range, for the frequency interval, *f*, from 0,1 to 100 Hz (for a total of 6 data points in logarithmic distribution). Additionally, the amplitude sweep tests gave information regarding the prevalent behaviour of the samples in the LVE range under a low frequency (1-1,592 Hz), regarding the shear strain applied and to check for the flow stress value, τ_f.

III.B.3.1.2.3.b Data transformation

Frequency sweeps, ran for a non-destructive deformation range (i.e. in the LVE region), gave information regarding the dependence of the dynamic viscosity, η', with the oscillation frequency, *f*, up to 100 Hz, the upper limit of the measuring geometries used.

The storage modulus G'(f_ρ) and loss modulus G''(f_ρ) values, at the frequency value f_ρ i.e., at the oscillation frequency produced in the oscillation-type density meter during the density measurement of each test sample (usually in the frequency interval of 273-279 Hz for liquid samples), were estimated by extrapolating the linear regressions of G'(*f*) and G''(*f*) (Eq. III.8 and III.9, respectively) determined with the experimental data.

$$\log(G') = a \log(f) + b \quad \text{(III.8)}$$

$$\log(G'') = c \log(f) + d \quad \text{(III.9)}$$

From the calculated values of G'(f_ρ) and G''(f_ρ), viscous portion $\eta'(f_\rho)$, i.e. dynamic viscosity, and elastic portion $\eta''(f_\rho)$ of samples behavior under shear at frequency f_ρ , were calculated from Eq. III.10 and III.11, respectively.

$$\eta'(f_\rho) = G''(f_\rho) / 2\pi f_\rho \quad \text{(III.10)}$$

$$\eta''(f_\rho) = G'(f_\rho) / 2\pi f_\rho \quad \text{(III.11)}$$

The loss or damping factor, $tan\ \delta(f_\rho)$, was calculated as the quotient of the loss ($G''(f_\rho)$) and the storage modulus ($G'(f_\rho)$). Thus, this parameter gives the ratio between the viscous and the elastic portion of the viscoelastic deformation.

$$tan\ \delta(f_\rho) = G''(f_\rho) / G'(f_\rho) \quad \text{(III.12)}$$

If $tan\delta > 1$ ($G'' > G'$) the sample is in fluid or liquid state ("sol state"), i.e., showing a behavior of a viscoelastic liquid, for $tan\ \delta < 1$ ($G' > G''$) the sample is in a gel-like or solid state, i.e., showing a behavior of viscoelastic solid, and for $tan\ \delta = 1$ a sol/gel transition will be met, i.e., having a viscoelastic behavior showing 50/50 ratio of the viscous and elastic portions.

III.B.3.1.2.3.c Thixotropic behaviour investigation tests

The thixotropic behaviour of the tested samples was investigated through shear rate ramps loops (upwards and downwards) measurements. Each one of these test was performed in controlled rate (CR) mode , and was divided in 3 parts: (1) rotational ramp for increasing shear rate $\dot{\gamma}$ values from 0,0001 s^{-1} to 100 s^{-1} (during 100 s for a total of 100 data points in linear distribution); (2) rotation at constant shear rate $\dot{\gamma}$ value of 100 s^{-1} (during 30 s for a total of 30 data points); and (3) rotational ramp for decreasing shear rate $\dot{\gamma}$ values from 100 s^{-1} to 0,0001 s^{-1} (during 100 s for a total of 100 data points in linear distribution).

Flow curves ($\tau(\dot{\gamma})$) were plotted for each sample and the hysteresis area of each one of the tests parts (i.e., upward shear rate ramp (A1); constant shear rate (A2) and downward shear rate ramp (A3)) were determined by rheometer's software (HAAKE RheoWin Datamanager®).

III.B.3.3 Results and Discussions

III.B.3.3.1 Comparison of the density results

To study the influence of samples' viscoelasticity on the density measurement results of an oscillation-type density meter, 7 different samples were prepared and rheologically characterized.

Because it is a static method of measuring the density of liquids, pycnometry was chosen to be used in comparison with the ones obtained with the oscillation-type density meter. As a static method it is expected that viscoelastic properties of samples would not influence density measurement results, as it might do in oscillation-type density meters. However, phenomena related to these properties were observed during the filling of the pycnometer which may have influenced the measurement results, and which cannot be easily accounted for.

The compilation of the density results of the 7 test fluids obtained at 20 ºC and ambient pressure by these two density measurement methodologies (oscillation-type density meter (ρ_{OD}) and pycnometer (ρ_{PN})) are given in Table III.25. A maximum relative expanded uncertainty of 0,0053 % was obtained for the density values obtained from the oscillation-type density meter ($\rho_{OD\ nc}$, $\rho_{OD\ c}$ and $\rho'_{OD\ c}$ values and the maximum uncertainty obtained for the pycnometric method was 0,010 % (Table III.25).

Table III.25 Compilation of the density results of the 7 test fluids obtained at 20 ºC and ambient pressure by using an oscillation-type density meter (DMA 5000, Anton Paar) (ρ_{OD}) and a pycnometer (ρ_{PN}).

F#	Oscillation-type density meter (OD)				Pycnometer (PN)	
	$\rho_{OD\ nc}$ (kg m^{-3})	$\rho_{OD\ c}$ (kg m^{-3})	$\rho'_{OD\ c}$ (kg m^{-3})	$U\ \rho_{OD}$ (kg m^{-3})	ρ_{PN} (kg m^{-3})	$U\rho_{PN}$ (kg m^{-3})
F1	1008,319	1008,183	1008,542	0,054	1007,87	0,10
F2	998,705	998,692	998,701	0,021	998,41	0,10
F3	999,801	999,753	999,905	0,054	999,23	0,10
F4	1008,335	1008,324	1008,335	0,020	1008,21	0,10
F5	1009,954	1009,727	1010,308	0,055	1011,52	0,10
F6	1049,012	1048,996	1049,005	0,021	1049,40	0,11
F7	1068.167	1068.164	1068.161	0.021	1067.55	0,11

Notes: F# - codification of the test fluids according to Table III.16; $\rho_{OD\ nc}$ - non-viscosity-corrected density value, $\rho_{OD\ c}$ - viscosity-corrected density value and $\rho'_{OD\ c}$ - density value corrected with the calibration curve obtained with the Newtonian liquids; U - expanded uncertainty stated as the standard measurement uncertainty multiplied by the coverage factor $k = 2$, which for a t-distribution corresponds to a coverage probability of approximately 95 %, obtained according to GUM methodology (JCGM 100:2008).

Table III.26 summarizes the density deviations, $\delta\rho$, of the results obtained by the oscillation-type density meter ($\delta\rho_{OD;\ PN}$)) and the results obtained by gravimetric method using a pycnometer (ρ_{PN}) of the 7 test fluids. The expanded uncertainties of the density deviations values, $\delta\rho_{OD;\ PN}$), were calculated by Eq. III.13.

$$U_{\delta\rho} = \sqrt{(u\rho_{OD\ nc})^2 + (u\rho_{PN})^2} \qquad \text{(III.13)}$$

Table III.26 Summary of the density deviations, $\delta\rho$, of the results obtained by the oscillation-type density meter (DMA 5000, Anton Paar) (ρ_{OD}) and the results obtained by gravimetric method using a pycnometer (ρ_{PN}) of the 7 test fluids.

F#	$\delta\rho(OD;\ PN)$			
	$\rho_{OD\ nc} - \rho_{PN}$ (%)	$\rho_{OD\ c} - \rho_{PN}$ (%)	$\rho'_{OD\ c} - \rho_{PN}$ (%)	$U_{\delta\rho}$ (%)
F1	0,045	0,031	0,067	0,011
F2	0,029	0,028	0,029	0,010
F3	0,057	0,052	0,067	0,011
F4	0,012	0,011	0,012	0,010
F5	-0,155	-0,178	-0,120	0,011
F6	-0,037	-0,038	-0,038	0,010
F7	0,058	0,058	0,057	0,010

Notes: F# - codification of the test fluids according to Table III.16; $\rho_{OD\ nc}$ - non-viscosity-corrected density value, $\rho_{OD\ c}$ - viscosity-corrected density value and $\rho'_{OD\ c}$ – density value corrected with the calibration curve obtained with the Newtonian liquids; $U\delta\rho$ – relative expanded uncertainty of the density deviations values, $\delta\rho(OD;\ PN)$ calculated by equation 5, stated as the relative standard measurement uncertainty multiplied by the coverage factor $k = 2$, which for a t-distribution corresponds to a coverage probability of approximately 95 %, obtained according to GUM methodology (JCGM 100:2008).

Table III.26 shows that even the density results corrected with the calibration curve obtained with the Newtonian liquids ($\rho'_{OD\ c}$) produce significant density deviations, up to a maximum value of ~ 0,12% ($\delta\rho_{OD;\ PN})_{max}$), when measuring viscoelastic samples, the, i.e. for all samples the density deviation obtained from the density value obtained with the pycnometer is larger than the expanded uncertainty of the density deviations values ($U\rho$) (from 0,010 to 0,011 %). Thus, the obtained density deviations obtained for the viscoelastic samples are 1 to 10 orders higher than the uncertainty of the relative expanded uncertainty of the density deviations values, $\delta\rho_{OD;\ PN}$). The same maximum density deviation value was obtained for the viscosity-corrected density indication value ($\delta\rho_{OD\ c;\ PN})_{max}$) given by the density meter. Since these two set of results were corrected according to the damping produce by

Newtonian materials it does not consider the possible effect of sample's elasticity at such high frequency.

III.B.3.3.2 Relation with samples' mechanical properties

The oscillation frequency f_ρ values (in Hz) of each sample during the density measurements with the oscillation-type density meter were calculated by the inverse of the period of the first harmonic oscillation (τ_1) measured by the density meter. As the tested density meter performs corrections of density values according to the damping in the oscillation period produced by the viscous part of the samples, the estimated value for the viscosity, $\eta_{est.}$, was also calculated using the approach applied in earlier studies (Furtado *et al.*, 2017). However, when testing viscoelastic samples, as the results in Table III.27 show, the same approach (Furtado *et al.*, 2017) was no longer valid to estimate the viscous portion of a sample. All the viscoelastic samples tested showed a damping factor, $tan\ \delta < 1$ (G' > G''), indicating that all the tested samples present a predominantly solid-like character, i.e., they behave as viscoelastic solids at the frequency f_ρ produced in the density meter (Table III.27).

Table III.27 Oscillation frequencies, f_ρ and dynamic viscosity $\eta_{est.}$ values estimated with the oscillation-type density meter (DMA 5000, Anton Paar) and viscous, $\eta'(f_\rho)$, elastic, $\eta''(f_\rho)$ complex, $|\eta^*(f_\rho)|$ viscosities and loss factor $tan\ \delta(f_\rho)$, for f_ρ, determined by extrapolation of the data obtained in frequency sweep tests performed with the rheometer.

F#	Density meter			Rheometer			
	f_ρ (Hz)	Q (1)	$\eta_{est.}$ (mPa·s)	$\eta'(f_\rho)$ (mPa·s)	$\eta''(f_\rho)$ (mPa·s)	$\lvert\eta^*(f_\rho)\rvert$ (mPa·s)	$tan\ \delta(f_\rho)$ (mPa·s)
F1	277,92	2,780	39,10	0,09	170	169,7	0,0006
F2	278,58	2,712	≤ 5,94	8,20	5088	5088,1	0,0016
F3	278,50	2,774	13,06	0,81	2456	2456,2	0,0003
F4	277,92	2,780	≤ 5,94	20,29	6164	6164,0	0,0033
F5	277,81	2,781	65,45	0,07	1088	1087,5	0,0001
F6	275,17	2,689	≤ 5,94	5,59	21784	21784,4	0,0003
F7	273,91	2,821	≤ 5,94	2,21	951	951,0	0,0023

Legend: f_ρ – oscillation frequency produced in the oscillation-type density meter (DMA 5000, Anton Paar) during the density measurement (Hz); Q – oscillation damping factor; Relative expanded uncertainty of viscosity estimation: $U'\eta_{est.}$ = 18 % (Furtado *et al.*, 2017); $U'\eta'(f_\rho) = U'\eta''(f_\rho)$ = 10-20 %.

Also to be noticed that, in general, the difference between the dynamic viscosity values estimated with the oscillation-type density meter, $\eta_{est.}$, by using the approach used with Newtonian fluids (Furtado *et al.*, 2017), and the viscous $\eta'(f_\rho)$ portion of the complex viscosity obtained by extrapolation of the data obtained in frequency sweep tests performed with the rheometer, is higher than the relative expanded uncertainty of viscosity estimations ($U'\eta_{est.}$ = 18 % (Furtado *et al.*, 2017); $U'\eta'(f_\rho) = U'\eta''(f_\rho)$ = 10-20 %) meaning that the approach used with Newtonian fluids (Furtado *et al.*, 2017) to estimate samples' viscosity values η_{est}, is not suitable for non-Newtonian fluids (Table III.27).

Table III.28 Summary of the viscoelastic prevalent behavior of the 7 tested samples in the linear viscoelastic range (in amplitude sweep tests at low frequency) and under high frequencies (in frequency sweep tests), performed at 20 ºC.

F#	Oscillatory tests	
	Amplitude sweep (f = 1 Hz) Viscoelastic behavior in the LVE range	Frequency sweep (f ~273-279 Hz) Viscoelastic behavior predicted for f_ρ
F1	G''> G', liquid-like	
F2	G' > G'', solid/gel-like	
F3	G''> G', liquid-like	
F4	G' > G'', solid/gel-like	G' > G", solid/gel-like
F5	G''> G', liquid-like	
F6	G' > G'', solid/gel-like	
F7	G' > G'', solid/gel-like	

Legend: for the fluid F5 the amplitude sweep test was performed at a constant frequency of 1,592 Hz.

In terms of viscoelastic behaviour one can group the test samples in three different groups, according to the results of the amplitude sweep tests: (1) samples F1, F3 and F5 (PVA and Borax, hydroxyethyl-cellulose and P(AAm-co-DADMAC) solutions) exhibited liquid-like behaviour (G'' > G') in the entire shear strain, γ, interval tested (i.e., from 0,1 to 100 %), therefore acting like viscoelastic liquids; (2) samples F2, F4 and F7 (carbomer solution, starch solutions and grape juice samples) exhibited a solid-like character (G' > G'') in the LVE range (Table III.28), with a flow stress, τ_f (G' = G'') between 1,8 – 2,7 m Pa, 10.6 – 16,5 m Pa, and 1,7 – 2,8 m Pa, respectively; (3) sample F6 (apple juice sample) showed a gel-like character (G' > G'') in the entire shear strain, γ, interval tested (Table III.28).

On the other hand, the rheological results, at the same frequency produced by the density meter, f_ρ, obtained by extrapolation of the frequency sweep test results, showed that all tested samples showed solid-like behaviour (G'' > G') (Table III.28), with a damping factor between 0,0006 and 0,0033 (Table III.19). As the damping factor $tan\ \delta(f_\rho)$ is the quotient of lost G'' (viscous portion) and storage modulus G' (elastic portion) (Eq. III.4), small values of $tan\ \delta$, i.e. < 1, are related with solid like behavior. Additionally, from frequency sweep tests, it was possible to realize that at low frequencies, F1, F2, F3, F4, F6 and F7 samples (PVA and Borax, carbomer, hydroxyethyl-cellulose, starch solutions and grape juice samples) presented a liquid-like behaviour (G'' > G'). F5 sample (P(AAm-co-DADMAC) solution was the only one showing a gel-like character (G' > G'') at low frequencies and presenting two crossover points (G'' = G') at frequencies f around 19,0 Hz and 59,3 Hz.

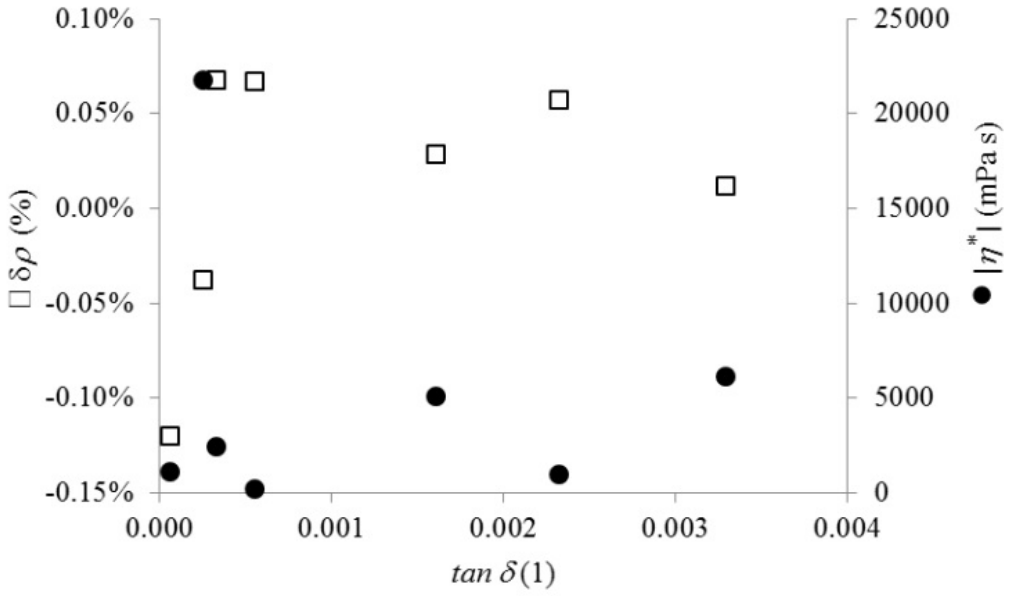

Figure III.25 Graphic representation of the density deviation $\delta\rho$ (i.e., $\rho'_{OD\,c}$ - ρ_{PN}) (white squares) and the complex viscosity $|\eta^*|$ (black filled circles) of the 7 viscoelastic samples, at 20 ºC, against the damping values *tan* δ (Table III.27) of the samples for frequency f_ρ..

At this point, the major concern of this investigation is to check if there is any causal relation between samples' viscoelastic character and density deviations $\delta\rho$ obtained by the density meter. For this, the density deviation $\delta\rho$ and samples' complex viscosity $|\eta^*(f_\rho)|$ were both plotted against samples' loss (damping) values *tan* δ, determined for frequency f_ρ in frequency sweep tests with the rheometer, in Fig. III.25. As previously described, if the viscous portion of a viscoelastic material is large enough (i.e., $tan\ \delta \to \infty$, viscoelastic liquid behavior) its absorption properties are enhanced causing damping effects on mechanical vibrations. However, all the tested samples presented solid-like (i.e., *tan* δ < 1 as G' > G'') for the oscillation frequency f_ρ produced in the density meter measuring cell during density measurements.

However, in contradiction with what was expected, for samples presenting low values of *tan* δ (i.e., $tan\ \delta \to 0$) and lower values of viscous $\eta'(f_\rho)$ the density deviations $\delta\rho$ are higher (Fig. III.25). The highest density deviation was obtained for the P(AAm-co-DADMAC) sample ($\delta\rho$ = -0,12% and *tan* δ= 0,0001).

As previously described, the measuring cell of the density meter when filled with the fluid under test will act as a damped harmonic oscillator due to the viscous portion of the sample, the *Q* factor (or oscillation damping factor), is therefore a ratio between the energy stored (in the oscillating resonator) and the energy dissipated during the oscillation by damping processes (in this case shear friction and shear heating). In this sense, it was expected that *Q* factor decreased for increasing viscosities in an exponential trend like describe in earlier studies (Furtado *et al.*, 2017) with Newtonian fluids (Fig. III.26).

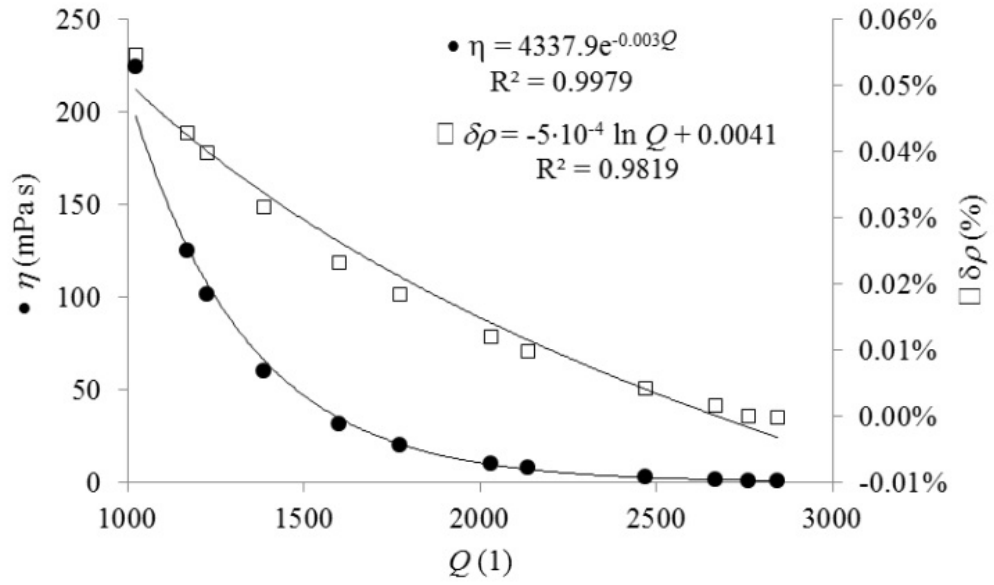

Figure III.26 Curves of the data obtained in (Furtado *et al.*, 2017) with Newtonian liquids by using oscillation-type density meters (DMA 5000M, Anton Paar). Dynamic viscosity η (black filled circles), at 20 ºC and 23 °C, and relative density deviation $\delta\rho$ (i.e., $\rho'_{OD\,c}$ - ρ_{PN}) (white squares), both against Q factor.

For viscoelastic samples, and when considering Q factor in function of complex viscosity $|\eta^*|$ (i.e., Q ($|\eta^*|$)) in general the trend is the same as the one obtain for Newtonian liquids, i.e. high values of $|\eta^*|$ produce lower values of Q, though, density deviations $\delta\rho$ do not fit the expected trend (black filled circles in Fig. III.27). Taking a deeper look into the trend of Q against the viscous η' portion of the complex viscosity $|\eta^*|$, the same trend is no longer existing (black filled circles in Fig. III.27). In theory, it was expected that more viscous samples (i.e., with high viscosity values (η')) would originate lower Q factor values.

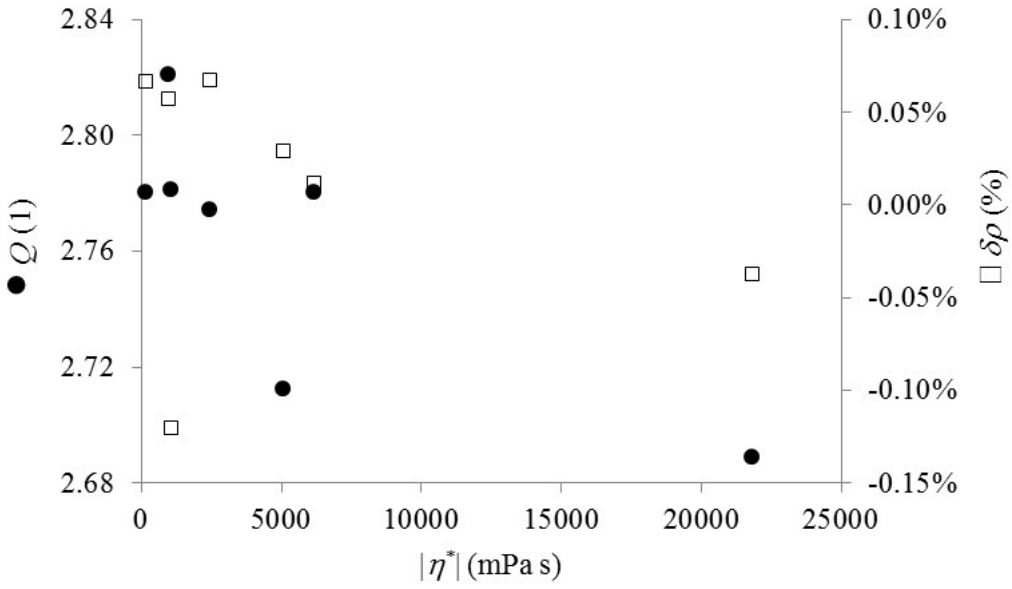

Figure III.27 Graphic representation of oscillation damping values Q (black filled circles) (Table III.27) and the the relative density deviation $\delta\rho$ (i.e., $\rho'_{OD\,c}$ - ρ_{PN}) (white squares) (Table III.26) of the 7 viscoelastic samples, at 20 ºC (Table III.27), against samples' complex viscosity $|\eta^*|$ (Table III.27) determined for frequency f_ρ in frequency sweep tests.

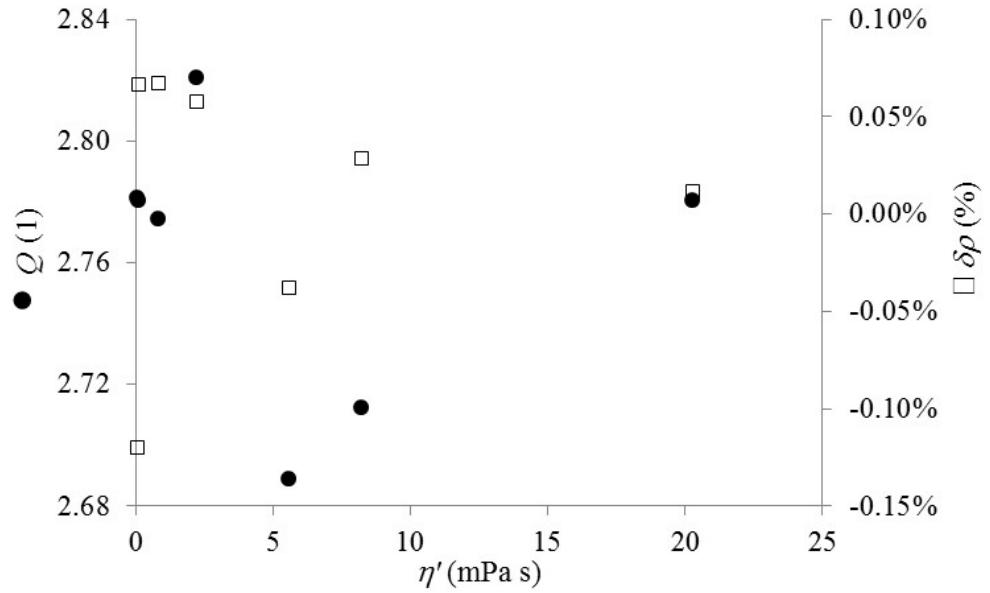

Figure III.28 Graphic representation of oscillation damping values Q (black filled circles) (Table III.27) and the the relative density deviation $\delta\rho$ (i.e., $\rho'_{OD\,c}$ - ρ_{PN}) (white squares) (Table III.26) of the 7 viscoelastic samples, at 20 ºC (Table III.27), against samples' viscous η' portion of the complex viscosity $|\eta^*|$ (Table III.27) determined for frequency f_ρ in frequency sweep tests.

Figure III.29 summarize the loss factor values $tan\,\delta$ (Table III.27) of the 7 viscoelastic samples determined for the frequency f_ρ in frequency sweep tests against the oscillation damping values Q (Table III.27). As the damping oscillation factor Q gives an indication of the ratio of the energy stored (i.e. elastic portion η'', or storage modulus G') by the energy dissipated (i.e. viscous portion η', or loss modulus G'') during the oscillation process, it was expected that Q vary inversely with the materials loss factor $tan\,\delta$ (resulting from G''/G' or η'/η''), however this is not the case as observed in Fig.III.29.

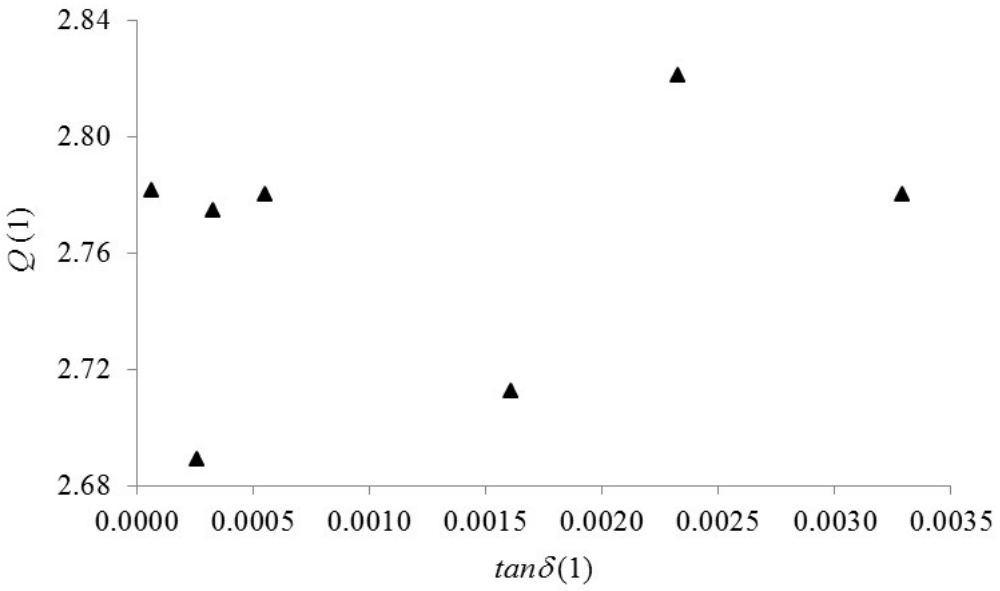

Figure III.29 Graphic representation of oscillation damping values Q against the loss factor $tan\,\delta$ of the 7 viscoelastic samples determined for the frequency f_ρ in frequency sweep tests (Table III.27).

III.B.3.3.3 Relation with samples' time-dependent relaxation/recovery behaviour

The sensibility of density measurements results to samples' time-dependent relaxation/recovery behavior was tested by measuring the same sample at two different relaxation times, i.e., time 0 and after ~ 5 min. From these measurements, all the relevant data given by the density meter, i.e. the first and second oscillations periods, τ_1 and τ_2, respectively and the damping indication parameter Q, were related (Table III.29). These results were also crossed with the results of the thixotropy tests (Table III.30).

Table III.29 Summary of sensibility of density measurements results to the 7 test samples' time-dependent relaxation/recovery behaviour in terms of variation of: density indication $\Delta\rho_{OD;}$ first and second oscillations periods, τ_1 and τ_2 and damping indication parameter Q.

F#	Δt (s)	$\Delta\rho_{OD\ c}$ (%)	$\Delta\rho_{OD\ nc}$ (%)	τ_1 (%)	τ_2 (%)	ΔQ (%)
F1	427	0,0002	0,0001	0,03	0,2	4
F2	353	-0,0004	-0,0003	0	16,7	5
F3	373	-0,0002	-0,0002	0	4,1	4
F4	507	-0,0004	-0,0004	0	4,2	4
F5	449	-0,0002	-0,0001	0	0,0	0
F6	357	0,0002	0,0006	0,14	11,8	0
F7	341	0,0005	0,0006	0,18	0,4	0

Legend: Δ means the difference between the values measured at time ~ 5 min and time 0; $\rho_{OD\ nc}$ - non-viscosity-corrected density value, $\rho_{OD\ c}$ - viscosity-corrected density value.

As was described, samples for which a positive value of resulting hysteresis area (i.e., Diff. in Table III.30) was obtained are thixotropic, and those with a negative value of hysteresis area are rheopectic. So, according to Table III.30, all the samples tested, with exception of F5 (i.e., P(AAm-co-DADMAC) solution), showed a thixotropic behavior, i.e. presented a reduction of its internal structural strength when subjected to a high-shear deformation, that is followed by a complete structural regeneration in the subsequent period of rest. This type of behavior is common for dispersions and gel samples.

Table III.30 Summary of the rotational tests results performed to characterize the thixotropic behavior of the 7 test fluids, at 20 ºC.

F#	Diff* (%)	A_1 (mPa s)	A_2 (mPa s)	A_3 (mPa s)
F1	21	1994000	139700	1739000
F2	34	15840	3,802	10520
F3	3	179500	30,59	174600
F4	37	14250	2,565	8948
F5	-1	2311000	569,4	2327000
F6	47	11220	3,329	5922
F7	44	12150	8,036	6851

Legend: *Resulting hysteresis area: Diff = $[(A_1+A_2-A_3)/(A_1+A_2-A_3)]\cdot 100$; Hysteresis areas A_1, A_2 and A_3 obtained in the tests for the upward shear rate ramp (A_1); constant shear rate (A_2) and downward shear rate ramp. The hysteresis areas values were integrated with rheometer's software (HAAKE RheoWin Datamanager®).

The relation between the density deviations ($\Delta\rho_{OD\ c}$ and $\Delta\rho_{OD\ nc}$) (Table III.29) and the hysteresis area (Table III.30) obtained in the thixotropic behaviour investigation tests is shown in Fig. III.30. Even if not possible to determine a casual relation between these two quantities, they seem to be more related then the first and second oscillations periods, τ_1 and τ_2 and damping indication parameter Q.

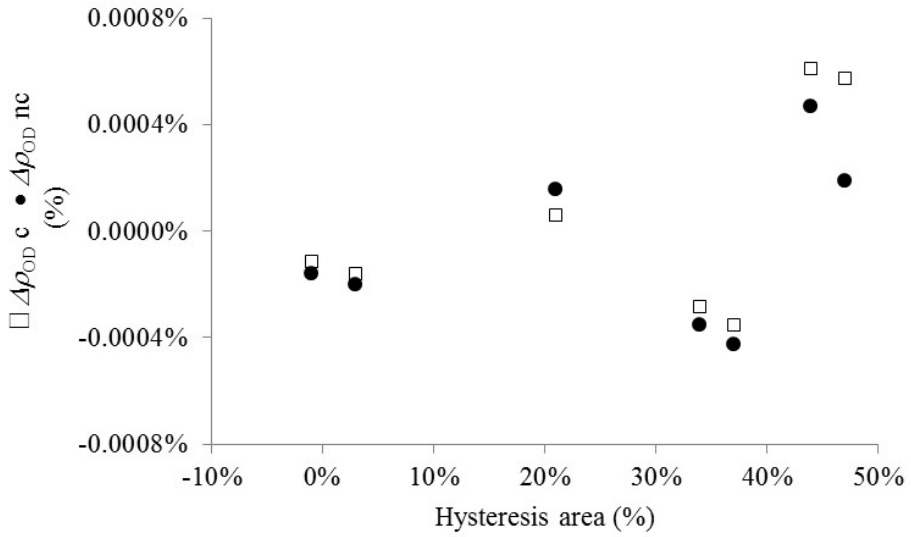

Figure III.30 Graphic representation of relation between density deviations, $\Delta\rho_{OD\,c}$ (white squares) and $\Delta\rho_{OD\,nc}$ (black filled circles), both in %, obtained by an oscillation-type density meter (DMA 5000, Anton Paar) when measuring the density of the 7 viscoelastic samples, and the hysteresis area obtained in time-dependent relaxation/recovery behaviour investigation tests performed at 20 ºC.

III.B.3.4 Conclusions

Oscillation-type density meters have shown to be convenient instruments to measure the density of Newtonian liquids in a wide range of density, viscosity and temperature, with an expanded uncertainty from 0,01 to 0,03 kg m^{-3}, by using a proper calibration curve, since the deviations due to viscosity may lead to a maximum density deviation of 0,62 kg m^{-3} in the viscosity interval up to 795 mPa s (Furtado *et al.*, 2017).

This study showed that the knowledge of samples' viscoelasticity effect on density measurements results using this kind of density meters is limited by the uncertainty of the pycnometer method 0,010 %, since these density meters can produce density results with much lower relative uncertainty (~0,0053 %). So, alternative method needs to be develop/improved as alternative to pycnometer method. An adapted hydrostatic method could be a good approach to be explored in further studies.

As already suspected in earlier studies (Furtado *et al.*, 2017), these results are other indication that oscillation of density meter cell, during density measurements, can cause modifications in the internal structure and arrangement of the molecules of the viscoelastic samples, leading to a non-well described density deviation trend, which may be essentially due to the elastic portion of the viscoelastic behavior of these samples. All the viscoelastic samples tested showed a damping factor, $tan\ \delta < 1$ (G' > G''), indicating that all the tested samples are in a solid-like state, i.e., showing a behaviour of viscoelastic solids at the frequency f_ρ produced in the density meter even when they are in liquid-like state in lower frequencies regimes (PVA and Borax, hydroxyethyl-cellulose, P(AAm-co-DADMAC) solutions and starch dispersion).

The frequency/temperature shift (FTS) method allows to extent various rheological parameters beyond the actual frequency range measured, within which no measuring data are available (Mezger, 2014;

Williams *et al*.,1955). And this could be a good alternative to the extrapolation methodology used in this paper to estimate the storage modulus G'(f_ρ) and loss modulus and G''(f_ρ) values, at the frequency value f_ρ i.e., oscillation frequency produced in the oscillation-type density meter during density measurements (usually in the frequency interval of 273-279 Hz for liquids samples), gave information regarding the dependence of the dynamic viscosity, η', with the oscillation frequency, f, up to 100 Hz, the upper limit of the measuring geometries used. However, FTS method is only applied to thermo-rheologically simple materials, not the case of dispersions and gels. For this reason, and since the mechanical characterization and the viscoelastic properties of fluids under such a high frequency value is not feasible by means of rheometry due to instrumental limitations, other methodologies might be use, e.g. by indirect method with Dynamic Mechanic Analysis (DMA) (ISO 4664-1:2011) up to 100 Hz and then for frequencies exceeding 1 kHz with a shift factor based on the Williams–Landel–Ferry (WLF) equation (Ferry, 1980), or by a direct method called Base Excitation Resonant Mass (BERM) (Darlow & Zorzi, 1981; (Shoyama & Fujimoto, 2018) suitable for measuring dynamic properties up to 1000 Hz (ISO 4664-1:2011), etc. However, the laboratory did not have access to these methodologies.

It was also observed that samples' time-dependent relaxation/recovery behaviour may produce density deviations up to 0,0006 % (for a resulting hysteresis area of 44 %) that showed no significance as the uncertainty of density determinations was ~0,0053 %.

As planned in the 17RPT02-*rhoLiq* EMPIR Project the viscoelasticity effect on density results need to be study by a measurement method with a low uncertainty such as the hydrostatic weighing. This may lead to means of comparison that will be able to use the oscillation-type density meters in their maximum metrological capability also with non-Newtonian samples. Or even to know the real limitation of this measuring instrument, to give the most accurate insights for reference documents, such as standards and guides.

Despite not being possible of establish a casual relation between samples' viscoelasticity and density errors, the results of this study gave the information that viscoelastic samples can produce density errors up to 0,18 % (when for the maximum obtained for the high viscosity samples was 0,069 % (Furtado *et al.*, 2017) with an uncertainty 0,011 % (limited by the uncertainty of the reference density measurement method used).

III.B.4 VISCOELASTICITY TESTS IN DMA 5000 M AND DMA HP

III.B.4.1 Materials and Methods

III.B.4.1.1 Test fluids

Two oscillation-type density meters, one DMA 5000M and a DMA HP, from Anton Paar, were tested with 4 non-Newtonian liquids samples (2 oil-based (NNTF1) samples and 2 water-based (NNTF2) polymeric solutions) with dynamic viscosity, at 23 °C, covering the interval from 50 to 2100 mPa·s. NNTF1 samples consisted in solutions of hydrogenated Isoprene Styrene copolymer (at 3 wt % and 6 wt %) in n-paraffin. NNTF2 samples consisted in ultra-pure water based solution of poly(acrylamide-co-dially dimethyl ammonium chloride (at 4 wt % and 8 wt %). The polymeric solutions showed different rheological characteristics which were also determined.

III.B.4.1.1 Viscoelastic samples characterization

III.B.4.1.1.1 Viscosity and density

The dynamic viscosity of the non-Newtonian liquids was measured in an MCR 502 rheometer from Anton Paar, using a coaxial-cylinder (CC27) measuring geometry. These measurements were performed at 23 °C, in controlled shear rate (CSR or CR) mode, for a constant shear rate of 30 s^{-1}.

The reference density of these liquids was measured by gravimetric method with a Gay-Lussac pycnometer, according to ISO 2811-1 (2011). The filling of the pycnometer with the non-Newtonian samples was performed with a peristaltic pump (ISM831C, ISMATEC) in order to avoid the formation of air bubbles. A Tygon HC F-4040-A tube (ISMATEC), specially formulated for hydrocarbons-based applications was used.

III.B.4.1.1.2 Rheological characterization

As the viscosity of non-Newtonian liquids changes with the oscillation frequencies produced by oscillation-type density meters, the rheological behaviour of the non-Newtonian liquids tested was investigated, with a rheometer MCR 502 (Anton Paar), to provide a deeper insight into the damping effects produced by these liquids. The measuring system used to perform these measurements was a Searle type coaxial cylinder (CC27) with a cup (i.e. the outer cylinder with a close base) with 26,66 mm of diameter, and a bob (i.e. the inner cylinder) with 28,92 mm of diameter. The temperature of the sample on the measuring system was controlled by an electrical heating and a cooling element (Peltier element), C-PTD200 from Anton Paar. The temperature of rheometer´s motor was regulated by a water thermostat (F6 and C25, HAAKE) at 23 °C. The temperature of the sample was measured indirectly by means of a temperature sensor incorporated in the temperature-control jacket surrounding the measuring system (C-PTD200, Anton Paar) together with a platinum resistance thermometer, connected to a data acquisition unit 34970A (Agilent), placed inside the hole of the cup of the coaxial-cylinder (CC27) measuring geometry (Fig. III.31). The temperature was measured continuously during the measurements.

Prior to the rheological measurements, and after charging the measuring geometry with the sample, the samples were left to recover any thixotropic structure and to achieve again the reference temperature. This time depended on the nature of the sample (ISO 3219:1993).

All the tests were performed at reference temperature of 23 ºC and ambient pressure, with exception of the temperature dependency test. Each test was made in triplicate.

The amplitude sweep tests were performed with a constant angular frequency (ω) of 10 rad/s (1,59 Hz) in controlled-shear-deformation (CSD) in the deformation rate (γ) interval from 0,01 % to 100 % (log. ramp).

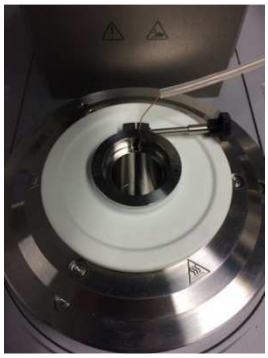

Figure III.31 Platinum resistance thermometer, connected to a data acquisition unit 34970A (Agilent), placed inside the hole of the cup of the coaxial-cylinder (CC27) measuring geometry, in the MCR 502 (Anton Paar) rheometer.

For the subsequent oscillatory tests, i.e. the frequency sweep, it was required that the measurements are carried out at strain levels within the linear viscoelastic (LVE) region. The amplitude sweeps tests were also used for determining yield stress, τ_y, (corresponding to the lowest shear stress, above which a sample shows an irreversible structural change; below the yield point it shows reversible elastic or viscoelastic behaviour) and flow stress τ_f (i.e. critical shear stress value above which a sample rheologically behaves like a liquid; with G' > G'', below the flow point it shows elastic or viscoelastic behaviour).

Frequency sweeps generally serve the purpose of describing the time-dependent behaviour of a sample in the non-destructive deformation range. High frequencies are used to simulate fast motion on short timescales, while low frequencies simulate slow motion on long timescale or at rest. In this case, the aim of using this test to investigate the effect of the oscillation frequency (occurred during density measurements) on the rheological properties of the viscoelastic samples (by determining sample's viscosity at that frequency).

The frequency sweep tests were performed with a deformation rate (γ) of 1 % (or a deformation rate value chosen from the linear viscoelastic (LVE) range pre-determined in the amplitude sweep test) in the angular frequency interval (ω) from 100 rad/s to 0,01 rad/s (15 Hz to 0,0159 Hz) (log. ramp).

III.B.4.2 Results and Discussion

III.B.4.2.1 Viscoelastic samples characterization

III.B.4.2.1.1 Viscosity and density

The values of dynamic viscosity, η and density, ρ, at 23 ºC, of the non-Newtonian liquids tested are presented in Table III.31.

Table III.31 Dynamic viscosity η and density values ρ, at 23 ºC, of the non-Newtonian liquids tested.

Non-Newtonian liquids	$\eta_{23\,°C}$ (1) (mPa·s)	$\rho_{23\,°C}$ (2) (kg·m^{-3})	U_ρ (kg·m^{-3})
NNTF1 (6 wt %)	774,99	749,781	0,075
NNTF1 (3 wt %)	48,68	744,810	0,074
NNTF2 (8 wt %)	2087,10	1016,70	0,10
NNTF2 (4 wt %)	308,55	1006,33	0,10

Legend: (1) The dynamic viscosity was measured at 23 °C, in CR mode at constant shear rate of 30 s^{-1}, in a MCR 502 rheometer from Anton Paar using a CC27 measuring geometry; (2) The reference density was measured by gravimetric method with a Gay-Lussac pycnometer; U – expanded uncertainty for a coverage factor k = 2.

III.B.4.2.1.2 Rheological characterization

III.B.4.2.1.2.a NNTF1

As can be seen in Fig. III.32, in the LVE region up to 1 %, the storage modulus G' (represented by the squares) is around one decade higher than the loss modulus G'' (represented by the triangles), G' > G''. Therefore, the NNTF1 sample displays a gel-liked structure, and can be termed as a viscoelastic solid material. This fact might be related with the links inside the material, for instance chemical bonds or physical-chemical interactions.

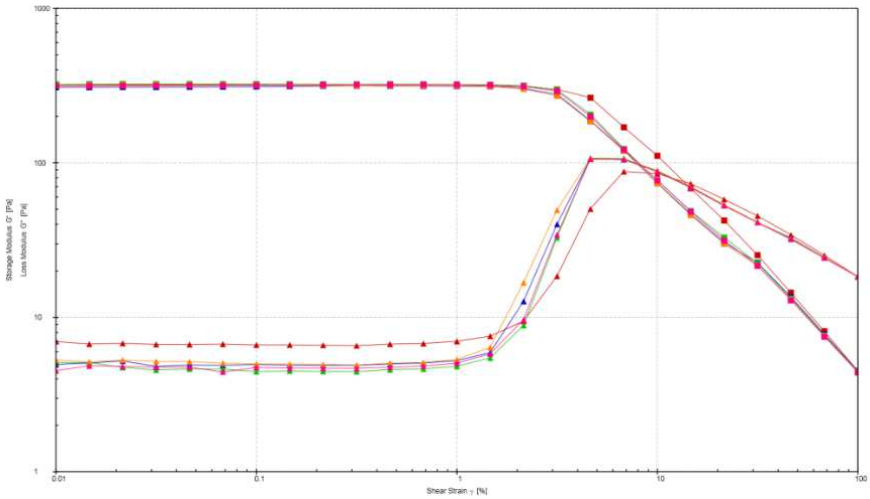

Figure III.32 Results of the amplitude sweep test of NNTF1, at 23 C, performed in a CC27, with a constant angular frequency, ω of 10 rad/s in CSD in the deformation rate, γ interval from 0,01 % to 100 %. Legend: squares – G' storage modulus; triangles - G'' loss modulus.

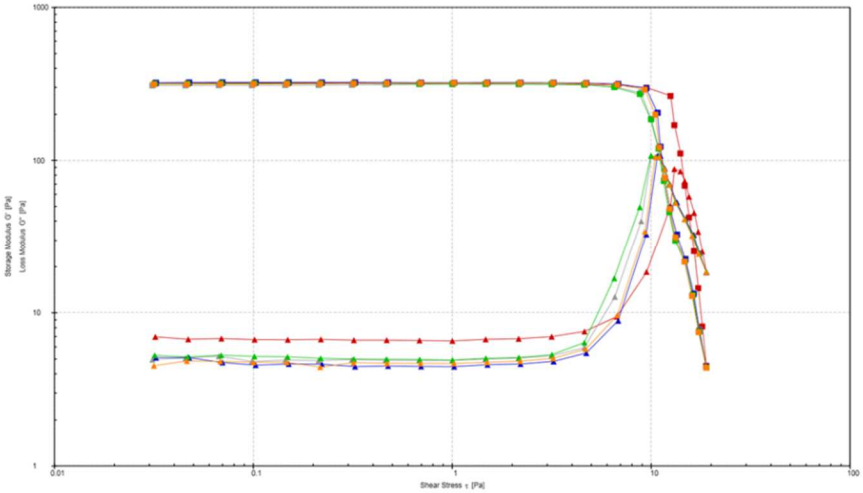

Figure III.33 Results of the amplitude sweep test in terms of shear stress (τ) of NNTF1, at 23 C, performed in a CC27, for a constant angular frequency (ω) of 10 rad/s in CSD in the deformation rate (γ) interval from 0,01 % to 100 %. Legend: squares – G' storage modulus; triangles - G'' loss modulus.

In the LVE region, NNTF1 sample shown a G' > G'', being in solid or gel state, after that, in the linearity limit presented a yield point τ_y of around 3 Pa and a flow point τ_f of around 10,2 Pa, corresponding to the crossover point G' = G''. For higher shear, G'' > G, and NNTF1 sample was in fluid state (Fig. III.33).

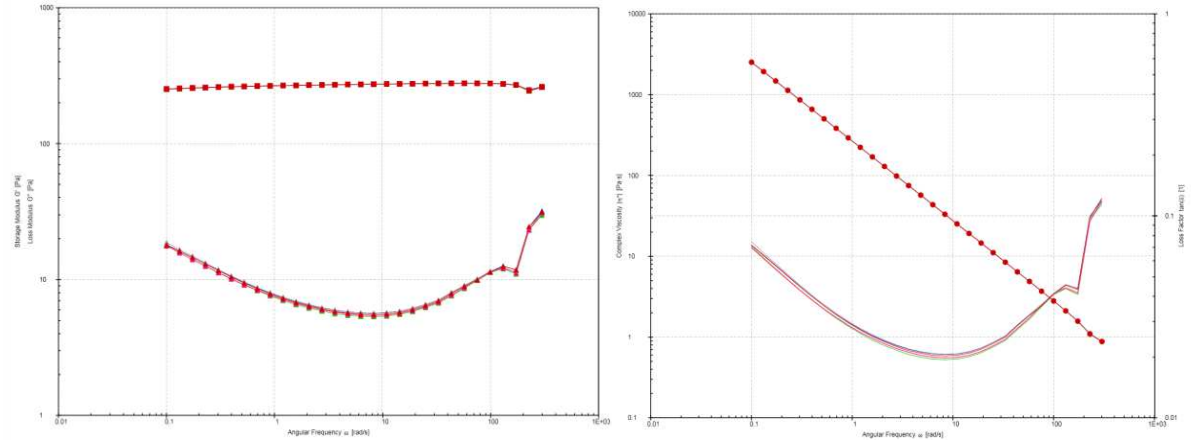

Figure III.34 Results of the frequency sweep test of NNTF1, at 23 C, performed in a CC27, with a constant deformation rate (γ) of 1 % in the angular frequency interval (ω) from 100 rad/s to 0,01 rad/s. Legend of 1st chart: squares – G' storage modulus; triangles - G'' loss modulus; 2nd chart: circles - $|\eta^*|$ complex viscosity; tan(δ) loss factor.

In the frequency sweep performed for a deformation rate γ of 1 % NNTF1 sample showed G' > G'' indicative of a gel-like structure (1st chart of Fig. III.34). The loss modulus G'' (triangles in the 1st chart of Fig. III.34) decreases with the increase of the angular frequency up to ~10 rad/s and then start to increase. On the other hand, the storage modulus G' (squares in the 1st chart of Fig. III.34) is mainly constant in the entire range of angular frequency tested (squares in the 1st chart of Fig. III.34). The complex viscosity $|\eta^*|$ of NNTF1 sample (circles in the 2nd chart of Fig. III.34) decreases constantly with the angular frequency ω.

III.B.4.2.1.2.b NNTF1 diluted 1:1 m:m

The results of the amplitude sweep of NNTF1 diluted show that the loss modulus G'' (represented by triangles) is higher than the storage modulus G' (represented by squares), G'' > G', in all range of shear strain tested (Fig. III.35), meaning that this sample presents mainly a liquid structure and can be termed as a viscoelastic liquid.

The reason for this might be related with the low concentration of polymer in this solution leading thus to a low number of entanglements among polymer chains. No flow point or yield point were therefore observed (Fig. III.36). Also, to be noticed, the scattering of G'' values caused by the approximation to rheometer's lower limit of sensitivity.

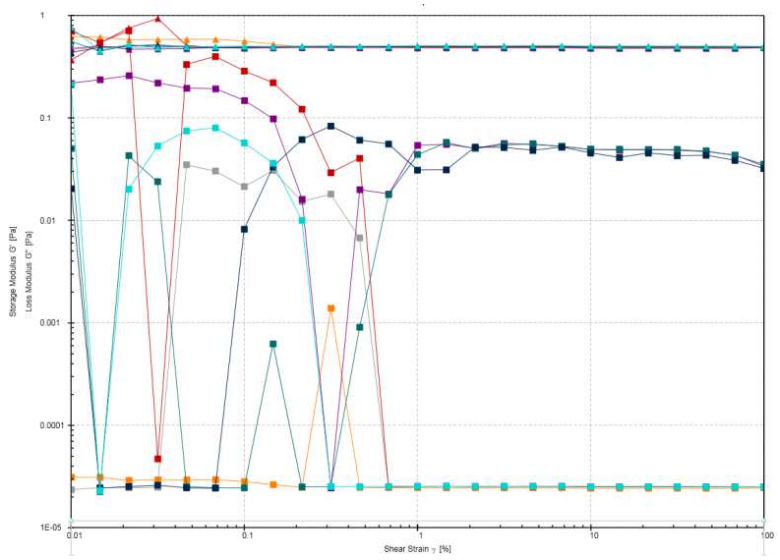

Figure III.35 Results of the amplitude sweep test of NNTF1 diluted 1:1 m:m, at 23 C, performed in a CC27, with a constant angular frequency (ω) of 10 rad/s in CSD in the deformation rate (γ) interval from 0,01 % to 100 %. Legend: squares – G' storage modulus; triangles - G'' loss modulus.

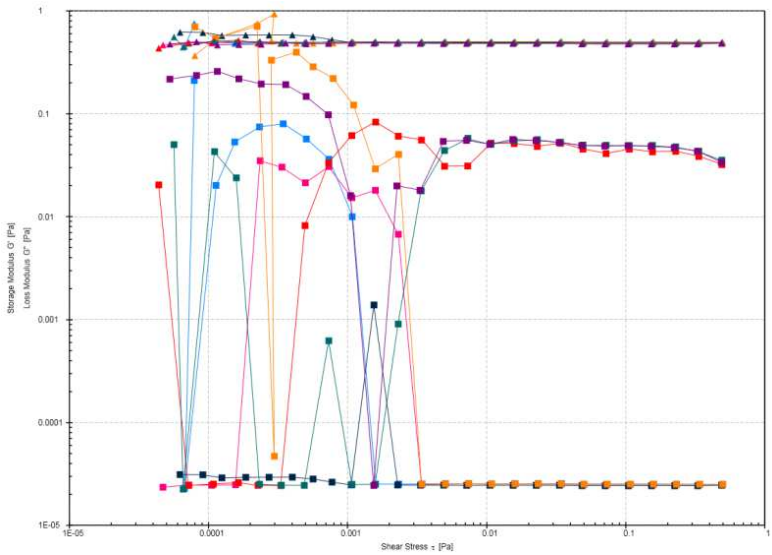

Figure III.36 Results of the amplitude sweep test in terms of shear stress (τ) of NNTF1 diluted 1:1 m:m, at 23 C, performed in a CC27, with a constant angular frequency (ω) of 10 rad/s in CSD in the deformation rate (γ) interval from 0,01 % to 100 %, with a MCR 502 (Anton Paar) rheometer. Legend: squares – G' storage modulus; triangles - G'' loss modulus.

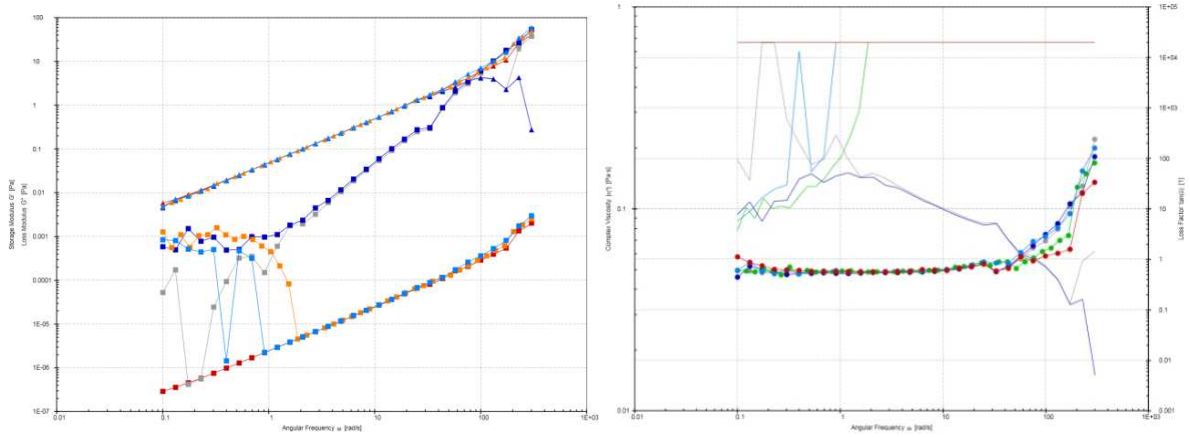

Figure III.37 Results of the frequency sweep test of NNTF1 diluted 1:1 m:m, at 23 C, performed in a CC27, with a constant deformation rate (γ) of 1 % in the angular frequency interval (ω) from 100 rad/s to 0,01 rad/s. Legend of 1st chart: squares – G' storage modulus; triangles - G'' loss modulus; 2nd chart: circles - $|\eta^*|$ complex viscosity; tan(δ) loss factor.

In the frequency sweep performed for a deformation rate γ of 1 % the NNTF1 diluted shown a G'' > G' indicative of a liquid behaviour (1st chart of Fig. III.37). As the angular frequency ω increases the G'' and G' also increase linearly (1st chart of Fig. III.37). The complex viscosity $|\eta^*|$ (circles in the 2nd chart of Fig. III.37) is mainly constant in the angular frequency ω range tested having an increase for angular frequencies higher than 30 rad/s.

III.B.4.2.1.2.c NNTF2

As can be seen in Fig. III.38 in the LVE region up to 10 %, the storage modulus G' (represented by the squares) is higher than the loss modulus G'' (represented by the triangles), G' > G'', the NNTF2 sample shows a gel-like structure, and can be termed a viscoelastic solid material. This might be due to the presence of links inside the material, for example chemical bonds or physical-chemical interactions.

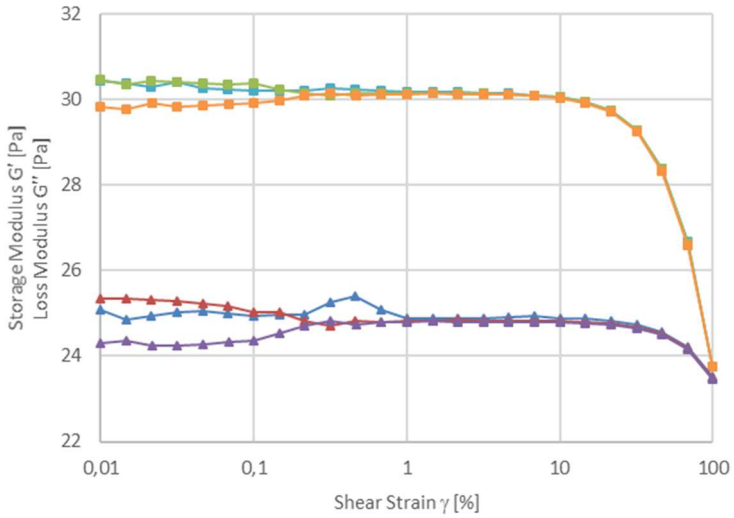

Figure III.38 Results of the amplitude sweep test of NNTF2, at 23 C, performed in a CC27, with a constant angular frequency (ω) of 10 rad/s in CSD in the deformation rate (γ) interval from 0,01 % to 100 %. Legend: squares – G' storage modulus; triangles - G'' loss modulus.

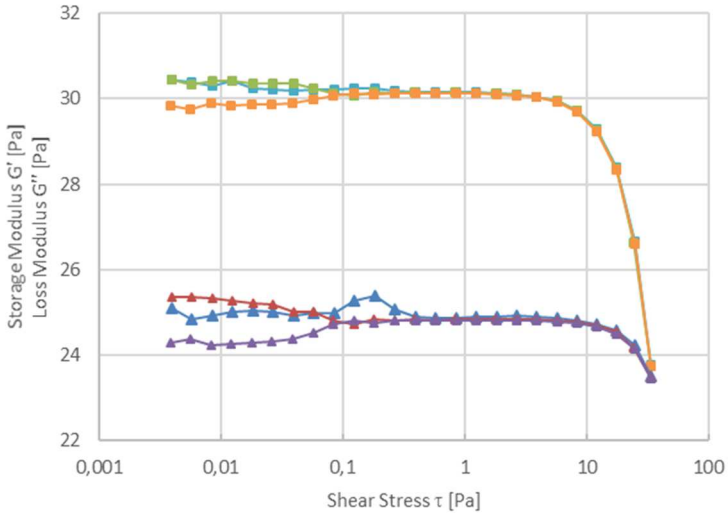

Figure III.39 Results of the amplitude sweep test in terms of shear stress (τ) of NNTF2, at 23 C, performed in a CC27, with a constant angular frequency (ω) of 10 rad/s in CSD in the deformation rate (γ) interval from 0,01 % to 100 %, with a MCR 502 (Anton Paar) rheometer. Legend: squares – G' storage modulus; triangles - G'' loss modulus.

In the LVE region, the NNTF2 sample shown a G' > G'', being in solid or gel state, after that, in the linearity limit presented a yield point τ_y of around 4 Pa and a flow point τ_f of around 33,4 Pa, corresponding to the crossover point G' = G''. For higher shear, G'' > G, and the NNTF2 sample was in liquid state (Fig. III.39).

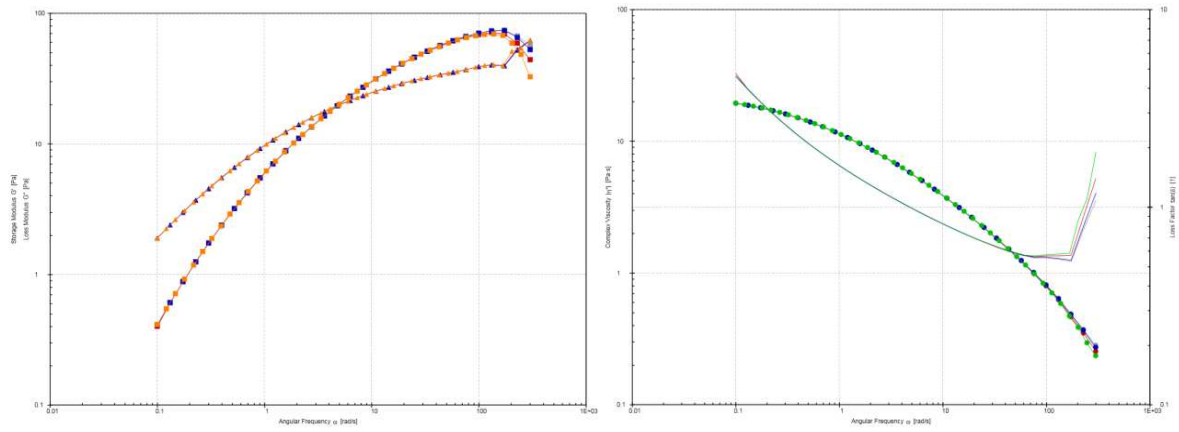

Figure III.40 Results of the frequency sweep test of NNTF2, at 23 C, performed in a CC27, with a constant deformation rate (γ) of 1 % in the angular frequency interval (ω) from 100 rad/s to 0,01 rad/s. Legend of 1st chart: squares – G' storage modulus; triangles - G'' loss modulus; 2nd chart: circles - $|\eta^*|$ complex viscosity; tan(δ) loss factor.

In the frequency sweep performed for a deformation rate γ of 1 %, within the LVE region, the NNTF2 shown a typical behaviour of an uncrossed polymer; in the lower frequency range, G'' > G' with predominantly viscous behaviour; in the upper frequency range, G' > G'' with prevailing elastic properties (1st chart of Fig. III.40). Thus, in between, there is the crossover point G' = G'' at ω = 3 rad/s (1st chart of Fig. III.40). The complex viscosity $|\eta^*|$ of NNTF2 (circles in the 2nd chart of Fig. III.40) decreases parabolically with the angular frequency ω.

III.B.4.2.1.2.d NNTF2 diluted 1:1 V:V

The results of the NNTF2 diluted amplitude sweep shown that the loss modulus G'' (represented by the triangles) is higher than the storage modulus G' (represented by squares), G'' > G', in all range of shear strain tested (Fig. III.41), meaning that this sample presents mainly a liquid structure and can be termed as a viscoelastic liquid. The reason for this might be related with the absence of bonds between the individual polymer molecules, i.e. uncross linked polymer molecules that are entangled but not chemically crosslinked, or also because of the low concentration of polymer in this solution leading thus to a low number of entanglements among polymer chains. No flow point or yield point were therefore observed (Fig. III.42).

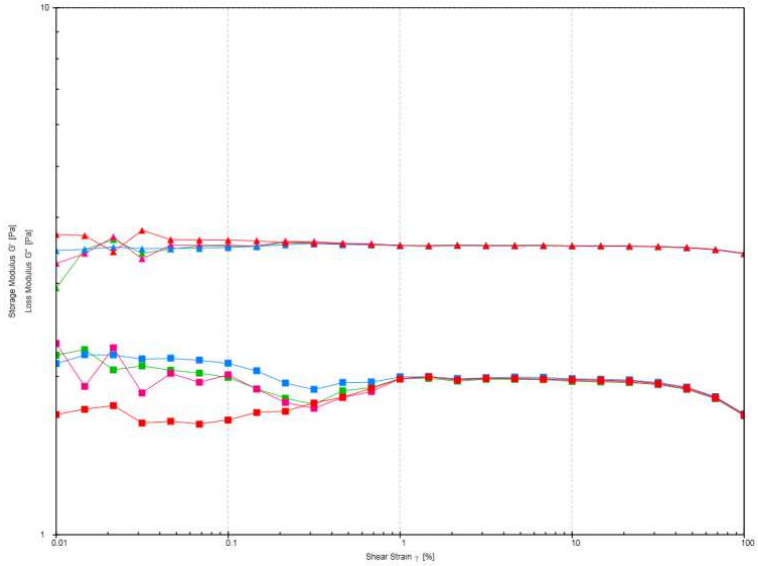

Figure III.41 Results of the amplitude sweep test of NNTF2 diluted 1:1 V:V, at 23 C, performed in a CC27, with a constant angular frequency (ω) of 10 rad/s in CSD in the deformation rate (γ) interval from 0,01 % to 100 %. Legend: squares – G' storage modulus; triangles - G'' loss modulus.

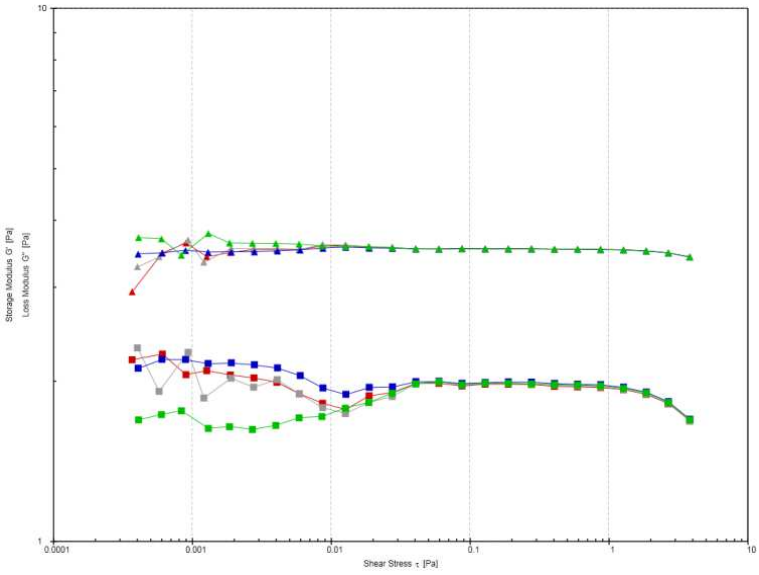

Figure III.42 Results of the amplitude sweep test in terms of shear stress (τ) of NNTF2 diluted 1:1 V:V, at 23 C, performed in a CC27, with a constant angular frequency (ω) of 10 rad/s in CSD in the deformation rate (γ) interval from 0,01 % to 100 %. Legend: squares – G' storage modulus; triangles - G'' loss modulus.

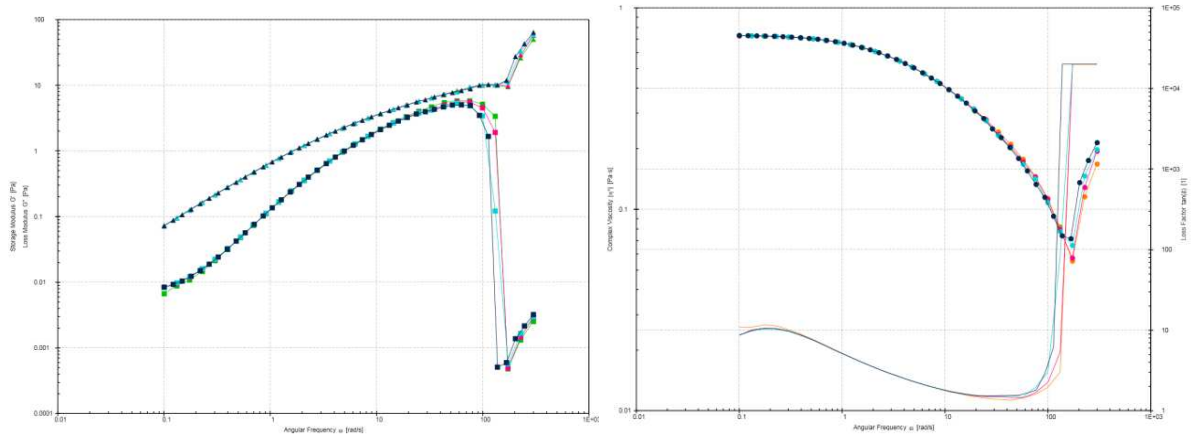

Figure III.43 Results of the frequency sweep test of NNTF2 diluted 1:1 V:V, at 23 C, performed in a CC27, with a constant deformation rate (γ) of 1 % in the angular frequency interval (ω) from 100 rad/s to 0,01 rad/s. Legend of 1st chart: squares – G' storage modulus; triangles - G'' loss modulus; 2nd chart: circles - $|\eta^*|$ complex viscosity; tan(δ) loss factor.

In the frequency sweep performed for a deformation rate γ of 1 % the NNTF1 diluted shown G'' > G' indicative of a liquid behaviour (1st chart of Fig. III.43). The loss modulus G'' (triangles in the 1st chart of Fig. III.43) increases with the increase of the angular frequency having a faster increase for angular frequencies higher than ~150 rad/s. On the hand, the storage modulus G' (squares in the 1st chart of Fig. III.43) also increase up to ~100 rad/s and then has an abrupt decrease up to ~200 rad/s and then start to increase again. The complex viscosity $|\eta^*|$ (circles in the 2nd chart of Fig. III.43) decreases parabolically with the angular frequency ω up to ~200 rad/s and then start to increase.

III.B.4.2.2 Viscoelasticity-induced errors

Density indication values, dnc and d, and density relative indication errors, $\delta\, dnc$ and $\delta\, d$, obtained, at 23 ºC, for the non-Newtonian liquid (NNL) samples are resumed in Tables III.32 and III.33, respectively.

Table III.32 Resume of the density indication values, dnc and d (in kg·m^{-3}), of a DMA 5000M and a DMA HP (Anton Paar) oscillation-type density meters obtained with non-Newtonian liquid (NNL) samples tested at 23 ºC.

Non-Newtonian liquids	DMA 5000M*					DMA HP*	
	d_{nc} (kg·m^{-3})	U_{dnc} (kg·m^{-3})	d (kg·m^{-3})	U_d (kg·m^{-3})	$(dnc - d)$ (%)	dnc (kg·m^{-3})	U_{dnc} (kg·m^{-3})
NNTF1 (6 wt %)	752,159	0,045	751,679	0,038	0,064	751,299	0,030
NNTF1 (3 wt %)	747,006	0,007	746,802	0,007	0,027	746,811	0,022
NNTF2 (8 wt %)	1017,789	0,061	1017,398	0,061	0,038	1017,742	0,020
NNTF2 (4 wt %)	1007,821	0,060	1007,623	0,060	0,020	1007,906	0,020

Legend: dnc – density indication not corrected for viscosity damping; d – density; U – expanded uncertainty for a coverage factor k = 2; *from Anton Paar.

Table III.33 Resume of the density relative indication errors, $\delta' dnc$ and $\delta' d$ (in %), of a DMA 5000 M and a DMA HP (Anton Paar) oscillation-type density meters obtained with non-Newtonian liquid (NNL) samples tested at 23 ºC

Non-Newtonian liquids	DMA 5000M*		DMA HP*
	$\delta' dnc$ (%)	$\delta' d$ (%)	$\delta' dnc$ (%)
NNTF1 (6 wt %)	0,317	0,253	0,202
NNTF1 (3 wt %)	0,295	0,268	0,269
NNTF2 (8 wt %)	0,107	0,068	0,102
NNTF2 (4 wt %)	0,148	0,128	0,156
NNTF1 (6 wt %)	0,317	0,253	0,202

Legend: dnc – density indication not corrected for viscosity damping; d – density; *from Anton Paar.

In general, the density relative indication errors obtained for the non-Newtonian liquids were higher than the ones obtained for Newtonian liquids, in both density meters (Fig. III.44 and III.45, respectively), specifically 2,3-fold for the DMA 5000M and 1,3-fold for the DMA HP (Tables III.32 and III.33, respectively). It was also observed that the mean density relative indication error of the DMA HP is 1,6-fold higher compared to the ones obtained and presented in previous sub-chapters with DMA 5000M for Newtonian liquids.

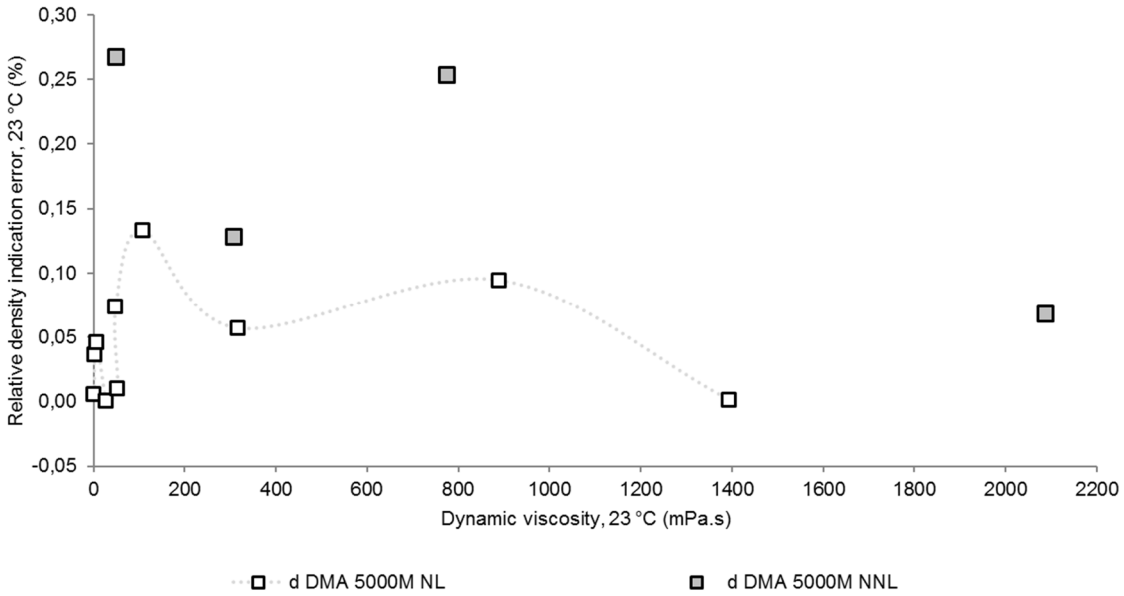

Figure III.44 Density relative indication errors results (in %) obtained, at 23 ºC, with a DMA 5000 M (Anton Paar) oscillation-type density meter, against the dynamic viscosity (in mPa·s) of the set of Newtonian (NL – represented by white filled squares) and of non-Newtonian (NNL – represented by grey filled squares) liquids samples tested.

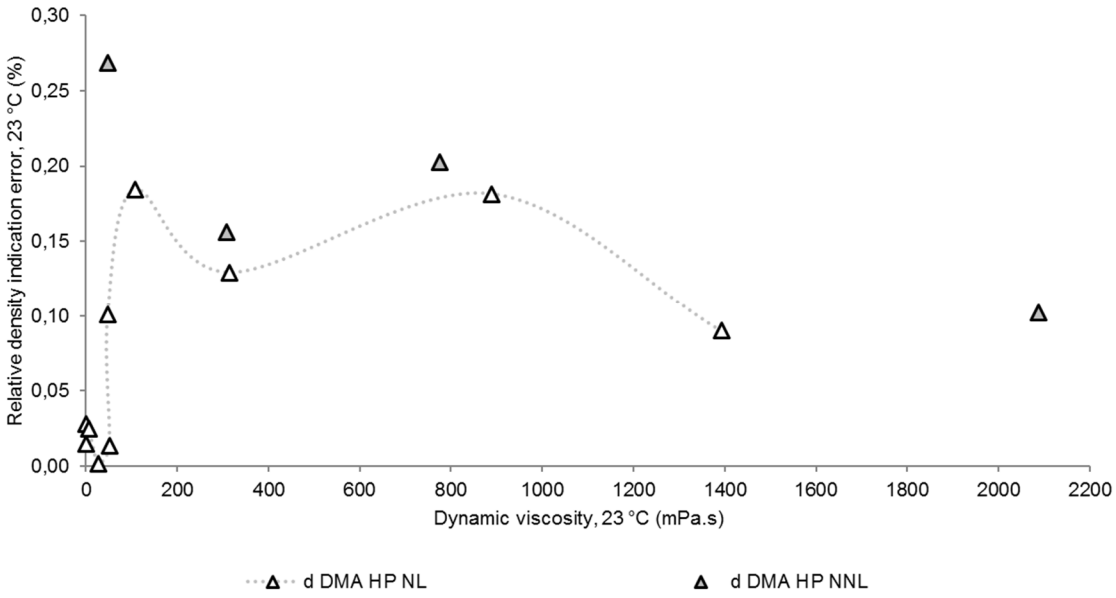

Figure III.45 Relative density indication errors results (in %) obtained, at 23 ºC, with a DMA HP (Anton Paar) oscillation-type density meter, against the dynamic viscosity (in mPa·s) of the set of Newtonian (NL – represented by white filled squares) and of non-Newtonian (NNL – represented by grey filled squares) liquid samples tested.

The difference between the two density indications ($dnc - d$) obtained by the DMA 5000 M density meter have been proofed in former studies (Furtado *et al.*, 2016) to have a relation with the viscosity of Newtonian liquids, when unbranched hydrocarbons and mineral oils were tested. As can be seen in Fig. III.46, with the data presented in Tables III.32 and III.33, the ($dnc - d$) values obtained for non-Newtonian liquids (represented by the grey filled circles) do not describe the same curve as the ($dnc - d$) values obtained for Newtonian liquids (represented by the black filled circles). For Newtonian liquids with viscosity above 315 mPa·s a plateau value of about 0,07 % was met for ($dnc - d$). As no Newtonian liquids with viscosity around 2087 mPa·s were tested, the ($dnc - d$) values were extrapolated in the curve being represented by the dashed red line. It was expected that for higher viscosities the difference between the two density indications would be constant as was observed for viscosities values above 315 mPa·s, however this was not the case as seen in Fig. III.45. The ($dnc - d$) values obtained for both solutions of NNTF1, 3 wt % with $\eta_{23\,^{o}C}$ ~49 mPa·s and 6 wt % with yield point and $\eta_{23\,^{o}C}$ ~775 mPa·s, showed values close to the ones obtained for Newtonian liquids with the same viscosity. On the other hand, the ($dnc - d$) values obtained for both solutions of NNTF2, 4 wt % with $\eta_{23\,^{o}C}$ ~309 mPa·s and 8 wt % with yield point and $\eta_{23\,^{o}C}$ ~2087 mPa·s, were around 3,5 and 2,4-fold lower, respectively, than the ones obtained with the Newtonian liquids. Despite no physical meaning could be attributed to these findings, one might conclude that non-Newtonian liquids cannot be included in the same rules used to predict viscosity from ($dnc - d$) values.

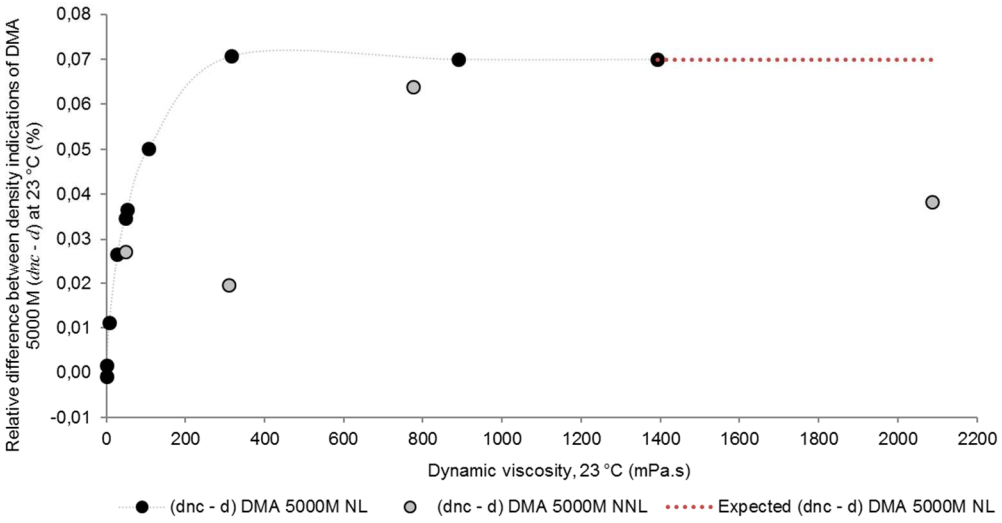

Figure III.46 Relative difference between density indications, ($dnc - d$) in %, against dynamic viscosity of the Newtonian (NL – black circles) and non-Newtonian (NNL – grey filled circles) liquids samples tested, at 23 ºC, with a DMA 5000 M (Anton Paar) density meter. (Legend: dnc – density indication not corrected for viscosity damping; d – density).

For viscosities values below 300 mPa·s, particularly for viscosities from 0,7 mPa·s to 107 mPa·s, Fig. III.47 shows that the data obtained can be fitted with the generic equation given by Furtado *et al.* (2017) as describing the dynamic viscosity of a Newtonian liquid from the density indications ($dnc - d$) of DMA 5000 M density meter from Anton Paar. The maximum residuals expected for this equation are 21 % in the viscosity interval from 0,7 to 7 mPa·s and 3,1 % in the viscosity interval 7 to 220 mPa·s. Despite the obtained residuals agreed with these values, dodecane (1,05 mPa·s) and the oil 50B (48,10 mPa·s) presented residuals above these values, 64,2 % and 8,3 %, respectively. These facts can be attributed to undetected experimental errors, for instance the possible presence of air bubbles in the sample that will lead to an incorrect higher viscosity and therefore to a higher difference between the density indications ($dnc - d$) given by the DMA 5000M density meter.

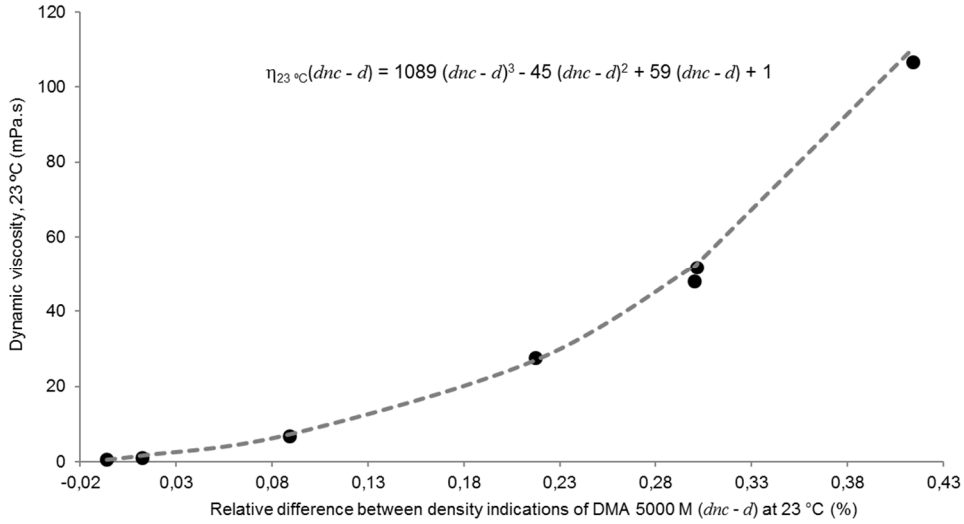

Figure III.47 Curve of dynamic viscosity against relative difference between density indications ($dnc - d$), at 23 ºC, obtained with the Newtonian liquids tested in the DMA 5000 M density meter, in the viscosity interval from (0,7 to 107) mPa·s. The grey dashed line represents the curve of the equation given in the chart. This equation was given by Furtado *et al.* (2016) as describing the dynamic viscosity of a Newtonian liquid from the density indications ($dnc - d$) of DMA 5000 M density meter.

III.B.4.3 Conclusions

As viscosity of non-Newtonian liquids changes with the oscillation frequencies produced by oscillation-type density meters, the rheological behaviour of the non-Newtonian liquids tested was investigated with a rheometer MCR 502 (Anton Paar). The oscillation periods of air and ultra-pure water were measured in an oscillation-type density meter (DMA 5000, Anton Paar) at 23 °C. For air an oscillation frequency of 373,69 Hz was measured, corresponding to a density of approximately 1,2 $kg \cdot m^{-3}$, and for ultra-pure water an oscillation frequency of 270,27 Hz, corresponding to a density of 998,203 $kg \cdot m^{-3}$. The interval of angular frequency analysed with the MCR 502 (Anton Paar) rheometer was from 1,6 10^{-9} Hz to 15 Hz. In terms of shear rate, an oscillation frequency of 300 Hz in the measuring cell of the oscillation-type density meter will correspond to a shear rate of 0,3 s^{-1}.

In the oscillation tests NNTF1 and NNTF2 show a rheological behaviour of a gel-like structure, the first with higher yield and flow points than the second one. This fact might be related with the higher deviation in the density indication of both density meters (DMA 5000M and DMA HP from Anton Paar) when comparing the results with Newtonian liquids with the same viscosity. On the other hand, both diluted solutions of NNTF1 and NNTF2 show a rheological behaviour typical for uncross linked polymeric solutions with a predominant viscous component. These two samples show lower density errors in the density meters measurements, higher than the ones obtained for Newtonian liquids, but still much lower than the non-diluted polymeric solutions.

Despite the low number of different non-Newtonian samples tested, and the fact of the oscillation tests were made for a maximum angular frequency of 15 Hz (the limit of this rheometer is 50 Hz), and the oscillation frequency in the density meter measuring cell be about 300 Hz, was possible to conclude that the oscillation of the density meter cell during the measurements of density may cause modifications in the internal structure and arrangements of the molecules of the non-Newtonian liquids. Further investigations should be conducted for an angular frequency up to 50 Hz.

In general, in both density meters the relative density indication errors obtained for the non-Newtonian liquids were higher than the ones obtained for Newtonian liquids. Despite no physical meaning could be attributed to these findings, it must be concluded that non-Newtonian liquids cannot be included in the same rules used to predict viscosity from ($dnc - d$) values.

III.C

PRESSURE-INDUCED ERRORS

Density is one of the most important properties in chemical industry. Accurate experimental density of pure fluids and their mixtures, as function of pressure and temperature, are required for many physical and chemical applications. The direct evaluation of its derived mechanical coefficients (isothermal compressibility and isobaric expansibility), the establishment of reliable equations of state (EOS) and the calculation of other important properties such as the molar isobaric heat capacity or dynamic viscosity (on the basis of kinematic viscosity measurements), are some of the intermediate steps leading to important scientific and technological applications, namely in heat and mass transfer in moving fluids (Lampreia & Castro, 2011). For instance, isothermal compressibility coefficients are required in solving many reservoir engineering problems, including transient fluid flow problems, and they are also required in the determination of the physical properties of the liquid fluids, with an intense and crucial use in oil industry (Ahmed, 2018).

Some studies have been undertaken to predict the metrological properties of these instruments at high-pressure (Lagourette *et al.*, 1992; Outcalt & McLinden, 2007, Lampreia & de Castro, 2011, Outcalt, 2018), however limited information is given concerning pressure-induced errors in non-Newtonian liquids.

Therefore, this part of the work aimed, first to design, produces, and validated a new methodology able to trace density measurement data for Newtonian and non-Newtonian liquids from atmospheric pressure up to 650 bar to determine the influence of pressure.

III.C.1 DEVELOPMENT OF A HIGH-PRESSURE DENSITY APPARATUS UP TO 650 bar

III.C.1.1 General Materials and Methods

III.C.1.1.1 Apparatus

The apparatus used for density measurements, from atmospheric pressure up to 650 bar, at 23 ºC, is a homemade assembling composed by: an oscillation-type density meter (DMA 5000M, Anton Paar) (Fig. III.48-A); a high-pressure density measuring cell (DMA HP, Anton Paar) (Fig. III. 48-B); a syringe pump (100DM, Teledyne ISCO) (Fig. III. 48-C); a pressure monitor (RPM4, Fluke) (Fig. III. 48-D); a recirculating water thermo regulated bath (C20 and CS20-D, Lauda) (Fig. III. 48-E); a membrane pump (MPC105T, Ilmvac) (Fig. III. 48-F); a turbomolecular pump with pirani-vacuummeter (Turbolab 80, Oerlikon) (Fig. III.48-G); stainless steel tube for high pressure (Swagelok); vacuum sensor (P30,WIKA) (Fig. III.48-J); inlet and outlet high pressure needle valves (SITEC) (Fig. III.48-V1 and V2); an inlet ball valve (Swagelok) (Fig. III.48-V3); two ball valves vacuum/air (Hoke) (Fig. III.48-V4) and other valves (Hoke) (Fig. III.48). In addition a set of 8 temperature sensors connected to a data acquisition unit 34970A from Agilent were distributed in different parts of the apparatus (one close to upper part of the syringe pump; one inside the temperature isolation box that contained the apparatus; one in the line to DMA HP; one in the line to pressure sensor; two inside the thermostatic bath and one outside the apparatus temperature isolation box to measure ambient temperature of the laboratory). The ambient conditions (room temperature, relative humidity and pressure) were measured by a combined sensor PTU300 from VAISALA. The DMA HP was stand with a 30 ° from the horizontal in order to avoid the formation of air bubbles.

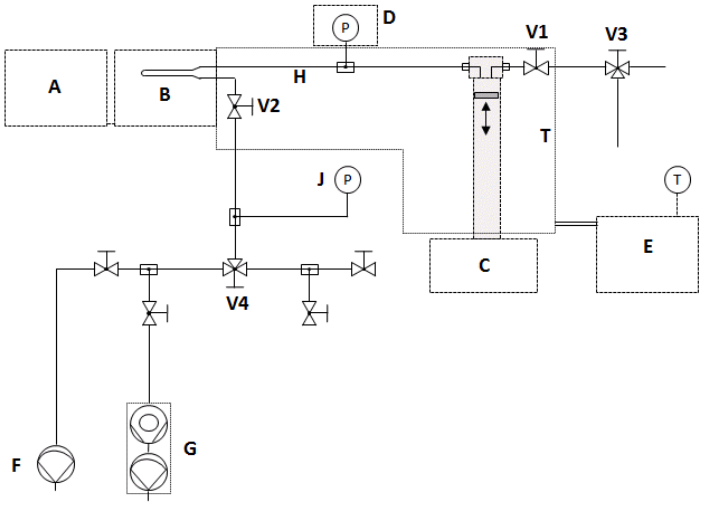

Figure III.48 Scheme of the assembling used to measure density, at 23 °C, in the pressure interval from atmospheric pressure up to 650 bar. Legend: A – Oscillation density-meter (DMA 5000 M, Anton Paar); B – Density measuring cell for high pressure (DMA HP, Anton Paar); C – Syringe pump (100DM, Teledyne ISCO); D – Pressure monitor (RPM4, Fluke); E – Recirculating water thermo regulated bath (C20 and CS20-D, Lauda); F – Membrane pump (MPC105T, Ilmvac); G – Turbomolecular pump with pirani-vacuummeter (Turbolab 80, Oerlikon) ; H – Stainless steel tube for high pressure; J - vacuum sensor (P30,WIKA); T - Thermostat-controlled area; V1 - Inlet high pressure needle valve (SITEC); V2 - Outlet high pressure needle valve (SITEC); V3 – Inlet ball valve (Swagelok); V4 - ball valve vacuum/air (Hoke); other valves (Hoke).

III.C.1.1.2 Samples tested

In order to investigate the metrological properties of oscillating U-tube density meters regarding viscosity (from 1 to 1650 mPa·s) and pressure (from atmospheric pressure up to 650 bar), 8 Newtonian liquids (ultra-pure water, mineral and polyalphaolefin (PAO) oils) and 5 non-Newtonian liquids (Table III.34) were used.

Table III.34 Composition and preparation procedure of the non-Newtonian liquids tested.

Non-Newtonian liquids / concentration	Composition / Preparation Procedure
NNTF1 (6 wt %)	6 wt % hydrogenated Isoprene Styrene copolymer in n-paraffin I (mixture of C_{10}-C_{13} hydrocarbons, with < 0,5 wt % C_{14} and < 0,2 wt % C_{15}) Gravimetric preparation and 70 min stirring at 125 °C
NNTF1 (3 wt % or designated as diluted 1:1 m:m)	100 g of NNTF1dissolved in 100 g of n-paraffin I Gravimetric preparation and overnight stirring at 350 rpm/min
NNTF2 (8 wt %)	8 wt % Poly(acrylamide-co-dially dimethyl ammonium chloride) solution (Sigma Aldrich) in ultra-pure water
NNTF2 (4 wt % or designated as diluted 1:1 v:v)	125 mL of NNTF2 dissolved in 125 mL of ultra-pure water Volumetric preparation and overnight stirring at 350 rpm/min

III.C.1.1.3 Samples preparation and loading

The samples tested, with exception of ultra-pure water, were degassed prior to the high-pressure measurements inside a vacuum oven (OVA031.XX1.5, GALLENKAMP). The samples were inserted in ambar glass bottles without lid (Fig. III.49). The vacuum was produced by evacuating the oven with a membrane pump (MPC105T, Ilmvac) until a pressure below 10 mbar was reached and left in these conditions overnight.

The degassing procedure of ultra-pure water (ISO 3696:1987) was based on boiling the water for 30 min and keeping it inside a closed glass bottle.

Figure III.49 Picture of the NNTF1 bottle inside the vacuum oven (OVA031.XX1.5, GALLENKAMP) showing the air bubbles formed in vacuum.

After degassing, the samples were introduced into the apparatus for density measurements via V3 inlet ball valve (Swagelok) (Fig. III. 48-V3). Prior to this, all the air contained inside the apparatus was pumped out, first with a membrane pump (MPC105T, Ilmvac) (Fig. III. 48-F) to remove liquid and solvent rests and then with a turbomolecular pump with pirani vacuummeter (Turbolab 80, Oerlikon) (Fig. III.48-G). The pressure inside the apparatus was measured with a vacuum sensor (P30, WIKA) (Fig. III.48-J). After achieving a stable value of vacuum inside the apparatus was reached, the outlet high pressure needle valve V2 (SITEC) (Fig. III. 8-V2) was closed. In a first step, the line was filled with the sample,

and in a second step the syringe pump (100DM, Teledyne ISCO) (Fig. III.48-C) was filled until 100 mL of volume capacity. The inlet-outlet high pressure needle valve V1 (SITEC) (Fig. III. 48-V1) was closed at the end of this process and the apparatus was ready to initiate the measurements after thermal equilibrium was achieved.

III.C.1.1.4 Apparatus cleansing

The cleansing procedure of the apparatus was dependent on the liquid tested. For aqueous solutions, ultra-pure water was used to flush the system. Hot water at 60 ºC was also used to potentiate the removal of the aqueous solutions of polymers, such as NNTF2 and NNTF2 diluted. For oil-based liquids and other organic compounds, petroleum ether was used, according the safety rules related with its use.

After finishing a set of measurements with a liquid, this was removed from the interior of the apparatus, first by emptying the syringe pump (100DM, Teledyne ISCO) (Fig. III. 48-C) and the rest of the liquid contained in the lines was then removed by pumping compressed air (with a particles filter), by opening the V2 outlet high pressure needle valve (SITEC), the V4 ball valve vacuum/air (Hoke) and the first valve (Hoke) on the right handed-side of valve V4. Then the cleansing liquid was inserted into the apparatus via the second valve (Hoke) on the right-handed side of V4 valve, by assembling a U-shaped metal tube that allowed to connect the apparatus inlet with a glass bottle of the cleansing liquid (Fig. III.48-V3). The cleansing liquid was pumped inside the apparatus by refilling the syringe pump with a high flow rate (20 mL/min). The cleansing liquid was removed via V1 and V3 valves into a glass bottle by running the syringe pump until being empty. This cycle was repeated at least 5 times for a volume of 20 mL and 1 to 3 times for the full capacity of the syringe pumps (102,6 mL).

The cleansing liquid remaining inside the apparatus was first removed by passing filtered compressed air via the valve located on the right-handed side of V4 valve, with valves V1 and V3 opened. This procedure was running at least overnight. After, the V3 valve was closed and V4 valve was turned for the left-handed side in order to connect the apparatus to the pumps. Then, the air contained inside the apparatus was pumped out, first with a membrane pump (MPC105T, Ilmvac) (Fig. III.48-F) until all the water was removed and then with a turbomolecular pump with pirani-vacuummeter (Turbolab 80, Oerlikon) (Fig. III.48-G). Pressure inside the apparatus was measured with a vacuum sensor (P30, WIKA) (Fig. III.48-J). After achieving a stable value of vacuum inside the apparatus, the outlet high pressure needle V2 valve (SITEC) (Fig. III.48-V2) was closed.

III.C.2.2 Calibration of the high-pressure density apparatus

III.C.2.2.1 Methods

The high-pressure density measurement cell, DMA HP from Anton Paar, was calibrated in density, with ultra-pure degassed water, at 23 ºC, in the pressure interval from atmospheric pressure up to 650 bar. The relative error of DMA HP density indication dependency with pressure, measured in the outlet with a pressure sensor RPM4 from Fluke, was obtained by using as reference values the CIPM formulation (because its use was endorsed by the International Committee for Weights and Measures (CIPM)) (Tanaka *et al.*, 2001) for water density. According to Tanaka *et al.* (2001) the density of de-aerated VSMOW (Vienna Standard Mean Ocean Water), in kg·m^{-3}, at a pressure of 101325 Pa and at t temperature, in ºC, expressed in terms of the ITS-90 is given by Eq. III.14. SMOW, or Standard Mean Ocean Water is an isotopic water standard defined in 1968 by the International Atomic Energy Agency (Tanaka *et al.*, 2001). The density of water has been given under the assumption that the water is air-free for a pressure p of 101325 Pa.

$$\rho_{water}(t,p) = a_5\left[1 - \frac{(t+a_1)^2(t+a_2)}{a_3(t+a_4)}\right] \quad \text{(III.14)}$$

Where: a_1 (ºC) = -3,983035 ± 0,00067; a_2 (ºC) = 301,797; a_3 (ºC^2) = 522528,9, a_4 (ºC) = 69,34881, and a_5 (kg m^{-3}) = 999,974950 ± 0,00084. The relative uncertainty of the density values given by Eq. III.6 is 1·10^{-6}. According to the same reference the compressibility factor, f_c, for the water density at pressure p, in Pa, and temperature t, in ºC, is given by Eq. III.15.

$$f_c = [1 + (k_0 + k_1 t + k_2 t^2)\Delta p] \quad \text{(III.15)}$$

Where: Δp (Pa) = p (Pa) – 101325 Pa; k_0 (10^{-11} Pa^{-1}) = 50,74; k_1 (10^{-11} Pa^{-1} ºC^{-1}) = -0,326 and k_2 (10^{-11} Pa^{-1} ºC^{-2}) = 0,00416. The relative uncertainty of the density values given by Equation 1 is 1 10^{-6}. The water density $\rho_{water}(t,p)$, in kg/m^3, at temperature t, in ºC, and pressure p, in Pa, results from the product of the water compressibility factor and the water density at temperature t and pressure p (Eq. III.16).

$$\rho_{water}(t,p) = f_c \cdot \rho_{water}(t,p_0) \quad \text{(III.16)}$$

III.C.2.2.2 Results

The apparatus for density measurements at high pressure (up to 650 bar) was calibrated with ultra-pure degassed water. The density values and the compressibility factors of ultra-pure water used as reference are described by Tanaka *et al.* (2001).

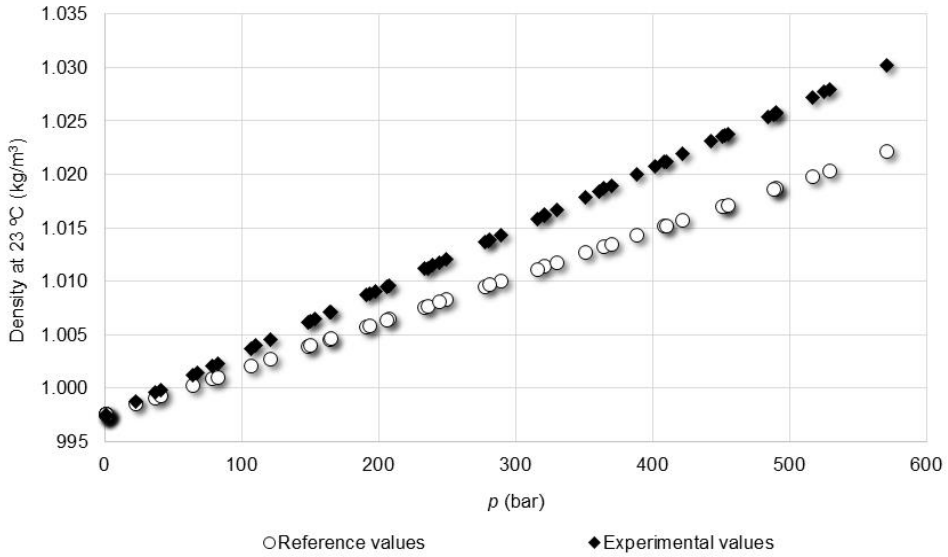

Figure III.50 Curves of reference density values from CIPM formulation (white circles), and density indication values given by the DMA HP (Anton Paar) (black rhombus), at 23 ºC, versus pressure, in the interval from 1 bar to 650 bar, for ultra-pure degassed water.

A calibration curve was plotted with the relative density deviation, in %, versus pressure, in bar (Fig. III.51) as well as a second-degree polynomial regression describing this relative density deviation on the pressure, of the DMA HP. A maximum residual of 0,009 %, corresponding to 0,05 kg·m^{-3}, was found for this polynomial equation.

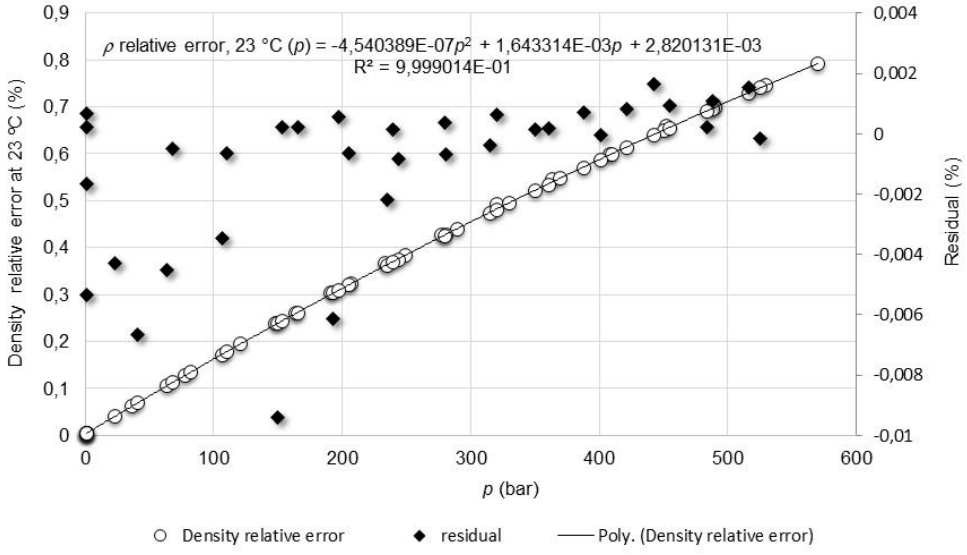

Figure III.51 Calibration curve of relative density deviation, at 23 ºC, versus pressure, in the interval from 1 bar to 650 bar of DMA HP, Anton Paar. (white circles – corresponds to the relative difference between the density indication values and the reference density values for ultra-pure water, at 23 °C, given by the ITS-90 formula (Tanaka *et al.,* 2001); black rhombus – corresponds to the difference between the experimental values of relative density deviation and the values obtained by the polynomial curve).

III.C.2.2.3Conclusions

The equation of a polynomial regression shown on Fig. III.51 can be used to correct the values of density indication of the DMA HP at 23 °C ($\rho_{\text{relative error, 23 °C}}$) for a given pressure measured by the pressure monitor (p).

III.C.2.3 Validation of density measurements obtained by the high-pressure density apparatus

III.C.2.3.1 Methods

Few data of density measurements result up to 650 bar with low uncertainty are available in literature. In order to validate the results obtained with the high-pressure density apparatus under test, the correlation equation for n-Nonane, at 23 °C, described by Schilling *et al.* (2008) was used for the pressure interval from (1 to 300) bar. The measurements reported in this paper have been carried out with a "single-sinker density meter" based on the Archimedes' buoyancy principle, first developed by Brachthäser *et al.* (1993) and later used for several authors (Klirneck *et al.*, 1998; Oaus *et al.*, 2003; Schilling, 2002). The total uncertainty of the measurements in density, for temperature below 413,15 K, was estimated to be 0,02 %.

III.C.2.3.2 Results

From Fig. III.52 one can observe that the slope of the n-Nonane corrected density values (white rhombus) is very similar to the n-Nonane literature values (black crosses) from Schilling *et al.* (2008).

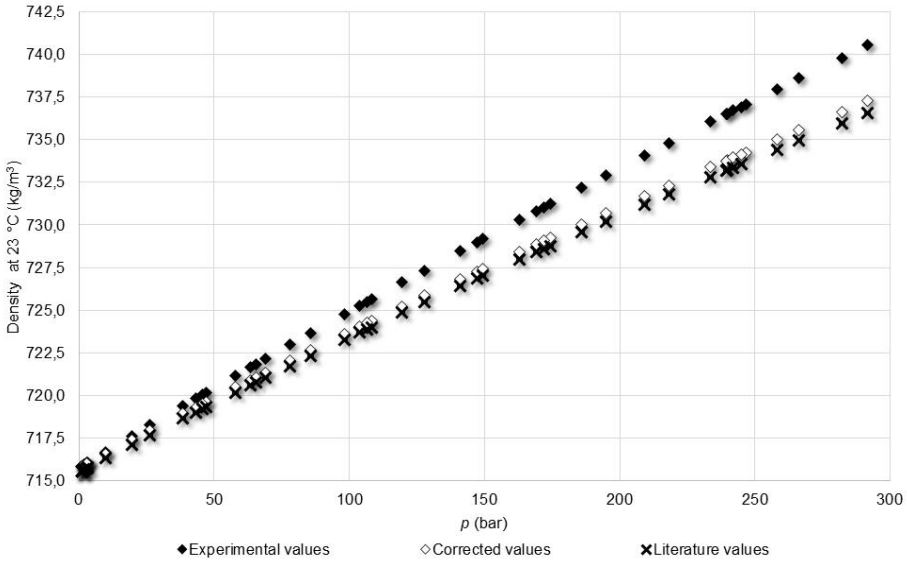

Figure III.52 Curve of n-Nonane density values, at 23 ºC, versus pressure, in the interval from 1 bar to 300 bar (black rhombus – corresponds to the density indication of DMA HP without corrections; white rhombus – corresponds to the density indication of DMA HP after correction with ultra-pure water calibration curve shown in Fig. III.35; white rhombus – corresponds to the difference between the experimental values and corrected values) and literature values of n-Nonane density, at 23 °C, in the pressure interval from 1 bar to 300 bar, obtained by Schilling *et al.* (2008) (black crosses).

For the uncertainty budget of the n-Nonane density measurements performed by the oscillation-type density meter DMA HP in the pressure interval from 1 bar to 300 bar, it was considered to have 3 major contributions: the uncertainty due to the DMA HP density resolution; the uncertainty of the DMA HP calibration with ultra-pure water including the drift and the uncertainty related with the maximum residual of the second degree polynomial regression of n-Nonane density at 23 °C versus pressure. Sensitivity coefficients of one were considered for all the uncertainty contributions.

Table III.35 Uncertainty budget for the n-Nonane density measurements, at 23 °C, in the pressure interval from 1 bar to 300 bar, performed by the high-pressure density apparatus.

Source of uncertainty	Relative standard uncertainty	Type of evaluation	Distribution	Degrees of freedom
DMA HP density resolution	$1{,}2{\cdot}10^{-5}$	B	Rectangular	50
DMA HP calibration with ultra-pure water (including drift)	$1{,}4{\cdot}10^{-5}$	B	Normal	50
Maximum residual of the second-degree polynomial regression	$4{,}0{\cdot}10^{-4}$	A	Normal	81
Relative combine standard uncertainty	$4{,}0{\cdot}10^{-4}$			
Relative expanded uncertainty	$6{,}7{\cdot}10^{-4}$			
Coverage factor k (95 %)	1,66			
ν_{eff}	81			

A maximum expanded uncertainty of the density measurements was estimated to be 0,50 kg/m^3, for a level of confidence of 95 % (Table III.35 and Fig. III.53). Schilling *et al.* (2008) describes a value of 0,14 kg/m^3 (Fig. III.35). The experimental density values (corrected with the ultra-pure water calibration curve – white rhombus) are represented in Fig. III.53 together with the literature values (Shilling *et al.*, 2008) (black crosses).

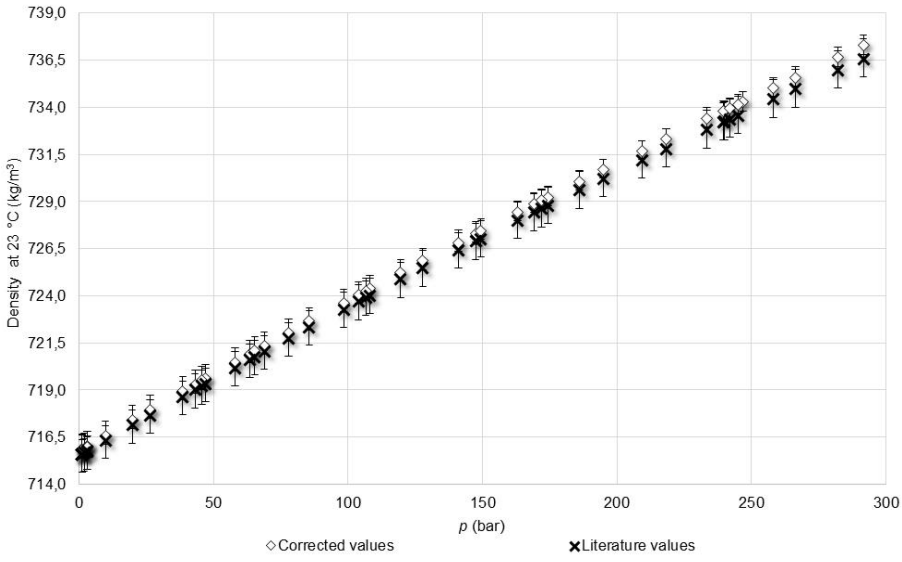

Figure III.53 Curve of n-Nonane density values, at 23 ºC, versus pressure, in the interval from 1 bar to 650 bar (white rhombus – corresponds to the density indication of DMA HP after correction with ultra-pure water calibration curve shown in Fig. III.35) and literature values of n-Nonane density, at 23 °C, in the pressure interval from 1 bar to 300 bar, obtained by Schilling *et al.* (2008) (black crosses). The vertical lines correspond to the expanded measurement uncertainty for a level of confidence of 95 %.

III.C.2.3.3 Conclusions

Through the comparison with the n-Nonane density values obtained for Schilling *et al.* (2008) one can conclude that the methodology applied to obtain density results at 23 °C and for pressures up to 300 bar is valid within the estimated measurement uncertainty of 0,50 kg·m^{-3}.

Further investigations must be done in order to validate the density data obtained for pressure higher than 300 bar.

III.C.2.4 Density measurements with the high-pressure density apparatus up to 650 bar

III.C.2.4.1 Methods

Each sample was tested for a set of 3 measurement cycles. In each cycle first, a decrease of volume of the syringe pump leading to an increase of pressure from atmospheric pressure up to 650 bar was performed, then an increase of volume of the syringe pump, conducting a decrease of pressure until the atmospheric pressure was reached again. The volume change of the syringe pump was performed with a constant flow rate of 0,25 mL/min for all the cycles. In the first cycle a volume step of 1 mL was used. In the second, 0,75 mL, and in the third 0,25 mL. A time interval of 5 minutes was used for each step after taking the density, temperature and pressure values of the liquid inside the apparatus.

III.C.2.4.2 Results

For each liquid the density indication of DMA HP for a pressure measured by the pressure monitor (RPM4, Fluke) was corrected using the calibration curve obtained for ultra-pure water (Fig. III.35). A graphical representation of the experimental density values, the corrected density values and the relative experimental deviation (difference between the experimental density values and the corrected values) was plotted for each liquid. For each sample a second-degree polynomial curve of the corrected density values versus the pressure was plotted as well as its residual analysis, i.e. difference between the corrected density values and the density values obtained through the regression curve.

III.C.2.4.2.1 Measurements results of Newtonian liquids

III.C.2.4.2.1.a. n-Nonane

A maximum relative density deviation of 0,86 % (corresponding to a 6,60 $kg \cdot m^{-3}$) for a pressure of 634,80 bar was observed for n-Nonane at 23 °C (Fig. III.54).

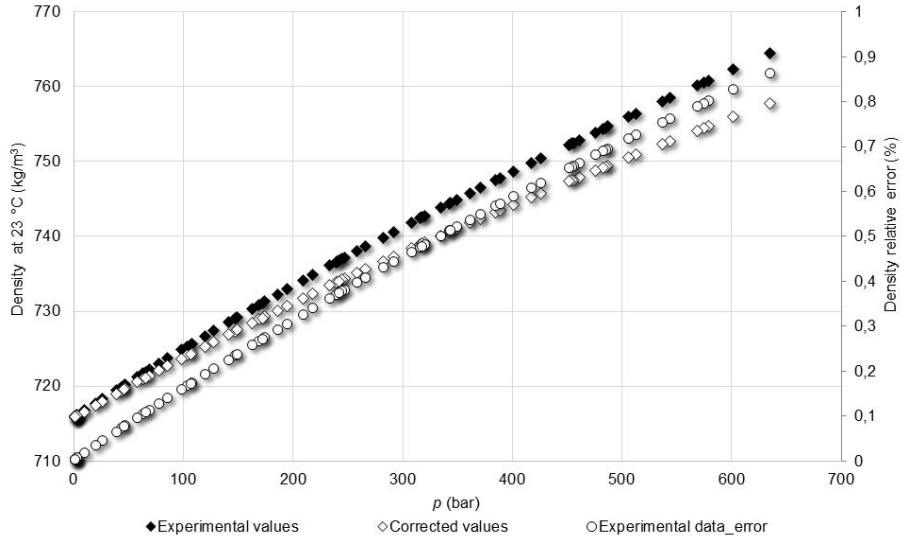

Figure III.54 Curve of n-Nonane density and density relative error values, at 23 ºC, versus pressure, in the interval from 1 bar to 650 bar (black rhombus – corresponds to the density indication of DMA HP without corrections; white rhombus – corresponds to the density indication of DMA HP after correction with ultra-pure water calibration curve shown in Fig. III.51; white circles – corresponds to the difference between the experimental values and corrected values).

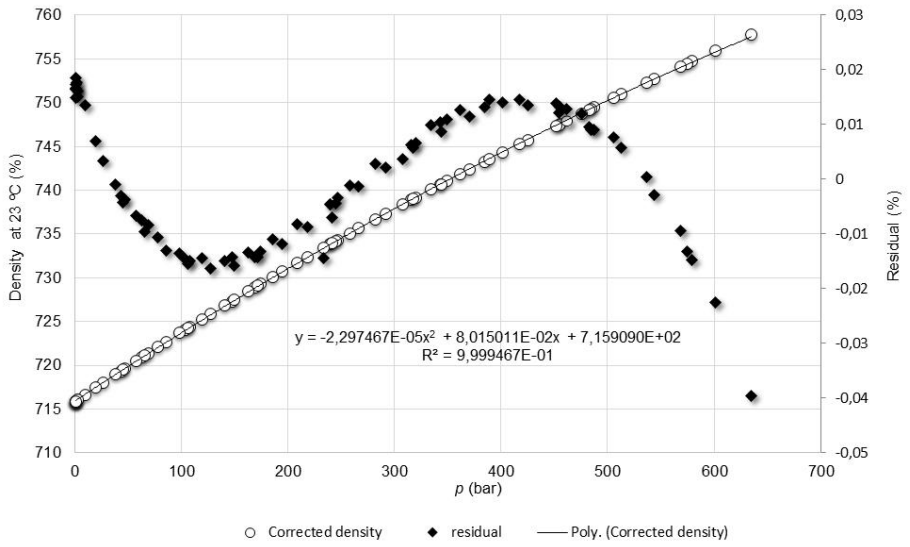

Figure III.55 Curve of n-Nonane density values, at 23 ºC, versus pressure, in the interval from 1 bar to 650 bar (white circles – corresponds to the density values of n-Nonane corrected with the calibration curve of water; black rhombus – corresponds to the difference between the corrected density values and the density values obtained through the second-degree polynomial equation shown on the graph).

The n-Nonane density (y) dependency on pressure (x), at 23 °C, is given by the second-degree polynomial equation shown on Fig. III.55. This equation presented a maximum residual, of 0,040 %, corresponding to 0,300 kg·m^{-3}.

III.C.2.4.2.1.b. Dodecane

A maximum relative density deviation of 0,87 % (corresponding to a 6,86 kg·m^{-3}) for a pressure of 638,00 bar was observed for dodecane at 23 °C (Fig. III.56).

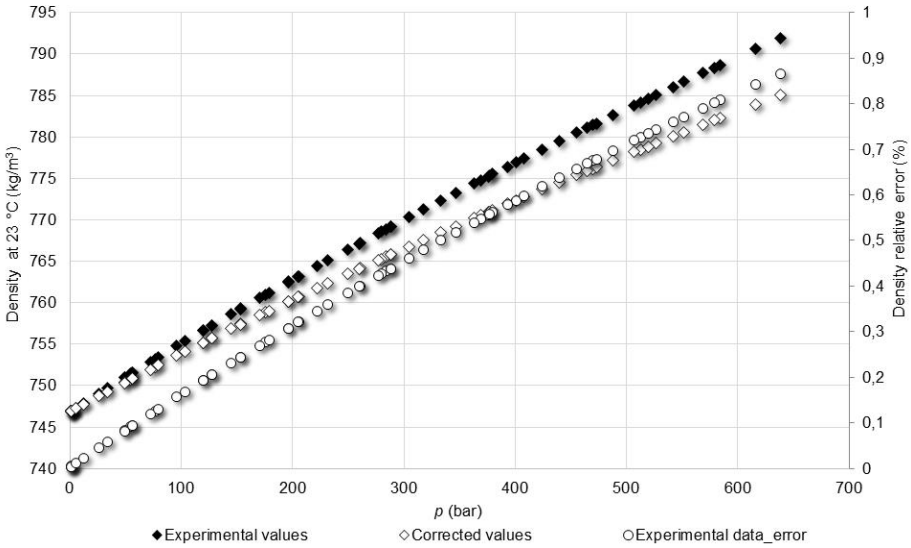

Figure III.56 Curve of dodecane density and density relative error values, at 23 ºC, versus pressure, in the interval from 1 bar to 650 bar (black rhombus – corresponds to the density indication of DMA HP without corrections; White rhombus – corresponds to the density indication of DMA HP after correction with ultra-pure water calibration curve shown in Fig. III.51; white circles – corresponds to the difference between the experimental values and corrected values).

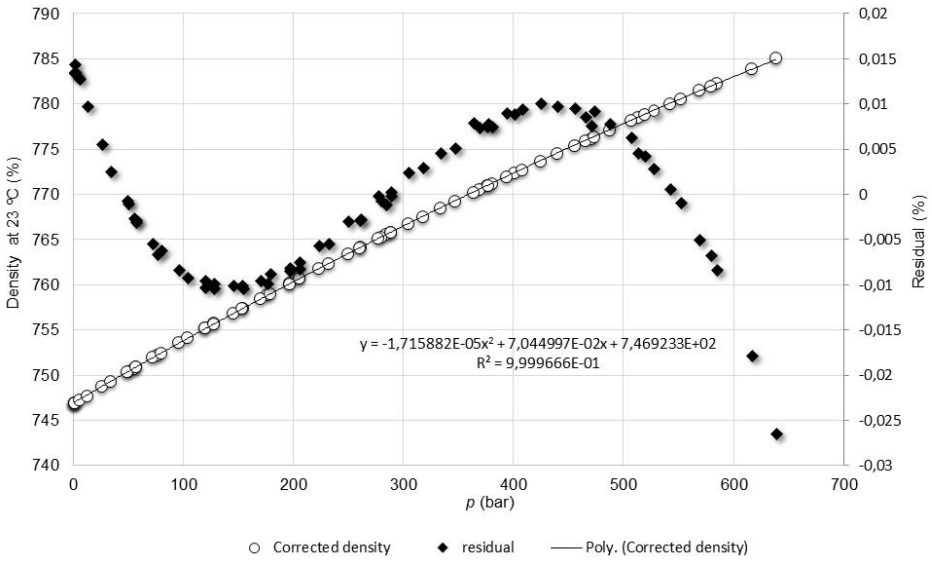

Figure III.57 Curve of dodecane density values, at 23 ºC, versus pressure, in the interval from 1 bar to 650 bar (white circles – corresponds to the density values of dodecane corrected with the calibration curve of water; black rhombus – corresponds to the difference between the corrected density values and the density values obtained through the second-degree polynomial equation shown on the graph).

The dodecane density (y) dependency on pressure (x), at 23 °C, is given by the second-degree polynomial equation shown on Fig. III.57. This equation presented a maximum residual, of 0,026 %, corresponding to 0,207 kg·m^{-3}.

III.C.2.4.2.1.c. Oil 50B

A maximum relative density deviation of 0,83 % (corresponding to a 7,46 kg/m^3) for a pressure of 601,64 bar was observed for oil 50B at 23 °C (Fig.III.58).

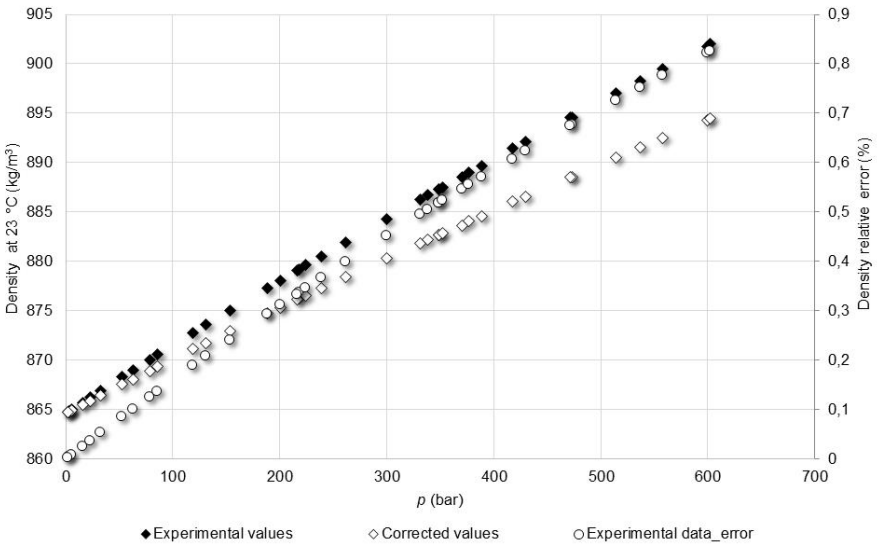

Figure III.58 Curve of oil 50B density and density relative error values, at 23 ºC, versus pressure, in the interval from 1 bar to 650 bar (black rhombus – corresponds to the density indication of DMA HP without corrections; white rhombus – corresponds to the density indication of DMA HP after correction with ultra-pure water calibration curve shown in Fig. III.51; white circles – corresponds to the difference between the experimental values and corrected values).

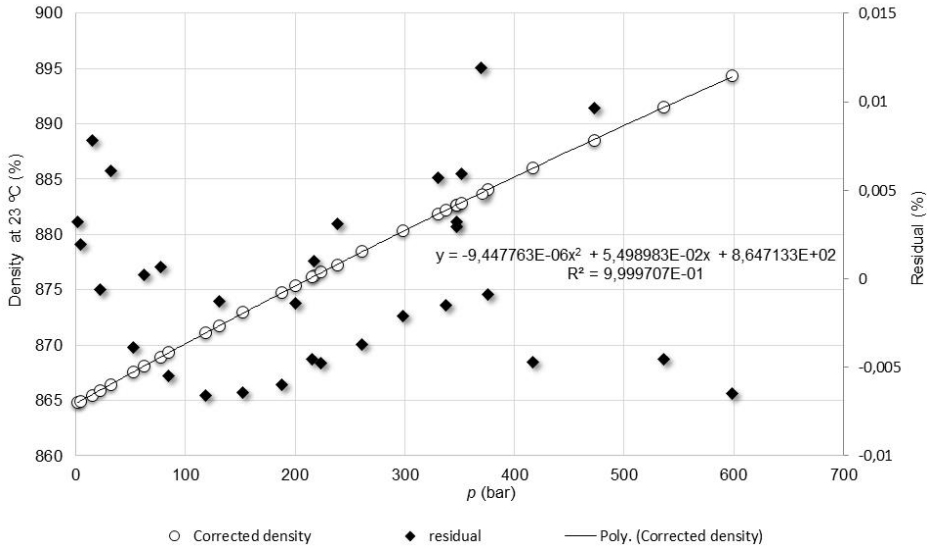

Figure III.59 Curve of oil 50B density, at 23 ºC, versus pressure, in the interval from 1 bar to 650 bar (white circles – corresponds to the density values of oil 50B corrected with the calibration curve of water; black rhombus – corresponds to the difference between the corrected density values and the density values obtained through the second-degree polynomial equation shown on the graph).

The oil 50B density (y) dependency on pressure (x), at 23 °C, is given by the second-degree polynomial equation shown on Fig. III.59. This equation presented a maximum residual, of 0,017 %, corresponding to 0,148 kg·m^{-3}.

III.C.2.4.2.1.d. Oil 100B

A maximum relative density deviation of 0,84 % (corresponding to a 7,20 kg/m^3) for a pressure of 608,57 bar was observed for oil 100B at 23 °C (Fig. III.60).

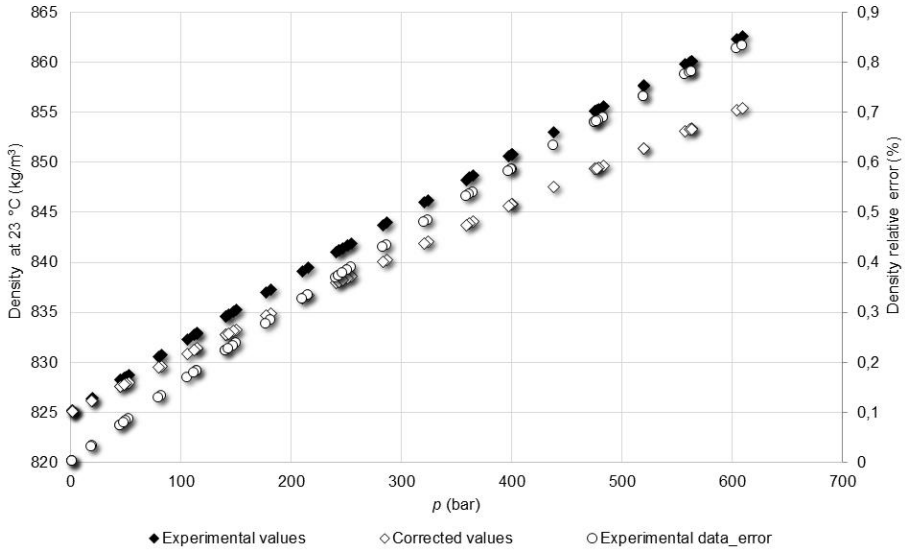

Figure III.60 Curve of oil 100B density and density relative error values, at 23 ºC, versus pressure, in the interval from 1 bar to 650 bar, measured with a DMA HP from Anton Paar (black rhombus – corresponds to the density indication of DMA HP without corrections; White rhombus – corresponds to the density indication of DMA HP after correction with ultra-pure water calibration curve shown in Fig. III.35; white circles – corresponds to the difference between the experimental values and corrected values).

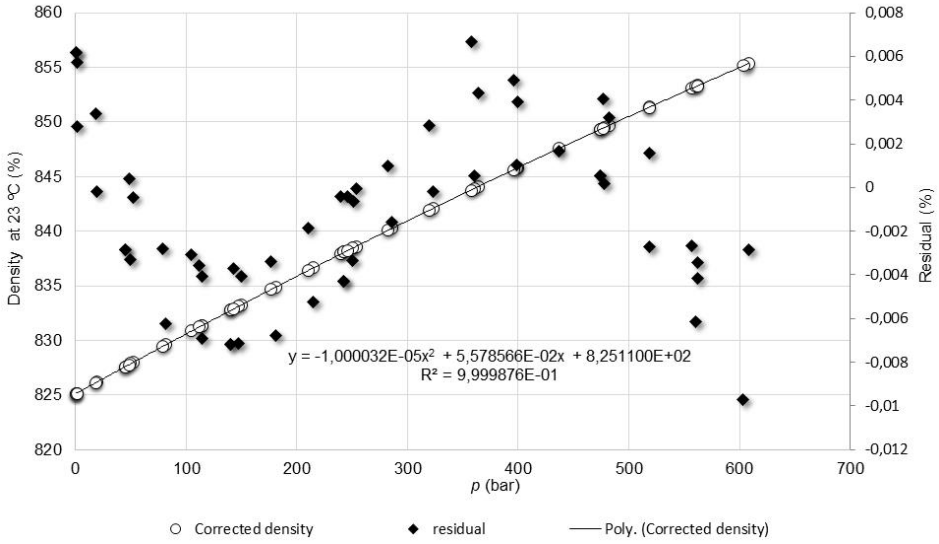

Figure III.61 Curve of oil 100B density relative error, at 23 ºC, versus pressure, in the interval from 1 bar to 650 bar (white circles – corresponds to the density values of oil 100B corrected with the calibration curve of water; black rhombus – corresponds to the difference between the corrected density values and the density values obtained through the second-degree polynomial equation shown on the graph).

The oil 100B density (y) dependency on pressure (x), at 23 °C, is given by the second-degree polynomial equation shown on Fig. III.61. This equation presented a maximum residual, of 0,010 %, corresponding to 0,083 kg·m^{-3}.

III.C.2.4.2.2 Measurements results of non-Newtonian liquids

III.C.2.4.2.2.a. NNTF1

A maximum relative density deviation of 0,87 % (corresponding to a 6,97 kg·m^{-3}) for a pressure of 644,19 bar was observed for NNTF1 at 23 °C (Fig. III.62).

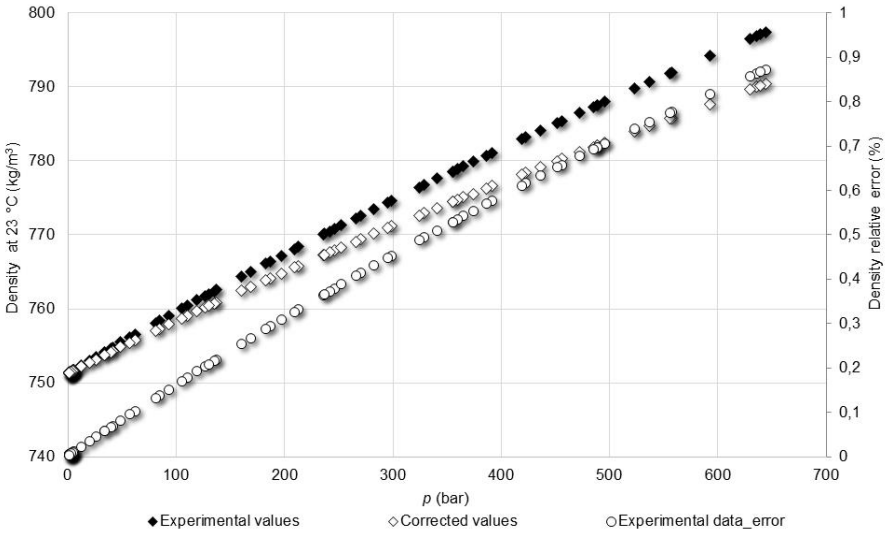

Figure III.62 Curve of NNTF1 density and density relative error values, at 23 ºC, versus pressure, in the interval from 1 bar to 650 bar (black rhombus – corresponds to the density indication of DMA HP without corrections; White rhombus – corresponds to the density indication of DMA HP after correction with ultra-pure water calibration curve shown in Fig. III.51; white circles – corresponds to the difference between the experimental values and corrected values).

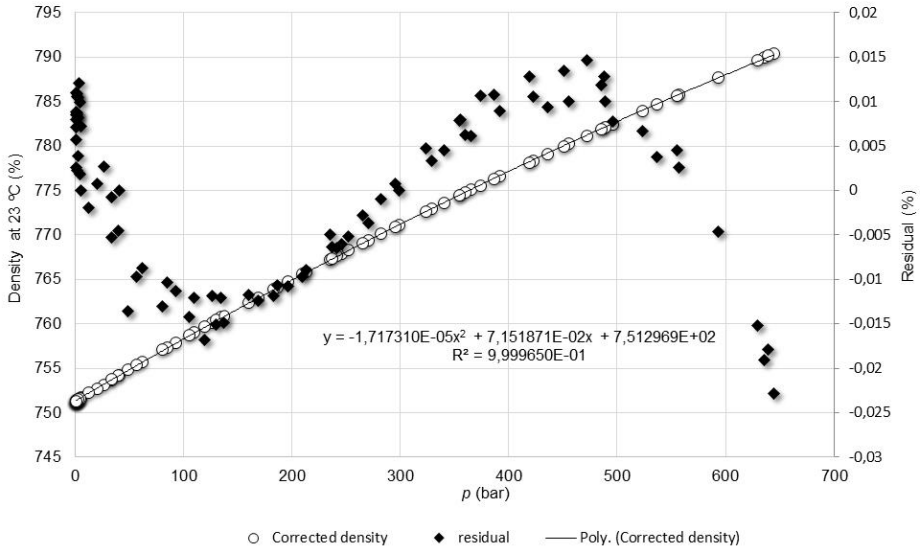

Figure III.63 Curve of NNTF1 density relative error, at 23 ºC, versus pressure, in the interval from 1 bar to 650 bar (white circles – corresponds to the density values of NNTF1 corrected with the calibration curve of water; black rhombus – corresponds to the difference between the corrected density values and the density values obtained through the second-degree polynomial equation shown on the graph).

The NNTF1 density (y) dependency on pressure (x), at 23 °C, is given by the second-degree polynomial equation shown on Fig. III.63. This equation presented a maximum residual, of 0,023 %, corresponding to 0,181 kg·m^{-3}.

III.C.2.4.2.2.b. NNTF1 diluted

A maximum relative density deviation of 0,83 % (corresponding to a 6,57 kg·m^{-3}) for a pressure of 605,01 bar was observed for NNTF1 diluted at 23 °C (Fig. III.64).

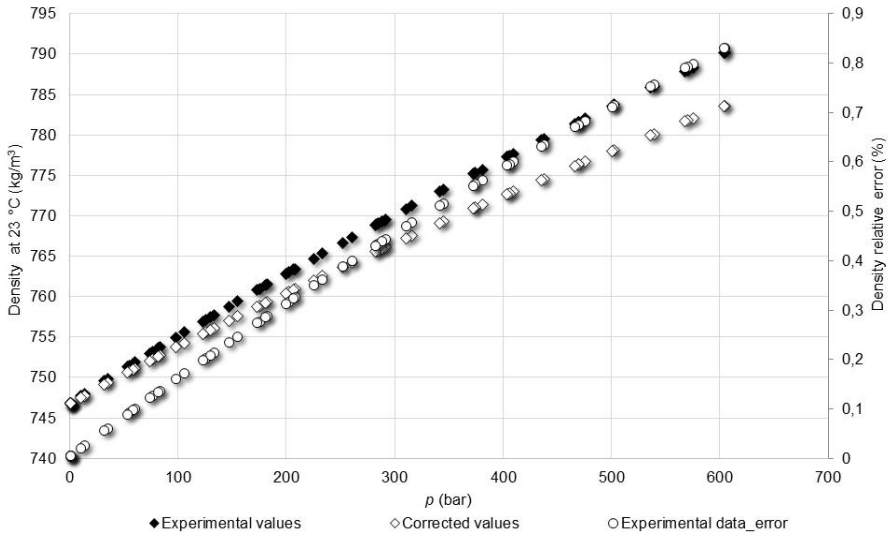

Figure III.64 Curve of NNTF1 diluted density and density relative error values, at 23 ºC, versus pressure, in the interval from 1 bar to 650 bar (black rhombus – corresponds to the density indication of DMA HP without corrections; white rhombus – corresponds to the density indication of DMA HP after correction with ultra-pure water calibration curve shown in Fig. III.51; white circles – corresponds to the difference between the experimental values and corrected values).

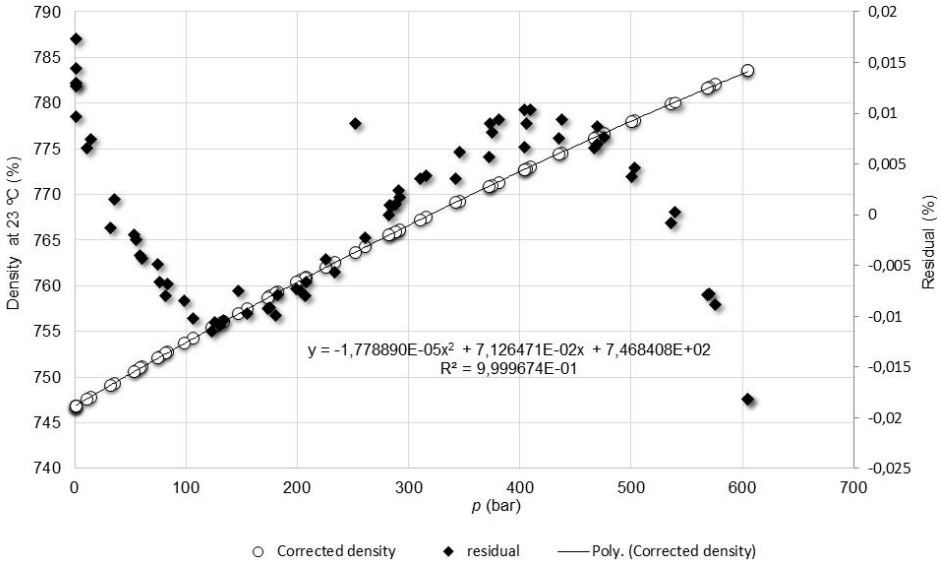

Figure III.65 Curve of NNTF1 diluted density relative error, at 23 ºC, versus pressure, in the interval from 1 bar to 650 bar (white circles – corresponds to the density values of NNTF1 diluted corrected with the calibration curve of water; black rhombus – corresponds to the difference between the corrected density values and the density values obtained through the second-degree polynomial equation shown on the graph).

The NNTF1 diluted density (y) dependency on pressure (x), at 23 °C, is given by the second-degree polynomial equation shown on Fig. III.49. This equation presented a maximum residual, of 0,018 %, corresponding to 0,142 kg·m^{-3}.

III.C.2.4.2.2.c. NNTF2

A maximum relative density deviation of 0,88 % (corresponding to a 6,57 kg·m^{-3}) for a pressure of 648,81 bar was observed for NNTF2 at 23 °C (Fig. III.66).

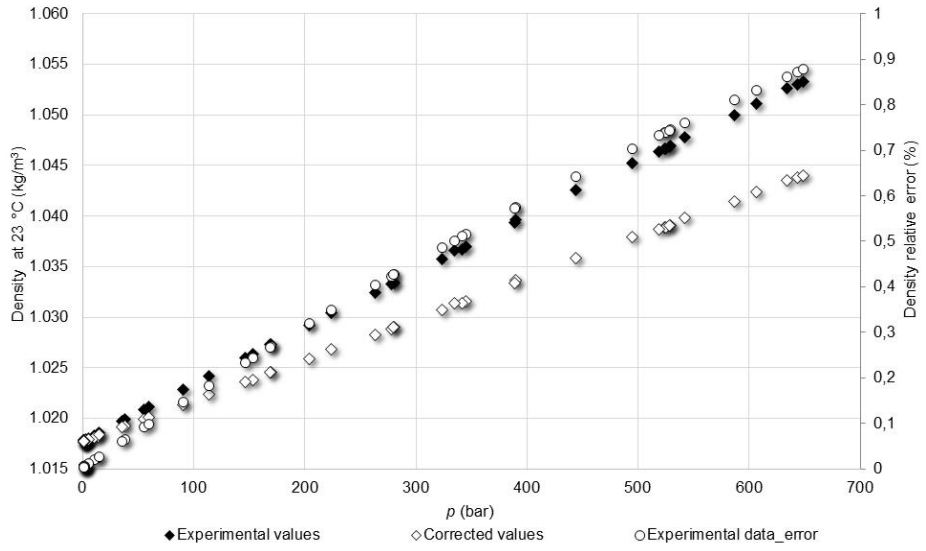

Figure III.66 Curve of NNTF2 density and density relative error values, at 23 ºC, versus pressure, in the interval from 1 bar to 650 bar, (black rhombus – corresponds to the density indication of DMA HP without corrections; white rhombus – corresponds to the density indication of DMA HP after correction with ultra-pure water calibration curve shown in Fig. III.51 white circles – corresponds to the difference between the experimental values and corrected values).

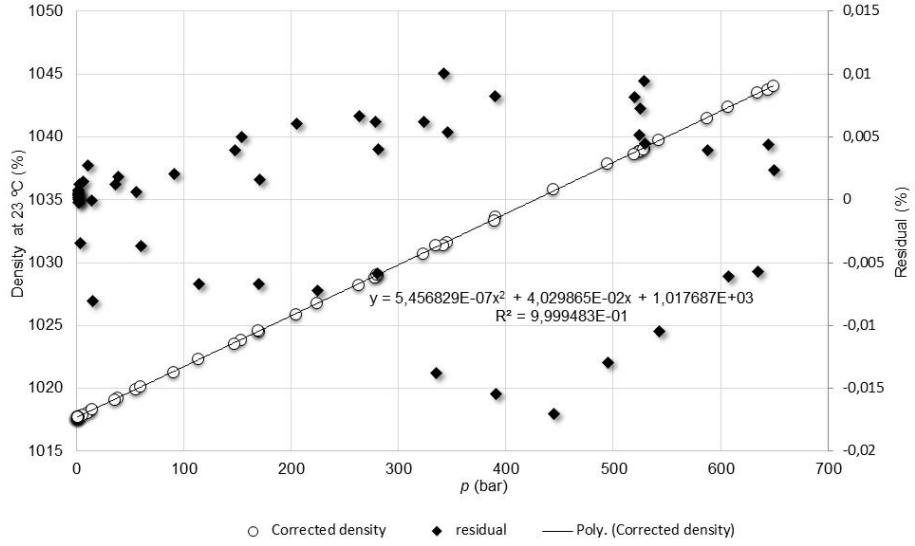

Figure III.67 Curve of NNTF2 density relative error, at 23 ºC, versus pressure, in the interval from 1 bar to 650 bar. (white circles – corresponds to the density values of NNTF2 corrected with the calibration curve of water; black rhombus – corresponds to the difference between the corrected density values and the density values obtained through the second-degree polynomial equation shown on the graph).

The NNTF2 density (y) dependency on pressure (x), at 23 °C, is given by the second-degree polynomial equation shown on Fig. III.67. This equation presented a maximum residual, of 0,017 %, corresponding to 0,176 kg·m^{-3}.

III.C.2.4.2.2.d. NNTF2 diluted

A maximum relative density deviation of 0,88 % (corresponding to a 9,18 kg·m^{-3}) for a pressure of 649,52 bar was observed for NNTF2 diluted at 23 °C (Fig. III.68).

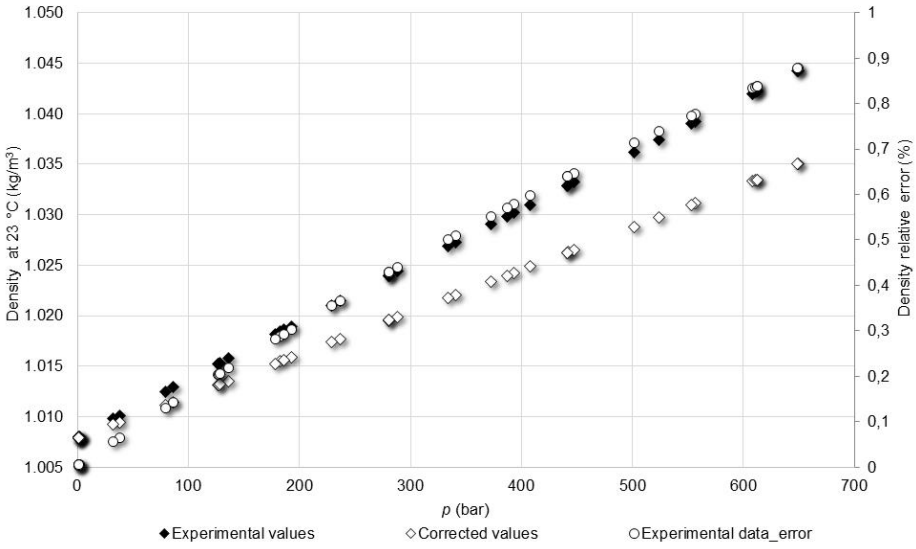

Figure III.68 Curve of NNTF2 diluted density values, at 23 ºC, versus pressure, in the interval from 1 bar to 650 bar (black rhombus – corresponds to the density indication of DMA HP without corrections; white rhombus – corresponds to the density indication of DMA HP after correction with ultra-pure water calibration curve shown in Fig. III.35; white circles – corresponds to the difference between the experimental values and corrected values).

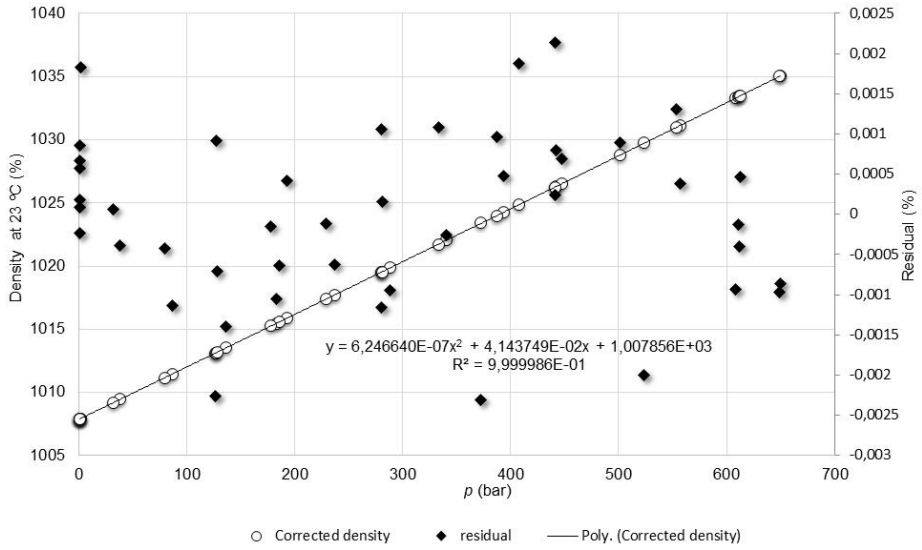

Figure III.69 Curve of NNTF2 diluted density and density relative error values, at 23 ºC, versus pressure, in the interval from 1 bar to 650 bar (white circles – corresponds to the density values of NNTF2 diluted corrected with the calibration curve of water; black rhombus – corresponds to the difference between the corrected density values and the density values obtained through the second-degree polynomial equation shown on the graph).

The NNTF2 diluted (y) dependency on pressure (x), at 23 °C, is given by the second-degree polynomial equation shown on Fig. III.69. This equation presented a maximum residual, of 0,002 %, corresponding to 0,024 kg·m^{-3}.

In Tables III.36 and III.37 are summarized the parameters of the second-degree polynomial equation of density, at 23 °C, dependence on pressure, in the interval from (1 to 650) bar, of the Newtonian and non-Newtonian liquids, respectively, measured with the apparatus under test. In addition, the expanded uncertainty of the density measurements results is presented in the Table III.38.

Table III.36 Parameters of the second-degree polynomial equation of density, ρ in kg·m^{-3}, at 23 °C, dependence on pressure, p in bar, in the interval from 1 to 650 bar, of the Newtonian liquids tested and expanded uncertainty, $U\rho$ (with k =2) of the density measurements.

Newtonian liquids	Second-degree polynomial equation $\rho_{23\,°C}(p) = a + b{\cdot}p + c{\cdot}p^2$						$U\rho$
	a (kg·m^{-3})	b (kg·m^{-3}·bar)	c (kg·m^{-3}·bar^{-2})	p (bar)	Max. residual (%)	Deg. of freedom (1)	(kg·m^{-3})
n-Nonane	7,159090·10^2	8,015011·10^{-2}	-2,297467·10^{-5}	1 to 635	0,040	81	0,50
Dodecane	7,469233·10^2	7,044997·10^{-2}	-1,715882·10^{-5}	1 to 638	0,026	73	0,34
Oil 50B	8,647133·10^2	5,498983·10^{-2}	-9,447763·10^{-6}	1 to 602	0,017	39	0,26
Oil 100B	8,251100·10^2	5,578566·10^{-2}	-1,000032·10^{-5}	1 to 609	0,010	57	0,14

Table III.37 Parameters of the second-degree polynomial equation of density, ρ in kg·m^{-3}, at 23 °C, dependence on pressure, p in bar, in the interval from 1 to 650 bar, of the non-Newtonian liquids tested and expanded uncertainty, $U\rho$ (with k =2) of the density measurements.

Non-Newtonian liquids	Second-degree polynomial equation $\rho_{23\,°C}(p) = a + b{\cdot}p + c{\cdot}p^2$						$U\rho$
	a	b	c	p	Max. residual	Deg. of freedom	
	(kg·m^{-3})	(kg·m^{-3}·bar)	(kg·m^{-3}·bar^{-2})	(bar)	(%)	(1)	(kg·m^{-3})
NNTF1	7,512969·10^{2}	7,151871·10^{-2}	-1,717310·10^{-5}	1 to 644	0,023	86	0,30
NNTF1 diluted	7,468408·10^{2}	7,126471·10^{-2}	-1,778890·10^{-5}	1 to 605	0,018	71	0,24
NNTF2	1,017687·10^{3}	4,029865·10^{-2}	5,456829·10^{-7}	1 to 649	0,017	52	0,30
NNTF2 diluted	1,007856·10^{3}	4,143749·10^{-2}	6,246640·10^{-7}	1 to 650	0,002	45	0,05

In the uncertainty budget density measurements, 3 major contributions where considered: the uncertainty due to the DMA HP density resolution; the uncertainty of the DMA HP calibration with ultra-pure water including the drift and the uncertainty related with the maximum residual of the second-degree polynomial regression of liquid density at 23 °C versus pressure (Table III.38). Sensitivity coefficients of one were considered for all the uncertainty contributions.

Table III.38 Uncertainty budget of the liquid's density measurements, at 23 °C, in the pressure interval from 1 to 650 bar, performed by the high-pressure density apparatus.

Source of uncertainty	Relative standard uncertainty	Type of evaluation	Distribution	Degrees of freedom
DMA HP density resolution	1,2·10^{-5}	B	Rectangular	50
DMA HP calibration with ultra-pure water (including drift)	1,4·10^{-5}	B	Normal	50
Maximum residual of the second-degree polynomial regression	(1)	A	Normal	(2)
Relative combined standard uncertainty	u_c			
Relative expanded uncertainty	$u_c{\cdot}k = U$			
Coverage factor (95 %)	k			
Effective degrees of freedom	ν_{eff}			

Legend: (1) Maximum residual of the second-degree polynomial regression and (2) Degrees of freedom described on Tables III.36 and III.37 for the Newtonian and non-Newtonian liquids tested, respectively. The relative combine standard uncertainty of the result, u_c, was obtained from the square root of the sum of the relative standard uncertainties, considering a unitary sensitive coefficient for all the contributions. The effective degrees of freedom, ν_{eff}, for the relative combine standard uncertainty were calculated by the Welch-Satterthwaite formula. The coverage factor, k, is chosen to be the $t_{1-\alpha/2,\nu}$ critical value from the t-table with ν_{eff} degrees of freedom. The relative expanded uncertainty of the result, U, was obtained by multiplying the relative combined standard uncertainty of the result, u_c, by the coverage factor, k. The presented terms are in accordance with GUM (JCGM 100:2008).

III.C.2.4.3 Conclusions

This work shows that it is possible to determine the equation of density dependence on pressure in the interval from 1 bar to 650 bar, at 23 °C, with the developed apparatus, with an expected density measurement uncertainty of 0,50 kg·m^{-3}, for both Newtonian and non-Newtonian liquids. On the contrary it is not possible to measure suspensions with this kind of apparatus mainly due to the heterogeneity of the sample and the possible deposition of the solid's parts inside the density meter measuring cell.

III.C.2.5 Determination of high-pressure density apparatus internal volume

III.C.2.5.1 Methods

The internal volume of the high-pressure density apparatus, to be used as a pVT apparatus, was determined by gravimetric method using degassed ultra-pure water as a standard.

The mass of water m_{water} was determined according to the Eq. III.17.

$$m_{water} = \left(m_{read\ final} - m_{read\ initial}\right)\left(\frac{1-\frac{\rho_{air}}{\rho_m}}{1-\frac{\rho_{air}}{\rho_w}}\right) - \Delta m_{capillary\ effect} - \Delta m_{surface\ tension\ effect} \quad \text{(III.17)}$$

Where the term $m_{read\ final} - m_{read\ initial}$ represent the difference between the balance readings in the end and in the beginning of the test; ρ_{air} the air density; ρ_m the density of the mass standards; ρ_w the water density according to CIPM formulation (Tanaka *et al.*, 2001); $\Delta m_{capillary\ effect}$ the correction of buoyancy effect of the capillary and $\Delta m_{surface\ tension\ effect}$ the correction of surface tension effect.

Due to the presence of a capillary in contact with the fluid to be weighted, capillary effects appear. The correction of the buoyancy effect caused by the capillary submerged in the water contained in the weighing vessel is given by the Eq. III.18.

$$\Delta m_{capillary\ effect} = \rho_w \cdot \pi\left(R_o^2 - R_i^2\right) \cdot l \quad \text{(III.18)}$$

Where: R_o the outer radius of the capillary; R_i the inner radius of the capillary and l the dipped length.

Other effect considered was that of surface tension. The correction of this effect is calculated according to Eq. III.19, where σ_w corresponds to surface tension of water (at test temperature) and g to gravitational acceleration (in the place where the test is taken place).

$$\Delta m_{surface\ tension\ effect} = \pi \cdot 2R_0 . \frac{\sigma_w}{g} \quad \text{(III.19)}$$

The volume of water V_{water} was then calculated by means of Eq. III.20.

$$V_{water} = \frac{m_{water}}{\rho_w} \quad \text{(III.20)}$$

A set of mass standards class OIML E1 (Häafner) were used for the substitution method.

Additionally, tests were made in order to determinate the error in volume of the syringe pump for 0,25 mL and 10 mL. The tests were performed at room temperature and ambient pressure.

III.C.2.5.2 Results

The determined internal volume of high-pressure density apparatus was 109,1469 mL (Table III.39) with an expanded uncertainty of $2{,}3 \cdot 10^{-3}$ mL (Table III.40).

Table III.39 Results of the determination of high-pressure density apparatus internal volume by gravimetric method using ultra-pure water.

Internal V (mL)	V relative standard-deviation (mL)	n (1)	V relative standard-deviation of the mean (mL)	Mean water t (ºC)	Standard deviation of water t (ºC)
109,1469	$1{,}8 \cdot 10^{-4}$	4	$9{,}0 \cdot 10^{-5}$	25,86	0,56

Table III.40 Uncertainty budget of determination of high-pressure density apparatus internal volume by gravimetric method using ultra-pure water.

Contribution	Relative standard uncertainty	Type of evaluation	Distribution	ν_{eff}
Balance resolution	$1{,}1 \cdot 10^{-7}$	B	Rectangular	3
Mass standards	$5{,}0 \cdot 10^{-7}$	B	Normal	50
Mass measurements repeatability	$9{,}0 \cdot 10^{-5}$	A	Normal	3
Relative standard uncertainty	$9{,}0 \cdot 10^{-5}$			
Relative expanded uncertainty	$2{,}1 \cdot 10^{-4}$			
Expanded uncertainty (mL)	$2{,}3 \cdot 10^{-3}$			
Coverage factor k (95 %)	2,35			
ν_{eff}	3			

The results of the error determination of the displaced volume of syringe pump (100DM, Teledyne ISCO) used in the high-pressure density apparatus by gravimetric method using ultra-pure water for the displaced volumes 0,25 mL and 10,00 mL are presented in Table III.41.

Table III.41 Results of the error determination of the displaced volume, V of syringe pump (100DM, Teledyne ISCO) used in the high-pressure density apparatus by gravimetric method using ultra-pure water.

V Indication (mL)	V indication mean error (mL)	V relative standard-deviation (mL)	n (1)	V relative standard-deviation of the mean (mL)	Mean water t (ºC)	Standard deviation of water t (ºC)
0,25	0,0019	$4{,}0 \cdot 10^{-3}$	13	$4{,}4 \cdot 10^{-3}$	25,86	0,56
10,00	0,0035	$1{,}4 \cdot 10^{-4}$	9	$4{,}7 \cdot 10^{-6}$		

The uncertainty budget of the error determination for displaced volumes 0,25 mL and 10,00 mL, are presented in Tables III.42 and III.43, respectively.

Table III.42 Uncertainty budget of the error determination of the displaced volume (0,25 mL) of syringe pump (100DM, Teledyne ISCO) used in the high-pressure density apparatus by gravimetric method using ultra-pure water.

Contribution	Relative standard uncertainty	Type of evaluation	Distribution	ν_{eff}
Balance resolution	$4{,}6 \cdot 10^{-5}$	B	Rectangular	12
Mass standards	$3{,}5 \cdot 10^{-6}$	B	Normal	50
Mass measurements repeatability	$4{,}4 \cdot 10^{-3}$	A	Normal	12
Relative standard uncertainty	$4{,}4 \cdot 10^{-3}$			
Relative expanded uncertainty	$7{,}9 \cdot 10^{-3}$			
Expanded uncertainty (mL)	$2{,}0 \cdot 10^{-3}$			
Coverage factor k (95 %)	1,78			
ν_{eff}	12			

Table III.43 Uncertainty budget of the error determination of the displaced volume (10 mL) of syringe pump (100DM, Teledyne ISCO) used in the high-pressure density apparatus by gravimetric method using ultra-pure water.

Contribution	Relative standard uncertainty	Type of evaluation	Distribution	ν_{eff}
Balance resolution	$1{,}1 \cdot 10^{-7}$	B	Rectangular	8
Mass standards	$3{,}0 \cdot 10^{-7}$	B	Normal	50
Mass measurements repeatability	$4{,}7 \cdot 10^{-6}$	A	Normal	8
Relative standard uncertainty	$4{,}7 \cdot 10^{-6}$			
Relative expanded uncertainty	$8{,}7 \cdot 10^{-6}$			
Expanded uncertainty (mL)	$8{,}7 \cdot 10^{-5}$			
Coverage factor k (95 %)	1,86			
ν_{eff}	8			

III.C.3.5.3 Conclusions

In this part of the work was designed, developed, characterized and validated a high-pressure density apparatus, able to ensure the traceability to SI of density measurements performed with oscillation-type density meters, within the pressure interval from 1 to 650 bar, with an estimated expanded uncertainty of ~0,23 to 0,50 $kg \cdot m^{-3}$, for both Newtonian and non-Newtonian samples. The developed apparatus and methodology are therefore suitable to be used for calibration purposes fulfilling the existing gap in high-pressure density traceability chain.

FACULDADE DE CIÊNCIAS E TECNOLOGIA
UNIVERSIDADE NOVA DE LISBOA

IV

METROLOGICAL COMPATIBILITY OF OSCILLATION-TYPE DENSIMETRY AND REFRACTOMETRY MEASUREMENT RESULTS

Refractometers and density meters are daily widely used to measure the refractive index and density, respectively, the most varied type of aqueous solutions, such as juice, grape must and seawater. It is very interesting to think that through the refractive index or density of these solutions it is possible to determinate other quantities of interest, e.g. the mass fraction in sugar, or as is usual called the degrees brix, that in SI units corresponds to cg of sucrose per g of solution. This quantity is traditionally used in the wine, sugar, fruit juice, and honey industries. In wine production the mass fraction in sugar of the grape must is determinate to provide an estimate of the wine alcohol content, based on the fermentation reaction of glucose into ethanol. This prediction is very important not only for the wine enhancement but also for the control of the necessary chemical that must be applied during the wine production in order to enhance the wine organoleptic characteristics.

Another example is the salinity measurements of seawater. Salinity is a measure of the dissolved solids in seawater, usually expressed in grams per kilogram or parts per thousand by weight. Salinity is an ecological factor of considerable importance, influencing the types of organisms that live in a body of water. These measurements provide key information to be applied in thermodynamic models of the oceans. One of the most direct ways is to measure its refractive index which is related to density and can therefore be related to the absolute salinity.

IV.1 DETERMINATION OF SUGAR AND SALT MASS FRACTIONS IN AQUEOUS SOLUTIONS

Several studies have been performed by Furtado *et al.* (2010 and 2013)[8] and Pellegrino *et al*. (2011a and 2011b)[9] to investigate the metrological compatibility of the mass fraction results of some compounds (glucose and sodium chloride) in aqueous solutions obtained by two different measuring techniques: refractometry and oscillation-type densimetry.

As definition, metrological compatibility is a property of a set of measurement results for a specified measurand, such that the absolute value of the difference of any pair of measured quantity values from two different measurement results is smaller than some chosen multiple of the standard measurement uncertainty of that difference. Indeed, the assignment of metrological compatibility to the measurement results, as defined in the International Vocabulary of Metrology, VIM (JCGM 200:2012), enables to decide whether the measurement results refer to the same measurand, when obtained by different measuring instruments, which would then be commutable.

In these studies, two measuring instruments were used: one digital refractometer RE 50 from Mettler Toledo and an oscillation-type density meter DMA 5000 from Anton Paar. In short, the measuring principle of a refractometer is based in Snell-Descartes Law where the critical angle is measured with a charge coupled device (CCD) after refraction in the solution contained in a cell illuminated by a light emitting diode (LED) at a wavelength of 589,3 nm. The operating principle of an oscillation-type density meter was already described in detailed in previous chapters.

Particularly, in the most recent study, Furtado *et al.* (2013), prepared, by weighing, a total of 12 aqueous solutions: 8 of glucose with mass fraction within the interval from 3 to 40 $cg \cdot g^{-1}$, and 4 of sodium chloride with mass fraction within the interval from 7 to 24 $cg \cdot g^{-1}$. The maximum mass fraction of glucose tested (40 $cg \cdot g^{-1}$) does not correspond to the saturation of glucose but rather the limit of the density reference tables (Circular NBS C440, 632, 1942; OJEC L 272,1990), that was the case of sodium chloride solutions.

[8] Furtado, A., Pellegrino, O., Alves, S., *et al.* (2010) Determinação da fracção mássica de soluções aquosas de glucose por refractometria e densimetria de tubo vibrante, In *CONFMET2010*.

Furtado, A., Oliveira, C., Pellegrino, O., *et al.* (2013) Metrological Compatibility of the Measurement Results of Aqueous Solutions Mass Fractions by densimetry and Refractometry, IMEKO International TC8, TC23 and TC24 - 3rd Symposium on Traceability in Chemical, Food and Nutrition Measurements.

[9] Pellegrino, O., Furtado, A., Alves, S., Spohr, I. & E. Filipe (2011a) Compatibilidade metrológica de resultados de medição da fracção mássica de glucose em soluções aquosas por densimetria de tubo vibrante e refractometria, In *4.º Encontro Nacional da Sociedade Portuguesa de Metrologia*.

Pellegrino, O., Furtado, A., Alves, S., Spohr, I. & E. Filipe (2011b) Refractometria e densimetria de tubo vibrante: técnicas complementares na determinação da fracção mássica de glucose em soluções aquosas?, In *XXII Encontro Nacional da Sociedade Portuguesa de Química.*

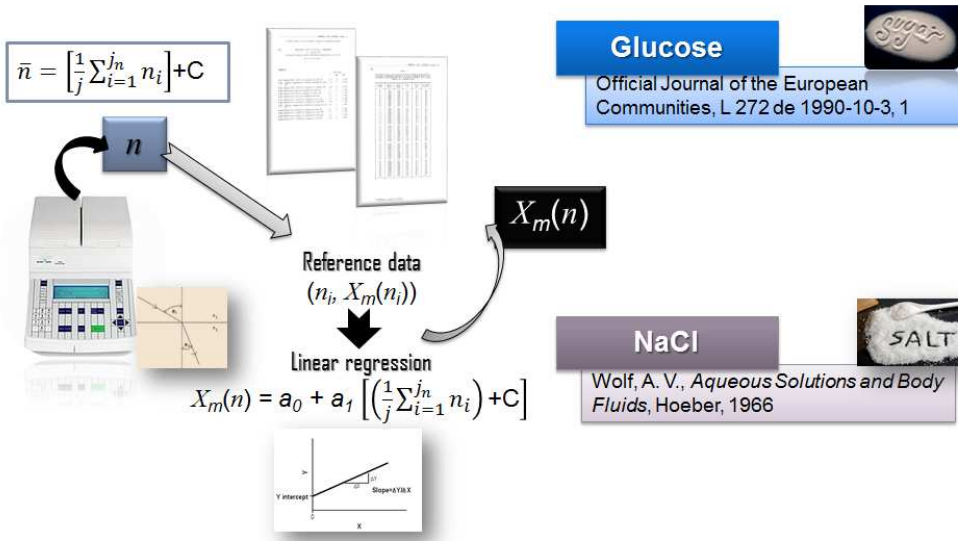

Figure IV.70 Schematics of the experimental methodology to obtain the mass fraction value of glucose and sodium chloride aqueous solutions from refractive index measurement results from a refractometer.

The employed methodologies to obtain the mass fraction value of the test samples included, in a first step, the measurement of the quantities of interest by the respective measuring instrument (i.e. refractive index, n with the refractometer and density, ρ with the density meter), and in a second step the conversion of this two quantities to mass fraction using references tables (i.e. n in $Xm(n)$ and ρ in $Xm(\rho)$), as can be seen in Fig.IV.70 and Fig.IV.71. The measurement equation for the average refractive index at a given temperature, $\bar{n}$ is represented in the Fig.IV.70 in the upper left corner, there C represents the refractive index correction based on certified reference materials used in refractometer calibration. The refractive index of glucose solutions was thus converted to mass fraction by linear regression of the reference values published in the Official Journal of the European Communities (OJEC L 272, 1990) and of aqueous solutions of sodium chloride through the reference values published by Wolf in 1966. The same logic was applied to density measurements, but where different reference data were used (Fig.IV.71). For glucose were considered the reference values published by the then National Bureau of Standards (Circular NBS C440, 632, 1942) and for sodium chloride were considered the reference values from Sohnel, 1985.

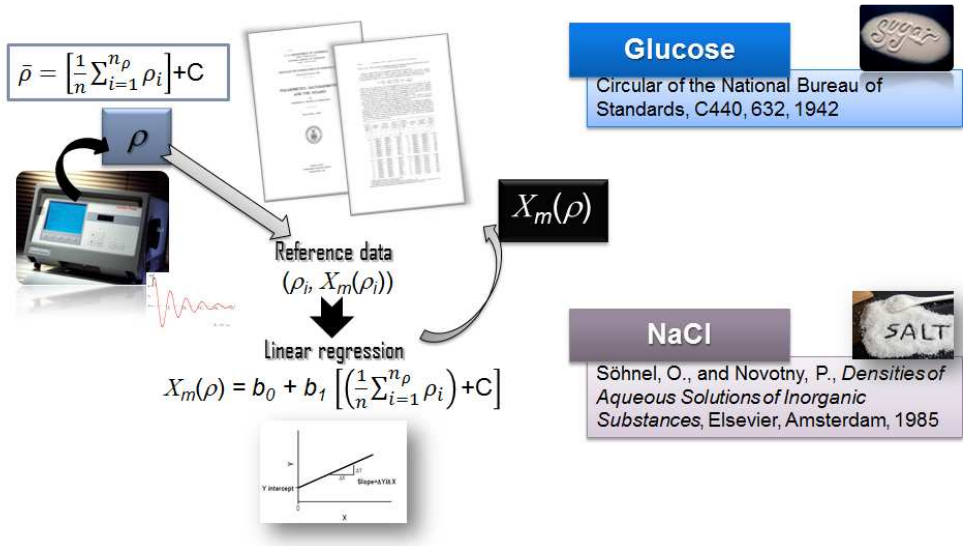

Figure IV.71 Schematics of the experimental methodology to obtain the mass fraction value of glucose and sodium chloride aqueous solutions from density measurement results from a density meter.

The results of the determination of the mass fraction in glucose, and in sodium chloride, at 20 ºC, by refractometry, $Xm(n)$ and densimetry, $Xm(\rho)$, are summarized on Table IV.44. As previously described, the metrological compatibility is a property of a set of measurement results for a specified measurand, in this case $Xm(n)$ and $Xm(\rho)$, such that the absolute value of the difference of any pair of measured quantity values from two different measurement results ($|X_{m(n)} - X_{m(\rho)}|$) is smaller than some chosen multiple, k of the standard measurement uncertainty of that difference, as can be seen in Eq. IV.1 (JCGM 200:2012). In this study the chosen multiple, k of the standard measurement uncertainty was a value of 2 corresponding to a level of 5 %.

$$|X_{m(n)} - X_{m(\rho)}| \leq k \cdot \sqrt{u^2{}_{Xm(n)} + u^2{}_{Xm(\rho)}} \qquad \text{(IV.1)}$$

As we can be seen in the results presented in the Table IV.44 for glucose solutions, all the mass fraction results in the interval from 3 to 40 cg·g^{-1}, obtained by refractometry and densimetry are metrologically compatibles, since the condition given by the Eq. IV.1 is fulfilled. However, for sodium chloride solutions the results were not so linear. It was observed that within the interval from 7 to 20 cg·g^{-1}the mass fraction values were compatibles but for the mass fraction near of saturated solution (around 26 cg·g^{-1}) it was not observed compatibility of the measurements (Table IV.44).

Table IV.44 Results of the determination of mass fraction at 20 ºC of the glucose aqueous solutions by refractometry, $Xm(n)$ and densimetry, $Xm(\rho)$, and respective uncertainty values.

Solution	$Xm(n)$ (cg·g^{-1})	$U_{Xm(n)}$ (cg·g^{-1})	$Xm(\rho)$ (cg·g^{-1})	$U_{Xm(\rho)}$ (cg·g^{-1})	$\Delta X_m = \lvert X_{m(n)} - X_{m(\rho)} \rvert$ (cg·g^{-1})	$\frac{\Delta X_m}{2.\sqrt{u^2{}_{X_{m(n)}} + u^2{}_{X_{m(\rho)}}}}$ (1)
1	3,16	0,10	3,23	0,10	0,07	0,51
2	5,73	0,10	5,79	0,10	0,06	0,41
3	10,50	0,10	10,43	0,10	0,07	0,52
4	11,64	0,10	11,66	0,10	0,02	0,19
5	19,56	0,10	19,56	0,10	0,00	0,01
6	26,80	0,10	26,78	0,10	0,02	0,19
7	34,66	0,10	34,65	0,10	0,01	0,06
8	40,36	0,10	40,28	0,10	0,08	0,55

Legend: U – expanded uncertainty for a coverage factor k =2.

The general conclusions of these studies were that the metrological compatibility for all range of glucose mass fraction tested was verified for the two methodologies used, indicating that these two methodologies can be used as redundant methods. Regarding the results of sodium chloride solutions for mass fractions near the saturation it was not observed metrological compatibility between the results obtained by refractometry and densimetry, and due to the great interest of these measurements for food science, health science, and oceanography, it is pointed out speed of sound as possible alternative methodology.

IV.2 Calibration of oscillation-type density meters for viscosity-induced damping with ICUMSA sucrose solutions[10]

Many of the laboratory and industrial oscillation-type density meters are daily used to measured high viscosity samples. In order to obtain accurate density values from the indication of these measuring instruments, they must be calibrated adequately by using viscous reference liquids. However, these reference liquids are not always available for the range of interest, or even for the similar matrix that the one of the liquids measured. The costs of such reference liquids can be also an additional difficulty that may lead to obtaining an inadequate or insufficient calibration. In this work, the suitability of the use of sucrose solutions, which density and viscosity were determinate via ICUMSA tables (ICUMSA SPS-3, 2000; ICUMSA SPS-4, 1998) by means of refractive index measurements.

Furtado *et al.* (2015) evidenced the applicability of the use of sucrose solutions to deduce calibrations curves for viscosity damping of a density meter in viscosity interval from 20 mPa·s to 55 mPa·s, at 20 ºC, with an expanded uncertainty of 0,030 $kg \cdot m^{-3}$. In this study, an interesting relationship between the difference of density indication without viscosity correction and density indication with viscosity correction was observed for DMA 5000 density meter (Anton Paar), allowing, without knowing the viscosity of the sample, to predict the correction to apply to density indication. The maximum deviations obtained in this work (Furtado *et al.*, 2015) were much larger than the one earlier described for this type of density meter (Fitzgerald, 2000).

IV.2.1 Introduction

The mass fraction, X_m of sugar aqueous solutions can be determined from the refractive index and density measurements.

Like for density measurements, the refractive index measurements allow to deduce the mass fraction values from correspondence tables between the measured quantity and the measurand, published by the ICUMSA (International Commission for Uniform Methods of Sugar Analysis) (ICUMSA SPS-4, 1998; ICUMSA SPS-3, 2000).

Previous studies (Pellegrino *et al.*, 2009)[11] displayed that linear interpolation in the interval of two successive referenced data was equivalent albeit with lower uncertainty value that least square linear regression upon at least 30 values. Therefore, the linear interpolation strategy in the two successive points intervals in followed in the present work for mass fraction measurement from density and refractive index measurements.

Metrological compatibility of mass fraction measurement results (JCGM 200:2008), by densimetry and refractometry, of glucose solutions, within the interval of 3 to 40 $cg \cdot g^{-1}$, was already demonstrated in previous work (Furtado *et al.*, 2013). There is some interest of studying aqueous solutions of sugars, as glucose and sucrose as they are used as reference materials for calibration and for metrological control of refractometers. Indeed, the refractive index values with respect to the sugar concentrations of these

[10] Furtado, A., Pellegrino, O., Pereira, J., Filipe, E. (2015) Oscillation-type density meter calibration in viscosity by ICUMSA sucrose solutions, XXI IMEKO World Congress, Book of Proceedings, Issue: 1, ISBN: 978-80-01-05793-3, TC09 Flow Measurement. This work was also presented as a poster communication at the XXI IMEKO World Congress, (August 30 to 4 September 2015, Prague, Czech Republic).

[11] Pellegrino, O., Furtado, A., & Filipe, E. (2009). Linear Fitting Procedures Applied to Refractometry of Aqueous Solutions. In XIX IMEKO World Congress.

solutions are well documented (ICUMSA SPS-4, 1998; ICUMSA SPS-3, 2000; *Jornal Oficial das Comunidades Europeias*, L 272, 1990).

Some test and industrial laboratory, which perform density measurements with oscillation-type density meters, works with very viscous samples, and therefore their density meter, must be calibrated with viscous reference liquid as well. No always CRM are available for the range of interest, or even for the similar matrix that the one of the liquids measured. The costs of such CRM can be also an additional difficulty that may lead to obtaining an inadequate or insufficient calibration.

In this part of the work, the suitability of the use of sucrose solutions, which density and viscosity were determinate via ICUMSA tables by means of refractive index measurements, to obtain calibrations curves for viscosity damping of a density meter in viscosity range of 20 to 55 mPa·s, at 20 ºC, it will be evaluated.

IV.2.2 Materials and Methods

VI.2.2.1 Density meter calibration for viscosity-induced damping

The deviation from density reference value of measuring results were analyzed for both density meter (DMA 5000, Anton Paar) indication of density with internal algorithm of correction of viscosity damping, $\delta\rho$, and for indication without internal corrections algorithm of correction, $\delta\rho_{nc}$. The difference between these two indications was also analyzed, ρ_{nc}-ρ. The uncertainty budget was performed according to GUM methodology (JCGM 100:2008) and as previously established (Furtado *et al.*, 2009).

IV.2.2.2 Determination of refractive index and density of sucrose solutions

Five D(+)-sucrose (extra pure, Scharlau) aqueous solutions, with mass fractions from 20 to 55 $cg \cdot g^{-1}$, were prepared gravimetrically with ultra-pure water (grade I) (ISO 3696:1987), produced by a MilliQ Advantage (Millipore), followed with a 2 hours stirring at room temperature.

The sucrose solutions refractive index, at 20 ºC, was measured with a digital refractometer RE 50 from Mettler Toledo, with a 10^{-5} resolution and a 0,01 ºC resolution thermostat. These measurements are traceable to SI using CRMs from the NMI of the USA, the NIST and from the NMI of Poland, the GUM.

The density of sucrose solutions was measured, at 20 ºC, with a oscillation-type density meter (DMA 5000 from Anton Paar).

The values of refractive index and density of different sucrose solutions were measured five times, from five different aliquots of the same sample, at 20 ºC, using internal procedures based on the Recommendation R124 from OIML (1997) and according to the standards ISO 15212 (1988), respectively.

IV.2.2.3 Determination of the density of sucrose solutions through ICUMSA tables

The mass fraction and the viscosity of each sucrose solution, through the refractive index mean values, were determinate by use of ICUMSA SPS-3 (2000) and SPS-5 (1994), respectively. The mass fraction obtained was then converted in density by mean of ICUMSA SPS-4 (1998). These density values were considered as reference values for the comparison with the density values obtained with the density meter.

IV.2.3 Results

The obtained results display that DMA 5000 density indication with viscosity correction, ρ, evidences a maximum deviation from the reference density value of 0,071 kg·m^{-3} and no dependence was observed with viscosity. On other hand, DMA 5000 density indication without viscosity correction, ρ_{nc}, increases with viscosity and evidences a similar behaviour to ρ_{nc}-ρ , as can be seen on Fig. IV.71.

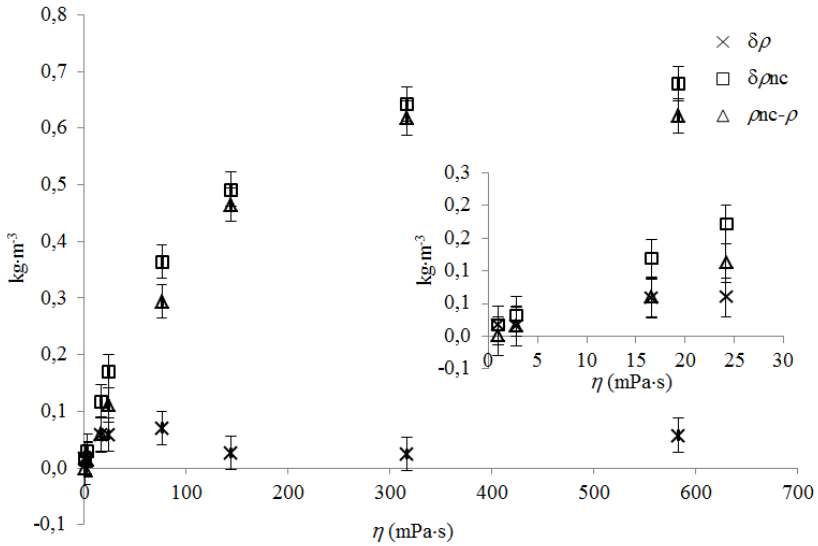

Figure IV.72 Density deviation, $\delta\rho_{nc}$, and difference between DMA 5 000 density indication without viscosity correction and with viscosity correctionρnc-ρ as a function of viscosity, at 20 ºC.

A linear relation can be observed between the density deviation of DMA 5000 density indication without viscosity correction, $\delta\rho_{nc}$, and the difference between the indication without and with viscosity correction, ρ_{nc}-ρ (Fig. IV.73). The maximum deviation of the linear curve presented in Fig. IV.69 is within the order of magnitude of the expanded uncertainty of the density measurements, i.e. 0,030 kg·m^{-3}.

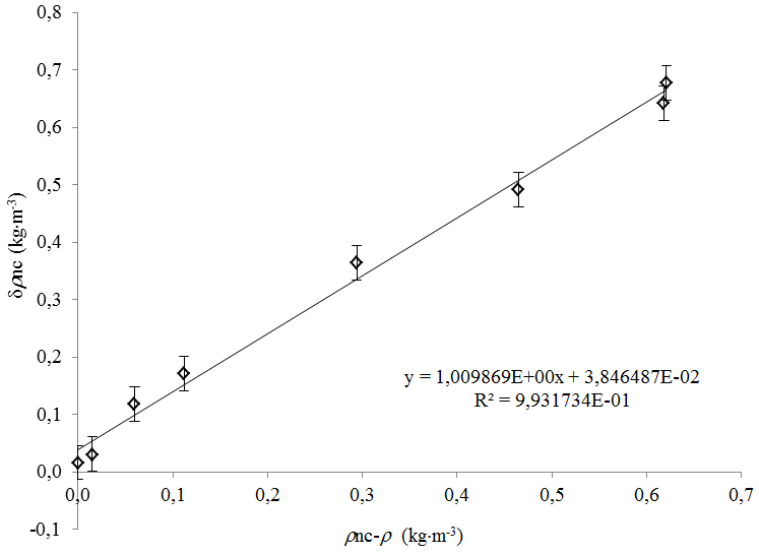

Figure IV.73 Relation between the deviation of DMA 5000 density indication without viscosity correction, $\delta\rho_{nc}$, and the difference between the indication without and with viscosity correction ρnc-ρ, at 20 ºC.

IV.2.3.1 Validation of damping curve with sucrose solutions

Through the ICUMSA tables (ICUMSA SPS-3, 2000), and from a refractive index with an expanded uncertainty of $2 \cdot 10^{-5}$, it was possible to deduce the density of the sucrose solutions with a maximum expanded uncertainty of 0,030 kg·m^{-3}.

The results presented in Table IV.45 show that the difference between the experimental values, $\delta\rho_{nc}$, and the values obtained by the curve of $\delta\rho_{nc}$ *vs* ρ_{nc}-ρ displayed in Fig. IV.73, $\delta\rho_{nc'}$, for the deviation of DMA 5000 density indication without viscosity correction is smaller than the expanded uncertainty of the density measurements, i.e. below 0,030 kg·m^{-3}.

Table IV.45 Results from validation of damping curve tests with sucrose solutions.

Sucrose X_m (cg·g^{-1})	η (mPa·s)	$\rho_{ref.}$ (kg·m^{-3})	$\delta\rho_{nc}$ (kg·m^{-3})	ρ_{nc}-ρ (kg·m^{-3})	$\delta\rho_{nc'}$ (kg·m^{-3})	$\delta\rho_{nc}$ –$\delta\rho_{nc'}$ (kg·m^{-3})
20,014	1,95	1081,038	0,040	0,005	0,044	0,003
30,007	3,19	1127,064	0,037	0,014	0,052	0,015
39,982	6,60	1176,426	0,107	0,046	0,085	-0,023
49,991	15,42	1229,607	0,134	0,100	0,139	0,005
54,994	28,05	1257,615	0,242	0,179	0,220	-0,022

Legend: $\delta\rho_{nc'}$- deviation from density reference value of DMA 5000 indication without internal corrections for viscosity obtained by the curve of $\delta\rho_{nc}$ *vs* ρ_{nc}-ρ obtained in Fig. IV.4.

IV.2.4 Conclusions

The use of sucrose solutions, the density values of whom were achieved by ICUMSA conversion tables (ICUMSA SPS-3, 2000), through refractive index measurements, allowed to validate the use of the linear relation between the deviation of DMA 5 000 density indication without viscosity correction, $\delta\rho_{nc}$, and the difference between the indication without and with viscosity correction ρ_{nc}-ρ, in the viscosity values range from 1 to 30 mPa·s, at 20 ºC, with an expanded uncertainty of 0,030 kg·m^{-3}. Sucrose is a cheap and a green reagent and the sucrose solutions are easy to prepare. For a test or industrial laboratory using a standard refractometer, it is possible to obtain a calibration curve for viscosity damping of a density meter.

IV.3 DETERMINATION OF ABSOLUTE SALINITY BY DENSIMETRY AND REFRACTOMETRY[12]

The salinity of seawater has been studied approximately for four decades, but indirectly determined through the electrical conductivity. This method is time consuming and gives results with a low accuracy. However, there are indirect methods capable of determining salinity, such as densimetry and refractometry. This work aimed to study the metrological compatibility of salinity determinations via these two methods. Sodium chloride solutions were prepared in ultrapure water and in two different artificial standard seawaters (OSIL and ERM), for later study of the matrix effect on the metrological compatibility of the salinity results obtained. The metrological compatibility of the salinity results obtained by measurement of the density and of the refractive index was verified in the [35,0; 200,0] g·kg^{-1}.

IV.3.1 Introduction

Seawater covers more than 70 % of the Earth's surface and accounts for about 97 % of Earth's water resources. On average, in each kilogram of seawater between 32 g and 37 g of salts are dissolved. This mass of dissolved salts found in seawater, brackish water, brine, or other saline solution, divided by the mass of the solution, defines salinity, S, usually expressed in SI units of grams per kilogram (g kg^{-1}), or expressed without the units given explicitly. Albeit some published works express S with the unit per mil, this is not recommended since the establishment of the Practical Salinity Scale (PSS78), in 1978 (IUPAC, 2008). Salinity interval values range from below a few g·kg^{-1}, for rivers and lakes, to 35 g·kg^{-1}, for seawater, 200 g·kg^{-1} for the Dead Sea up to brine salinity values as high as around 260 g·kg^{-1}.

The salt content or salinity of the oceans is one of the most important parameters in oceanography. Its importance has long been recognized in studies of water mass movements in the open ocean (Feistel, 2008). Salinity or more precisely *Absolute Salinity* is a term used to quantify the total mass of substances dissolved in pure water to form a given mass of seawater (Feistel *et al.*, 2015). Improving knowledge of sea surface salinity leads to a better estimation of the global hydrological cycle which, ultimately, will contribute towards a better understanding of climate change. Salinity is also an important parameter of marine science having a considerable influence as an ecological factor on marine organisms, affecting algal blooms, movement of fish stocks, shellfish productivity, and aquaculture. Two main kinds of salinity can be defined. Absolute salinity, S_A, essentially represents the total dissolved salts whereas practical salinity, S, is calculated from the conductive components only. The former, S_A, offers several advantages over the latter, S, for oceanographic purposes. For instance, it has no limitations by scale (as in PSS78), improves ocean models (as S_A is truly conservative), and enables reducing density errors in the Equation of State for seawater. Hence, new algorithms have been formulated for density, enthalpy, entropy, potential temperature, and sound speed in terms of absolute salinity, temperature and pressure (Feistel, 2008).

A remarkable characteristic of seawater is that its relative chemical composition is fairly uniform around the world (Nayar, Scharqawy and Banchik, 2016), which allows it to be treated as an aqueous solution of a single salt concentration by using the quantity *Absolute Salinity* (Millero *et al.,* 2008). The physical properties of seawater can thus be expressed as a function of temperature, pressure, and salinity. However, the mass fraction of dissolved salt in seawater is difficult to measure directly. Thus, several salinity scales have been historically used to approximate it: *Knudsen Salinity* (SK) (Knudesn, 1901), *Chlorinity* (Cl) (Jacobsen and Knudsen, 1940), *Practical Salinity* (SP) (Lewis and Perkin, 1978), and,

[12] This work was submitted for publication to the *Measurement Journal* on the 6th of September 2019, as: Furtado, A., Napoleão, A., Pereira, J., Quendera, R., Pellegrino, O., Cidade, M.T., Oliveira, C.R., & Sousa, J.A. Determination of absolute salinity by refractometry and oscillation-type densimetry as compatible methods.

most recently, *Reference Salinity* (SR) (Millero *et al.*, 2008). Indeed, this quantity cannot be measured directly in seawater or other natural waters because of the difficulty of drying the salts from these waters being the salinity usually calculated from other quantities, such as chlorinity or the electrical conductivity, whose relationship to salinity is well known (IUPAC, 2008). These properties, however, cannot be accurately measured, and that is why precise measurements of salinity are required specially by the oceanographic community.

Among the experimental techniques that allow the quantitative analysis of the compounds in aqueous solutions, densimetry and refractometry have shown to be reliable and easy to use for aqueous solutions of sodium chloride. For instance, the metrological compatibility of their obtained results for sodium chloride aqueous solutions, in the NaCl mass fraction $X_{m\mathrm{NaCl}}$ interval from 7 cg g^{-1} to 24 cg g^{-1} (corresponding to a Salinity interval of 70 to 240 g·kg^{-1}), had already been demonstrated (Furtado *et al.*, 2010, 2013[13]; Pellegrino *et al.*, 2011a, 2011b). To this purpose, and due to the complexity of measuring the contents of multi-components aqueous solutions, the mass fraction of one salt dissolved in water may be determined through the above-mentioned analytical techniques. As it is the main dissolved component in seawater, sodium chloride in water is a good candidate to be a model of seawater. In this study, these two methodologies, based on refractometry and densimetry, were used with sodium chloride aqueous solutions to test the compatibility (JCGM 200:2012) of salinity determinations in a wider interval of S_A [20; 260] g·kg^{-1}. Additionally, the matrix effect of seawater was also tested with these methodologies by using two artificial standard seawater samples (OSIL and ERM) as matrix and incrementing the salinity by addition of sodium chloride.

IV.3.2 Materials and Methods

The present work was divided into two experimental parts. The first one consisted on the study of the metrological compatibility of absolute salinity values, S_A, obtained by two different measurement techniques: refractometry and densimetry. For this purpose, a set of 13 sodium chloride solutions in ultrapure water, corresponding to a [20; 260] g kg^{-1} S_A salinity interval, was prepared and tested at 20 ºC. In a second part, two sets of solutions based in two artificial standard seawaters (SSW) were prepared, with the aim of studying the effect of the matrix, i.e. the different saline compositions, on the results of the absolute salinity obtained and compare them to the ones in ultrapure water aqueous solutions.

IV.3.2.1 Preparation of test solutions

The NaCl (pellets, 99,7 % purity, PanReac) solutions were gravimetrically prepared in order to obtain absolute salinity values S_A between 20 and 260 g·kg^{-1}, by y using a mass comparator of Mettler Toledo, PR 2004, bringing the salinity values to the standard uncertainty of about 1 g·kg^{-1}. The ultrapure water (type I) (ISO 3696:1987) used in the preparation of the solutions was produced by the Milli Q Advantage water system from Merck Millipore. Finally, to ensure good homogeneity and the absence of precipitates, all solutions were agitated on a stirring plate for at least 60 minutes. Table IV.46 summarizes the density, ρ and refractive index, n, values, at 20 ºC obtained (Söhnel and Novotny, 1985; Wolf, 1966).

[13] Furtado, A., Oliveira, C., Pellegrino, O., *et al.* (2013) Metrological Compatibility of the Measurement Results of Aqueous Solutions Mass Fractions by densimetry and Refractometry, In *IMEKO International TC8, TC23 and TC24 - 3rd Symposium on Traceability in Chemical, Food and Nutrition Measurements.*

Table IV.46 Summary of the density, ρ and refractive index, n values, at 20 ºC, corresponding to the absolute salinity, S_A interval studied (*(Söhnel and Novotny, 1985); **(Wolf, 1966)).

S_A (g·kg^{-1})	ρ^* (g·cm^{-3})	n^{**} (1)
20	1,0125	1,3365
35	1,0232	1,3391
50	1,0340	1,3418
75	1,0523	1,3462
100	1,0707	1,3505
150	1,1085	1,3594
175	1,1280	1,3639
200	1,1478	1,3684
210	1,1558	1,3702
230	1,1721	1,3739
260	1,1972	1,3795

IV.3.2.2 Refractive index measurements

The refractive index, n, of a solution can vary with its composition, concentration, temperature, and the wavelength of light incident. The relationship between the solution concentration and the refractive index has many applications including salt concentration measurement. According to the Snell-Descartes law, the direction of propagation of the light going through a solution, linearly change with its concentration. The refractive indexes of the samples were measured with a refractometer Abbemat 550 from Anton Paar, with a [1,300 000; 1,720 000] measuring interval, with SI traceability by calibration using certified reference materials for the refractive index from 3 National Metrology Institutes (GUM - Poland; NIST - USA and PTB - Germany), ensuring a 0,000 01 refractive index standard uncertainty. Measurements of the Snell-Descartes law critical angle were performed by a charge coupled device (CCD) after refraction in the solution located in an approximately 0,4 mL cell, maintained at 20,00 ºC and illuminated by a light emitting diode (LED) at a 589.3 nm wavelength.

IV.3.2.3 Density measurements

The density measurements were performed with an oscillation-type density meter DMA 5000 from Anton Paar.

IV.3.2.4 From refractive index and density to absolute salinity

The employed methodology to obtain the absolute salinity value of the test samples was like the one previously used (Furtado *et al.*, 2013; Napoleão *et al.*, 2018). Once the quantity of interest, the refractive index, n, or the density, ρ, was measured, internationally recognized reference tables were used to convert it into mass fraction, for the 20 ºC reference temperature, as the quantities are temperature dependent. Linear interpolation in the intervals of the two successive tabled data are performed to deduce mass fraction value, as it provides a smaller uncertainty deduced value (Pellegrino, Furtado & Filipe, 2009). NaCl mass fractions were determined from refractive index measurements, using reference values published in 1966 (Wolf, 1966) still in use, whereas the density reference values were published in 1985 (Söhnel & Novotny, 1985). For instance, to obtain NaCl mass fraction value, $X_m(n_p)_p$ from the average of N measurement values of the refractive index, at 20 ºC, after correction with the calibration curve of the refractometer (Eq. IV.2), an interpolation was done by using a set of pairs of values $(n_{(p-1)}, X_m(n)_{(p-1)})$ and $(n_{(p+1)}, X_m(n)_{(p+1)})$ from the reference values published by Wolf (1966), according to Eq. IV.3. The *C* value represents the refractive index correction based on CRM used in refractometer calibration.

$$n_p = \frac{\sum_{i=1}^{N} n_i}{N} + C \quad \text{(IV.2)}$$

$$X_m(n_p)_p = \frac{[n_p - n_{(p-1)}][\mathrm{X}_m(n)_{(p-1)} - \mathrm{X}_m(n)_{(p+1)}]}{n_{(p-1)} - n_{(p+1)}} + X_m(n)_{(p+1)} \quad \text{(IV.3)}$$

From the interpolated value of the mass fraction in NaCl $X_m(n_p)_p$, in cg g^{-1}, (Eq. IV.2), the value of absolute salinity, S_A, was obtained by multiplication of a factor of 10, i.e. $S_A = 10\ X_m(n_p)_p$, in g·kg^{-1}. The same methodology was applied to density values by using the density meter calibration curve and the respective set of pairs of values from the reference values published by Söhnel and Novotny (Söhnel and Novotny, 1985).

IV.3.2.5 Uncertainty budget of determination of the absolute salinity values from density and refractive index

The cause-effect diagram displayed in Fig. IV.74 represents the different contributions to the standard uncertainty of the determination of absolute salinity, S_A ($S_A(n)$ and $S_A(\rho)$), from the different input quantities (refractive index, n, and density, ρ) as well as the uncertainty inherent to interpolation, that have the contribution of the linear regression uncertainty (in the form of residuals) and from the reference data. The uncertainty associated with each input quantity is a combination of three main sources of uncertainty: measurements repeatability, i.e. dispersion; the correction of the temperature of the sample; and component for calibration of the measuring instruments (C). Additionally, the components of measurement uncertainty were grouped into two categories, Type A and Type B, according to whether they were evaluated by statistical methods or other methods (Type A), and how they are combined to yield a variance according to the rules of mathematical probability theory (Type B). The uncertainty budget was calculated according to the GUM (JCGM 100:2008).

The calculation of the standard uncertainty of the differences of pairs of absolute salinity results and ($S_A(n)_i$, $S_A(\rho)_i$) are performed according to the GUM methodology (JCGM 100:2008), considering that the absolute salinity results $u^2(S_{A,i})$ by both refractometry and densimetry are uncorrelated. Albeit the temperature uncertainty component is present in expressions of uncertainties of all analytical techniques, its contribution is around 1000 times smaller than the greatest contribution uncertainty component, which allowed us to neglect its covariance term in the expression $[u^2(S_A(n)_i) + u^2(S_A(\rho)_i)]^{1/2}$.

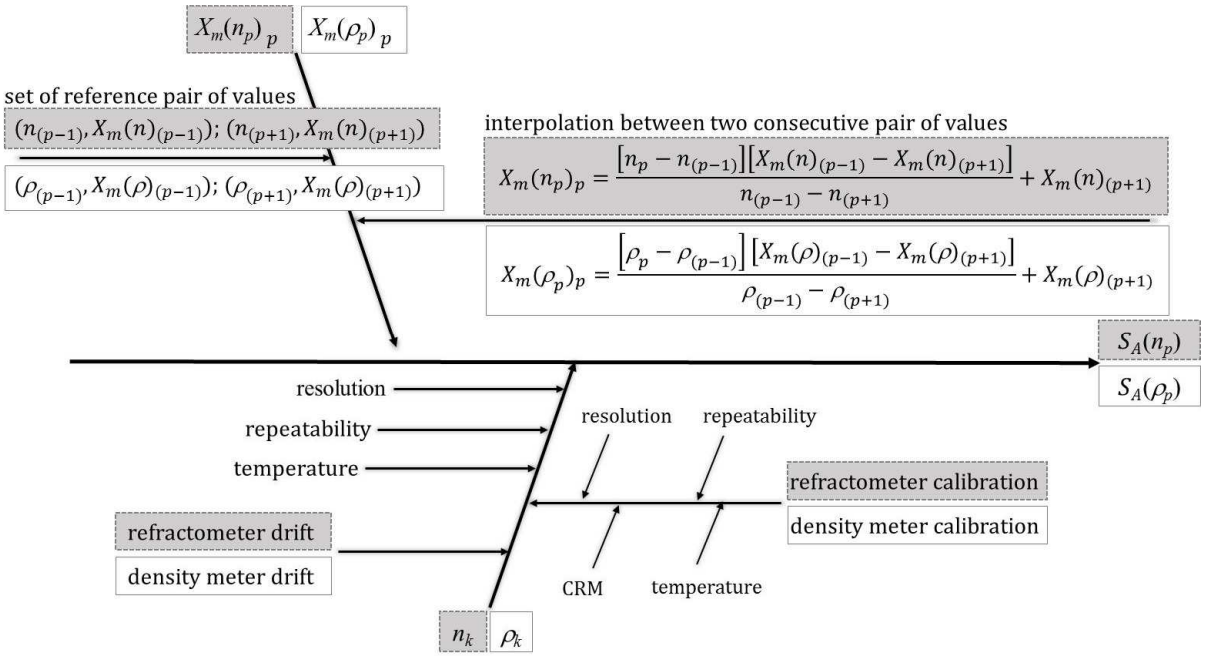

Figure IV.74 Cause-and-effect diagram of the contributions to the standard uncertainty of the determination of the absolute salinity results, S_A, from the different input quantities refractive index, n and density, ρ.

As shown in Fig. IV.74, reference data used in developing correlations present its one uncertainty (Söhnel and Novotny, 1985; Wolf, 1966), which is generally given by the rounding accuracy with which the numbers are expressed. Furthermore, the uncertainty associated with the use of interpolation between reference data, sometimes may result in deviations between the reference data and the interpolated value.

The combined standard uncertainty of the measurand, i.e. $S_A(n)$ and $S_A(\rho)$ at 20 ºC, is determined by taking the value of the square root of its variance deduced from the input quantities and from the influence quantities using the GUM (JCGM 100:2008) formalism based on the Law of propagation of the uncertainties. This law consists on calculating the different uncertainty components $u_i(y) = |\frac{dy}{dx_i}| u(x_i)$ of y due the input quantities x_i, in which $u(x_i)$ represents the standard uncertainty of the input quantity x_i and $\frac{dy}{dx_i}$ are the sensitivity coefficients that are derived from the calculation algorithm. The number of effective degrees of freedom was calculated according to the Welch-Satherwaite formula, given by Eq. II.C.7.

The calculation of the expanded uncertainty, U, gives a confidence interval where the true value of the measurement is expected to lie. The expanded uncertainty is obtained by multiplying the combined uncertainty value, $u_c(y)$, by an expansion factor, k, assuming a normal distribution, i.e. $U = k \cdot u_c(y)$. Then, the measurement result lies in the interval [y - U; y + U].

The uncertainty budget of the absolute salinity results, S_A, obtained via density, $S_A(\rho)$ and refractive index, $S_A(n)$ measurements, at 20 ºC, is given on Table IV.47.

Table IV.47 Uncertainty budget of the absolute salinity results, S_A, obtained via density, $S_A(\rho)$ and refractive index, $S_A(n)$ measurements, at 20 ºC.

Contribution	Standard uncertainty	Type of evaluation	Distribution	Degrees of freedom
Instruments[1] resolution	$\frac{1 \cdot 10^{-6}}{\sqrt{12}}$	B	Rectangular	50
Instruments[1] calibration (including drift)	$n \rightarrow 1 \cdot 10^{-5}$ $\rho \rightarrow 1 \cdot 10^{-5}$	B	Normal	50
n and ρ measurements repeatability	$\frac{\sigma}{\sqrt{n}}$	A	Normal	n-1
Temperature[2]	-	A	Normal	50
Interpolation (including reference values[3,4] and residuals)	$n \rightarrow 2 \cdot 10^{-2}$ $\rho \rightarrow 6 \cdot 10^{-3}$	B	Rectangular	50

Legend: σ – standard deviation of the mean value of the measurements; for refractive index n: 1 - refractometer Abbemat 550 from Anton Paar; 3 – set of reference pair of values (n, X_m), given by (Wolf, 1966, with an uncertainty of $U_n = (1 \cdot 10^{-4})/(12)^{1/2}$ for refractive index values and $U_{XmNaCl} = (1 \cdot 10^{-1})/(12)^{1/2}$ for NaCl mass fraction values; for density, both with rectangular distributions; ρ: 1 – oscillation-type density meter DMA 5000 from Anton Paar; 4 – set of reference pair of values (ρ , X_m), (Söhnel and Novotny, 1985), with an uncertainty of $U_{XmNaCl} = (1 \cdot 10^{-1})/(12)^{1/2}$ for density values and $U_\rho = (1 \cdot 10^{-4})/(12)^{1/2}$ for NaCl mass fraction values, both with rectangular distributions; 2 – the uncertainty due to the temperature measurements of the samples is already taken into account in the uncertainty of the calibration of the refractometer and of the density meter, since the dependency $n(t)$ and $\rho(t)$ is also tested for the CRM used in the calibration.

IV.3.2.6 Study of the metrological compatibility of the absolute salinity values obtained by refractometry and by densimetry

The metrological compatibility is a property of a set of measurement results for a specified measurand, such that the absolute value of the difference of any pair of measured quantity values from two different measurement results is smaller than some chosen multiple of the standard measurement uncertainty of that difference. Indeed, the assignment of metrological compatibility to the measurement results, as defined in the VIM (JCGM 200:2012), enables to decide whether the measurement results refer to the same measurand, when obtained by different measuring instruments, which would then be commutable.

To study the metrological compatibility of the absolute salinity values obtained by refractometry and by densimetry in the [20; 260] g·kg^{-1} S_A interval, 13 solutions of sodium chloride in ultrapure water were prepared according to point IV.2.2.1. The refractive index and the density of these solutions were measured, at 20 ºC, according to the description of IV.3.2.2 and IV.3.2.3, respectively. These values were finally converted to $S_A(n)$ and $S_A(\rho)$ values (point IV.3.2.4) with associated uncertainties $U\,S_{A(n)}$ and $U\,S_A(\rho)$ (point IV.3.2.5). The assessment of the metrological compatibility of these salinity results was performed as described in point IV.2.2.8.

IV.3.2.7 Study of the effect of the seawater matrix on the determination of the absolute salinity by refractometry and by densimetry

In this part of the work, the analysis of the effect of the seawater matrix on the determination of the absolute salinity, S_A, by refractometry and by densimetry for aqueous solutions in the [35; 200] g·kg^{-1} salinity interval, was performed. The solutions were prepared based on two samples of artificial standard seawater (OSIL and ERM-CA403) and NaCl was added to obtain the desired salinity according to Tables IV.9-11. The measurement of the density of these solutions was carried out according to the methodology described above.

IV.3.2.8 Assessment of the metrological compatibility of the absolute salinity results

The chosen multiple, k, of the standard measurement uncertainty was a value of 2 corresponding to a level of 5 %. In short, if the ratio $\frac{\Delta S_A}{U_{\Delta S_A}}$, of a certain pair of salinity values obtained by refractometry and by densimetry ($S_A(n)_i$; $S_A(\rho)_i$), respectively, for a same solution, is less or equal to 1, the set of measurement results are consider metrologically compatible (within the interval of confidence chosen) and the experimental techniques are commutable.

IV.3.3 Results and Discussion

IV.3.3.1 Study of the metrological compatibility of the absolute salinity values obtained by refractometry and by densimetry

The absolute salinity results obtained from the measured values of refractive index, $S_A(n)$, and density, $S_A(\rho)$, at 20 °C and the respective expanded uncertainties, U, of the 14 aqueous solutions of NaCl in ultrapure water are given in Table IV.6; those of the 13 solutions of NaCl in OSIL SSW are presented in Table IV.7 and those of the 13 solutions of NaCl in artificial ERM SSW in Table 5. On average, the relative uncertainty for obtaining $U_{S_A(n)}$ from the measured refractive index values is about 7 times higher than the relative uncertainty for obtaining $U_{S_A(\rho)}$ from the values of density for the case of NaCl solutions in ultrapure water, about 5 times higher in the case of NaCl solutions in OSIL SSW and about 11 times higher in the case of NaCl solutions in ERM SSW (Tables IV.48-50).

Table IV.48 Absolute salinity, S_A results of the solutions of sodium chloride in ultrapure water obtained from the measured values of refractive index, $S_A(n)$, and density, $S_A(\rho)$, and respective expanded uncertainties, U_{S_A} (k =2).

$S_{A,\text{nom.}}$	$S_A(n)$	$U_{S_A(n)}$		$S_A(\rho)$	$U_{S_A(\rho)}$	
(g·kg^{-1})	(g·kg^{-1})	(g·kg^{-1})	(%)	(g·kg^{-1})	(g·kg^{-1})	(%)
35	34,74	0,30	0,86	34,957	0,060	0,17
50	49,56	0,20	0,40	49,700	0,060	0,12
70	70,00	0,20	0,29	70,200	0,060	0,09
74	73,59	0,30	0,41	73,858	0,060	0,08
98	98,41	0,60	0,61	97,863	0,060	0,06
144	143,86	0,20	0,14	143,992	0,060	0,04
166	166,39	0,10	0,06	166,441	0,060	0,04
188	188,20	0,30	0,16	188,424	0,060	0,03
197	197,73	0,80	0,40	196,929	0,060	0,03
201	201,27	0,24	0,12	200,939	0,060	0,03
211	211,39	0,55	0,26	210,859	0,060	0,03
215	214,63	0,40	0,19	214,234	0,060	0,03
231	231,57	0,70	0,30	230,834	0,060	0,03

Legend: U – expanded uncertainty for a coverage factor k =2.

Table IV.49 Absolute salinity, S_A results of the solutions of sodium chloride solutions in OSIL SSW obtained from the measured values of refractive index, $S_A(n)$, and density, $S_A(\rho)$, and respective expanded uncertainties, U_{S_A} (k =2).

$S_{A,\text{nom.}}$	$S_A(n)$	$U_{S_A(n)}$		$S_A(\rho)$	$U_{S_A(\rho)}$	
(g·kg^{-1})	(g·kg^{-1})	(g·kg^{-1})	(%)	(g·kg^{-1})	(g·kg^{-1})	(%)
37,4	37,74	0,13	0,35	37,878	0,060	0,16
37,7	37,22	0,16	0,44	37,386	0,060	0,16
37,8	38,17	0,11	0,29	38,282	0,060	0,16
38,6	39,02	0,19	0,48	39,204	0,060	0,15
39,4	39,75	0,11	0,29	39,864	0,060	0,15
41,0	41,27	0,23	0,55	41,497	0,060	0,14
41,8	41,96	0,29	0,69	42,252	0,060	0,14
42,6	42,90	0,25	0,58	43,147	0,060	0,14
75,0	73,02	0,47	0,64	73,484	0,060	0,08
100,0	97,41	0,30	0,30	97,707	0,060	0,06
150,0	143,56	0,22	0,15	143,777	0,060	0,04
175,0	170,43	0,06	0,04	170,491	0,060	0,04
200,0	196,19	1,31	0,67	194,883	0,060	0,03

Legend: U – expanded uncertainty for a coverage factor k =2.

Table IV.50 Absolute salinity, S_A results of the solutions of sodium chloride in ERM SSW obtained from the measured values of refractive index, $S_A(n)$, and density, $S_A(\rho)$, and respective expanded uncertainties, U_{S_A} (k =2).

$S_{A,\text{nom.}}$	$S_A(n)$	$U_{S_A(n)}$		$S_A(\rho)$	$U_{S_A(\rho)}$	
(g·kg^{-1})	(g·kg^{-1})	(g·kg^{-1})	(%)	(g·kg^{-1})	(g·kg^{-1})	(%)
36,2	36,23	0,74	2,05	35,487	0,060	0,17
36,2	36,22	0,77	2,13	35,451	0,060	0,17
36,6	36,61	0,74	2,01	35,873	0,060	0,17
37,4	37,44	0,73	1,94	36,718	0,060	0,16
38,2	38,20	0,68	1,79	37,515	0,060	0,16
39,8	39,72	0,63	1,58	39,088	0,060	0,15
40,6	40,72	0,79	1,95	39,927	0,060	0,15
50,0	49,07	0,30	0,61	48,772	0,060	0,12
75,0	73,39	0,42	0,57	72,971	0,060	0,08
100,0	97,57	0,57	0,59	96,996	0,060	0,06
150,0	145,73	0,77	0,53	144,959	0,060	0,04
175,0	170,47	0,59	0,35	169,880	0,060	0,04
200,0	194,78	0,86	0,44	193,926	0,060	0,03

Legend: U – expanded uncertainty for a coverage factor k =2.

The results of the compatibility analysis of the absolute salinity values, S_A obtained from the measured refractive index values, n and density ρ, at 20 °C, of the NaCl solutions in ultrapure water, of the NaCl solutions in OSIL SSW and those of the NaCl solutions in ERM SSW, are given in Tables IV.51-53, respectively, in the form of ΔS_A' corresponding to the relative difference between a pair of salinity values obtained by refractometry and by densimetry $\Delta S_A'$, that is given by $\frac{|S_{A(n)}-S_{A(\rho)}|}{S_{A,nom}}$ 100, the correspondent relative uncertainty $U'_{\Delta S_A}$, and their ratio $\frac{\Delta S_A}{U_{\Delta S_A}}$.

Table IV.51 Assessment of the metrological compatibility of the relative differences between pairs of salinity values obtained by refractometry and by densimetry $\Delta S_A'$, and their correspondent relative uncertainty $U'_{\Delta S_A}$ obtained for sodium chloride solutions in ultrapure water.

$S_{A,\mathrm{nom.}}$ (g·kg^{-1})	$\Delta' S_A$ (%)	$U'_{\Delta S_A}$ (%)	$\frac{\Delta S_A}{U_{\Delta S_A}}$ (1)
35	-0,63	0,87	0,7
50	-0,27	0,42	0,7
70	-0,29	0,30	1,0
74	-0,36	0,41	0,9
98	0,56	0,62	0,9
144	-0,09	0,15	0,6
166	-0,03	0,07	0,5
188	-0,12	0,16	0,7
197	0,40	0,41	1,0
201	0,16	0,12	1,3
211	0,25	0,26	1,0
215	0,18	0,19	1,0
231	0,32	0,30	1,0
262	0,40	0,42	1,0

Legend: U' – expanded uncertainty for a coverage factor k =2.

Table IV.52 Assessment of the metrological compatibility of the relative differences between pairs of salinity values obtained by refractometry and by densimetry $\Delta S_A'$, and their correspondent relative uncertainty $U'_{\Delta S_A}$, obtained for sodium chloride solutions in OSIL SSW.

$S_{A,\mathrm{nom.}}$ (g·kg^{-1})	$\Delta S_A'$ (%)	$U'_{\Delta S_A}$ (%)	$\frac{\Delta S_A}{U_{\Delta S_A}}$ (1)
3,74	-0,36	0,39	0,9
3,77	-0,43	0,46	0,9
3,78	-0,29	0,33	0,9
3,86	-0,48	0,51	1,0
3,94	-0,29	0,33	0,9
4,10	-0,56	0,58	1,0
4,18	-0,69	0,70	1,0
4,26	-0,59	0,60	1,0
7,50	-0,62	0,63	1,0
10,00	-0,30	0,30	1,0
15,00	-0,14	0,15	1,0
17,50	-0,04	0,05	0,7
20,00	0,66	0,66	1,0

Legend: U' – expanded uncertainty for a coverage factor k =2.

Table IV.53 Assessment of the metrological compatibility of the relative differences between pairs of salinity values obtained by refractometry and by densimetry $\Delta S_A'$, and their correspondent relative uncertainty $U'_{\Delta S_A}$, obtained for sodium chloride solutions in ERM SSW.

$S_{A,nom.}$ (g·kg^{-1})	$\Delta S_A'$ (%)	$U'_{\Delta S_A}$ (%)	$\frac{\Delta S_A}{U_{\Delta S_A}}$ (1)
3,62	2,05	2,05	1,0
3,62	2,13	2,14	1,0
3,66	2,01	2,01	1,0
3,74	1,94	1,95	1,0
3,82	1,79	1,80	1,0
3,98	1,58	1,58	1,0
4,06	1,95	1,96	1,0
5,00	0,60	0,61	1,0
7,50	0,55	0,56	1,0
10,00	0,57	0,58	1,0
15,00	0,51	0,51	1,0
17,50	0,34	0,34	1,0
20,00	0,43	0,43	1,0

Legend: U' – expanded uncertainty for a coverage factor k =2.

Following the methodology described previously (in point IV.2.2.8), it can be concluded that the absolute salinity values determined by the refractometry and densimetry measurement results are metrologically compatible, since the condition $\Delta S_A \leq U_{\Delta S_A} \Leftrightarrow \frac{\Delta S_A}{U_{\Delta S_A}} \leq 1$ is fulfilled almost whatever the absolute salinity value given in Tables IV.51-53.

IV.3.3.2 Study of the effect of the seawater matrix on the determination of salinity by refractometry and by densimetry

The effect of the seawater matrix on the determination of the absolute salinity of aqueous solutions, by refractometry and by densimetry, at 20 ºC, was studied in the [35; 200] g·kg^{-1} salinity interval SA. The test solutions were prepared based on two artificial standard seawater samples (OSIL and ERM-CA403) by addition of certain mass of NaCl to obtain the desired salinity.

Fig. IV.75 and IV.76 display the variation of the relative expanded uncertainty $U'S_A$ values of the absolute salinity, S_A obtained from the measured values of density, ρ, at 20 °C, depending on the nominal value of the absolute salinity, S_A of the solutions of NaCl in ultrapure water (UPW), and in SSW from OSIL and ERM. In the case of the values of $U'S_{A(\rho)}$, there is no dependence on the type of matrix (i.e. ultrapure water, OSIL or ERM) (Fig. IV.76). A maximum value of $U'Xm_{\mathrm{NaCl}(\rho)}$ of 0,20 % (Fig. IV.76) was obtained, for NaCl solutions in ERM, with a $U'S_{A(n)}$ between 0,1 % and 0,9 %, and finally the NaCl solutions in OSIL SSW with a $U'S_{A(n)}$ between 0,3% and 2,1 %, then NaCl solutions in type I water, with a $U'S_{A(n)}$ between 0,1 % and 0,7 % (Fig. IV.75).

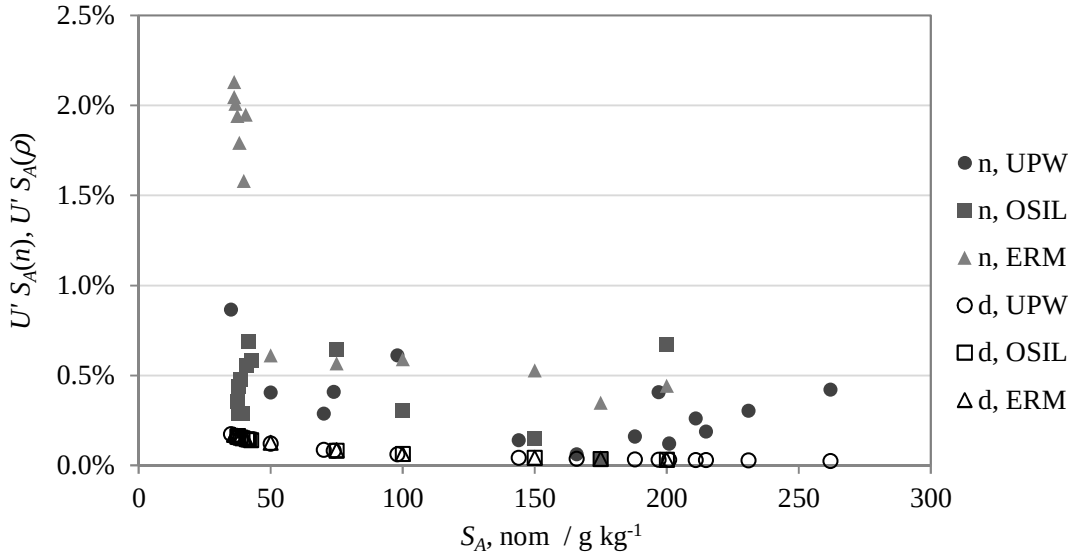

Figure IV.75 Relative expanded uncertainty, $U'\ S_A(n)$ and $U'\ S_A(\rho)$, of the absolute salinity values, S_A obtained from the measured values of refractive index, n (represented as n) and density, ρ (represented as d), at 20 °C, for the solutions of NaCl in ultrapure water (UPW - circles), in OSIL SSW (squares) and in ERM SSW (triangles).

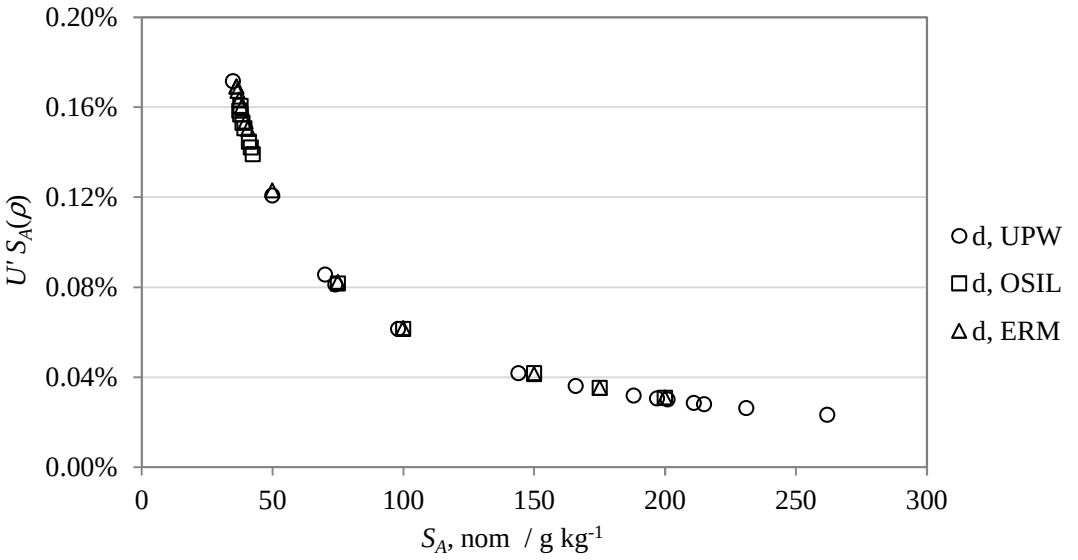

Figure IV.76 Relative expanded uncertainty, $U'\ S_A(\rho)$, of the absolute salinity values, S_A obtained from the measured values of density, ρ (represented as d), at 20 °C, for the solutions of NaCl in ultrapure water (UPW –circles), in OSIL SSW (squares) and in ERM SSW (triangles).

By analyzing the relative differences $\Delta S_A'$, between the values of the absolute salinity obtained from the measured values of refractive index, $S_A(n)$, and of density, $S_A(\rho)$, at 20 °C, as a function of the nominal value of the absolute salinity, S_A, shown in Fig. IV.77, it is possible to verify that the technique used presents the same deviations for the OSIL SSW as for the NaCl solutions in ultrapure water, albeit for the ERM SSW the deviations are higher. The uncertainties obtained for the lower levels of S_A values are higher for the smaller absolute salinities.

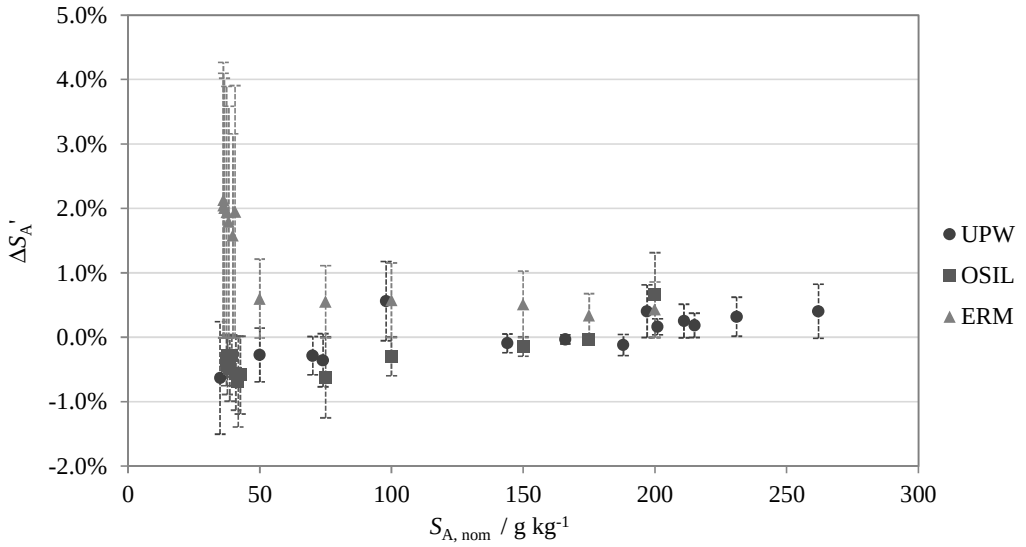

Figure IV.77 Relative difference between pairs of salinity values obtained by refractometry and by densimetry $\Delta S_A'$ as a function of the nominal value of the absolute salinity, S_A, for the solutions of NaCl in ultrapure water (UPW – black circles), in OSIL SSW (dark grey filled squares) and in ERM SSW (light grey filled triangles). Legend: the vertical bars represent the relative expanded uncertainty of the relative differences, $U_{\Delta S_A'}$, for a 95 % confidence level.

IV.3.4 Conclusions

The knowledge and characterization of the physicochemical properties of the liquid matter are common objectives of the laboratories LPL, that performs density measurements, and LFR, that performs refractometry measurements, of the IPQ, the Portuguese Metrology Institute. Although each laboratory is specialized in an area of metrological knowledge, it is often the case that knowledge intersects in order to better characterize a particular sample.

The results obtained for the salinity of the aqueous solutions of NaCl through both the refractive index, n, and the density, ρ, showed metrological compatibility in the [35; 200] g·kg^{-1} salinity interval. However, the salinity uncertainties of the results of NaCl solutions in ultrapure water obtained from refractometry were seven times greater than the uncertainties obtained from densimetry. In the case of NaCl solutions in OSIL SSW, the salinity uncertainties were five times greater and for NaCl in ERM SSW eleven times greater from refractometry than those obtained from densimetry. These results allow one to conclude that, in situations where very low uncertainties are required, the use of the densimetry technique through the oscillation-tube density meter should be chosen. However, if very small uncertainty is not required and only fast results are necessary, it is better to use refractometry, because it is a fast and inexpensive technique, which proved to be compatible with the previous one.

FACULDADE DE CIÊNCIAS E TECNOLOGIA
UNIVERSIDADE NOVA DE LISBOA

V

General Conclusions & Future Work

The main goal of this work consisted in the study of the influence of physical and mechanical properties of fluids when using oscillation-type density meters to measure density, at ambient and high pressure. The influence of viscosity, in Newtonian liquids, and of viscoelasticity, in non-Newtonian fluids, on the accuracy and precision of density measurements were investigated by using as comparison methods hydrostatic weighing and pycnometry, respectively. The mechanical characterization of the viscoelastic samples was conducted by rheometry.

These investigations aimed to fulfil an actual gap of liquids' density metrology knowledge and to give answer to the actual needs of Society, in terms of industry, customers, research and development. In general, the obtained results from this research gathered new knowledge regarding the robustness of oscillating-tube density meters with regard to: density (from 650 to 1615 $kg \cdot m^{-3}$); temperature (from 10 to 50 ºC); viscosity (from 0,7 to 1400 mPa·s); viscoelasticity (polymeric solutions, gels, particulate systems, etc.) and pressure (from ambient pressure up to 650 bar).

As would be expected, during this work it was not possible to test all brands and models of oscillation-type density meters currently available on the market. However, although these density meters may vary in their configuration or in underlying technologies, they all share the same principle of measurement, so the calibration methodologies presented in this work may be found useful in investigating the density errors induced by the physical and mechanical properties of fluid samples (as viscosity and viscoelasticity) and the ones induced by measurement characteristics (like temperature and pressure), thus allowing a more complete assessment of the accuracy and precision of the density measurements produced.

The knowledge gained will be disseminated in international guides and standards for scientific, applied (EURAMET guides and ISO standards) and legal metrology (OIML and WELMEC documents) and this will address the lack of documentation on this issue.

Density and Viscosity → This work proved that oscillation-type density meters are suitable instruments to measure the density of Newtonian liquids in a wide range of density, viscosity and temperature, with an expanded uncertainty from 0,01 to 0,03 $kg \cdot m^{-3}$, by using a proper calibration curve, since the deviations due to viscosity-induced damping may lead to a maximum density deviation of 0,62 $kg \cdot m^{-3}$ in the viscosity interval up to 795 mPa·s.

Viscoelasticity → One of the limitations identified during this work was the high uncertainty of the density measurements of non-Newtonian fluids obtained with pycnometers by gravimetric method. It is a fact that nowadays is the most used method for this type of liquids, since the potential effects on hydrostatic weighing method is not yet well-described. These investigations showed that the knowledge of samples' viscoelasticity effect on density measurements results using this kind of density meters is limited by the (relative) uncertainty of the pycnometer method, 0,010 %, since these density meters can produce density results with much lower relative uncertainty (~0,0053 %). For this reason, it was found essential further works to design, develop and optimize a new measuring system (for e.g. based on gravimetric, optics methods, or other adequate methodologies) able to measure the density of non-Newtonian fluids at 20 ºC and atmospheric pressure, with a target uncertainty of 0,010 $kg \cdot m^{-3}$ (at least better than 0,5 $kg \cdot m^{-3}$ which correspond to the uncertainty obtained when using a pycnometer). This new method should also be designed in order to overcome other limitations of the pycnometry, such as: high sample's volume required; difficulty in stabilizing sample's temperature; difficulty in handling viscous samples with the possibility of bubble formation, etc. This may lead to means of comparison that will be able to use the oscillation-type density meters in their maximum metrological capability also with non-Newtonian samples. Or even to know the real limitation of this measuring instrument, to give the most accurate insights for reference documents, such as standards and guides. The 17RPT02-rhoLiq EMPIR Project will address this subject in further joint investigations.

Despite not being possible of establish a casual relation between samples' viscoelasticity and density errors, the results of these studies gave the information that viscoelastic samples can produce density errors up to 0,18 % (when for the maximum obtained for the high viscosity samples was 0,069 % with an uncertainty 0,011 % (limited by the uncertainty of the reference density measurement method used). It was also proofed that samples' time-dependent relaxation/recovery behaviour may produce density deviations up to 0,0006 % (for a resulting hysteresis area of 44 %) that showed no significance as the uncertainty of density determinations was ~0,0053 %.

Other limitation found during these investigations was the extrapolation methodology used to estimate samples' viscosity values at the oscillation frequency value produced in the oscillation-type density meter during density measurements (usually in the frequency interval of 273-279 Hz). This extrapolation since the mechanical characterization and the viscoelastic properties of fluids under such a high frequency value is not feasible by means of rheometry due to instrumental limitations, other methodologies might be use in future works such as: indirect method with Dynamic Mechanic Analysis (DMA) (ISO 4664-1:2011) up to 100 Hz and then for frequencies exceeding 1 kHz with a shift factor based on the Williams–Landel–Ferry (WLF) equation (Ferry, 1980); or direct method called Base Excitation Resonant Mass (BERM) (Darlow & Zorzi, 1981; (Shoyama & Fujimoto, 2018) suitable for measuring dynamic properties up to 1000 Hz (ISO 4664-1:2011), etc.

High pressure → During this work, a high-pressure density apparatus was developed, characterized and validated ensuring the traceability to SI of density measurements performed with oscillation-type density meters at high pressure (up to 650 bar). This work allowed to conclude that it is possible to determine the equation of density dependence on pressure in the interval from 1 to 650 bar, with the developed apparatus, with an expected density measurement uncertainty of 0,50 $kg\ m^{-3}$, both for Newtonian and non-Newtonian liquids. On the contrary, it showed that it is not possible to measure suspensions with this kind of apparatus, mainly due to the heterogeneity of the sample and the possible

deposition of the solid's parts inside the density meter measuring cell. The developed apparatus and methodology are suitable to be used for calibration purposes, as recommended by the standard ASTM D7961 (2017), fulfilling this existing gap in density traceability chain. Another step needs to be done, in future works, is to build or to adapt this apparatus to be used in a wider temperature range.

New calibration methods → In this work was also evidenced the applicability of the use of sucrose solutions to deduce calibrations curves for viscosity damping of a density meter in viscosity interval from 1 to 30 mPa·s, at 20 ºC, with an expanded uncertainty of 0,030 $kg \cdot m^{-3}$. Also, an interesting relationship between the difference of density indication without viscosity correction and density indication with viscosity correction was observed for DMA 5000 density meter, allowing, without knowing the viscosity of the sample, to predict the correction to apply to density indication.

Salinity → Another highest-level aspect is the determination of seawater salinity in the European marginal seas, being important for the description of oceanic currents as base for climate modelling. So, several investigations were performed to prove the compatibility of salinity determinations by means of density and refractive index measurements. The results obtained for the salinity of the aqueous solutions of NaCl through both the refractive index, n, and the density, ρ, showed metrological compatibility in the [35; 200] g kg^{-1} salinity interval. These results allowed concluding that, in situations where very low uncertainties are required, the use of the densimetry technique through the oscillation-tube density meter should be chosen. However, if very small uncertainty is not required and only fast results are necessary, it is better to use refractometry, because it is a fast and inexpensive technique, which proved to be compatible with the previous one.

REFERENCES

Ahmed, T. (2018). *Reservoir engineering handbook*. Gulf Professional Publishing.

Al-Malah, K. (2006). Rheological properties of carbomer dispersions. *ANNUAL TRANSACTIONS-NORDIC RHEOLOGY SOCIETY*, *14*, 123.

Alves, S., Furtado, A., Spohr, I., & Filipe, E. (2011). Reducing Uncertainty in the Density Determination of Liquids: Application of the Substitution Method in Oscillation-Type Densimetry, EURACHEM.

ASTM D7961-17, Standard Practice for Calibrating U-tube Density Cells over Large Ranges of Temperature and Pressure.

ASTM E2509–14, Standard Test Method for Temperature Calibration of Rheometers in Isothermal Mode.

ASTM E2510-07(2013), Standard Test Method for Torque Calibration or Conformance of Rheometers.

ASTM E2975–15, Standard Test Method for Calibration of Concentric Cylinder Rotational Viscometers.

Batista, E. M., Godinho, I., do Céu Ferreira, M., Furtado, A., & Lucas, P. (2017). Comparison of infusion pumps calibration methods. Measurement Science and Technology. https://doi.org/10.1088/1361-6501/aa8474.

Batista, E., Almeida, N., Furtado, A., *et al.* (2015a). Assessment of drug delivery devices. *Biomedical Engineering / Biomedizinische Technik*, doi:10.1515/bmt-2014-0138.

Batista, E., Furtado, A., Almeida, N., Moura, S, Martins, R., Sousa, L., & Filipe, E. (2015b). Calibration of infusion pumps using liquids whose physical properties differ from those of water, *Journal of Physics: Conference Series* 588, 012053 doi:10.1088/1742-6596/588/1/012053.

Batista, E., Godinho, I., do Céu Ferreira, M., Furtado, A., Lucas, P., & Silva, C. (2017). Comparison of infusion pumps calibration methods. *Measurement Science and Technology,* 28(12), 124003. https://doi.org/10.1088/1361-6501/aa8474.

Bauer, H., & Boese, N. (1990). Rheological Properties of a Micelle System in Solution to be Used as Reference Liquid with Viscoplastic Behaviour. In *Third European Rheology Conference and Golden Jubilee Meeting of the British Society of Rheology* (pp. 37-40). Springer Netherlands.

Bauer, H., & Boese, N. (1990). Rheological Properties of a Micelle System in Solution to be Used as Reference Liquid with Viscoplastic Behaviour. In *Third European Rheology Conference and Golden Jubilee Meeting of the British Society of Rheology* (pp. 37-40). Springer, Dordrecht.

Becker, P., Bettin, H., Kuetgens, U., HallmannSeiffert, B., & Riemann, H. (2005). Silicon for primary metrology: the effect of hydrogen on its perfection. *J. Phys. D: Appl. Phys.* 38 4109–4114

Benyounes, K., Remli, S., & Benmounah, A. (2018). Rheological behavior of Hydroxyethylcellulose (HEC) Solutions. In *Journal of Physics: Conference Series* (Vol. 1045, No. 1, p. 012008). IOP Publishing.

Bettin, H., Borys, M., & Nicolaus, R. A. (2008). Density: From the Measuring of a Silicon Sphere to Archimedes' Principle. Special Issue / *PTB-Mitteilungen* 118, No. 2 and No. 3.

BIPM, I., IFCC, I., ISO, I., & IUPAP, O. (2008). Evaluation of Measurement Data - Guide to the Expression of Uncertainty in Measurement GUM 1995 with minor corrections. *Joint Committee for Guides in Metrology, JCGM*, *100.*

Borys, M.; Scholz, F., & Firlus, M. (2008). Realization of the Mass Scale. *PTB-Mitteilungen* 118, 10–15.

Bouchot, C., & Richon, D. (2001). An enhanced method to calibrate vibrating tube densimeters. *Fluid Phase Equilibria*, *191*(1-2), 189-208.

Cabiati, F., & Bich, W. (2009). Realization and dissemination of units in a revised SI. *Measurement*, *42*(10), 1454-1458.

Chara, Z., Zakin, J. L., Severa, M., & Myska, J. (1993). Turbulence measurements of drag reducing surfactant systems. *Experiments in Fluids*, 16(1), 36-41.

Chmielewski, C., & Jayaraman, K. (1993). Elastic Instability in Cross-Flow of Polymer-Solutions through Periodic Arrays of Cylinders, *J. Non-Newton Fluid Mech.* 48, 285-301.

Cuckow, F.W. (1949). A new method of high accuracy for the calibration of reference standard hydrometers. *Journal of the Society of Chemical Industry*, *68*(2), 44-49.

Darlow, M., & Zorzi, E. (1981). Mechanical design handbook for elastomers (the design of elastomer dampers for application in rotating machinery) [Final Report].

DIN 53019-4:2016, Rheometry - Measurement of rheological properties using rotational rheometers - Part 4: Oscillatory rheology.

DIN 53019-1:2009, Viscometry - Measurement of viscosities and flow curves by means of rotational viscometers - Part1: Principles and measuring geometry.

DIN 53019-2:2001, Viscosimetry - Measurement of viscosities and flow curves by means of rotation viscosimeters – Part 2: Viscosimeter calibration and determination of the uncertainty of measurement.

DIN 53019-3:2008, Viscometry- Measurement of viscosities and flow curves by means of rotational viscometers – Part 3: Errors of measurement and corrections.

Directive 2007/45/EC of the European Parliament and of the Council of 5 September 2007, laying down rules on nominal quantities for prepacked products, repealing Council Directives 75/106/EEC and 80/232/EEC, and amending Council Directive 76/211/EEC.

Ehlers, S., Könemann, J., Ott, O., Wolf, H., Šetina, J., Furtado, A., & Sabuga, W. (2019). Selection and characterization of liquids for a low pressure interferometric liquid column manometer. *Measurement*, *132*, 191-198.

Ewoldt, R. H., Johnston, M. T. & Caretta, L. M. (2015). Experimental challenges of shear rheology: How to avoid bad data. In *Complex Fluids in Biological Systems* (pp. 207-241). Springer New York.

Fehlauer, H., & Wolf, H. (2006). Density reference liquids certified by the Physikalisch-Technische Bundesanstalt. *Measurement Science and Technology*, *17*(10), 2588.

Feistel R (2008). A Gibbs Function for Seawater Dynamics for -6 ºC to 80 ºC and Salinity up to 120 g/kg. *Deep Sea Research* I 55: 1639-1671.

Feistel, R., Wielgosz, R., Bell, S. A., Camões, M. F., Cooper, J. R., Dexter, P., ... & Hellmuth, O. (2015). Metrological challenges for measurements of key climatological observables: oceanic salinity and pH, and atmospheric humidity. Part 1: overview. *Metrologia*, *53*(1), R1.

Ferry, J.D. (1980). *Viscoelastic Properties of Polymers*, John Wiley & Sons, New York.

Fitzgerald, D. (2000). Technical Assessment of the Anton Paar DMA5000 density meter. *H&D Fitzgerald Ltd., UK.*

Fritz, G., Scherf, G., & Glatter, O. (2000). Applications of densiometry, ultrasonic speed measurements, and ultralow shear viscosimetry to aqueous fluids. *The Journal of Physical Chemistry B*, *104*(15), 3463-3470.

Fujii, K. (2006). Precision density measurements of solid materials by hydrostatic weighing. *Meas. Sci. Technol.* 17, 2551–2559.

Fujita, Y., Zubler, T., Mastropierro, J.,Trujillo, S., Cekiel, I., Malta, D., Lorefice, S., Ballereau, P., Meury, P., Zhang, Z., Wolf, H., Trochta, D., Sakarya, O., Van Andel, I., Buchner, C., Spohr, I., Furtado, A., Lugadiru, B., Mekawy, M., Jonker, D., Kumar, A. and Anuar, Z., CCM. V-K3: CCM Key Comparison of Viscosity. *Metrologia*, 55(1A), 07010.

Furtado, A., Batista, E., Ferreira, M.C., Godinho & I., Lucas, P. (2017). Uncertainty calculation in the calibration of infusion pumps using the comparison method. In *book of proceedings of the AMCTM XI and IMEKO TC21*, 31-29 August 2017, Glasgow, Scotland.

Furtado, A., Batista, E., Spohr, I., & Filipe, E. (2009). Measurement of Density Using Oscillation-Type Density Meters Calibration, Traceability and Uncertainties. In *Proceedings of the 14ème Congrès International de Métrologie*.

Furtado, A., Moura, S., Pereira, J., Moutinho, J., Oliveira, F., Godinho, I. (2016). The importance of the use of adequate reference materials in density measurements performed in hemodialysis treatments. *Measurement*, 79, 349-353. doi:10.1016/j.measurement.2015.07.032.

Furtado, A., Moutinho, J., Moura, S., Oliveira, F., & Filipe, E. (2015). The role of adequate reference materials in density measurements in hemodialysis. In *Journal of Physics: Conference Series* (Vol. 588, No. 1, p. 012051). IOP Publishing. doi:10.1088/1742-6596/588/1/012053

Furtado, A., Oliveira, C., Pellegrino, O., Pereira, C., Mateus, C., Queirós, A., ... & Filipe, E. (2013). Metrological compatibility of the measuring results of aqueous solutions mass fractions by densimetry and refractometry. In *book of proceedings of the Joint IMEKO International TC8, TC23 and TC24 Symposium*.

Furtado, A., Pagel, R., Lorenz, F., Godinho, I. & Wolf, H. (2017). Estimation of nominal viscosity of Newtonian liquids from data obtained by an oscillation-type density meter, In *Annual Transactions of the Nordic Rheology Society*, Vol. 25.

Furtado, A., Pellegrino, O., Alves, S. *et al*. (2010). Determinação da fracção mássica de soluções aquosas de glucose por refractometria e densimetria de tubo vibrante. In *book of proceedings of the CONFMET2010,* Lisbon, Portugal, 4-5 November 2010.

Furtado, A., Pellegrino, O., Pereira, J. & Filipe, E. (2015c). Oscillation-type density meter calibration in viscosity by ICUMSA sucrose solutions, In b*ook of proceedings of the XXI IMEKO WORLD CONGRESS*, Issue: 1, ISBN: 978-80-01-05793-3, TC09 Flow Measurement.

Furtado, A., Pereira, J., Schiebl, M., Mares, G., Popa, G., Bartos, P., ... & Neuvonen, P. (2018). Establishing traceability for liquid density measurements in Europe: 17RPT02-rhoLiq a new EMPIR joint research project. *Journal of Physics: Conference Series* (Vol. 1065, No. 8, p. 082013). IOP Publishing. doi:10.1088/1742-6596/1065/8/082013.

Gavina, J., Furtado, A., Pereira, J., & Sousa, J. (2018). Indirect and direct temperature calibration methodology of a rheometer using a Newtonian reference material. *Journal of Physics: Conference Series* (Vol. 1065, No. 4, p. 042055). IOP Publishing. doi:10.1088/1742-6596/1065/4/042055

Giesekus, H., & Langer, G. (1977). Die Bestimmung der wahren Fließkurven nicht-newtonscher Flüssigkeiten und plastischer Stoffe mit der Methode der repräsentativen Viskosität. *Rheologica Acta*, *16*(1), 1-22.

Gupta, S.V. (2002). *Practical Density Measurement and Hydrometry*, IOP Publishing.

Highgate, D. J. & Whorlow, R. W. (1969). End effects and particle migration effects in concentric cylinder rheometry. *Rheologica Acta*, *8*(2), 142-151

Holcomb, C. D., & Outcalt, S. L. (1998). A theoretically-based calibration and evaluation procedure for vibrating-tube densimeters. *Fluid phase equilibria*, *150*, 815-827.

ICUMSA Method. Specification and Standard SPS-5 “Viscometry”, 1994.

ICUMSA Methods. Specification and Standard SPS-3 “Refractometry and Tables - Official”, 2000.

ICUMSA Methods. Specification and Standard SPS-4 “Densimetry and Tables: sucrose, glucose, fructose and inverted sugars”, 1998.

International Recommendation “Hierarchy scheme for density measuring instruments” produce by the Subcommittee TC 9/SC4 of the ORGANISATION INTERNATIONALE DE METROLOGIE LEGALE (OIML).

ISO 13528:2015 - Statistical methods for use in proficiency testing by interlaboratory comparison.

ISO 15212-1:1998. Oscillation-type density meters - Part 1: Laboratory instruments.

ISO 15212-2:2002. Oscillation-type density meters - Part 2: Process instruments for homogeneous liquids.

ISO 1652:2011, Rubber Latex-Determination of Apparent Viscosity by Brookfield Test Method.

ISO 17034:2016 (E): General requirements for the competence of reference material producers.

ISO 2555:1989, Plastics – Resins in the Liquid State or as Emulsions or Dispersions-Determination of Apparent Viscosity by the Brookfield Test Method.

ISO 2811-1:2016. Paints and varnishes - Determination of density - Part 1: Pycnometer method.

ISO 3585:1998 - Borosilicate glass 3.3 – Properties.

ISO 3696:1987 – "Water for analytical laboratory use – Specification and test methods".

ISO 4664-1:2011- Rubber, vulcanized or thermoplastic - Determination of dynamic properties -Part 1: General guidance

ISO 80 000-4:2006(E) Quantities and units — Part 4: Mechanics.

ISO 80 000-7:2008(E) Quantities and units — Part 7: Light.

ISO Guide 30:2015, Reference materials — Selected terms and definitions.

ISO TR 3666:1998 (E): *Viscosity of water*.

ISO/IEC 17025:2017. General requirements for the competence of testing and calibration laboratories

IUPAC Recommendations (2008). from the IUPAC Analytical Chemistry Division, Subcommitee on Solubility and Equilibrium Data, prepared for publication by Gamsjäger H, Lorimer JW, Scharlin P and Shaw DG 2008 Glossary of terms related to solubility. *Pure and applied chemistry* 80(2): 233-276. DOI: 10.1351/pac200880020233.

Jacobsen, J.P. & Knudsen, M. (1940). Urnormal (1937) Or Primary Standard Sea-water 1937, Association D'Océanographie Physique. *Union Géodésique et Géophysique Internationale, Publication Scientifique* No. 7.

JCGM 100:2008 (2008). Evaluation of measurement data – Guide to the expression of uncertainty in measurement. BIPM.

JCGM 200:2012 (2012). International Vocabulary of Metrology – Basic and General Concepts and Associated Terms. VIM 3rd edition. BIPM.

Jornal Oficial das Comunidades Europeias, L 272 de 3.10.1990, 1.

Kelessidis, V.C., Maglione, R. & Bandelis, G. (2010). On the end-effect correction for Couette type oil-field direct-indicating viscometers for Newtonian and non-Newtonian fluids. *Journal of Petroleum Science and Engineering*, *71*(1), 37-46.

Knudsen M. (1901). Hydrographische Tabellen. G.E.C. Gad, Copenhagen, L. Friederichsen & Company, Hamburg, Buchdruckerei Bianco Luno.

Koh, C.J., Hookham, P. & Leal, L.G. (1994). An Experimental Investigation of Concentrated Suspension Flows in a Rectangular Channel, *J. Fluid Mech.* 266, 1-32.

Koshiba, T., Mori, N., Sugiyama, S. & Nakamura, K. (1999). Elongational effects in the flow of viscoelastic fluid through a wavy channel, *Rheol. Acta*, 38, 375-383.

Lagourette, B., Boned, C., Saint-Guirons, H., Xans, P., & Zhou, H. (1992). Densimeter calibration method versus temperature and pressure. *Measurement Science and Technology*, *3*(8), 699.

Lampreia, I.M., & de Castro, C.A.N. (2011). A new and reliable calibration method for vibrating tube densimeters over wide ranges of temperature and pressure. *The Journal of Chemical Thermodynamics*, *43*(4), 537-545.

Laun, M., Auhl, D., Brummer, R., Dijkstra, D. J., Gabriel, C., Mangnus, M. A., ... & Handge, U. A. (2014). Guidelines for checking performance and verifying accuracy of rotational rheometers: viscosity measurements in steady and oscillatory shear (IUPAC Technical Report). *Pure and Applied Chemistry*, *86*(12), 1945-1968.

Le Menn, M., Albo, P.A.G., Lago, S., Romeo, R., & Sparasci, F. (2018). The absolute salinity of seawater and its measurands. *Metrologia* 56, pp. 1-10.

Lee, J., Chen, Y., Pope, T., Hanson, E., Cozzens, S., & Batmaz, T. (2008). U.S. Patent No. 7,341,980. Washington, DC: U.S. Patent and Trademark Office.

Lewis, E.L., & Perkin, R.G. (1978). Salinity: its definition and calculation. *J. Geophys. Res.* 83: 466. DOI: 10.1029/JC083iC01p00466.

Lorefice, S., & Saba, F. (2017). The Italian primary kinematic viscosity standard: the viscosity scale. *Measurement*, *112*, 1-8.

Lorefice, S., & Sardi, M. (2012, September). Calibration of a reference vibrating tube densimeter. In *XX IMEKO World Congress–Metrology for Green Growth, Busan–Republic of Korea*.

Lucas, P., & Klein, S. (2015). Metrology for drug delivery. *Biomedical Engineering/Biomedizinische Technik*, 60(4), 271-275.

Melvad, C., Krühne, U., & Frederiksen, J. (2010). Design considerations and initial validation of a liquid microflow calibration setup using parallel operated syringe pumps. *Measurement Science and Technology*, 21(7), 074004.

Mezger, T.G. *The Rheology Handbook* (E. Coatings, 4th edition, Vincentz Network, 2014)

Millero, F.J., Feistel, R., Wright, D.G., & McDougall, T.J. (2008). The composition of Standard Seawater and the definition of the Reference-Composition Salinity Scale. *Deep Sea Research Part I: Oceanographic Research Papers* 55(1): 50-72. DOI: 10.1016/j.dsr.2007. 10.001.

Napoleão, A., Furtado, A., Pereira, J., Quendera, R., Pellegrino, O., Cidade, M.T., & Oliveira, C.R. (2018). Salinity determinations by refractometry and oscillation-type densimetry as compatible methods: from salinity to pH. *Journal of Physics: Conference Series* (Vol. 1065, No. 7, p. 072037). IOP Publishing. doi:10.1088/1742-6596/1065/7/072037.

Nayar, K.G., Sharqawy, M.H., & Banchik, L.D. (2016). Thermophysical properties of seawater: a review and new correlations that include pressure dependence. *Desalination* 390: 1-24.

OIML G 14:2011 (E). Density measurement.

OIML International Recommendation “Hierarchy scheme for density measuring instruments” produce by the Subcommittee TC 9/SC4 of the OIML.

OIML R 124 “Refractometers for the measurement of the sugar content of grape must”, 1997

Outcalt, S. L., & McLinden, M. O. (2007). Automated densimeter for the rapid characterization of industrial fluids. *Industrial & Engineering Chemistry Research*, *46*(24), 8264-8269.

Outcalt, S.L. (2018). Calibration Fluids and Calibration Equations: How Choices May Affect the Results of Density Measurements Made with U-Tube Densimeters. *Journal of Research of the National Institute of Standards and Technology*, *123*, 1-10.

Pellegrino, O., Furtado, A., & Filipe, E. (2009). Linear fitting procedures applied to refractometry of aqueous solutions. In: 3rd Symposium on Traceability in Chemical, Food and Nutrition Measurements, Lisbon, Portugal, 6-11 September 2009. *Proc. XIX IMEKO World Congress Fundamental and Applied Metrology*.

Pellegrino, O., Furtado, A., Alves, S., Spohr, I. & Filipe, E. (2011a). Compatibilidade metrológica de resultados de medição da fracção mássica de glucose em soluções aquosas por densimetria de tubo vibrante e refractometria, In 4.º Encontro Nacional da Sociedade Portuguesa de Metrologia.

Pellegrino, O., Furtado, A., Alves, S., Spohr, I. & Filipe, E. (2011b). Refractometria e densimetria de tubo vibrante: técnicas complementares na determinação da fracção mássica de glucose em soluções aquosas?, In XXII Encontro Nacional da Sociedade Portuguesa de Química.

Pellegrino, O., Furtado, A., Cortez, L., & Filipe, E. (2008). Estimativa de incerteza para função de medição linear; Aplicação em refractometria das soluções líquidas. In *3.º Encontro Nacional da Sociedade Portuguesa de Metrologia* (SPMet).

Picard, R. S. Davis, M. Gläser, K. Fujii (2008). Revised formula for the density of moist air (CIPM-2007). *Metrologia*, vol. 45, pp. 149-155.

Resolution 1 of the 26th CGPM (2018). Metrologia, 2019, 56, 022001. Available on: https://www.bipm.org/en/CGPM/db/26/1/

Resolution of the 1st CGPM (1889). CR p.34-38. Available on: https://www.bipm.org/en/CGPM/db/1/1/

Resolution of the 3rd CGPM (1901). CR p.70. Available on: https://www.bipm.org/en/CGPM/db/3/2/

Savins, J.G. (1968). Shear thickening phenomena in poly (vinyl) alcohol-borate complexes. *Rheologica Acta*, *7*(1), 87-93.

Schilling, G., Kleinrahm, R., & Wagner, W. (2008). Measurement and correlation of the (p, ρ, T) relation of liquid n-heptane, n-nonane, 2, 4-dichlorotoluene, and bromobenzene in the temperature range from (233.15 to 473.15) K at pressures up to 30 MPa for use as density reference liquids. *The Journal of Chemical Thermodynamics*, *40*(7), 1095-1105.

Schindelin, J., Arganda-Carreras, I., Frise, E., Kaynig, V., Longair, M., Pietzsch, T., Preibisch, S., Rueden, C., Saalfeld, S., Schmid, B.,Tinevez, J.Y., White, D.J., Hartenstein, V., Eliceiri, K., Tomancak, P., & Cardona, A. (2012). Fiji: an open-source platform for biological-image analysis, *Nature Methods* 9(7): 676-682.

Schmidt, H., Wolf, H., & Hassel, E. (2016). A method to measure the density of seawater accurately to the level of 10− 6. *Metrologia*, *53*(2), 770.

Schramm, G. (1994). *A practical approach to rheology and rheometry* (pp. 53-56). Karlsruhe: Haake.

Shapley, N.C., Armstrong, R.C., & Brown, R.A. (2002). Laser Doppler velocimetry measurements of particle velocity fluctuations in a concentrated suspension. *J Rheol*. 46:1, 241–72.

Shapley, N.C., Armstrong, R.C., & Brown, R.A. (2004). Evaluation of particle migration models based on laser Doppler velocimetry measurements in concentrated suspensions. *J Rheol*. 48:2, 255–79.

Shirakashi, M., Ito, H., & James, D.F. (1998). LVD measurement of the flow field in a constant extensional-rate channel, *J. Non-Newtonian Fluid Mech.* 74, 247-262.

Shoyama, T., & Fujimoto, K. (2018). Direct measurement of high-frequency viscoelastic properties of pre-deformed rubber. *Polymer Testing*, *67*, 399-408.

Söhnel, O., & Novotny, P. (1985) Densities of Aqueous solutions of Inorganic Substances. Amsterdam: Elsevier.

Sousa, A.T. (1994). Density and Viscosity of Homogeneous Systems, Ph.D. Thesis, University of Lisbon.

Spieweck, F., & Bettin, H. (1992). Review: Solid and liquid density determination. *Technisches Messen*, 59, 237–244, 285–292.

Stabinger, H. (1994). Density Measurement using modern oscillating transducers, South Yorkshire Trading Standards Unit, Sheffield.

Stabinger, H., Leopold, H., & Kratky, O. (1967). A new method for precision measurement of the density of liquids. *Monthly Bulletins for Chemistry / Chemical Monthly*, *98* (2), 436-438.

Swindells, J.F., Coe, J.R., & Godfrey, T.B. (1952). Absolute Viscosity of water at 20 °C. In: *J. Res. NBS 48*, p. 1 - 31.

Tanaka, G., Okamoto, K., & Madarame, H. (2000). Experimental investigation on the interaction between polymer solution jet and free surface, *Exp. Fluids* 29, 178-183.

Tanaka, M., Girard, G., Davis, R., Peuto, A., & Bignell, N. (2001). Recommended table for the density of water between 0 °C and 40 °C based on recent experimental reports, *Metrologia*, Vol. 38: 301-309.

Toms, B.A. (1949). Some observations on the flow of linear polymer solutions through straight tubes at large Reynolds numbers, *Proceedings of International Congress on Rheology*, vol. 2, North Holland, Amsterdam, pp. 135–141.

Wagner, W., & Kleinrahm, R. (2004). Densimeters for very accurate density measurements of fluids over large ranges of temperature, pressure, and density. *Metrologia,* 41, S24–S39.

Webster, J. G., & Eren, H. (2016). *Measurement, instrumentation, and sensors handbook: spatial, mechanical, thermal, and radiation measurement*. CRC press.

Wein, O., Pěnkavová, V., & Havlica, J. (2015). End effects in rotational viscometry II. Pseudoplastic fluids at elevated Reynolds number. *Rheologica Acta*, *54*(11-12), 903-914.

WELMEC Guide 6.4. Guide for packers and importers of e-marked prepacked products.

Williams, M. L., Landel, R. F., & Ferry, J. D. (1955). The temperature dependence of relaxation mechanisms in amorphous polymers and other glass-forming liquids. *Journal of the American Chemical society*, *77*(14), 3701-3707.

Wolf, A.W. (1966). Aqueous solutions and body fluids, their concentrative properties and conversion tables. New York: Harper and Row Publishers.

Wolf, H.; Bettin, H., & Gluschko, A. (2006) Water density measurement by a magnetic flotation apparatus. *Meas. Sci. Technol.* 17, 2581–2587

Won, C., Jin, Y. I., Kim, M., Lee, Y., & Chang, Y. H. (2017). Structural and rheological properties of potato starch affected by degree of substitution by octenyl succinic anhydride. *International journal of food properties*, *20*(12), 3076-3089.